Investigation into Cytosine Epigenetic State in Bladder Cancer

By

Alrayan Abass Albaz

The University Of Sheffield.

A thesis submitted in partial fulfilment of the requirements for the degree of

Doctor of Philosophy

The University of Sheffield
Department of Oncology and Metabolism
Faculty of Medicine, Dentistry and Health

Submission Date

October 2018

Abstract

Bladder cancer is a common malignancy that is best classified into high and low grade disease. Low-grade cancers are indolent in nature but expensive to manage. High-grade cancers can be invasive at diagnosis and have a poor prognosis. Molecular studies suggest high and low grade tumours are biologically distinct. All bladder cancers are characterised by heterogenous cell populations, high mutational burden and can be classified into molecular sub-groups using RNA expression and cell surface markers. Here I have explored these subgroups further and look at heterogenicity in primary muscle invasive bladder cancers (MIBC).

Firstly, I extracted different cell populations from fresh MIBC biopsies. I developed protocols to handle these specimens and used flow cytometry to isolate subpopulations. I discovered different cell populations exist, in different fractions, and that this information may reveal tumour subgroups. For example, subpopulations expressing CD44 and CD49f (indicators of a terminally differentiated urothelial subtype) were common and there was often a lack of CD90 cell surface receptor expression (an indicator of the basal differentiated subtype).

Secondly, I examined changes in epigenetic traits at cytosine residues to explore the frequency and extent of hydroxymethyl cytosine for the first time in bladder cancer. Using a 450K microarray I identified patterns of change that could affect key carcinogenic genes and could distinguish benign and malignant tissues using 5 methyl and 5 hydroxy methyl cytosine residues. Pathway analysis revealed several biochemical signalling pathways and over 30 genes to have altered cytosine residues. Finally, I validated these epigenetic findings in individual tumours and normal urothelium as well as in subpopulations identified in flow cytometry.

Although this research took a modest approach towards addressing queries raised by epigenetic alterations, it could serve as groundwork for future research. These include development of a primary tissue culture technique for malignant urothelial tissues and to identify the least differentiated bladder subpopulations. The genes and pathways identified using the array data should be investigated in further detail using murine models to better understand their role in urothelial carcinomas.

Acknowledgments

In the name of Allah, the most gracious and most merciful.

First of all, I would like to express my sincere gratitude to my supervisor Professor James Catto, for his support, patience and invaluable advice and guidance throughout my PhD.

My sincerest appreciation to the Ministry of Higher Education of Saudi Arabia for the financial support while doing my PhD at the University of Sheffield.

I would like to thank all of the friendly members (past and present) of the oncology and human metabolism department who made my time great during this PhD. Thanks to Andy Platts for his help with technical issues and Anil Ganesh for his advice and support during my PhD. Special thanks for Louise Goodwin for helping me in collecting tissues specimens, Sarah Bottomely for her support and Maggie Glover for her support and advice in primary tissue culture. Also, I would like to thank Dr. Paul Heath and Matthew Wyles from SITran for their help to perform the array experiment.

At the last but not least, a massive thank you from the bottom of my heart for my father Abass (may Allah rest his soul in peace) who supported me in all of my life and to my mother Fawziah who was always caring for me and assured me in this life whenever I faced difficulties. Also big thanks to my sisters Aljohara, Kholud and Alanoud and my brothers Ahmad and Hattan who supported me during my studies.

I would like to finally express my deepest love and appreciation to my lovely wife and son. Afnan support's and caring had a huge impact on both real and study life. Also my little lion Azzam, his positive energy made me stronger through my difficult times. I would like to say that without all my family members I would not be able to do my PhD.

Table of Content

List of Figures

List of Tables

List of Abbreviation

5-fC	5-formaylcytosine
5-hmC	5-hydroxymethylcytosine
5-mC	5-methylcytosine
ADCY4	Adenyl Cyclase Type 4
ADRA1A	Adrenergic Receptor Alpha 1-A
AGTR1	Angiotensin II Receptor Type 1
AJCC	American Joint Committee on Cancer's
APC	Adenomatous Polyposis Coli
ASR	Age-Standardised mortality Rates
BCSC	Bladder Cancer Stem Cells
BDNF	Brain-Derived Neurotrophic Factor
BS	Bisulfite sequencing
BTG2	B-cell Translocation Gene 2
CAM	Cell Adhesion Molecules
CCEG	Cystitis Cystica Et Glandularis
CD	Cluster of Differentiation
CDR	Crude Death Rates
CGH	Comparative Genomic Hybridisation
CIS	Carcinoma In Situ
CpG	Cytosine-Phosphate-Guanine
CSC	Cancer Stem Cells
CT	Computed Tomography
CTOS	Cancer Tissue Originated Spheroid
DAPK	Death-Associated Protein Kinase
DMEM	Dulbecco's Modified Eagle's Medium
DMP	Different Methylated Positions
DMSO	Dimethyl Sulphoxide
DNA	Deoxyribonucleic acid
DNMT	DNA MethylTransferases
dsDNA	Double Stranded DNA
EBV	Epstein-Barr Virus

ECS	E-Cigarette Smoking
EDNRB	Endothelin Receptor Type B
EDTA	Ethylene Diamine Tetra Acetic Acid
EGF	Epidermal Growth Factor
EMA	Epithelial Membrane Antigen
ERBB2	Erb-B2 Receptor Tyrosine kinase 2
EZH2	Enhancer of Zeste Homologue 2
FACS	Fluorescence-Activated Cell Sorting
FCS	Foetal Calf Serum
FGF	Fibroblast Growth Factor
FISH	Fluorescence In Situ Hybridisation
GALR1	Galanin Receptor 1
GRIA1	Glutamate Receptor 1
GRIN2A	Glutamate Ionotropic receptor NMDA Type subunit 2A
GST	Glutathione S-Transferases
GWAS	Genome wide association studies
HBSS	Hank's Balanced Salt Solution
HPV	Human Papilloma Virus
HR	High Risk
HSV	Herpes Simplex Virus
IL-6	Interleukin 6
IM	Intestinal Metaplasia
ISUP	International Society for Urological Pathology
ITH	Intra-Tumour Heterogeneity
KEGG	Kyoto Encyclopedia of Genes and Genomes
KIU	20-Kallikrein Inactivating Units
KSFMc	Keratinocyte Serum Free Media complete
LEP	Leptin
LEPR	Leptin Receptor
LNGFR/P75NTR	Low-Affinity Nerve Growth Factor
LMP	Low Malignant Potential
MI	Methylation Index
MIBC	Muscle Invasive Bladder Cancer

MM	Multiple Myeloma
MRI	Magnetic Resonance Imaging
MSK1	Mitogen-Activated and Stress-Activated Protein Kinase 1
MVC	Micro Vessel Count
NE	Neuroendocrinal
NEAA	Non-Essential Amino Acid
NET	Neuroendocrine Tumour
NGS	Next Generation Sequencing
NHU	Normal Human Urothelium
NMF	Non-negative Matrix Factorisation
NMIBC	Non-Muscle Invasive Bladder Cancer
NMIUC	Non-Muscle Invasive Urothelial Carcinoma
NOS1	Nitric Oxide Synthase 1
NPFFR2	Neuropeptide FF Receptor 2
NRXN1	Neurexin-1 Alpha
NSAIDS	Non-Steroidal anti-Inflammatory Drugs
NTSR1	Neurotensin receptor type 1
OXBS	Oxidative Bisulfite Sequencing
PCA	Principal Components Analysis
PCR	Polymerase Chain Reaction
PI3K	Phosphatidyl Inositol 3 Kinase
PPAR	Peroxisome Activator Pathway Receptor
PRC2	Polycomb-Repressive Complex 2
PUNLMP	Papilloma, papillary Urothelial Neoplasms of Low Malignant Potential
qMSP	Quantitative Methylation-Specific-PCR
RASSF1A	Ras association domain Family 1 isoform A
RB	Retinoblastoma
RBC	Red Blood Cells
RFS	Recurrence Free Survival
RUNX3	Runt-related transcription factor 3
SCC	Squamous Cell Carcinoma
SCCB	Small Cell Carcinoma of the Bladder
SD	Standard Deviation

SEYLLp	Standard Expected Years of Life Lost Per living person
SHH	Sonic Hedgehog
SMG	Significantly Mutated Genes
SNP	Single Nucleotide Polymorphism
ssDNA	Single Stranded DNA
SSTR1	Somatostatin Receptor 1
TACR	Tachykinin Receptor 3
TCGA	The Cancer Genomic Atlas
TET	Ten-Eleven Translocation
TIC	Tumour-Initiating Cells
TNF	Tumour Necrosis Factor
TNM	Tumour, Node and Metastasis
TrkB	Tropomyosin Receptor Kinase
TURBT	Transurethral Resection of the Bladder Tumour
UTR	Untranslated Region
VEFG	Vascular Epithelial Growth Factor
VIP	Vasoactive Intestinal Peptide (VIP
VIPR2	Vasoactive Intestinal Peptide Receptor 2
VSA	Vascular Surface Area
WHO	World Health Organization
µg	Microgram
µL	MicroLitre

CHAPTER ONE

1 INTRODUCTION

1.1 Understanding cancer

1.1.1 Definition of cancer

Cancer is a term used to define 'a diseased state' in which normal human cells divide and proliferate uncontrollably. This uncontrolled proliferation can potentially spread (metastasis) to healthy regions of the body via the blood stream or lymphatic vessels (Sudhakar, 2009). The term cancer was coined from the Greek term 'karkinos' meaning non-healing swelling/ ulcerous formation, while tumours or carcinoma where coined from another Greek term 'karkinoma' meaning non-healing cancer (Papavramidou et al., 2010). Cancer has been classified into various types on the basis of its tissue of origin and differentiation; these include carcinomas, arising from epithelial cells (such as adenocarcinoma or squamous carcinoma), sarcomas, which originate from connective tissue, leukaemia and lymphomas, which have a haematopoietic origin, germ cell tumours, which develop from pluripotent cells, and blastomas, which arise from embryonic cells. The most common human cancers include breast, prostate, lung, colorectal, skin and bladder cancer (Jemal et al., 2011).

The multifaceted development of cancer is definitively guided by aberrant signalling pathways, which foster an unstable genome and support genetic diversity. Cancer progression occurs through the acquisition of aberrant genetic coding and inflammation. There are certain traits or hallmarks that are unique to cancers (Hanahan and Weinberg, 2000). Identification of these hallmarks has made it easier to characterise the phenotypes of cancer. Cancer hallmarks are listed in Table 1.1 (Hanahan and Weinberg, 2011).

Table 1.1 The Hallmarks of Cancer: The Next Generation (Hanahan and Weinberg, 2011)

1	Continuous proliferation signals
2	Overriding normal growth suppression
3	Resistance to apoptosis
4	Unlimited replicative potential
5	Continuous angiogenesis
6	Infiltrating spread and metastasis
7	Reprogrammed energy assimilations
8	Immune extinction

Common aetiological factors of cancer include aging, alcohol abuse, the use of tobacco and exposure to carcinogenic substances, including ionising radiation (Sloan and Gelband, 2007). The use of tobacco is one of the most common exposures leading to cancer mortality (Vineis et al., 2004). Chronic infections by pathogens like human papilloma virus (HPV) and Helicobacter pylori (Graham, 1997), lack of proper diet and nutrition (Sala et al., 2004) have also been identified to cause cancer. Other causes include occupational hazards like polycyclic aromatic amines (Cumberbatch et al., 2015), asbestos (Donoghue, 2004), ionising radiation (Cardis et al., 1995), and pollutants (Boffetta, 2006).

1.1.2 International cancer statistics

The modern age has brought about a change in human lifestyle and habits as well as an evolution in the techniques used for diagnosing diseases. Concurrent with these changes, there has been a rise in the number of reported cancer cases across the globe. With the incidence rate projected to grow by over 70% in the next decades, this problem requires urgent attention. For example, in 2012 alone, 14 million new cases of cancer were identified globally. Cancer is the second highest cause of mortality with over 8.8 million cases being reported in 2015 alone behind heart disease (https://gco.iarc.fr/). Populations

residing in low and middle-income countries are especially susceptible to cancer and cancer associated mortality. The top ten occurring cancers include cancers of the lung, breast, colon and rectum, prostate, stomach, liver, cervix, oesophagus, bladder and pancreas (https://gco.iarc.fr/), (https://www.wcrf.org/). The prevalence rate for cancer is 625 cases per 100,000 individuals irrespective of gender. Cancer prevalence is higher among women (with a prevalence rate of 660.5/100000) than in men (with a prevalence rate of 589.4/100000) due to the high frequency of breast cancer (https://gco.iarc.fr/).

1.1.3 The human bladder – an anatomical perspective

The urinary bladder in humans serves as a muscular repository for urine and is located in the anterior pelvis. This organ is distensible in nature and possesses a tetrahedral shape when empty and an ovoid shape when full of urine (Macarak and Howard, 1999). In men, the bladder position is between the rectum and the pubic symphysis, while in females it is between the rectum and uterus/vagina (Hickling et al., 2015). The pubic symphysis is isolated from the urinary bladder by the Space of Retzius. Other anatomical differences include the resting point of the bladder, which in males is between the endopelvic fascia and the pelvic floor muscles. In females, the basal portion of the bladder, as well as the urethra, is fixed to the anterior wall of the vagina (Gosling, 1985). The roof of the bladder is enclosed by the peritoneum, with the bladder neck being affixed to neighbouring structures by the pelvic fascia and the pelvic ligaments. The body of the bladder is buttressed against the pelvic diaphragm in females and by the prostate in men. Lateral support ensured by the obturator internus and the levator ani muscles. Normal physiology and functionality of the urinary bladder is ensured by the concerted actions of smooth and striated muscles, driven by musculoskeletal, neurological and psychological inputs (Fowler et al., 2008). This in turn permits the collection and draining of the bladder contents. The underlying regulator of these efforts is the contraction and relaxation of the detrusor muscles as well as the muscles lining the bladder neck and pelvic floor (Sam and LaGrange, 2018).

A well-organised muscular bladder neck acting as the sphincter governs micturition in women, while in men the bladder neck is contiguous with the prostate and thus assists as an in-house urethral sphincter. This region has three distinct layers of muscle – the inner longitudinal muscle layer, the middle circumferential muscle layer and the outer longitudinal muscle layer. The inner longitudinal smooth muscle forms the urethral tube while the middle circumferential muscles are the most prominent around the muscle neck and the outer longitudinal layer is directed towards the pubovesical muscles on the posterior side of the pubic bone (Ellis, 2005, Hill, 2015).

The vascular supply for the urinary bladder arises from the internal iliac artery and the superior vesicular branch of this artery is one of the major arteries supplying the bladder. This is supplemented by the inferior vesicular artery in males and the vaginal arteries in females. In both males and females, the obturator and inferior gluteal arteries also provide blood supply to the bladder. The bladder is drained by the vesical venous plexus, which empties into the internal iliac vein. The lymphatic drainage of the bladder is carried out by vessels that drain into the obturator, iliac (external & internal) as well as the common iliac lymph nodes (Augurio et al., 2008).

The mucosa of the human urinary bladder is known as the urothelium and is made up of transitional epithelial cells. This transitional epithelium is bound to the muscle lined bladder walls by connective tissue called lamina propria. The lamina propria serves as a submucosa and is lined by dense layer of microvessels, which covers the detrusor muscle. Fatty connective tissue covers the anterior and lateral portions of the bladder, while the peritoneum overlaps the posterior portion. The bladder mucosa along the luminal surface is shielded by a glycosaminoglycan layer (Parsons, 1993).

1.2 Understanding bladder cancer

1.2.1 Introduction to bladder cancer

Bladder cancer is a common malignancy worldwide (Freedman et al., 2011). Exposure to carcinogenic substances via the use of tobacco has been suggested to be the single most common factor leading to the development of this disease (Freedman et al., 2011) . Other causative factors include exposure to heavy metals like arsenic (Christoforidou et al., 2013) or nitrates (Espejo-Herrera et al., 2015) in drinking water. Early symptoms of this malignancy include haematuria and irritative urinary symptoms (DeGeorge et al., 2017). A conclusive histological understanding of the disease is best obtained through transurethral resection of the bladder tumour (TURBT), allowing staging and primary treatment. The TURBT procedure (Furuse and Ozono, 2010) is often supplemented by adjuvant intravesical bacilli Calmette-Guérin treatment (Fuge et al., 2015) or intravesical chemotherapy (Shen et al., 2008). Muscle invasive bladder cancer usually requires more radical options, such as radical cystectomy, radical radiation therapy (Stein et al., 2001) and neoadjuvant therapy (Vale, 2005). Low and high-grade bladder cancer are molecularly distinct; with the former following a papillary/luminal pathway (non-muscle invasive tumours) and the latter a nonpapillary/basal pathway (muscle invasive tumours) (Blaveri et al., 2005).

1.2.2 Epidemiology

Bladder cancer is the ninth most common cancer and the thirteenth most common form of cancer in terms of mortality worldwide (Ferlay et al., 2015). In 2012, there were 430,000 new cases of this disease reported worldwide (Antoni et al., 2017); and up to 76,960 new cases of bladder cancer were reported in USA in the year 2016, with the vast majority of this disease afflicting men (58,950 new cases) (Siegel et al., 2016). Meanwhile, up to 10,171 cases of bladder cancer where reported in the United Kingdom in the year 2015 with an elevated mortality rate of 5,369. The mean age of British patients identified with bladder cancer has been reported to be around 71.3 years with total treatment costs being around 55.39

million British pounds (Sangar et al., 2005). Cumulative expenditure associated with bladder cancer in the European Union has been estimated to be not less than 4.9 billion euros in 2012 (Leal et al., 2016).

Incidence rates are particularly high in populated regions of Southern and Western Europe as well as in North America. The disparity in the distribution of the population afflicted with bladder cancer is influenced particularly by risk factors like tobacco usage, occupational chemical hygiene and Schistosoma haematobium infections (Antoni et al., 2017). A geographic pattern of bladder cancer is seen, reflecting that urothelial carcinoma is more widespread in Western Europe and the USA, while squamous cell bladder cancer is more common in Africa (Mostafa et al., 1999). The highest incidence rates for bladder cancer have been reported in Western Europe and USA while the Eastern European nations and Asiatic states have the lowest rates (Pelucchi et al., 2006). This is likely to change with smoking rates falling in many Western countries (Rushton et al., 2012). The high frequency, nature of surveillance and high prevalence creates a significant economic burden on the healthcare sector (Leal et al., 2016).

1.2.2.1 Risk factors

A number of occupational, non-occupational or environmental exposures are risk factors for the development of bladder cancer. Cigarette smoking accounts for the majority of the reported cases of bladder cancer, especially in developed countries (Jankovic and Radosavljevic, 2007). Cigarette smokers have a 2-5 times greater probability of developing bladder cancer than non-smokers (Ferris et al., 2013). Individuals using alternatives to cigarettes like cigars, pipes and smokeless tobacco still appear at risk of developing bladder cancer (Letasiova et al., 2012). E-cigarette smoking (ECS) has been linked with DNA damage and reduced cellular repair activities in the bladder in turn elevating the risk of the development of bladder cancer (Lee et al., 2018, Bourke et al., 2017). Occupational chemicals account for 5-10% of cases in developed countries (Jankovic and Radosavljevic, 2007, Cumberbatch et al.,

2015). Common occupational carcinogens include aromatic amines, polycyclic aromatic hydrocarbons and heavy metals (Carreon et al., 2006). Aromatic amines connected to bladder cancer include 4-aminobiphenyl, 2-naphthylamine and benzidine, as well as phenyl moieties like 4,4'-methylenebis (2-chloroaniline) (Letasiova et al., 2012). Individuals working in the chemical, dye and rubber industries are particularly at risk of exposure to these hydrocarbons on a daily basis. Professionals working as hairdressers and barbers have also been identified to be at risk due to their regular exposure to dyes and other chemicals containing aromatic hydrocarbons (Harling et al., 2010). Exposure to drinking water contaminated with the heavy metal arsenic, in concentrations ranging from 300-500 μg/l, have been strongly correlated with bladder cancer (Meliker and Nriagu, 2007). Chromium chlorination by products in drinking water has also been associated with bladder cancer oncogenesis (Golabek et al., 2017).

Individuals with the 'slow acetylator' phenotype of the gene N-acetyltransferase 2, which has been associated with phase II detoxification of aromatic amines, are particularly at risk of developing bladder cancer (Marcus et al., 2000). Knockdown of Glutathione S-transferases (GST) enzymes/genes (GSTA1, GSTM1, GSTP1 and GSTT1) (involved in cellular detoxification) has been associated with elevated bladder cancer susceptibility (Matic et al., 2013). Meta-analysis has also revealed GSTM1 and GSTT1 gene polymorphisms to be associated with bladder cancer susceptibility (Yu et al., 2017). Infectious microorganisms, including both Gram-negative bacteria (e.g. Pseudomonas, Klebsiella, Enterobacter) and Gram-positive bacteria (Staphylococcus) have all been associated with cystitis or chronic inflammation of the bladder lining (Grover et al., 2011). Cystitis cystica et glandularis (CCEG) and intestinal metaplasia (IM) have been identified to be harbinger stages of bladder adenocarcinoma (Smith et al., 2008). Other non-occupational hazards include infectious pathogens like Schistosoma haematobium (which causes the water-borne disease Schistosomiasis/ Bilharzia), exposure to chemotherapeutic agents and ingestion of analgesics. Furthermore, the administration of the chemotherapeutic agent, cyclophosphamide, has been linked to urotoxicity with afflicted individuals

developing urothelial carcinoma in the long term (Talar-Williams et al., 1996). Ifosfamide, an alkylating agent commonly used as a chemotherapeutic agent, has also been linked with the development of bladder cancer (Sannu et al., 2017). A similar oncogenic effect has been observed in the bladders of patients treated with the chemotherapeutic agent chlornaphazine (Laursen, 1970), with cancer appearing up to 3-10 years after chlornaphazine dose administration (Thiede and Chr. Christensen, 2009). Regular use of analgesics like phenacetin (Piper et al., 1985) and other non-steroidal anti-inflammatory drugs (NSAIDS) have been linked to bladder cancer incidence (Fortuny et al., 2007).

Other risk factors for bladder cancer include exposure to ionising radiation amongst individuals working in the nuclear industry. Low dose ionising radiation from nuclear fallout, e.g. as in Chernobyl, has been identified as causing chronic inflammation and proliferative atypical cystitis, also called Chernobyl cystitis. This stage has been considered to lead to later bladder cancer oncogenesis (Romanenko et al., 2009). In addition, there appears to be a positive association between diabetes mellitus and the risk of developing bladder cancer (Fang et al., 2013), and low blood serum levels of 25-hydroxy vitamin D (25(OH)D) have also been associated with bladder cancer susceptibility in male populations (Mondul et al., 2010). Diet is also likely to play a role, with a higher intake of red and processed meats having been identified as a bladder cancer risk factor (Li et al., 2014), as is elevated saturated fat intake and chronic obesity (Brinkman et al., 2011). Conversely, increasing total fluid intake and the consumption of fruits and vegetables has been associated with a reduction in the risk of bladder cancer. Aberrant expression of leptin an important regulator of body weight apparent in some bladder cancer specimens suggests a role for leptin in bladder carcinogenesis (Yuan et al., 2004).

1.2.2.2 Morbidity and mortality

Mortality rates appear to be highest in regions of Europe and Africa (Northern and Sub-Saharan Africa) and lowest in Asia and Central America (Chavan et al., 2014). The age-standardised mortality rates

(ASR) for bladder cancer in 2012 were 4.5/100,000 for Europe. Poland (ASR 6.3) and Spain (ASR 6.5) had some of the highest mortality rates irrespective of gender. A decade long study of bladder cancer afflicted individuals in the USA identified that 17% of deaths in men and 23% of deaths in women were caused as a direct result of this disease (Scosyrev et al., 2012). Mortality rates were at 7.6/100000 persons for American men but only at 2.2/10000 persons for American women. Men had higher bladder cancer mortality across Europe (ASR 8.5) while women had comparatively lower rates at ASR 1.8. Mortality rates were at ASR 7.3 for men and 2.8 for women in the UK for the same period. The highest mortality rates amongst women were in Denmark, with elevated ASR values of 3.8. Crude death rates (CDR) indices for bladder cancer increased from 10.79 per 100000 individuals in 2000 to 14.30 per 100000 individuals by 2014 in Poland. Standard expected years of life lost per living person (SEYLLp) indices associated with bladder cancer increased from 202.9 to 243.4 in Poland during the same period (Jobczyk et al., 2017). The median age at death was highest in individuals in the age group 75-84 (32.2%) followed by >84 (30.4%) (https://seer.cancer.gov/statfacts/html/urinb.html). Stage T1 bladder cancer had elevated rates of recurrence, while stages Tis and T1 were associated with a greater risk of disease advancement and mortality (Chamie et al., 2013). Older individuals (≥ 70) had higher mortality rates following radical cystectomy (Nielsen et al., 2007).

1.2.3 Economics

As stated, the high prevalence and nature of surveillance make bladder cancer one of the most expensive human malignancies (Leal et al., 2016, Gore and Gilbert, 2013). Costs are particularly high for patients in the final stages of bladder cancer (Parkin, 2006). Inability to afford expensive therapies often results in a shortened lifespan. High costs also reflect the constant monitoring needed throughout the afflicted individual's lifespan to identify any signs of recurrence (Svatek et al., 2014). The treatment costs per patient from bladder cancer diagnosis till the final phase range from $89,287 to $202,203 in the USA. While in the UK, the costs incurred for bladder cancer management are about £55.39 million or £8,349

per patient (Sievert et al., 2009). Perioperative chemotherapy often prescribed to patients diagnosed with bladder cancer is considered a cost-effective measure towards disease management; cauterisation and fulguration is also considered cost effective for patients with low-grade bladder cancer (Ferlay et al., 2015). The treatment costs associated with radiographic and cystoscopy protocols are lower when patients are prescribed bladder cancer surveillance measures. Increased post-operative care reduces morbidity rates following radical cystectomy and this also lowers the costs associated with perioperative care. Moreover, it is essential for the patients to be aware of the surgical benefits so as to be able to make an informed decision about whether the treatment benefits accrued are worthwhile. Diagnosis at the early stages of carcinogenesis results in lower treatment costs (Bauer et al., 2015) with chances of recurrence being minimised. Early disease diagnosis also helps in reducing disease mortality and unnecessary burden.

1.2.4 Histological subtypes

Bladder cancer is histologically classified into urothelial and non-urothelial subtypes, with multiple further subtypes of urothelial bladder cancer based on its variant histologic features (which are also referred to as divergent differentiation) (Chalasani et al., 2009). Classifying divergent differentiation patterns in the urothelium following transurethral resection, therefore, could be helpful in identifying tumours that might turn invasive and may need more aggressive treatment (Wasco et al., 2007). Such invasive urothelial bladder cancer has also been further subdivided as listed in Table 2.1.

Table 1.2 Variants of Invasive urothelial carcinoma

Variants of Invasive urothelial carcinoma
Squamous differentiation
Glandular differentiation
Nested pattern
Micropapillary
Microcystic
Lymphoepithelioma-like(Pantelides et al., 2012)(Pantelides et al., 2012)
Plasmacytoid and lymphoma-like
Sarcomatoid/carcinosarcoma
Trophoblastic differentiation
Giant cell
Lipid cell
Clear cell
Undifferentiated

Adapted from previously published literature (Chalasani et al., 2009)

Following the identification of variant histological patterns, urothelial bladder cancer has been classified into three major classes – squamous carcinoma, adenocarcinoma and small cell carcinoma. Squamous cell carcinoma (SCC) can occur in both Schistosomiasis/ bilharzia afflicted bladders (Godwin and Hanash, 1984) as well as in non-bilharzial bladders (Shokeir, 2004). Non-bilharzial SCC is primarily caused by chronic inflammation following urethral catheterisation of the bladder calculi. Schistosomiasis (also known as bilharzia), or even recurring urinary tract infection, can cause the bilharzial variant of SCC (Mostafa et al., 1999). Adenocarcinoma is another type of bladder cancer and exhibits characteristic growth patterns on the basis of which it has been further classified. These

histological classifications include enteric, mucinous, signet-ring cell, adenocarcinoma not otherwise specified, and mixed patterns (Dadhania et al., 2015). Adenocarcinomas tend to possess a papillary, nodular, flat or ulcerated architecture with some variants having the tendency to be more aggressive and recurring often (Roy and Parwani, 2011). Small cell carcinoma of the bladder (SCCB) is an aggressive form of bladder cancer which is usually diagnosed only at advanced stages (Ismaili, 2011). SCCB is a form of neuroendocrine tumour (NET) arising along the bladder epithelium (Ghervan et al., 2017). Given the limited case studies currently available on this form of bladder cancer, further research must be directed towards this variant so as to identify an appropriate treatment regime (Sehgal et al., 2010).

1.2.5 Staging, grading, diagnosis and symptoms of bladder cancer

Staging – Bladder staging is done using the American Joint Committee on Cancer's Tumour, Node and Metastasis (TNM) classification scheme (AJCC- TNM). Utilisation of this scheme is helpful in identifying the extent and scale of the disease at the time of diagnosis. Each bladder case identified is classified in terms of T (representing extent of tumour), N (representing metastasis towards the lymph nodes) and M (representing distant metastasis) (Youssef and Lotan, 2011). Identification of the 'T' stage is usually performed after examination of afflicted tissue following TURBT. The 'T' stage has been further subdivided into pTa (tumours confining the bladder lining only), pT1 (tumours occupying the lamina propria but not the muscularis propria), pT2 (tumours appearing in the muscularis propria), pT3 (tumours appearing in the perivesicular tissue) and pT4 (tumours spreading into other organs) (Kirkali et al., 2005). The 'N' & 'M' staging analyses are distinguished using either Computed Tomography (CT) scans or Magnetic Resonance Imaging (MRI) scans (Boustead et al., 2014).

Table 1.3 Bladder staging Node and Metastasis (TNM) classification.

Stage	Tumour	Lymph node involvement (N)	Metastasis (M)
Stage Ta	Ta: non-invasive papillary carcinoma	N0	M0
Stage Tis	Tis: Carcinoma in situ	N0	M0
Stage 1	T1: has grown into connective tissue	N0	M0
Stage 2	T2a: has grown into inner half of muscle layer	N0	M0
	T2b: has grown into outer half of muscle layer	N0	M0
Stage 3	T3a: microscopic invasion of surrounding fatty tissue	N0	M0
	T3b: macroscopically detectable invasion of surrounding fatty tissue	N0	M0
Stage 4	T4a: spread into prostate (men) and uterus (women)	N0	M0
	T4b: has grown into pelvic or abdominal wall	N0	M0

Any T	N1-3: lymph node involvement in proximal or distal lymph nodes	M0
	Any N: any lymph node involvement	M1: metastasis present

(N0 -no lymph node involvement; M0 - no signs of metastasis) adapted from previously published literature (Smolensky et al., 2016).

Grading - The World Health Organization/International Society for Urological Pathology (WHO/ ISUP) grading classification is standard globally (Epstein et al., 1998). Bladder neoplasms are graded as normal urothelial, hyperplastic urothelial (flat and papillary hyperplasia), flat lesions with atypia [reactive atypia, dysplasia, carcinoma in situ (CIS)] and papillary neoplasms (papilloma, papillary urothelial neoplasms of low malignant potential (PUNLMP), low-grade papillary carcinoma and high-grade papillary carcinoma) (Epstein et al., 1998).

Due to the heterogeneous nature of bladder cancer and the existence of several different histologic grades within the same tumour, appropriate intervention strategies can only be planned after performing histological grading. Urothelial carcinomas are graded as papilloma, low malignant potential (LMP), Grade 1, Grade 2 and Grade 3.

Diagnosis –Populations exposed to occupational hazards deemed to be at a high risk of developing bladder cancer should be screened for bladder cancer (Larre et al., 2013). Typical individuals deemed fit for screening have characteristic signs associated with bladder cancer development like haematuria and frequent voiding of urine. Tests used include bladder imaging, cystoscopy, urinalysis and cytology (Bangma et al., 2013).

Symptoms – The most common symptom of bladder cancer is haematuria (or blood in the urine). This symptom is present in the vast majority of cancers (Steiner et al., 2008). Other symptoms of bladder cancer include irritative urinary symptoms and urinary infections. Weight loss and abdominal pain are also common in metastatic forms of this malignancy. All these symptoms are associated with microscopic or macroscopic haematuria (Jewett, 1973).

1.3 Molecular biology of bladder cancer

Previous research has indicated the existence of several aberrant genetic pathways that eventually lead to the genesis of this malignancy. These aberrant pathways are deleterious either due to mutations in any of their individual genes or due to malfunctioning of their regulatory framework. Several such instances have been identified, e.g. in the tumour suppressor p16 (INK4A/MTS-1/CDKN2A) gene coding for cell cycle control (Liggett and Sidransky, 1998), KDM6A involved in chromatin regulation (Gui et al., 2011), and tyrosine kinases (Lu et al., 1997). Research has also revealed that these deleterious mechanisms are sometimes not confined to bladder cancer alone. For example, the basal and luminal forms of bladder cancer share similar gene expression signatures to those of breast cancer (Damrauer et al., 2014). Studies on bladder cancer specimens have also identified that the proto-oncogene HRas (GTPase HRas/ transforming protein p21) is associated with tumour recurrence (Burchill et al., 1994). Other genes linked to the development of bladder cancer include tuberous sclerosis 1 (TSC1) (Guo et al., 2013) and tumour protein p53 (TP53) (Ecke et al., 2008).

The development of bladder cancer through distinct pathways is a direct result of changes in the genetic code, whether through mutation, deletion or amplification. These modifications can either result in the formation of an aberrant protein or else change their expression profile along the bladder wall (Ayan et al., 2001, Cowan et al., 2016). Gene expression profiling has revealed the existence of four distinct groups/clusters of bladder tumours. Each of these has significantly different mutations and at times

separate morphologies (Cancer Genome Atlas Research, 2014, Seok Ju, 2017). Cluster I contains mutations leading to the presentation of papillary tumours that have altered FGFR3 and lowered expression of FGFR3 down regulators miR-99a and miR-10. Elevated expressions of GATA3, FOXA1, UPK3A and ERBB2 are characteristic of Cluster I and Cluster II. Cluster III are akin to basal/squamous tumours and have elevated expression of cytokeratins like KRT14, KRT5, KRT6A as well as EGFR. Cluster IV tumours lack any of the alterations present in the other groups and tend to be unique.

1.3.1 Genetic pathways that match clinical phenotypes

Modification of genetic pathways via genetic and epigenetic changes leads to carcinogenesis in the human bladder (Li et al., 2016). These aberrant alterations induced by accumulation or exposure to carcinogens cause abnormal tumorigenic cells to form at specific sites (Sadikovic et al., 2008). These sites, referred to as CIS or in situ neoplasms, develop into high-grade invasive tumours, which later metastasise (Zieger et al., 2009). While hyperplasia along the normal urothelium develops into low-grade non-invasive papillary tumours which recur often (Pasin et al., 2008); these in turn can develop into high-grade invasive tumours, which also later metastasise (Tuncer et al., 2014).

Genetic assessment has shown the presence of atypical signal transduction pathways that tend to be unique to each subtype (McConkey et al., 2015). Mutations in genes encoding for fibroblast growth factor receptor 3 (FGFR3) and epidermal growth factor (EGF) have been identified to match clinical phenotypes (van Rhijn et al., 2002, Dodurga et al., 2011). Aberrant expression of these genes has been identified to have a deleterious cascade effect along their signalling pathways resulting in clinical subtypes of bladder cancer (Rotterud et al., 2007, Chae et al., 2017).

1.3.1.1 Low-grade papillary urothelial carcinoma

Mutations of HRAS, FGFR3, hTERT promoter, STAG2, KDM6A (UTX) are most common in this bladder cancer phenotype (Haugsten et al., 2010, Poyet et al., 2015). DNA sequencing has revealed the methylation of tumour suppressor genes like Adenomatous Polyposis Coli (APC), ARF tumour suppressor (p14ARF) and Ras association domain family 1 isoform A (RASSF1A) (van der Weyden and Adams, 2007). Patients were also found to have elevated methylated sequences for apoptosis-related genes, like death-associated protein kinase (DAPK) (Christoph et al., 2006). Other tumour suppressor pathways, like the retinoblastoma (RB) and p53 signalling cascades, are inactivated while the Ras mitogen activated protein kinase (RAS-MAPK) pathway involved in cellular proliferation is activated (Sears and Nevins, 2002).

The inactivation and activation of the above-mentioned signalling cascades are not concurrent across all specimens examined, thus necessitating expression profiling of multiple pathways (Mitra et al., 2006). Alterations that induce these changes might occur at multiple sites and may be led by a combination of genetic and epigenetic changes at a number of sites across the genome (Kanwal and Gupta, 2012). These modifications might include alterations in oncogenes, single nucleotide polymorphism (SNP), tumour suppressor gene deletion or modification (Ye et al., 2014). This makes it imperative to use advanced molecular biological techniques, like DNA microarrays, on a much larger scale (Sanchez-Carbayo and Cordon-Cardo, 2003).

1.3.1.2 RAS-MAPK signal transduction pathway

A single signal transduction pathway, i.e. the RAS-MAPK, is perturbed at multiple levels in bladder cancer (Dangle et al., 2009). During the normal developmental processes, the RAS-MAPK signalling cycle regulates moieties, promoting an increased transcription of genes involved in cellular proliferation (Santarpia et al., 2012). Under aberrant conditions, as in tumour cells, increased activation of this

pathway leads to uncontrolled cellular proliferation (Dunn et al., 2005). Pathway activation occurs due to the binding of growth factors onto receptor tyrosine kinases, which induce receptor dimerisation and auto phosphorylation (Xing et al., 1996). This in turn causes modification of inactive Ras into its active form (Vetter and Wittinghofer, 2001). The activated Ras sets off a signalling cascade via three different signalling families; these include the extracellular signal-regulated kinase [ERK (the classical MAPK pathway)], c-Jun N-terminal Kinase/stress- activated protein kinase (JNK/SAPK) and p38 kinase (Zhang and Liu, 2002).

Activation of these MAPK pathways induces a physiological response, which includes cellular proliferation, differentiation and apoptosis (Johnson and Lapadat, 2002). Other physiological responses involve chromatin modelling, brought about by mitogen-activated and stress-activated protein kinase 1 (MSK1) (Deak et al., 1998). MSK1, a H3 kinase (Kim et al., 2008a), is a downstream target of the RAS-MAPK pathway and induces post-translational modification of histones along the chromatin, thus making it transcriptionally available for further downstream targets like c-Myc (a cell cycle deregulator) in the RAS-MAPK pathway (Sawicka and Seiser, 2012).

Activation of Ras is the prelude to a series of downstream events that eventually lead to the activation of the tumorigenic process in the human bladder. Prime activation moieties include mutations causing an overexpression of receptors in either FGFR or EGF receptor families (Naik et al., 2011, Guancial et al., 2014). Several other such factors exist along the same pathway including mutations in the Ras gene (Oxford and Theodorescu, 2003) or c-Myc (Schmitz-Drager et al., 1997). Silencing of the tumour suppressor RASSF1A (Dammann et al., 2003) via DNA methylation has also been reported to have an influence on the RAS-MAPK pathway activation (Chan et al., 2003). RASSF1A, meanwhile, acts as an antagonist towards RAS pathway promotion in normal tissue.

1.3.1.3 Fibroblast growth factor receptor 3 (FGFR3)

Mutations in FGFR3, a receptor tyrosine kinase, are common in bladder tumours. Originally identified in non-lethal skeletal disorders, it has been suggested that afflicted individuals could be prone to developing bladder cancer (van Rhijn et al., 2002). FGFR3 overexpression has been identified in low-grade papillary bladder tumours as well as in muscle invasive bladder tumours (Gust et al., 2013). Although identified to possess heterogeneous molecular target sites, FGR3 has been identified as a prime candidate for an adjuvant-based anti-FGF3 treatment (Pouessel et al., 2016). FGFR3 can also co-occur with PIK3CA mutations (Kompier et al., 2010) while it has been found to be limited to Ras mutations (Jebar et al., 2005). This has been proposed to be the reason why both FGFR3 and Ras present the same phenotype.

Immune staining of bladder tumour specimens has shown that tumour angiogenesis might be provoked by elevated FGFR3 expression (Bertz et al., 2014). Parameters such as micro vessel count (MVC), vascular surface area (VSA) and expression levels of Fibroblast Growth Factor (FGF) and Vascular Epithelial Growth Factor (VEGF) may be useful for prognosis of tumour angiogenesis (Dickinson et al., 1994). Meanwhile due to its expression in low-grade bladder carcinomas, FGFR3 mutations have been considered to be a predictive biomarker for use with tumour tissues and urinary isolates (Knowles, 2007). Examination of FGFR3 mutations in afflicted bladder specimens using comparative genomic hybridisation (CGH) has shown a low number of genetic alterations across tumour specimens (Junker et al., 2008).

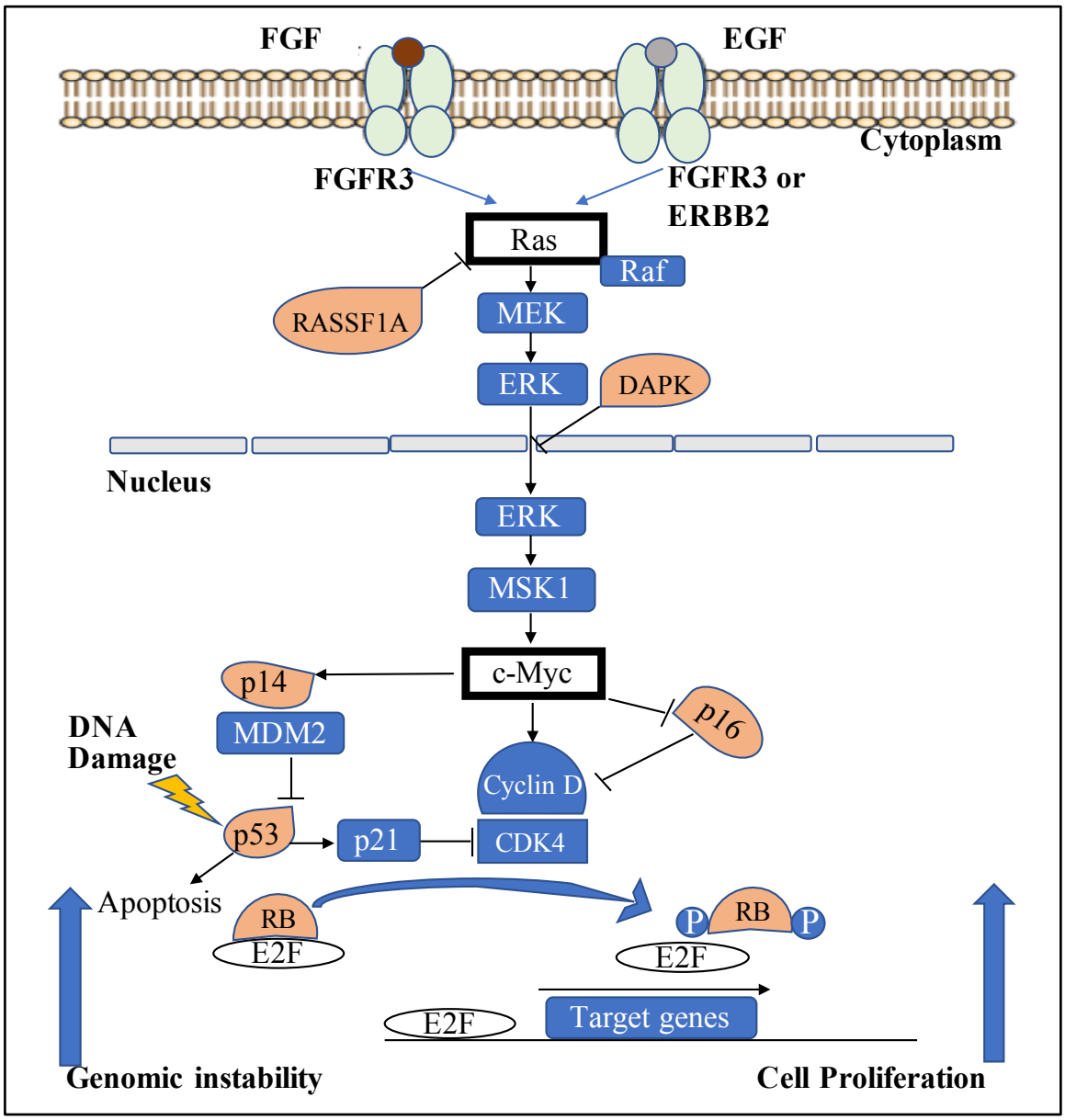

Figure 1.1 The processes (both genetic and epigenetic) driving bladder cancer oncogenesis.

Protein encoded by tumour suppressor genes, or with decreased expression, are presented in orange whereas protein encoded by oncogenes, or with increased expression, are presented in clear boxes with a black border. Redrawn and adapted from. EGF, epidermal growth factor; FGF fibroblast growth factor; FGFR3, fibroblast growth factor receptor 3; ERBB2, erythroblastic leukemia viral oncogene homolog 2; Ras, GTPase HRas; Raf, RAF proto oncogene serine/threonine-protein kinase; RASSF1A, Ras association (RalGDS/AF-6) domain family 1; MEK, MAPK/ERK kinase MSK1, mitogen-activated and stress-activated protein kinase 1 P, phosphorylated; DAPK, death-associated protein kinase; c-Myc, Myc proto-oncogene protein; CDK4, cyclin-dependent kinase 4; MDM2, p53-binding protein Mdm2; RB, retinoblastoma-associated protein; E2F, member of E2F family of transcription factors. Redrawn and adapted from (Wolff et al., 2005).

1.3.1.4 KDM6A/ UTX

Frequent modification of the telomerase (TERT) gene promoter has been identified as causing mutations in the histone lysine (K)-specific demethylase 6A (KDM6A)/ ubiquitously transcribed tetratricopeptide repeat, X chromosome (UTX) gene. These somatic alterations co-exist with the BRCA1 associated protein -1 (BAP1) gene mutations in afflicted bladder specimens (Nickerson et al., 2014). Resultant changes included modifications along the deubiquitinase active site and a loss of nuclear localisation signal, which in turn caused a loss of KDM6A signal resulting in a bladder cancer phenotype. A similar loss of the UTX gene expression in multiple myeloma (MM) specimens resulted in elevated proliferation, clonogenicity, adhesion and tumorigenicity (Ezponda et al., 2017). Next generation sequencing (NGS) on bladder specimens from high risk (HR) non-muscle invasive urothelial carcinoma (NMIUC) has revealed particularly upregulated levels of chromatin remodelling genes (Scott et al., 2017). The loss of KDM6A expression results in enhanced activity of Polycomb-repressive complex 2 (PRC2) containing the enzymatic subunit enhancer of zeste homologue 2 (EZH2) (Ler et al., 2017). PRC2 is a complex that mediates transcriptional silencing by methylation of lysine 27 of histone H3 using the EZH2 subunit (Kim and Roberts, 2016). With urothelial specimens exhibiting loss of KDM6A being dependent on EZH2 for cellular proliferation, an inhibition of EZH2 has been shown to delay in vivo onset of tumour growth (Ler et al., 2017) thus making EZH2 an ideal therapeutic target. Meanwhile, recent research has revealed a gender specific bias, with more mutations in the KDM6A gene in females than in males for non-invasive tumours (Hurst et al., 2017).

1.3.2 Muscle invasive bladder cancer (MIBC)

This variant of bladder cancer is particularly aggressive, with standard treatment options primarily involving radical cystectomy or radiation therapy (Gilligan et al., 2003), and can be caused by an assortment of factors such as missense mutations as in the case of Erb-B2 Receptor Tyrosine kinase 2 (ERBB2) (Groenendijk et al., 2016), loss of tumour suppressor genes such as TP53 (Wu et al., 1996)

and retinoblastoma 1 (RB1) (Pollack et al., 1997). With the development of advanced molecular biological and screening methodologies, several other genes and genetic mechanisms have been implicated in muscle invasive bladder cancer. These include:

1.3.2.1 Mutations of oncogenes and tumour suppressor genes

Oncogenes: Next generation sequencing and expression profiling tools have been utilised to identify mutations driving muscle invasive bladder tumours (Lerner et al., 2015). Up to 32 significantly mutated genes (SMG) have been identified, some of which are key drivers of cell cycle regulation, chromatin remodelling and DNA damage response (Lerner, 2015); these include CDKN2A, RB1, CREBBP, LRP1B, FOXQ1, and KDM6A. Other novel somatic mutations identified include those in RNA binding motif protein, HECW1, and zinc finger protein 271 (Pan et al., 2016). Knock down of the oncogene fibulin-3 (FBLN3/ EFEMP1), an extracellular matrix glycoprotein, has been identified to reduce the invasive potential of MIBC's in a murine model (Han et al., 2017). Somatic mutations, especially those observed in the gene Adenomatous Polyposis Coli (APC) (a tumour suppressor gene), and nuclear-b catenin accumulation, have been considered to be evidence for Wnt signal transduction pathway activity in bladder cancer oncogenesis (Kastritis et al., 2009).

Several techniques currently exist to identify lineage specific mutations in bladder tumours (Li et al., 2012). This has been particularly beneficial in identifying the existence of mutations and has enabled tumour characterisation into T-cell inflamed and non-T-cell inflamed tumours, on the basis of the tumour microenvironment. The non-T cell inflamed tumours have up regulated expression of tumour suppressor genes like PD-L1 (Kleinovink et al., 2017), IDO (Muller et al., 2010), and FOX-P3 (Wang et al., 2010), while T-cell inflamed tumours have activated pathways for β-catenin, PPAR-γ and FGFR3 (Sweis et al., 2016). The low T-cell receptor assortment, elevated neoantigen loads and high numbers of somatic mutation have all been identified to contribute to higher recurrence free survival (RFS) rates (Choudhury

et al., 2016). Somatic mutations in DNA repair genes also have prognostic value since carriers of these have been found to have significantly elevated RFS rates (Yap et al., 2014).

1.3.2.2 Chromosomal aneuploidy

Gain of function mutations associated with p53 function cause chromosomal instability, which in turn often results in aneuploidy (Santos et al., 2003). Identification of DNA aneuploidy is of prognostic value as an important predictor of tumour stage and overall disease progression (Puntoni et al., 2007). Fluorescence in situ hybridisation (FISH) studies have revealed the existence of both trisomy and tetrasomy in chromosome 7 and chromosome 17, while monosomy has been identified in chromosome 9 (Cézar et al., 2002). Elevated aneuploidy rates have not, however, been corroborated with the loss of tumour suppressor genes, e.g. Cohesion subunit SA-2 (STAG2) (Balbás-Martínez et al., 2013). Existing data suggests that bladder cancer disease progression results in peridiploid aneuploidy, doubling of DNA content as well as chromosomal loss (Shackney et al., 1995).

Whole genome sequencing of muscle invasive bladder tumours had previously shown a correlation between the tumour grade and the number of somatic mutations and copy number variations (Cazier et al., 2014). In addition, deep re-sequencing has revealed that there is an intra-tumour heterogeneity (ITH) between heterogeneous tumour subpopulations referred to as sub clones which could be evidence for a multifocal disease (Thomsen et al., 2017). The existence of such sub clones could be utilised to identify genetic drivers of muscle invasive bladder tumour and to distinguish unifocal disease (Yap et al., 2014). Characterisation of these unstable sub clones could also be utilised for monitoring clonal evolution so as to predict the predominant sub clone in the malignant tumour. These could also be utilised to plan therapeutic intervention strategies specifically designed to counter these recurring sub clones (Liu et al., 2017a). Prime targets for such intervention strategies include the neoantigens generated by such somatic alterations (Choudhury et al., 2016).

1.3.2.3 Viral oncogenesis

Chronic inflammation and viral transfection have been identified as potentiating factors in muscle invasive bladder cancer genesis. Schistosomiasis (Zaghloul, 2012) and urethral catheter induced trauma (West et al., 1999) have been identified as causing severe chronic inflammations. Although viral transcripts have been identified in bladder cancer specimens, their roles in oncogenic processes are not yet clear (Abol-Enein, 2008). Viruses identified as risk factors include human papilloma virus (Lopez-Beltran and Escudero, 1997), Epstein-Barr virus (EBV) (Abe et al., 2008), herpes simplex virus (HSV) (Badawi et al., 2010) and BK polyoma viruses (Fioriti et al., 2003). The frequent detection of viral transcripts in bladder cancer specimens could also be due to the homologies that exist, as was observed between the human bladder cancer EJ oncogene and the Harvey sarcoma virus ras gene (Parada et al., 1982). The ability of HSV type II to selectively induce tumour specific immunity has been suggested to be useful as an intravesicle therapeutic solution (Martuza, 2000). Recent research has also suggested the possibility of using alpha viruses like M1 to selectively eradicate bladder cancer cells (Hu et al., 2018).

1.3.2.4 RNA expression subtypes

Integrated genomic analysis had originally revealed the existence of four different expression subtypes in MIBC using RNA sequencing data (Cancer Genome Atlas Research, 2014). Later, a fifth expression sub-type was identified using unbiased Bayesian non-negative matrix factorisation (NMF) consensus clustering of a larger RNA sequencing dataset (Robertson et al., 2017). These expression subtypes include luminal, luminal-infiltrated, luminal-papillary, neuronal and basal-squamous; all of which were corroborated with cancer survival rates (Robertson et al., 2017). The identification of different expression subtypes has confirmed the need for patient stratification and treatment regimens for MIBC (Hurst and Knowles, 2014). The basal expression subtype of MIBC has enhanced p63 activation and squamous differentiation, while luminal subtypes has enhanced FGFR3 mutations and elevated

peroxisome activator pathway receptor (PPAR) activation (Choi et al., 2014). Meanwhile, whole transcriptome analysis has suggested that the basal expression subtype responds most to neoadjuvant chemotherapy (Seiler et al., 2017). MIBC's exhibiting a p53-like phenotype (Cordon-Cardo et al., 1994) exhibited elevated chemoresistance to neoadjuvant MVAC (Methotrexate Vinblastine Adriamycin Cisplatin) therapy (Choi et al., 2014). Cluster wise analysis of microarray data has revealed elevated expression levels of the markers CD44, Keratin 6B (KRT6B), Keratin 5 (KRT5), and Keratin 14 (KRT14) in basal subtypes. Luminal subtypes, meanwhile, have enhanced expression levels of the markers Uroplakin 3A (UPK3A), Uroplakin 2 (UPK2) and Uroplakin 1B (UPK1B) (Damrauer et al., 2014). This molecular stratification has been suggested as indicating an underlying susceptibility to tailor-made chemotherapeutic regimes (Sjodahl et al., 2012).

The luminal-papillary subtype was identified in tumours with papillary morphology while being enhanced with FGFR3 mutations. Specimens from this subtype had lowered carcinoma in situ (CIS) scores (Dyrskjot et al., 2004) while retaining sonic hedgehog signalling (SHH), indicating its development from a precursor non-muscle invasive bladder cancer (NMIBC) (Robertson et al., 2017). The luminal infiltrated subtype is discernible from the luminal variants of MIBC by lymphocytic infiltrates while demonstrating significant expression of smooth muscle and myofibroblasts (Robertson et al., 2017). Elevated expression levels of several markers like CD274 (PDL-1) and PDCD1 (PD-1) were apparent in this subtype, clarifying their responsiveness to anti-PDL-1 therapy (Rosenberg et al., 2016). Neuronal subtypes included tumours of both neuroendocrinal (NE) and non-NE origin. This subtype was characterised by the poor survival rates characteristic of aggressive neuroendocrine bladder cancers, as well as elevated expression levels of neuronal differentiation and developmental genes (Robertson et al., 2017).

1.4 Epigenetic changes in bladder cancer

1.4.1 Overview of the epigenetics of cancer

The term 'epigenetics' refers to the study of variations in the organism caused by alteration of gene expression in the absence of a concomitant change in the genotype (Ruden et al., 2003). In mammalian cells epigenetic modifications of gene expression may arise from changes in histone modifications, changes in DNA and RHAS methylation and from non-coding RNA expression (Chen et al., 2017). The accumulation of epigenetic changes leads to cellular reprogramming and the initiation of carcinogenesis (Sharma et al., 2010). Epigenetic changes in cell phenotypes are appealing therapeutic targets due to their reversible nature (Mair et al., 2014). Epigenetic changes may hinder normal development and tissue maintenance, however, and induce alterations in gene function causing malignancies. These epigenetic modifications are a key feature of cancer.

In contrast to aberrant somatic changes like gene mutations and copy number variations, epigenetic changes regulate gene expression without any change in the genetic code. Epigenetic changes modify the transcriptome leading to carcinogenesis and cancer progression (You and Jones, 2012). Conversely, epigenetic instability can be created through mutations to epigenetic regulator genes like DNA methyltransferases (Jin and Robertson, 2013), chromatin modifiers (Lunning and Green, 2015) and chromatin regulators. Expression profiling of bladder cancer tumours has revealed that a vast majority have mutations present in their chromatin regulatory genes e.g. KDM6A (Cancer Genome Atlas Research, 2014, Hurst et al., 2017). The genetic drivers of such heightened epigenetic dysregulation in bladder cancers require further investigation.

1.4.2 The role of DNA methylation

DNA methylation refers to the process by which a methyl group is added via a covalent reaction to the cytosine ring of a DNA molecule (Weissbach, 1993). The methylation event induced by DNA methyltransferases (DNMT) occurs at the C5 position of 5'-CG-3' dinucleotides (CpG) (Singal and Ginder, 1999). In mammals, the majority of the DNA methylation occurs at CpG sites; in embryonic stem cells, however, (ESC) methylation events occur along non-CpG sites (Lister et al., 2009). Methylated CpG sites are susceptible to deamination into uracil, resulting in a genome short at these sites; the exception being the strands of nucleotides referred to as 'CpG islands' (CGI), which contain the expected CpG content and are mostly unmethylated (Takai and Jones, 2002). Methylation of CpG sites along a gene's promoter sequence causes gene silencing (Jones and Liang, 2009) while CGI's along actual gene sequences is linked to gene expression (Yang et al., 2014).

CpG methylation is primarily catalysed by DNA methyltransferase 1 (DNMT1), DNMT3A and DNMT3B. Continued DNMT1 expression is essential for preserving methylation levels and in turn preventing mitotic defects during tumorigenesis, thus accounting for tumorigenic potential (Chen et al., 2007). While DNMT1 provides for the continuous methylation activity along repetitive sequences, methylated sequences have increased levels of partially methylated DNA. These sites undergo de novo methylation brought about by DNMT2A and DNMT3B, thereby ensuring maintenance (Liang et al., 2002).

Upregulated DNMT1 expression is linked to reduced patient survival rates, while downregulation of the same causes reduced tumour outgrowth and elevated radiosensitivity (Wu et al., 2011). Population studies have revealed DNA hypomethylation to be a characteristic biomarker for bladder cancer susceptibility; this is due to its ability to promote genomic instability and elevate cancer risk (Moore et

al., 2008). Moreover, increased methylation frequencies of the genes CDH1, RASSF1A, APC and CDH13 are linked to elevated methylation index (MI), an indicator of poor bladder cancer prognosis.

DNMT1 expression and DNA methylation maintained by phosphatidylinositol 3-kinase/protein kinase B pathway observed in MIBC (Sun et al., 2007). In muscle invasive bladder cancer (MIBC), down regulation of the B-cell translocation gene 2 (BTG2) was found to cause an increase in DNMT1 and DNMT3A transcription; this caused a spike in methylation levels and has been reported to account for the invasive potential of MIBC compared to non-muscle invasive bladder cancer (NMIBC) (Devanand et al., 2014). A potential inhibitor of these enzymes is the flavonoid compound kaempferol, which modulates DNMT3B degradation (Qiu et al., 2017). Another possible antagonist of DNMT activity is zebularine, which prevents sustained remethylation and gene resilencing (Cheng et al., 2004).

1.4.3 DNA hydroxymethylation

The epigenetic mechanisms involved in the evolution of bladder cancer may not just be restricted to DNA cytosine methylation. Following modification of the cytosine moiety into methylcytosine (5mC), an oxidative step could cause its demethylation into 5-hydroxymethylcytosine (5hmC). This conversion is catalysed by dioxygenases belonging to the ten-eleven translocation (TET) family of genes like TET1, TET2 and TET3 (Kriaucionis and Heintz, 2009, Tahiliani et al., 2009). This demethylation step could also occur following DNA replication in the absence of DNMT's (Guibert and Weber, 2013). The 5hmC molecule is then transformed into 5-formylcytosine (5fC) and 5-carboxylcytosine (5caC) by TET enzymes (Ito et al., 2011). The covalent bonds in this 5fC molecule give it a unique ability to alter the structure of the DNA helix and nucleosome positioning via histone-DNA interactions (Raiber et al., 2015). Cleavage of the covalent C-C bond of 5fC residue results in it being switched with an unbound cytosine (Iwan et al., 2018).

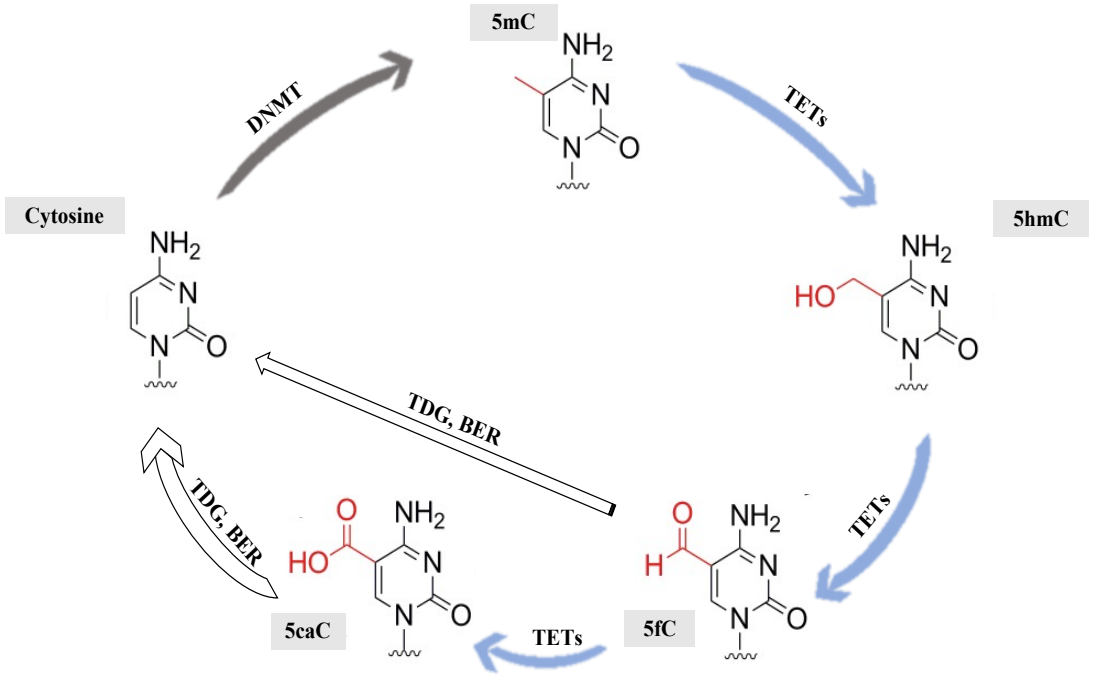

Figure 1.2 Cytosine methylation catalysed by DNMT and TET proteins.

DNA methyltransferase (DNMT) catalyses Cytosine at the C5 position inducing methylation. The 5-methylcytosine (5-mC) demethylation process occurs through oxidation by ten eleven translocation (TET) proteins which convert 5-mC into 5-hydroxymethylcytosine (5-hmC), 5-formylcytosine (5-fC) and 5-carboxylcytosine (5-caC). Thymine-DNA glycosylase (TDG) can identified and cleaved to both 5-fC and 5-caC via the base-excision repair pathway thereby restoring the unmethylated cytosine. Redrawn and adopted from (Xing et al., 2013).

Hydroxymethylation is common in many tumour suppressor genes, like POU Class 4 Homeobox 2 (POU4F2) and protocadherin 17 (PCDH17). Non-invasive techniques like urine sediment analysis are recommended over invasive procedures like cystoscopy for detecting hypermethylation levels in bladder cancer patients. Combinatorial approaches featuring both sediment analysis and quantitative methylation-specific-PCR (qMSP) could be utilised for screening for bladder cancer (Wang et al., 2016). qMSP has also been proven to be effective for the estimation of hypermethylation amongst promoter regions of other tumour suppressor genes, like RASSF1A and APC, allowing early detection and monitoring of bladder cancer (Hoque et al., 2006).

1.4.4 Chromatin remodelling - Histone modifications

Histones are key conserved sequences of genetic material which when bound together as an octamer form the nucleosome. Multiple units of such nucleosomes together form the chromatin (Luger et al., 1997). In addition to DNA methylation, post-translational modification of histone tails, such as glycosylation (Lakatos and Jobst, 1989), sumoylation (Shiio and Eisenman, 2003), ubiquitylation (Cao and Yan, 2012), and carbonylation (Garcia-Gimenez et al., 2012), changes their configuration. Histone modification events are either a locally acting chromatin event (Qiang et al., 2011) or occur on a widespread scale (Schubeler et al., 2004). The detection of such global histone methylation events (to histones H3K9 and H3K27) using tissue microarray has been utilised to predict tumour prognosis in bladder cancer (Ellinger et al., 2014). Trimethylation of histone H4K20 has been associated with invasive bladder cancer and its presence is crucial when recommending adjuvant therapy (Schneider et al., 2011).

1.4.5 MicroRNA's

These are small non-coding RNA sequences that act as epigenetic regulators via post-translational modification of gene expression, often via down regulation (Dweep et al., 2011). MicroRNA's are initially transcribed into primary miRNA (pri-miRNA) in the nucleus by RNA polymerase II (Han et al., 2004) and then into hairpin shaped precursor miRNA (pre-miRNA) by the enzyme drosha (Han et al., 2004). It is then transported into the cytoplasm where it is modified into single stranded miRNA's by enzymes like dicer (Koscianska et al., 2011). On attaining its active form, it enters into the miRNA silencing complex (miRISC) and starts to trigger mRNA degradation (Mah et al., 2010). mRNA silencing occurs following miRNA's binding to the 3' untranslated region (UTR) of mRNAs (Didiano and Hobert, 2008).

1.5 Cell surface markers for bladder cancer

Epithelial and stromal cells within a bladder tumour are heterogeneous but exhibit a homogenous morphology and express numerous cell surface markers (Liu et al., 2012). This intratumoral heterogeneity arises due to the selective pressure exerted by genetic and epigenetic changes during tumour evolution (Chan et al., 2009). Comparative transcriptome analysis can be used to identify panels of differentiation (CD) markers (Welby et al., 2017) that could sort bladder cancer types, including stem cells (Liu et al., 2012). Several bladder cancer cell surface markers have been identified, including CD104 (Liu et al., 2012), CD44 (Wu et al., 2017), CD49f (Santos et al., 2017), CD90 (Takeuchi et al., 2016). Identification of cell surface markers specific for cancer stem cells could be utilised to design therapeutic strategies aimed towards resolving cancer (Medrano et al., 2017).

A tumour initiating cell subpopulation has been sorted from primary bladder cancer cells using cell surface markers $CD44^{+}CK5^{+}CK20^{-}$. On further transplantation as xenograft tissue these cells were able to regenerate into a heterogeneous tumour markedly similar to the original tumour (Chan et al., 2009). Meanwhile an activated gene signature similar to aggressive bladder cancer was observed in microarray analysis of gene expression (Chan et al., 2010). Subsequent research done to select urothelial cancer cells for cisplatin resistance suggests that the utility of CD90 as a cancer stem cell marker is not exact. This could be because of the existence of phenotypic plasticity contributing towards the absence of CD90 marker in cell lines exhibiting all tumour subpopulation characteristics (Skowron et al., 2015). Similar research has also shown that bladder cancer cells can be classified into three distinct subtypes characterised by the expression of the cytokeratins – keratin 20 (KRT20), keratin 5 (KRT5) and keratin 14 (KRT14) (Volkmer et al., 2012).

Summary

Molecular studies have investigated the heterogeneity of bladder cancer and characterised it into molecular subgroups, either by RNA expression or cell surface markers. This necessitates growing cells from fresh bladder tumour biopsies in order to obtain primary epithelial cells in culture. This has been a particularly challenging task for scientists, however. Previous research has characterised various differentiation states in bladder cancer by sorting specific cell surface markers. Although this approach has been well studied, the underlying epigenetic changes in these subpopulations is yet to be fully investigated. Similarly, 5hmC residues in bladder cancer have not yet been explored on the basis of quantitative sequencing at a single base resolution using DNA methylation array. To bridge these gaps in awareness regarding bladder cancer heterogeneity the following hypotheses and aims were proposed for this research:

Hypotheses

That primary tissue cultures of bladder cancer cells could serve as ideal models to examine unique characteristics.

That distinct subpopulations exist in bladder cell lines and tissues.

That discrete variations exist in the cytosine residues of the methylome of normal and bladder tumour tissues.

Aims

- To develop a primary tissue culture protocol for malignant urothelial tissues using different serum free media and techniques aiming to collect/retrieve bladder stem cells.
- To sort distinct bladder subpopulations using cell surface markers CD44, CD47, CD49f and CD90 via Fluorescence-Activated Cell Sorting (FACS).

- To investigate the epigenetic profile of 5hmC in normal and malignant bladder tissue by using the new oxidative bisulfite sequencing (OXBS), which allows quantification of 5hmC sites through Illumina Infinium HumanMethylation450K array.
- To ascertain the differences in methylation level between BS and OXBS sequencing.
- To correlate the methylation level with publicly available normal bladder and matched bladder tumour gene expression data from the cancer genomic atlas (TCGA).
- To explore 5hmC sites in a distinct bladder subpopulation using a qPCR detection technique.

CHAPTER TWO

2 MATERIALS AND METHODS

2.1 Patients and Tumour Samples

2.1.1 Ethics statements

Fresh and frozen tissue specimens were isolated after approval was obtained from the local Research Ethics Committee (Investigation of Molecular Instability in the Pathogenesis of Urothelial Cancer, STH 15574). Written consent was obtained prior to specimen excision and collection from bladder cancer patients. Collected specimens were analysed anonymously. During the tissue collection process both healthy and afflicted bladder tissue were collected and secured. Guidelines used during the tissue collection process were in accordance to the principles set out in the Declaration of Helsinki. The usage of tissue specimens was in compliance with the Human Tissue Act, 2004.

2.1.2 Patient samples

A total of 78 bladder specimens were freshly isolated from patients who were under surgical treatment at the Royal Hallamshire Hospital, Sheffield, UK. An experienced histopathologist performed tumour sampling and sectioning. Tissue samples that needed to be cultured or sorted were collected in a sterile medium; tumour tissue samples meanwhile were stored immediately at -80°C for molecular analysis later or DNA extraction. In addition, normal tissues were collected from healthy individuals who had undergone surgical removal of prostate (radical prostatectomy) and was then stored at -80°C for future use. Details of all cases examined in this study are summarised in Appendix 1.

2.2 Materials

2.2.1 General Laboratory Equipment and Consumables

Tables below contain the general equipment, consumables and chemicals that were used in this study. The materials and reagents which are method-specific are described in the subsequent sections.

Table 2.1: Laboratory Equipment

Product	Company
Agarose gel electrophoresis	Apollo Instruments
Benchtop centrifuge - eppendorfs	Fisher Scientific
Biological safety cabinet	Forma Scientific
FACSAria™ III cell sorter	Becton Dickinson
Haemocytometer	Hawksley
Heat block	Grant Instruments
Ice machine	Scotsman
Incubator – tissue culture	Sanyo
Inverted microscope	Nikon Instrument
Nanodrop 2000 system	Thermo Scientific
Pipette aid	Drummond
Pipettes	Gilson
Power pack	Bio-Rad
Thermal cycler	Applied Biosystem
UV transilluminator	Bio-Rad
Vortex	Fisons Scientific Equipment
Water baths	Grant Instruments

Table 2.2: Laboratory Consumables

Product	Company
Centrifuge tubes – 15 ml	Corning
Centrifuge tubes – 25 ml	Sarstedt
Centrifuge tubes – 50 ml	Fisherbrand
Cryovials	Nalgene
Culture plates - 6 well	Cellstar
Eppendorf tubes - 0.5 ml and 2 ml	Sarstedt
Eppendorf tube– 1.5 ml	Greiner bio-one
Filter pipette tips	StarLab
Gel loading tips	StarLab

Latex examination gloves	Schottlander
Plastic disposable pipettes	Fisherbrand
Refill pipette tips	StarLab
Sterile petri dishes	Corning
Sterile plastic syringes	Becton Dickinson
Sterile scalpels	Swann Morton
Tissue culture flasks - T25 and T75	Thermo Scientific
Tissue culture sterile petri dish	Corning

Table 2.3: Laboratory Chemicals

Product	**Company**
Agarose powder	Fisher Scientific
Bovine serum albumin	Sigma-Aldrich
Ethanol	Fisher Scientific
Ethidium bromide	Sigma-Aldrich
Iso-Propanol	Fisher Scientific
Methanol	Fisher Scientific
Methylene blue	Sigma-Aldrich
Sodium chloride	Fisher Scientific
Tris-base	Fisher Scientific

2.2.2 Cell Culture Materials and Reagents

Established cell lines: Two established cell lines have been used in this study, the EJ cell line, from invasive bladder carcinoma cells and the RT112 cell line from transitional cell carcinoma. Both were purchased from the American Type Culture Collection (ATCC) at the start of the project.

Subpopulation cell lines: EJ serves as the original population for all subpopulation cell lines. These are D4 and G7, which is a single cell-derived colony obtained from the original EJ cell line.

Cisplatin resistance cell line: The EJ-R cell line was developed from the EJ cell line after treating the cells for a prolonged period until they became resistant to cisplatin.

Dulbecco's Modified Eagle's Medium (DMEM) (Lonza): The medium contains (4.5 gm/ l) glucose and L-glutamine. To maintain established cell lines in culture, the medium was supplemented with 10% foetal calf serum (FCS) (Lonza), (100 µg/ml) penicillin (Lonza) and (100 µg/ml) streptomycin (Lonza).

Phosphate buffer saline (PBS) (FisherFisher Scientific): Available in tablet form, with each tablet being dissolved in 100 ml of deionised water. The resulting solution was then autoclaved at 121 °C for 15 minutes prior to use.

Dimethyl sulphoxide (DMSO) (Sigma Aldrich): DMSO was added to cell culture media prior to freezing cultured cell lines to prevent cell desiccation or rupture.

The trypsin-versene/EDTA mixture (Lonza-BioWhittaker): It has 0.5 g/L trypsin and 2.0 g/L versene/EDTA. It was stored at -20 °C and was warmed to 37 °C before use.

2.2.3 Primary Tissue Culture Materials

Table 2.4 Culture media and their components

Medium Name	Component (CONC)	Supplier
Dulbecco's Modified Eagle's Medium (DMEM)	(FCS) (10%) Penicillin (100 µg/ml) Streptomycin (100 µg/ml) Non-essential amino acids (5 ml)	Lonza
Hank's Balanced Salt Solution (HBSS)	Mg2+ and Ca2+ Kallikrein inactivating units (KIU) (20 units) Penicillin (100 µg/ml) Streptomycin (100 µg/ml)	Gibco
Stem-Pro Human Embryonic Stem Cells (hESCs)	DMEM/F12 + GlutaMAXTM-I Stem-Pro hESCs Supplement Bovine Serum Albumin (25%) Fibroblast Growth Factor (FGF) (10 µg/ml) 2-Mercaptoethanol (55 mM)	Gibco

EpiLife Medium	Calcium (6 0 μM) Bovine Pituitary Extracts (BPE) (25 μg/ml) Epidermal Growth Factor (EGF) (0.5 ng/ml) (3 mM) glycine (1%) Non-Essential Amino Acids (1%) Insulin-Transferrin-Selenium (ITS) (1%) FCS (1%) Penicillin and Streptomycin (100 μg/ml)	ThermoFisher Scientific
Keratinocyte serum-free medium (KSFM)	Epidermal Growth Factor (EGF) (5 ng/ml) Bovine Pituitary Extracts (BPE) (50 ng/ml) Penicillin and Streptomycin (100 μg/ml)	ThermoFisher Scientific

Table 2.5 Enzymes and materials used in primary tissue culture

Enzymes/Materials	**Supplier**
Stem Pro Accutase	ThermoFisher Scientific
Liberase DH (5 mg)	Roche
bFGF fibroblast growth factor-basic	Invitrogen
0.1 mM 2-mercaptoetha-nol	Life Technologies
Falcon™ Cell Strainers (70 μm)	BD Biosciences

2.2.4 Human Tumour Dissociation Materials

The human tumour dissociation kit (Miltenyi Biotec) was comprised of dissociation enzymes, gentleMACS™ dissociator, MACSmix™ tube rotator, gentleMACS C tubes, and MACS smartstrainers. The GentleMACS™ dissociator is an automated machine that comes with pre-defined programs and was used to obtain single-cell suspensions by using GentleMACS C tubes. MACSmix™ is a tube rotator with a versatile application that can be used at temperatures ranging from 2-42 °C. GentleMACS C tubes were used to bring about the dissociation of cells while maintaining a safe and sterile environment for

the sample. MACS smartstrainers have a size of 70 µm and were used to obtain a single-cell suspension from cell aggregation or large particles.

2.2.5 Flow Cytometry Materials

Table 2.6: List of reagents used in flow cytometry

Reagent	Supplier
Cell staining buffer	BioLegend
10X Red Blood Cell (RBC) Lysis buffer	BioLegend
LIVE/DEAD™ Fixable Dead Cell Stain	ThermoFisher Scientific

Table 2.7: List of antibodies used in the study and their characteristics

Antibody	Isotype	Reactivity	Supplier
Phycoerythrin (PE) anti- human CD47	Mouse IgG1,κ	Human	BioLegend
Allophycocyanin (APC) anti- human CD44	Mouse IgG1,κ	Human	BioLegend
PE anti-human CD90 (Thy1)	Mouse IgG1,κ	Human	BioLegend
PE anti- human/mouse CD49f	Rat IgG2a,κ	Human, Mouse	BioLegend

2.2.6 DNA Extraction Materials

A DNeasy® Blood and Tissue Kit (Qiagen) was used to extract DNA and comprised of Tissue Lysis Buffer (Buffer ATL), Proteinase K, Wash Buffers (Buffers AW1 and AW2), Lysis Buffer (Buffer AL), , Elution Buffer (Buffer AE), collection tubes and DNeasy® mini spin columns.

2.2.7 True Methyl Array Materials

The materials used for this analysis were purchased from CEGX Cambridge Epigenetic, and included:

Purification and denaturation reagents and other equipment*:*

- Binding Buffer 1, stored at 2-8 °C.
- Binding Buffer 2, stored at 2-8 °C.

- Magnetic Bead Solution, stored at 15-25 °C.
- Denaturing Solution, stored at 15-25 °C.
- HPLC Grade 100% Acetonitrile, stored at 15-25 °C.

Oxidation reagents:

- Oxidant Solution, stored at -20 °C.
- Ultra-Pure Water, stored at 15-25 °C.

Bisulphite conversion reagents:

- Bisulphite Reagent Aliquot.
- Bisulphite Diluent.
- Bisulphite Additive.
- Desulfonation Buffer Concentrate.
- Elution Buffer.

All stored at 15-25 °C.

Digestion control enzymes:

- Digestion Control.
- Digestion Control FWD PCR Primer.
- Digestion Control REV PCR Primer.
- Cutting Control DNA.

All stored at -20 °C.

Other reagents, equipment and kits used:

- Uracil tolerant DNA polymerase (KAPA HiFi Uracil).
- 10X TaqαI Buffer.
- TaqαI Restriction Enzyme.
- 100x BSA.

All stored at -20 °C.

- **GeneJET ™ PCR Purification Kit** (ThermoFisher Scientific).
- **Qubit® Fluorometer machine** (Life Technologies™) was used with ssDNA and dsDNA measurement dyes.
- **Magnetic Separation Rack**.
- **PCR Thermos Cycler Bench Top Machine**.

2.2.8 Gel-electrophoresis materials

All components below were used for performing gel electrophoresis.

Agarose Gel: Agarose powder (ThermoFisher Scientific) was used for the casting of the gel, which was used as a medium for separating DNA.

50X TAE Buffer: 10x Tris-Acetate-EDTA (TAE) buffer was diluted 1 in 5 from 50X TAE stock solution running buffer before use. Stock solution was prepared by dissolving 242 gm of Tris base and 18.6 gm of EDTA to approximately 700 ml of distilled water. Then, 57.1 ml of Glacial acetic acid was added, and the volume was adjusted to 1000 ml. The solution was stored at room temperature.

Electrophoresis unit: The unit components include a gel casting tray (15 x 7 cm), sample comb (for 25 samples) and electrophoresis tank (Geneflow).

Ethidium bromide (Sigma): 1 gm of ethidium bromide of was dissolved in 100 ml distilled H_2O to prepare 10 mg/ml ethidium bromide solution. The solution was wrapped in foil and stored at 4 °C.

DNA ladder (**Promega):** 1 KB DNA ladder was used, it was stored at 4 °C before use.

Loading buffer: 6X loading buffer was prepared by mixing 25 mg bromophenol blue in 3 ml glycerol and the final volume was brought up to 10 ml by adding distilled water. The prepared solution was stored at 4 °C.

2.2.9 Illumina 450K BeadChip Array Materials

Table 2.8: List of reagents provided in Illumina 450K BeadChip Array kit

Reagent	Description
ATM	Anti-Stain Two-Colour Master Mix
FMS	Fragmentation solution
MA1	Multi-Sample Amplification 1 Mix
RPM	Random Primer Mix
MSM	Multi-Sample Amplification Master Mix
PB1	Reagent used to prepare BeadChips for hybridisation
PB2	Humidifying buffer used during hybridisation
PM1	Precipitation solution
RA1	Resuspension, hybridisation, and wash solution
STM	Superior Two-Colour Master Mix
TEM	Two-Colour Extension Master Mix
XC1	XStain BeadChip solution 1
XC2	XStain BeadChip solution 2
XC3	XStain BeadChip solution 3
XC4	XStain BeadChip solution 4
0.4 N NaOH	Stored at 2-8 °C before use

Equipment used for array

- Multi-Sample BeadChip Alignment Fixture.
- Illumina Hybridisation Oven Scanner.
- Hybridisation Gasket Slide.
- Hyb Chamber Inserts.
- MSA4 Plate.

2.2.10 Quest 5-hmC Detection Kit Materials

Enzymes

- 5-hmC Glucosyltransferase (2 units/µl).
- 10X UDPG (Uridine Diphosphoglucose) [1 mM].
- 10X 5-hmC GT Reaction Buffer.
- MspI Restriction Enzyme (10 units/µl).
- Quest 5-hmC Control DNA.
- Quest qPCR Primers 1 & 2 [20 µM].

All stored at -20 °C.

DNA clean and concentrator TM - 5

- DNA Elution Buffer.
- DNA Wash Buffer.
- DNA Binding Buffer.
- Collection Tubes.
- Zymo-SpinTM Columns.

All stored at 15-25 °C.

Other enzymes and reagents used:

- QuestTaq qPCR PreMix.
- Locus Specific qPCR Primers (forward/reverse).
- DNase/RNase- Free H_2O.

All stored at -20 °C.

2.3 Methods

2.3.1 Cell culture methods

Mammalian cell culture

Tumour cells were maintained as monolayers in full culture media, e.g. Dulbecco's Modified Eagle's Media (DMEM). They were supplemented with 10% foetal calf serum (FCS) and 5 ml of non-essential amino acids (NEAA). The cultured cells were allowed to grow in an incubator at a temperature 37 °C with 5% CO_2 and a relative humidity of 95% air atmosphere. Cells were harvested in a T75 flask and were brought to 50-70% confluence prior to being utilised in any of the assays. When the confluence of the cells reached 80-90%, they were transferred to a new T75 flask in order to continue the logarithmic growth phase. Then, cell passaging was performed using 10 ml PBS for removal of cellular debris. Next, the cells were incubated at 37 °C for 3-5 minutes in the presence of 2 ml of trypsin in order to detach the cells. Then, 10 ml of media was added to the T75 flask to inactivate the trypsin. After that, the detached cells were collected and centrifuged at 2,000 rpm for 3 minutes and the supernatant was discarded. 15 ml of fresh culture medium was added to the pellet and then transferred into a new T75 flask. A sterile working environment was maintained by carrying out all cell culture work in a safety laboratory cabinet (Sanyo). The cabinet was always cleaned with industrial methylated spirit (IMS) before and after use to prevent contamination. Also, mycoplasma testing was routinely performed to ensure that there was no contamination in the cell lines used in this study.

Freezing and thawing of cells

Preserving the cells for the long term by freezing them does not affect the stability of the cells in culture. Cells to be frozen were trypsinised and resuspended as mentioned above and then transformed into pellet form by centrifuging at 2,000 rpm for 3 minutes and again resuspending them in a fresh culture medium with 10% DMSO. 1 ml aliquots of the same cells were preserved by transferring them into cryovials and cooling them slowly to -80 °C. Aliquots of these cells intended for long-term storage were stored in

liquid nitrogen. Cells present in frozen aliquots could then be transferred into 10 ml of fresh culture medium and pelleted via centrifugation after being thawed at room temperature as described above. The cells were then resuspended in 10 ml of fresh media to allow them to recover and then transferred into a new flask. Both the freezing and thawing steps had to be carried out rapidly to avoid the toxic effects of DMSO.

2.3.2 Primary tissue culture methods

The three methods that were used are detailed below:

Explant method

The explant method described previously was used to obtain cells from tissue. A small tissue sample was obtained by gently scraping the urothelial portion of the specimen. The isolated cells were then placed on a sterile petri dish with a few drops of culture media. The solution was later made up to 10 ml with culture media and then centrifuged at 1000 rpm for 5 min at room temperature. The isolated cells were collected as pellet and resuspended in 7 ml of fresh media and subsequently transferred to T25 flasks. The same was then placed in an incubator at 37 °C with 5% CO_2 at a relative humidity of 95%. The culture media was changed at intervals of 2-3 days as required (Hendijani, 2017).

Stripping HBSS method

The stripping HBSS method was used to chemically disaggregate the tumour tissue. Specimens were left in an incubator at 37 °C with 5% CO_2 and a relative humidity of 95% for 4 hours in 15 ml of HBSS (without Mg^{2+} and Ca^{2+} ions medium). The HBSS contained 1% EDTA (ethylenediaminetetraacetic acid, disodium salt) solution, 1 M HEPES (4-(2-hydroxyethyl)-1-piperazineethanesulfonic acid*)* and 20 KIU/ml aprotinin. After the incubation, the urothelial part was mechanically disaggregated and prepared for tissue culture by placing it in a T25 flask containing 10 ml of fresh media.

CTOS method

Primary culture of the cells was done by following the Cancer Tissue Originated Spheroid (CTOS) method (Kondo et al., 2011). In this method, the tissue sample was placed in a 50 ml centrifuged tube with 20 ml of DMEM which was supplemented with 100 µg/ml penicillin and 100 µg/ml streptomycin. Tissue culture was performed immediately after tumour resection or biopsy, or stored at 4 °C until initiation of the CTOS method.

The DMEM medium was discarded and the sample was washed with 20 ml HBSS that contained Mg^{2+} and Ca^{2+}. The wash step was performed by inverting the tube. The HBSS wash solution was discarded and 20 ml of fresh HBSS was added. Then the HBSS medium and samples were transferred to a 10-cm tissue culture dish. The necrotic tissues were removed by using forceps and razor blades and then the remaining sample was transferred to a new 10 cm tissue culture dish with 30 ml HBSS. The tissue was minced with forceps or razor blades into small pieces. The sample with media was transferred to a 50 ml centrifuge tube and centrifuged at 1000 rpm at 4 °C for 5 minutes. The supernatant was discarded and the sample washed with 20 ml fresh HBSS by inverting the tube. The wash step was repeated by performing centrifugation at 1000 rpm at 4 °C for 5 minutes. Again, the supernatant was discarded and the sample washed with HBSS solution. The pellet was collected and resuspended in 20 ml DMEM which was supplemented with 100 units/ ml penicillin, 100 µg/ ml streptomycin, and 0.28 units/ ml Liberase DH. The digestion mixture was then transferred to a 100 ml sterile conical flask. The digestion of the sample was performed by frequent stirring for 2 hours in a 37 °C water bath. Then, the digestion media was transferred to 50 ml centrifuge tube and centrifuged at 1000 rpm at 4 °C for 5 minutes. After that, the media was discarded. Next, the washing step was performed by adding 20 ml HBSS and inverting the tube. The samples were filtered through a 500 µm stainless-steel wire mesh and then the filtrate was transferred to a 50 ml centrifuge tube. The sample was again filtered through a 70 µm cell strainer in a 10 cm tissue culture dish containing 30 ml HBSS medium. This meant that organoids sized >70 µm remained in the cell strainer and these were collected using a pipette and then centrifuged at

1000 rpm at 4 °C for 5 minutes. The sample was washed with 20 ml HBSS by inverting the tube and centrifuging at 1000 rpm at 4 °C for 5 minutes and the HBSS solution was then discarded. 4 ml serum-free stem cell medium supplemented with 0.1 mM 2-mercaptoethanol, 8 ng/ml bFGF, 100 µg/ ml streptomycin, 100 units/ml penicillin and 25 µg/ml amphotericin B was added to both the organoids and filtrate and then were transferred to a 6 cm nontreated dish and incubated at 37 °C with 5% CO_2 at a relative humidity of 95 % for 24 h. Then, both organoids and filtrate were observed under a microscope.

2.3.3 Tumour dissociation methods

Tumour dissociation was used to obtain single tumour cells from the solid tumour tissue for subsequent culture and characterisation. Tumour dissociation is dependent on successful disruption of the extracellular matrix, which is achieved mainly by enzymatic degradation.

Preparation of enzymes:

Enzyme H was prepared by dissolving lyophilised powder of enzyme H vials in 3 ml DMEM and was filtered prior use.

Enzyme R was prepared by dissolving the lyophilised powder in 2.7 ml DMEM.

Enzyme A was prepared by dissolving with 1 ml of buffer (A) that was provided with the kit.

All enzymes were prepared in aliquots and stored at -20 °C.

Tumour dissociation steps:

Following the manufacturer protocol provided by Miltenyi Biotec, excised tumour specimens were spliced into 2-5 mm pieces. Necrotic, fat and fibrous areas were then removed. The shortened sections were then transferred to a gentleMACS C Tube that contained a mixture of all three enzymes. The C tube was inverted and attached onto the sleeve of the dissociator and the program h_tumor_01 was run. At the end of this program, the specimens were incubated for 30 minutes at 37 °C. Meanwhile using the MACSmix Tube Rotator was used for continuous rotation. Again, the C tube was attached onto the

Dissociator and this time the program h_tumor_02 was run. Then, the sample was incubated for 30 minutes at 37 °C and the MACSmix Tube Rotator was used for continuous rotation during the incubation. Then again, the C Tube was attached onto the Dissociator and this time the program h_tumor_02 was once again run. A short centrifugation process was performed at 1,000 rpm at room temperature which yielded the sample as a pellet at the bottom of the tube. This pellet was resuspended and filtered to SmartStrainer MACS (70 μm) that was placed in a 50 ml tube. The MACS SmartStrainer was washed using 20 ml DMEM and centrifuged at 300xg for 7 minutes. The sample that was obtained was resuspended for further use. Erythrocytes and dead cells were removed by applying the Red Blood Cell Lysis buffer (10×).

2.3.4 Flow cytometry

After obtaining the desired cell or tissue, it was prepared for single cell suspension in a cell staining buffer. 15 ml of the cell staining buffer was added to the cells and centrifuged at 2000 rpm for 5 minutes after which the supernatant was discarded. Red blood cells were lysed by applying the Red Blood Cell Lysis Buffer at 1X working concentration and the pellet was resuspended in 3 ml of 1X RBC Lysis Buffer. The sample was then incubated for 5 minutes and 15 ml of the cell staining buffer was added and then centrifuged at 2000 rpm for 5 minutes. Then, the supernatant was discarded, and the viable cells were counted using a haemocytometer. The cells were then diluted to a concentration at 5-10 x 10^5 cells/ml and resuspended in cell staining buffer before being distributed into micro centrifuge plastic tubes at 100 μl/tube of cell suspension (5-10 x 10^5 cells/tube). To block nonspecific binding of antibody in the immunofluorescent staining, the cells were subjected to pre-block before performing staining by incubating with irrelevant purified Ig which was obtained from the same species with same isotype. Cell surface staining with antibody was done by adding purified primary antibody that was conjugated with a fluorescent molecule and then incubated in the dark for 15-20 minutes on ice prior use. The washing step was repeated twice with 2 ml of cell staining buffer through centrifugation for 5 minutes at 350×g.

The cell pellet was resuspended in 0.5 ml of cell staining buffer and 5 µl (0.25 µg)/million cells of Dead Cell Stain was added to exclude dead cells. Then the tube was incubated on ice in the dark for 3-5 minutes and then finally it was analysed with a flow cytometer machine. The results were then analysed using FlowJo software.

2.3.5 DNA Extraction Methods

DNA was extracted following the Qiagen DNeasy® Blood and Tissue Kit protocol. The kit firstly lyses the sample, then binds it to the DNeasy membrane, before elution of the DNA with an intermediate washing step. The membrane is silica based, and has the ability to bind selectively with the DNA. The washing steps are performed to remove contaminants from the sample.

Cell/tissue preparation and lysis

To prepare the lysate from frozen tissue, 10-20 mg of frozen tissue was taken and treated with 20 µl of Proteinase K and 180 µl of Tissue Lysis Buffer ATL in a clean nuclease free 1.5 ml microfuge tube. Then the mixture was incubated on a heat block at 56 °C for > 8 hours in order to dissolve the tissue completely. The mixture was prepared for the spin column method by adding a mixture of 200 µl of Buffer AL and 200 µl of absolute ethanol.

Cultured cells

The lysate of cultured cells was prepared by treating the cells with trypsin and then centrifuging them. About 2×10^7 cells were taken and PBS was added for resuspension of the cells. 200 µl of this cell suspension was drawn in a 1.5 ml microfuge tube and treated with 20 µl of Proteinase K and 200 µl of Buffer AL. In order to dissolve the cells completely, this was incubated at 56 °C for 30 minutes. The preparation for the spin column method was done by adding with 200 µl of absolute ethanol to the suspension.

a. DNA absorption

DNA from the cell lysate was extracted through the spin column by performing centrifuging at 6,000×g for 1 minute. The contents were discarded and the spin column placed in a fresh collection tube.

b. Washing

The washing step was performed by adding 500 µl of Buffer AW1 to the spin column and centrifuging at 6,000 × g for 1 minute. The flow through was collected and the spin column was transferred to a new tube. A second washing step was performed by adding 500 µl of Buffer AW2 and then centrifuging at 16,000×g for 3 minutes.

c. DNA elution

After the washing step, DNA elution was done by adding Buffer AE to the spin column and incubated for 1 minute at room temperature before centrifugation at 6,000×g for 1 minute. After obtaining the required amount of DNA, the spin column was then discarded and the eluted DNA was stored at -20 °C.

2.3.6 True-Methyl Array Kit Methods

This method was performed following the CEGX® True-Methyl Array Kit protocol. The kit was used to detect and quantify the level of cytosine methylation (5-mC). The kit contains all the required enzymes for site specific oxidation, bisulphite conversion and PCR amplification. The oxidant solution converts the 5-hmC bases to its formyl derivative 5-fC which then undergoes bisulphite conversion. In the bisulphite conversion, 5-fC is converted to uracil through decarbonylation and deamination. After the conversion of unmethylated cytosine and formylated cytosine to uracil, magnetic beads are used to recover the DNA through elution.

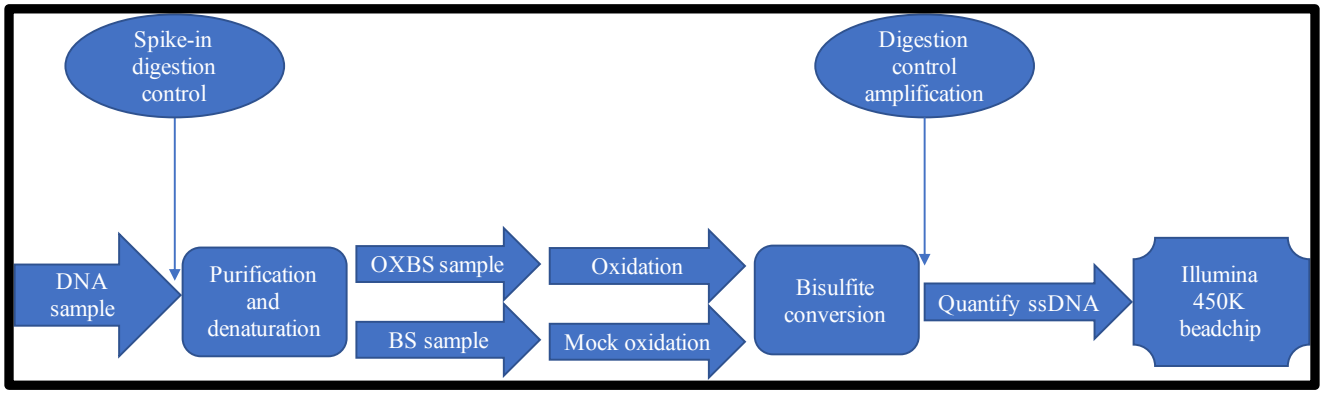

Figure 2.1 Flow chart of the True-Methyl assay

a) Solutions:

Desulfonation buffer was prepared by adding 37.5 ml of 100% ethanol to 16 ml of Desulfonation buffer concentrate and vortexed and stored in 2-8 °C.

Magnetic Bead Binding solution 1 was prepared by adding 120 µl of Magnetic Bead Solution into 6 ml of Binding Buffer 1, which was mixed thoroughly by pipetting up and down then stored at 2-8 °C.

Magnetic Bead binding solution 2 was prepared by adding 720 µl of Magnetic Bead Solution into 60 ml of Binding Buffer 2, and mixed though pipetting. All the mixtures were vortexed and stored at 2-8 °C.

b) Quantifying HMW Genomic DNA sample and spike in the digestion control:

The CEGX® TrueMethyl Array Kit used 1 µg high molecular weight genomic DNA (HMW gDNA) per sample for processing of 500 ng of sample through each of the BS and OXBS conversion processes. Quantification of the genomic DNA was done by adding 1 µg HMW gDNA in a 1.5 ml microcentrifuge tube with ultra-pure water also being added to make up the final volume to 49 µL. The digestion control was thawed before 1µL was added to the genomic DNA to make up the total volume to 50 µL.

c) DNA oxidation workflow

Solution preparation

Fresh stock of acetonitrile was prepared by mixing 3.0 ml 100% acetonitrile with ultra-pure water from the TrueMethyl Array Kit to make up 80% Acetonitrile. The mixture was mixed through vortexing and all the beads were performed at room temperature.

Purification

100 µL of Magnetic Bead Binding Solution 1 was added to each of the 1.5 ml microcentrifuge tubes containing 50 µl HMW gDNA sample and vortexed. Then, the microcentrifuge tubes were incubated at room temperature for 20 minutes. The tubes were then briefly microcentrifuged to collect the pellet. The tubes were placed into a magnetic separation rack and beads were pelleted for 5 minutes at room temperature. Then, the supernatant was carefully discarded without displacing the tubes from the magnetic separation rack. Next, 1.0 ml of 80% Acetonitrile wash was added to the tubes without disturbing the bead pellet. The 1.0 ml 80% Acetonitrile wash was removed and discarded taking care to avoid aspiration of the bead pellet. This Acetonitrile washing step was repeated two further times so that 3 x 1.0 ml 80% Acetonitrile washes were performed in total. Finally, the pellets were air dried for 5 minutes at room temperature.

Denaturation steps

50 µL denaturing solution was added to the bead pellet which was then removed from the magnetic separation rack. The bead pellet was resuspended and vortexed. Then it was incubated at room temperature for 5 minutes and incubated at 37 °C for 30 minutes. Then, a brief spin down was performed to the 1.5 ml microcentrifuge tube and the sample was collected from the bottom of the tube. The tubes and pellet beads were then placed in a magnetic separation rack for 5 minutes at room temperature. The 50 µl elute was then transferred to a new 0.2 ml PCR tube and was placed on ice.

DNA oxidation

For the DNA oxidation reactions, i.e., OXBS and BS reactions, the components were mixed into two new 0.2 ml PCR tubes to prepare the oxidation reaction. For the OXBS reaction, 24 µl denatured DNA and 1 µl oxidation solution was mixed. For the BS reaction, 24 µl denatured DNA and 1 µl ultra-pure water was mixed. The total volume for both reactions was 25 µl each. The oxidation reaction mix was then incubated at 40 °C for 30 minutes in a PCR thermocycler. The mix was then centrifuged at 14000×g for 10 minutes at room temperature to pellet any black precipitate. An orange coloured supernatant was the indication of successful oxidation. The supernatant was then transferred to a new 0.2 ml PCR tube for further downstream processing.

d) Bisulfite conversion

Bisulfite conversion preparation

Bisulfite aliquots were dissolved by adding 4.2 ml of the Bisulfite Diluent to each aliquot and then the solution was incubated at 60°C for 15 minutes, after that, the solution was vortexed until it fully dissolved.

Bisulfite conversion reaction

The Bisulfite conversion reaction mix was prepared by mixing DNA solution from the DNA oxidation step at 25 µl, Bisulfite reagent solution at 170 µl and Bisulfite additive at 5 µl, to make a total volume of 200 µl. The mix was vortexed and centrifuged for collection of the sample at the bottom. The 0.2 ml PCR tube containing the Bisulfite Conversion Reaction mix was placed into a thermocycler with heated lid and Bisulfite DNA conversion was performed using a thermal profile with a repeat i.e., done in two cycles. The thermal profile that was used in sequence was denaturation for 5 minutes at 95 °C, incubation for 20 minutes at 60 °C, denaturation for 5 minutes at 95 °C, incubation for 40 minutes at 60 °C,

denaturation for 5 minutes at 95 °C, incubation for 165 minutes at 60 °C and lastly for an indefinite period at 20 °C.

Clean up

Fresh stock of 70% ethanol also was prepared. After completion of the bisulfite reaction, the 0.2 ml PCR tubes were centrifuged at 14000×g for 10 minutes without disturbing the pellet, 195 µl of the supernatant was collected and transferred to a new 1.5 ml microcentrifuge tube. 1.0 ml of Magnetic Bead Binding Solution 2 was added to each of the 1.5 ml microcentrifuge tubes containing 195 µL bisulfite converted sample. The sample was vortexed immediately to mix it, with the tube was kept at a 45° angle to ensure proper mixing. Then it was incubated for 20 minutes at room temperature. After the incubation, a brief spin down was performed, and the tube was placed in a magnetic separation rack. After 30 minutes incubation, the clear supernatant was discarded without disturbing the bead pellet.

Wash steps:

1.4 ml of 70% ethanol was added to the tubes without disturbing the bead pellet and then the ethanol was discarded while avoiding aspiration of the bead pellet.

Desulfonation steps:

For desulfonation, 1.0 ml Desulfonation Buffer was added to the tubes while keeping them in a magnetic separation rack, i.e., directly to the bead pellet, after that, the tubes were removed from the rack. As the pellets were resuspended in the buffer, the tubes were subjected to spin down. Again, the tubes were put in a magnetic separation rack and incubated for 5 minutes. Then the supernatant was discarded taking care to avoid disturbing the bead pellet.

Wash steps:

1.0 ml of 70% ethanol was added to the tubes for washing and then discarded. This wash step was repeated once more, and then the pellets were air dried for 15 minutes.

Elution step:

15 µl of elution buffer was directly added onto the bead pellet and vortexed to fully resuspend the bead pellet into the elution buffer. Then it was incubated for 20 minutes at room temperature to elute the DNA from the beads. Then the DNA sample was spun down to collect the sample at the bottom of the tube. Next the tubes were transferred to a magnetic separation rack and allowed to form pellet beads for 5 minutes. A 13-15 µl quantity of elution was collected within which was the recovered DNA sample. The converted DNA sample was quantified using the Qubit® ssDNA kit.

e) Digestion control PCR amplification and digestion control amplicon

PCR Amplification preparation

Table 2.9: List of reagents used for PCR amplification and their quantity

Reagent	Quantity of the reagent (µl)
10X polymerase buffer	5
Digestion Control Fwd PCR primer (100 µM)	0.5
Digestion Control Rev PCR primer (100 µM)	0.5
Uracil tolerant DNA polymerase HiFi Uracil+	5U
DNA (recovered template)	1
Ultra-Pure Water	39
TOTAL volume	50

The digestion control was then amplified according to the following thermal cycling condition. The amplification step was divided into three segments: the first segment comprised one cycle with temperature of 95 °C and a duration of 120 s, the second segment comprised 40 cycles with temperatures of 95 °C, 60 °C and 72 °C and durations of 30 s, 30 s and 15 s, respectively, and the third segment comprised one cycle with a temperature of 4 °C and unlimited duration.

PCR purification

The amplicons were cleaned up using a PCR purification kit and then the concentration of the amplicons was determined using the Qubit® dsDNA kit according to the manufacturer's instructions.

Digestion preparation:

Table 7: list of reagents used for digestion and their quantity

Reagents	Quantity of the reagent (µl)		
	Digestion +ve Control	Digestion –ve Control	Cutting Control
Taq RE (20 U/ µl)	40U	-	40U
Processed Digestion Control amplicon DNA (10 ng/µl)	10	10	-
100x BSA	0.2	0.2	0.2
10X Taq buffer	2	2	2
Cutting Control DNA (20 ng/µl)	-	-	5
Ultra-Pure Water	5.8	7.8	10.8
TOTAL volume	20	20	20

The digestion mixture was incubated for 18 hours at 65 °C. Then it was denatured at 80 °C for 20 minutes. Finally, it was run using gel electrophoresis by following the method in the next section 2.3.7.

2.3.7 Gel Electrophoresis Methods

1% Agarose gel was prepared by dissolving 1 gm Agarose in 100 ml 1X TAE buffer. The mixture was gently heated to dissolve the agarose. The solution was left to cool for about 3 minutes before 5 µl of ethidium bromide was added, stirred and then poured onto a gel-casting tray with combs. After the gel had cooled and solidified at room temperature the comb was removed carefully and the gel placed in an electrophoresis tank, which was loaded with 1X TAE running buffer. 5 µl of DNA sample was mixed with 1 µl of 6x loading buffer and the resulting mixture was loaded into a single well of the agarose gel. To determine DNA fragment size 5 µl of 1KB DNA ladder was loaded into another well. Electrophoresis

was allowed to occur at 80V for 60-90 minutes. The resulting bands were visualised using a UV trans-illuminator and photographed.

2.3.8 Illumina 450K BeadChip array methods

This method was performed following the Infinium HD Methylation protocol for the Infinium HumanMethylation450K assay.

MSA4 Plate preparation

An MSA4 barcode label was applied to a new 0.8 ml microplate (MIDI). 20 µl MA1 was dispensed into the MSA4 plate wells and 7 µl of the DNA sample was also transferred to the wells. 1 µl 0.4N NaOH was dispensed into each of the wells in the MSA4 plate that contained MA1 and the tips were exchanged between DNA samples. Next, the MSA4 plate was sealed with the 96-well cap mat. The plate was vortexed at 1600 rpm for 1 minute. This was then pulse centrifuged at 280 × g and incubated for 10 minutes at room temperature. The cap mat was carefully removed and 68 µl RPM was dispensed into each well of the MSA4 plate wells containing the samples followed by 75 µl MSM into each of the wells containing samples. The MSA4 plate was sealed with the cap mat and was vortexed at 1600 rpm for 1 minute. After the MSA4 plate was centrifuged it was then incubated in an Illumina Hybridisation oven for at least 20 hours at 37 °C.

DNA fragmentation

Next, the cap mat was carefully removed and 50 µl of FMS was added to each well containing a sample. The MSA4 plate was sealed with the 96-well cap mat. The plate was vortexed at 1600 rpm for 1 minute and then placed on the 37 °C heat block for 1 hour.

DNA precipitation

In the MSA4 plate, the wells that contained samples, had 100 µl of PM1 added to them. The plate was sealed with the cap mat and then vortexed at 1600 rpm for 1 minute and incubated for 5 minutes at 37 °C. Then, the cap mat was removed carefully and discarded. Each well that contained a sample, had 300 µl of 100% 2-propanol added to it, and then the MSA4 plate was sealed with a new cap mat. The plate

was inverted thoroughly at least 10 times to mix the contents and then incubated at 4 °C for 30 minutes. The sealed MSA4 plate was centrifuged at 3000 × g at 4 °C for 20 minutes. After centrifugation, the MSA4 plate was immediately removed and the cap was discarded. The MSA4 plate was inverted to decant the supernatant. To ensure that all the wells were devoid of liquid, the MSA4 plate was tapped firmly for 1 minute. The uncovered, inverted, plate was left on the tube rack for 1 hour at room temperature to air dry the pellet.

DNA resuspension

46 µl of RA1 was added to each of the wells in MSA4 plate. To seal in the heat, foil was applied to the MSA4 plate and heated to seal. The sealed plates were then incubated for 1 hour in the Illumina Hybridisation oven at 48 °C. Then plates were vortexed for 1 minute at 1800 rpm.

BeadChip Hybridisation

For denaturing, the MSA4 plate was placed on the heat block at 95 °C for 20 minutes. The BeadChips were removed from their 2 °C to 8 °C storage. When the incubation was carried out, the Hybridisation Chambers were prepared and the BeadChips were placed into the BeadChip Hybridisation Chambers. 400 µl of PB2 was added into the humidifying buffer reservoirs of the chambers and the lids were closed. After the incubation was complete, the MSA4 plate was kept at room temperature for 30 minutes, and then centrifuged at 280×g for 1 minute. The BeadChips were placed in the Hybridisation chamber insert and 15 µl of DNA sample was added to each BeadChip. It was then necessary to wait for some time to allow the DNA sample to disperse over the BeadChip. Then, the Hybridisation Chamber inserts containing BeadChips were loaded into the Illumina Hybridisation Chamber and placed in the Illumina Hybridisation Oven at 48 °C and incubated for at least 16 hours.

BeadChip washing steps

Each Hybridisation Chamber was removed from the Illumina Hybridisation Oven and placed on the benchtop to cool for 30 minutes. A wash rack was submerged in a washing dish filled with 200 ml of PB1. The Hybridisation Chamber inserts were removed from the Hybridisation Chambers and each

BeadChip was also removed from the Hybridisation Chamber insert. Each BeadChip cover seal was removed and each BeadChip was slid into the wash rack; it was made sure that the BeadChips were submerged in the PB1, then for 1 minute the wash rack was moved up and down with slow agitation.

Assemble flow through champers

After washing steps, a black frame was placed into the BeadChip alignment fixture. The BeadChip alignment fixture was prefilled with PB1. The BeadChip was then aligned to the alignment fixture. Then to the top of each BeadChip a clear spacer was placed. On top of the clear spacer covering each BeadChip a glass back plate was placed. To create a reservoir against the BeadChip surface, the barcode end of the BeadChip was facing inwards the plate reservoir. To the flow-through chambers a metal clamps were attached.

BeadChip extension

The water circulation reservoir was filled with water to the appropriate level and the temperature of the chamber rack was set at an equilibrium of 44 °C. 330 ml of 100% ethanol was added to the XC4 bottle and made up to a final volume of 350 ml. The XC4 bottle was shaken vigorously for complete resuspension. Then it was used at room temperature or stored at 2 to 8 °C. A mix of following reagents was then dispensed into the reservoir of each flow-through chamber.

Table 2.10: List of reagents and their quantity added to the flow through chamber

Reagent	Quantity of the reagent	Time of incubation
RA1	150 µl	30 sec, repeated 5 times
XC1	450 µl	10 minutes
XC2	450 µl	10 minutes
TEM	200 µl	15 minutes
95% formamide/1 mM EDTA	450 µl	1 minute, repeated once
-	-	Incubated for a total of 5 minutes
XC3	450 µl	1 minute, repeated once

BeadChip staining

Table 2.11: List of reagents, their quantity and incubation time

Reagent	Quantity of the reagent	Incubation time
STM	250 µl	10 minutes
XC3	450 µl	1 minute, with one repeat
Wait for 5 minutes		
ATM	250 µl	10 minutes
XC3	450 µl	1 minute, with one repeat
Wait for 5 minutes		
STM	250 µl	10 min
XC3	450 µl	1 minute, with one repeat
Wait for 5 minutes		
ATM	250 µl	10 minutes
XC3	450 µl	1 minute, with one repeat
Wait for 5 minutes		
STM	250 µl	10 minutes
XC3	450 µl	1 minute, with one repeat
Wait for 5 minutes		

BeadChip coating

310 ml of PB1 was added to the dish in which the BeadChips were submerged. Following this, the dish was placed in the staining rack. The surface of the reagent was broken down by slowly moving the rack while the BeadChips remained submerged in the PB1. Another dish was marked with "XC4" and 310 ml of XC4 was added to it. The staining rack was removed from the dish labelled PB1 and placed in the dish labelled with XC4 and allowed to soak in it. The BeadChips were then placed in a tube rack after removing them from the staining rack. The BeadChips were vacuum dried for 50-55 minutes at 675 mm Hg.

BeadChip imaging

The iScan microarray scanner system was used to scan the BeadChips.

2.3.9 Quest 5hmc detection kit methods

Detection of 5hmC in DNA was done through the step where the samples are first modified through glucosylation and then treated with digestion enzyme MspI. Then ultra-pure DNA was eluted through the spin column which was subjected to qPCR for locus-specific analysis of 5hmC. This method was performed following the quest 5hmC qPCRdetection kit protocol from Zymo Research.

Glucosylation Steps

Each DNA to be tested were divided into two separate tubes (+ve glucosylation and -ve glucosylation).

Table 2.12: List of reagents for +ve glucosylation and -ve glucosylation

Reagent	**+ve Glucosylation**	**-ve Glucosylation**
Test DNA [100-500 ng]	5 µl	5 µl
10X UDPG	5 µl	5 µl
5-hmC GT Enzyme	2 µl	-
10X 5-hmC GT Reaction Buffer	5 µl	5 µl
ddH2O	33 µl	33 µl
Total	**50 µl**	**50 µl**

The reagents in the table were mixed and the final volume was made up to 50 µl. The mixture was then incubated for more than 2 hours at 37 °C.

Digestion step

After incubation, the mixture was treated with 30 units of MspI enzyme (in the case of both the +ve Glucosylation and -ve Glucosylation reaction setups) and incubated at 37 °C for more than 4 hours.

Clean-up

DNA binding buffer at a 5:1 ratio was added to each reaction mixture; in other words, 250 µl of the binding buffer was added to 50 µl of reaction mixture. The sample was placed into the spin column and then centrifuged at 10,000xg for 30 seconds. After that, the flow through was discarded, and 200 µl of DNA wash buffer was added to the spin column and then centrifuged at 10,000xg for 30 seconds. This

was repeated once more. The spin column was placed into a new 1.5 microcentrifuge tube. 6 µl of DNA elution buffer was added to the centre of the spin column and then was incubated at room temperature for one minute. For collection of DNA the elute was collected after centrifugation at 10,000xg for 30 seconds.

Locus-specific 5-hmC Detection

Three tubes of the same DNA samples were used to the qPCR reaction set up. These tubes are: +ve Glucosylation (test sample), -ve Glucosylation (0% control) and no treatment DNA (100% control). Primers (forward/reverse) were designed and purchased from Sigma-Aldrich. Details of these primers are listed in appendix 2.

Table 2.13 5-hmC detection reaction set up

Component	**Volume**
Test DNA [10-50 ng]	2 µl
2X Quest*Taq* qPCR PreMix	10 µl
Primer forward [20µM]	0.4 µl
Primer reverse [20µM]	0.4 µl
ddH2O	17.2 µl
Total volume	**20 µl**

Table 2.14 qPCR cycle parameters

Steps	Temperature	Time
1 Denaturation	95°C	1 minute
2 Denaturation	95°C	30 sec
3 Annealing	50°C	15 sec
4 Elongation	72°C	15 sec
5 Cycling	Go to step 2	40X
6 Final Elongation	72°C	5 minutes

2.3.10 Statistical analysis

Flowjo software analysis (version 10) was used to analyse the cell surface markers used in the flow cytometry chapter.

SPSS statistics version (25.0.0.1) and Microsoft Excel version (16.14.1) were used for statistical analysis and figure representation of flow cytometry chapter 4.

R studio software (version 3.4.1) was used for DNA methylation 450K array analysis. All packages were downloaded from the Bioconductor website and were used for data analysis for the Illumina 450K methylation array data. The Minfi package was the main package used which called for most of the analysis workflow in the array chapter 5. R scripts that contain codes used for DNA methylation analysis were uploaded to a respiratory in Github website and can be accessed using the following link (https://github.com/A-Albaz/Methyltion-Analysis).

CHAPTER THREE

3 PRIMARY CULTURE OF BLADDER CANCERS *IN VITRO*

3.1 Introduction

Placing isolated cells in an artificially supplemented growth media is a commonly used technique to study developmental complexities, disease progression and signalling mechanisms (Philippeos et al., 2012). Bladder cell lines or primary tissue culturing of human bladder tissue explants, either from healthy donors or from oncogenic bladder tissue material (Rahman et al., 1987) have served as ideal sources for stem cell isolation (Falso et al., 2012) and investigation of chemotherapeutic intervention strategies (Flieger et al., 2008). Culturing of scarce bladder tumours alleviates the necessity for frequent surgical intervention while ensuring access to human primary cells of high purity and low passage numbers (Woodman et al., 2011). This technique also ensures maintenance of quality control while avoiding contamination from other cell lines (Bonazza et al., 2016).

Primary bladder cancer tissues have been recognised as repositories of bladder cancer stem cells (CSC) which possess aggressive tumorigenic characteristics (Chan et al., 2010). Since tumour cells from bladder cancer biopsies have been identified as being capable of forming xenografts on immune-compromised animals, it is necessary to examine and characterise bladder cancer stem cells in detail (Goodwin Jinesh et al., 2014). Meanwhile recent research in different bladder cancer subtypes has identified the possibility of their characterisation using CSC's, which in turn possessed unique cell surface markers (Liu et al., 2012). Such characterisation of CSC's could enable follow-up of the factors triggering relapses driven by therapeutic resistance to chemotherapy (Zhao, 2016).

Several epigenomic processes have been identified as driving changes in this unique subset of stem cells, including DNA methylation (Toh et al., 2017), which in turn accounts for factors like invasiveness, drug resistance and metastasis, as observed in papillary bladder cancer (Li et al., 2017). Genome wide association studies (GWAS) have shown that impaired DNA methyltransferases silenced genes like DNA (cytosine-5)-methyltransferase 1 (DNMT1) (Spada et al., 2007), ensuring the survival of cancer

stem cells (De Carvalho et al., 2012). DNA methylation functionality is very discriminatory in nature, with its occurrence being locus specific and modest in magnitude (Bock et al., 2012). Runt-related transcription factor 3 (RUNX3), a polycomb target gene expressed in urothelial stem cells, has been identified to be preferentially methylated, thus causing the evolution of the perpetually replicating cancer stem cells (Wolff et al., 2008). Meanwhile hypermethylation of Glutamate receptor 1 (GRIA1) is associated with severe outcomes in basal bladder cancer and has also been hypothesised to be expressed in cancer stem cells (Tilley et al., 2017).

Other markers, like Octamer-binding transcription factor-4 (OCT-4) and CD133, have been identified to be helpful in selectively isolating particular subsets of cancer stem cell markers (Sedaghat et al., 2017). Meanwhile the basal layer of the urothelium, long hypothesised to be the potential source of cancer stem cells, was realised to be positive for the stem cell markers Epithelial Membrane Antigen (EMA) and CD44 variant 6 (CD44v6) (Yang and Chang, 2008). Improved techniques, such as magnetic cell sorting, has made possible the examination of the colony-forming properties of cells positive for this marker. Lineage tracing methods has previously proven the existence of a tumour-initiating cells (TIC) signature $CD44^{+}CK5^{+}CK20^{-}$ in a subpopulation of cancer stem cells in primary bladder cancer (Chan et al., 2009).

3.2 Isolation and culture methods of bladder CSC's

Explant cultures enable observation and manipulation of biopsied tissues in controlled environments while maintaining intercellular communication between individual bladder cancer cells (Locke et al., 2005, Bull et al., 2011, Shamir and Ewald, 2014). These cultures thus maintain the tumour microenvironment, enabling them to be used as ideal test beds for assessing therapeutic compounds (Benbrook, 2006). However, these tissue culture systems lack integrated physiological systems, which are yet to be assessed using a therapeutic index (Sugibayashi et al., 2004).

Cell isolation using the Hank's Balanced Salt Solution (HBSS) buffer-based stripping approach has proven ideal for isolating bladder CSCs. The isolation and culturing of these cells involves disaggregation of cells from primary tissue using enzymatic, chemical and mechanical disaggregation techniques (Ng et al., 2011). The buffer serves to segregate the primary tissue (urothelium from stromal part) while the mechanical disaggregation approach further isolates the cells into single cells. This speeds up the process of setting up the cell culture, but is disadvantageous since a differentiation of CSCs is not possible at this stage. Since primary cell culture conditions are often insufficiently optimised there exists a potential for lowered cellular viability with the added risk of cross-contamination by other cells/cell lines.

A novel cell propagation approach using 3D spheres has been identified to address the majority of these issues (Ochs et al., 2003). 3D spheroids were used in cultivating human mammary CSCs in an anchorage independent manner in a serum free medium containing clones called tumorospheres. These tumorospheres serve to enrich CSCs from several cell lines (Ponti et al., 2005). Propagation of CSCs using tumorospheres enhances their proliferative potential while preserving clonogenicity (Kondo et al., 2011). The key factor promoting cancer cell survival under *in vitro* conditions is primarily the cell-to-cell contacts (Hofmann et al., 2007), with such contacts being advantageous, especially with cancer tissue originating from spheroid (CTOS) cultures (Kondo et al., 2011). The CTOS-based approach utilises disaggregated cells of colorectal cancer tissue to form spheroids, which form xenograft tumours while retaining the features of parent tumours. Tumorosphere cells, however, whilst enriched in CSCs, are unable to maintain this enrichment in a cell line dependent manner (Calvet et al., 2014).

Several growth factors have also been identified using a base medium free of serum, Dulbecco's Modified Eagle's Medium (DMEM), with the CSC population of urothelial cells being grown on BD Falcon chambered culture slides (Dimov et al., 2010). Similarly, EMA (-) cells and $CD44v6^{+}$ have been

isolated via a magnetic sorting approach using serum free DMEM in order to identify colony forming, self-renewing and proliferating cells (Yang and Chang, 2008).

Hypothesis

It is hypothesised that bladder cancer stem cells can be retrieved and grown from primary bladder tumour cultures.

It is also hypothesised that in vitro growth of bladder cancer stem cells may be used to study their characteristics.

Aim

To establish primary tumour cultures with the aim of collecting/retrieving bladder cancer stem cells (CSCs).

3.3 Materials and Methods

3.3.1 Patients and Tumour Samples

30 bladder tissue biopsies were obtained from patients following surgical removal of the bladder tissue at the Royal Hallamshire Hospital, Sheffield UK. These were used in this study (Table 3.1). Informed consent was obtained from all patients (Investigation of Molecular Instability in the Pathogenesis of Urothelial Cancer, STH 15574) Patient ages ranged from 49-97 years with a mean age of 78 years. Out of 30 samples, there were 23 males and 7 females included in this study. Details of all cases examined in this chapter are summarised in Appendix 1.

Table 3.1 Tumour samples and numbers used in primary culture

Stage & Grade	**No.**
pTa	6 (20%)
pT1	7 (23%)
≥pT2	17 (57%)
Total	**30**
G2	5 (17%)
G3	25 (83%)
Total	**30**

3.3.2 General Primary Tissue Culture Plan

The following plan was used to select the best methods and materials in order to obtain primary tissue cultures of bladder tumour tissues (figure 3.1).

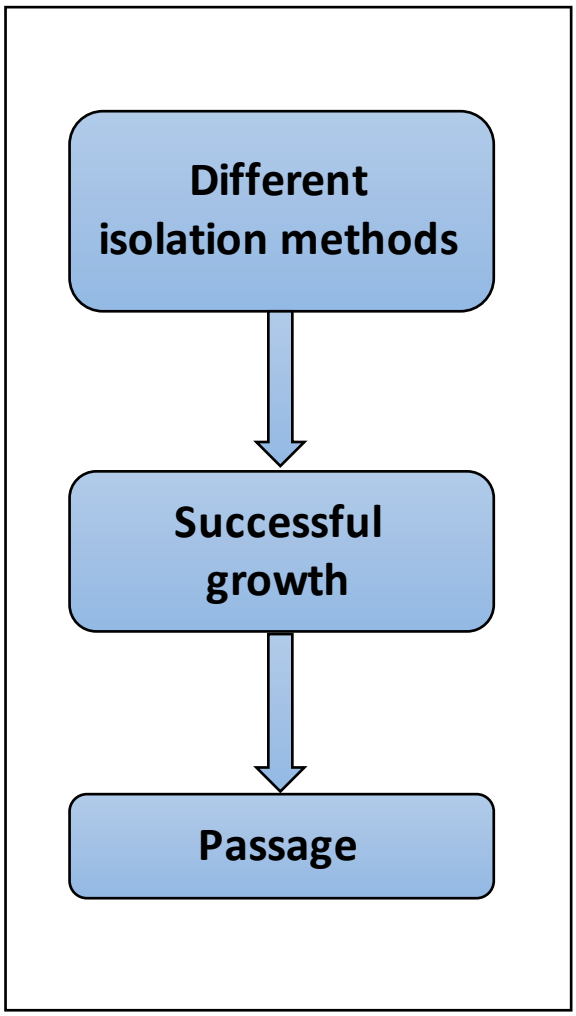

Figure 3.1 Plan used for primary tissue culture.

3.3.3 Tumour collection and processing

The biopsied tumours used in this study were sourced from patients who had undergone surgical removal either via transurethral resection of bladder tumour (TURBT) or cystectomy. Samples were collected immediately after surgery in 20 ml of the transport medium Hank's balanced salt solution (HBSS), with Mg^{2+} and Ca^{2+} containing 20-kallikrein inactivating units (KIU) aprotinin, 100 µg/ml of penicillin and 100 µg/ml of streptomycin. Upon delivery, the tumour samples were handled under sterile conditions in a safety laboratory cabinet using sterile equipment. Three methods were primarily used in this study to isolate cells from the bladder tumour biopsies. Details were described previously in the materials and

methods chapter (section 2.3.2). Illustrations of the explant and stripping HBSS methods are shown below (Figures 3.2 and 3.3, respectively).

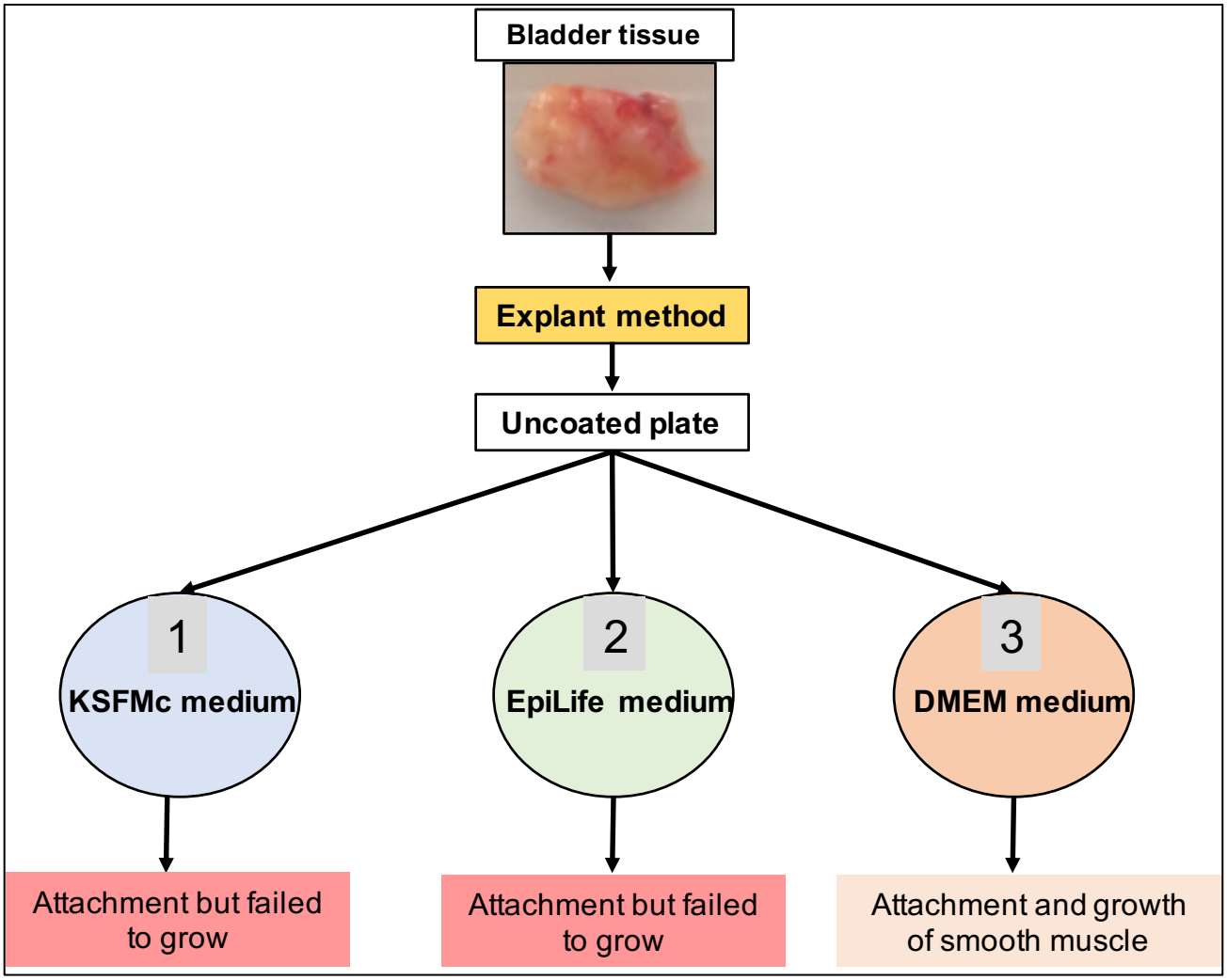

Figure 3.2 Schematic representation of the explant isolation method.

The Figure illustrates the explant isolation procedure for the primary tissue culture of bladder tumour tissue using three different mediums.

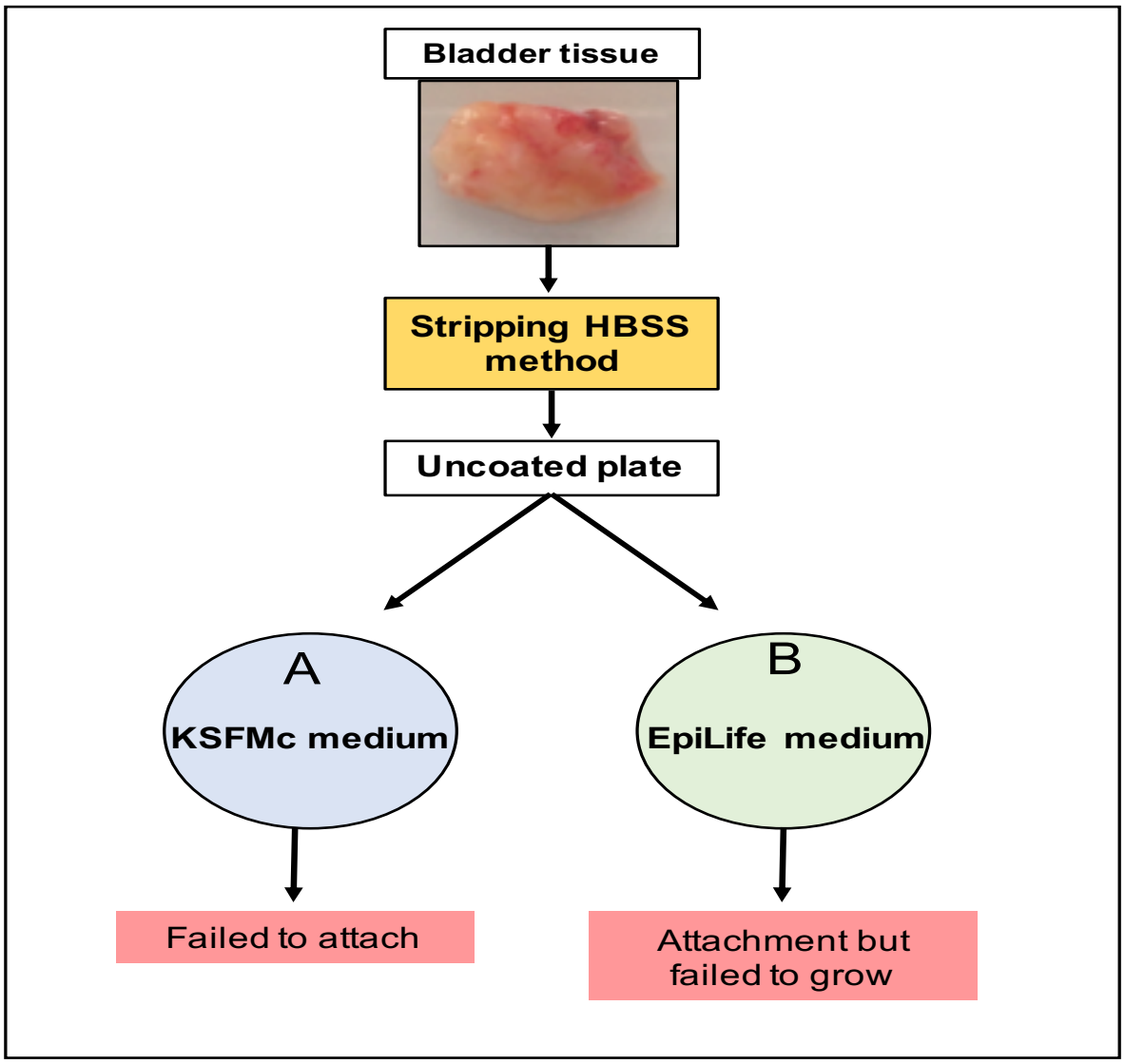

Figure 3.3 Schematic representation of the stripping HBSS isolation method.

The figure illustrates the stripping HBSS isolation procedure for the primary tissue culture of bladder tumour tissue using two different serum free media.

3.3.4 Cell culture growth and passage

Different media were used in this study in order to achieve successful growth. Details were provided in the materials and methods chapter (section 2.2.3). Cultured cells were initially maintained in DMEM medium supplemented with 1% non-essential amino acid (NEAA), 10% foetal calf serum (FCS), 100 µg/ml of penicillin and 100 µg/ml of streptomycin to improve the cellular adhesion to the culture plate. The media was later switched with a serum free medium so as to grow epithelial cells selectively.

The coating matrix kit was composed of proteins not of animal origin and contained 0.5 ml of sterile recombinant type I human collagen. This extracellular matrix coating the culture plate served to enhance the adhesion and growth of keratinocyte cells *in vitro* (Seifert et al., 2007).

Different enzymes were used in order to achieve a successful culture passage. First, a Trypsin-versene/EDTA mixture containing 0.5 g/l trypsin and 2.0 g/l versine/EDTA. EDTA helps to remove the magnesium and calcium ions from the cell surface, which normally help in cell-cell adhesion, and thereby allows trypsin (a serine protease) to hydrolyse specific peptide bods. Then a trypsin inhibitor or medium containing serum was used to halt the trypsin activity. StemPro® Accutase containing proteolytic and collagenolytic enzymes free of bacterial or mammalian derived protein serves as a replacement for the traditional trypsin enzyme and is useful for the detachment of cells grown in standard as well as coated culture plates.

3.4 Results

3.4.1 Selection of isolation method for urothelial cell growth

3.4.1.1 Explant method

The explant method was initially performed on freshly biopsied bladder tumour tissue by scraping the urothelial part of the tissue. Cells obtained were then placed onto three uncoated plastic plates named 1, 2 and 3, with each plate containing a different medium, namely KSFMc, EpiLife and DMEM, respectively (as shown above in Figure 3.2).

The resection tissue specimens were able to attach in the tissue culture plates containing each of these three media. This cellular attachment did not lead to out-growth in the plates containing KSFMc and EpiLife media, however. On the other hand, the resectioned tissue placed in the plate containing DMEM was able to attach and grow into smooth muscle-like cells (Figure 3.4).

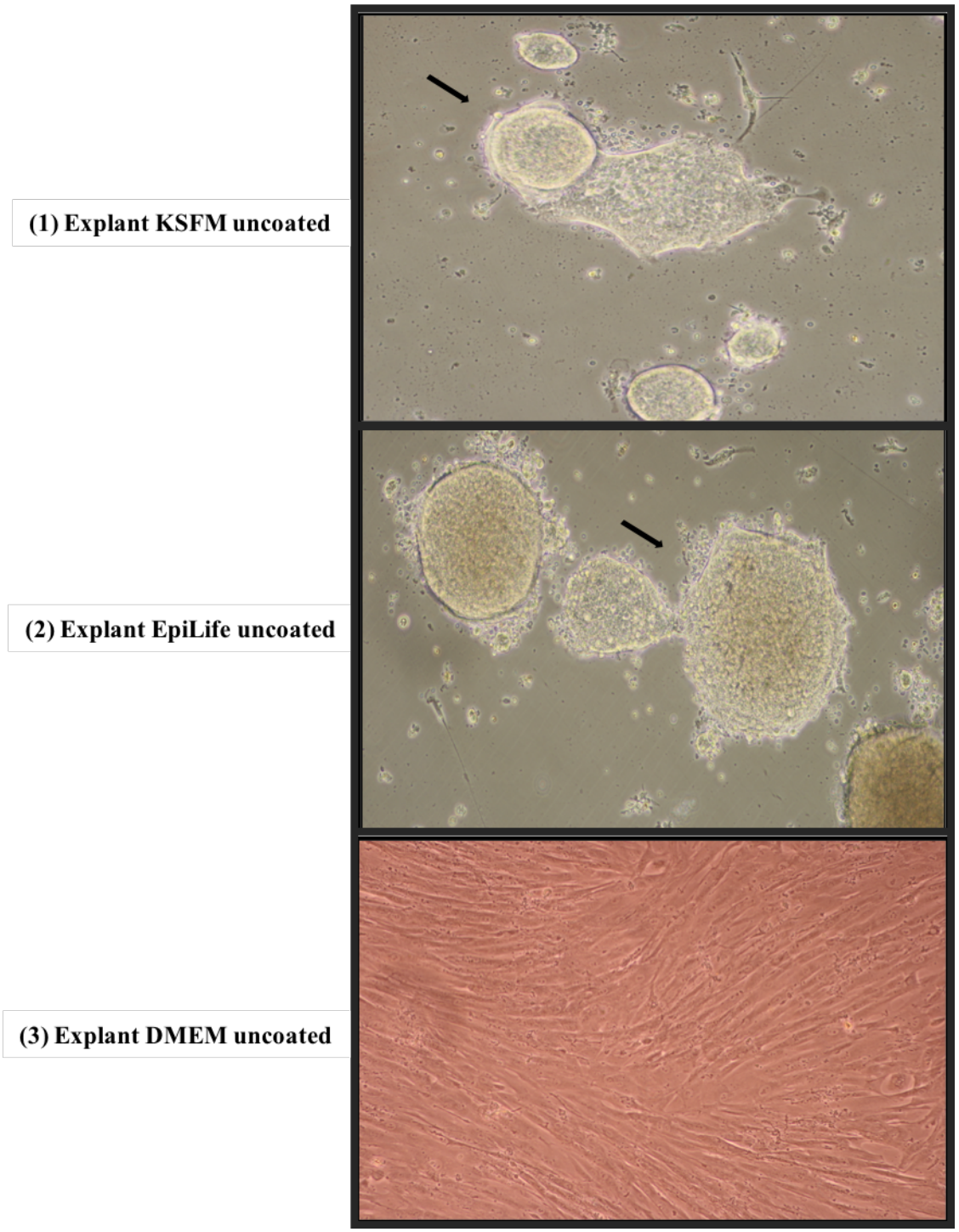

Figure 3.4 Primary bladder tumour tissue culture performed using the explant method.

Adherent tumour tissue (black arrow) in two different growth media KSFMc (1) and EpiLife (2). Outgrowth of primary bladder tumour into fibroblast-like or stromal like cells in DMEM media (3). Images were captured at X40 magnification.

3.4.1.2 Stripping HBSS method

A different method, called the stripping HBSS method (illustration shown above figure3.3), was also used in order to observe if there were any significant differences in cellular growth compared to the explant method.

When the stripping HBSS method was used, single cell attachment was observed in the two uncoated culture plates, but no outgrowth was observed in plate (A) when KSFMc medium was used over the next three days. While growth was observed on plate (B) when EpiLife medium was used, proliferation stopped after one week in culture (Figure 3.5).

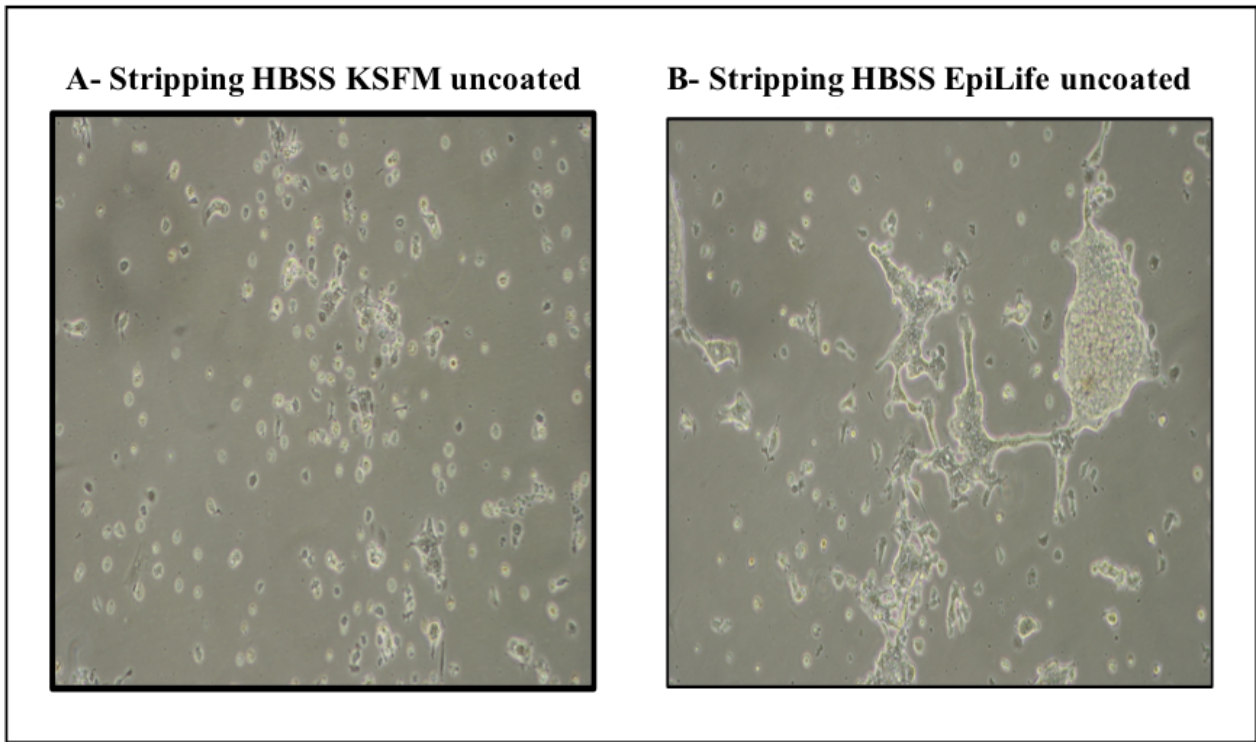

Figure 3.5 Primary bladder tumour tissue culture using the stripping HBSS method.

A) Primary bladder tumour culture using the stripping HBSS method in the serum free medium KSFMc. B) Primary bladder tumour culture using the stripping HBSS method with the serum free medium EpiLife. Images were captured at X40 magnification.

3.4.1.3 Utilising coated matrices

Culture plates with coated matrices were used in order to ease cellular anchorage during primary bladder tissue culturing. These were then tested together with the explant methods using serum free media. Interestingly, there was an initial attachment of tumorospheres onto the coated plates. Cells were also initially seeded onto DMEM medium supplemented with 20% foetal calf serum (FCS) for the first 24hrs of culture in order to enhance tissue attachment and was later changed to serum-free EpiLife medium. Following this, many differently sized spheres were seen attached after 24 hours of seeding the tumour tissue onto these coated plates [Figure 3.6 (A and B)]. After five days of incubation, spheres start to make contact with other spheres, and cells started to migrate out of colonies, (black arrows) [Figure 3.6 (C and D)]. After two weeks, cells started to proliferate and fill the space between colonies (black arrow) [Figure 3.6 (E and F)].

Unfortunately, after three weeks of culture, a co-culture was observed as the cultures were realised to have been contaminated with fibroblasts. (black circle) [Figure 3.6 (G)]. Also, multiple layers of cell clusters were developed on the culture plate [Figure 3.6 (H)] and spheres had edges that were rounded off, as shown in Figure 3.6 (I), and which started to detach from the plate surface after three weeks in culture.

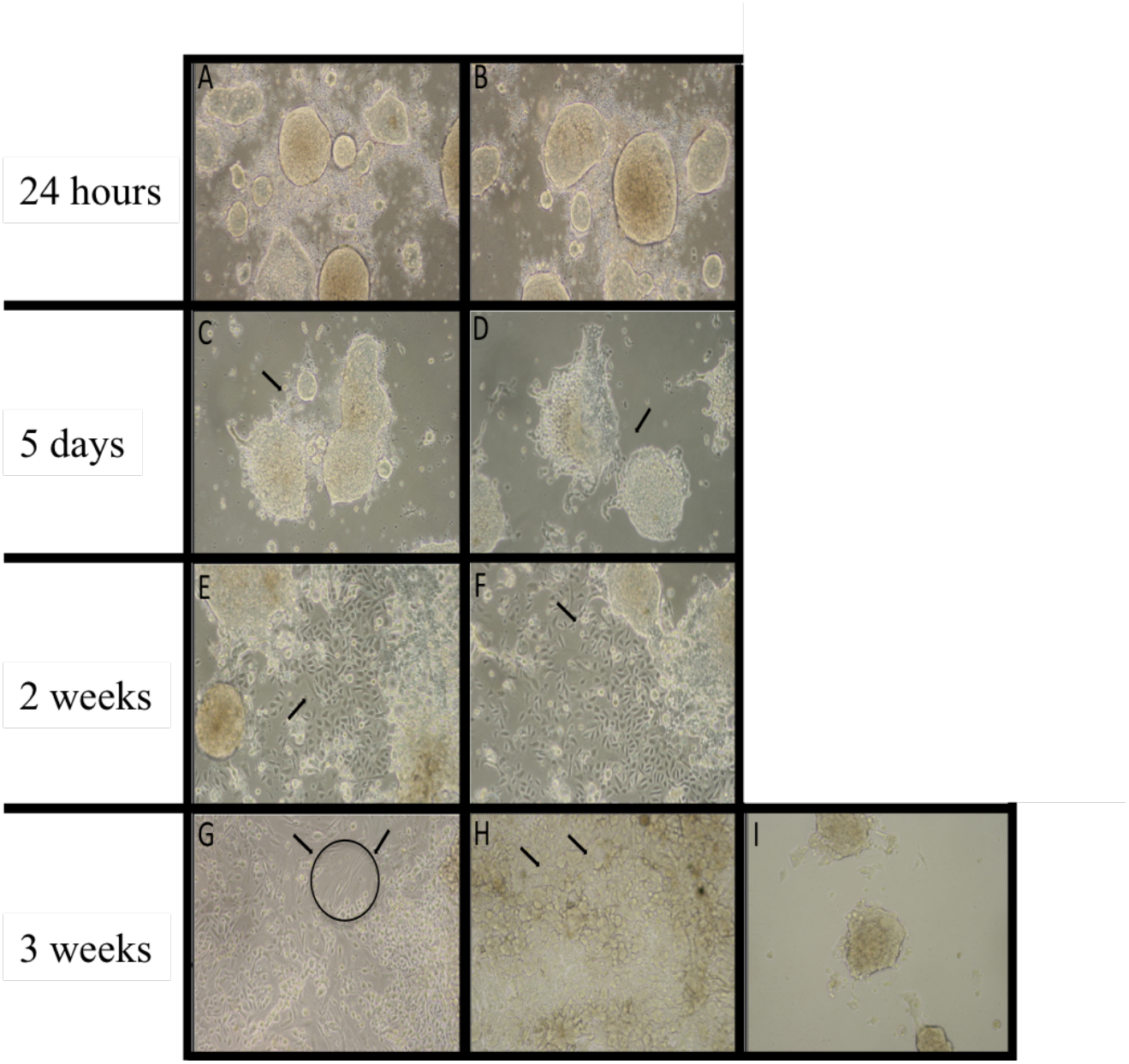

Figure 3.6 Primary bladder tumour cells grown using the explant method on coated plates containing serum free EpiLife media.

Attachment of bladder tumours cells evident after 24 hrs (A, B). Plated bladder tumour cells start to migrate out from colonies after day 5 (C and D). Proliferation of bladder tumour cells was apparent after two weeks (E and F). Fibroblast contamination (circled) evident after three weeks in some of the culture-containing plates (G). Multi-layered cell clusters and spheres round off around this stage (H and I). Images were captured at X40 magnification.

3.4.2 Selection of new serum free medium

The explant method enabled successful isolation and establishment of bladder tumour tissue on extracellular matrix-coated plates containing serum free EpiLife medium. Co-cultures were observed to form later in the said culture, however, which disadvantaged such an approach. Recent research (Kondo et al., 2011) has suggested the ability of cancer tissue originated spheroid (CTOS) to form spheres from colorectal cancer tissue samples in coated culture plates with serum free StemPro® media. Here, we attempted to use exactly the technique described in Kondo et al. on bladder samples but in this case it failed to provide cell attachment and induce growth.

When the explant method was used with StemPro® media, however, successful attachment and better growth were observed in the culture (Figure 3.7). On day five, a few pieces of tissue sample were attached to the plate and cells were observed to be migrating out to fill the space [Figure 3.7 (A, black arrow)]. In Figure 3.7 (B and C), cells had proliferated across the plate with no fibroblast contamination observed. After prolonged growth and daily re-feeding with StemPro medium, the cells stopped growing and started to detach, becoming bloated and apoptotic in appearance [Figure 3.7 (D, E and F)].

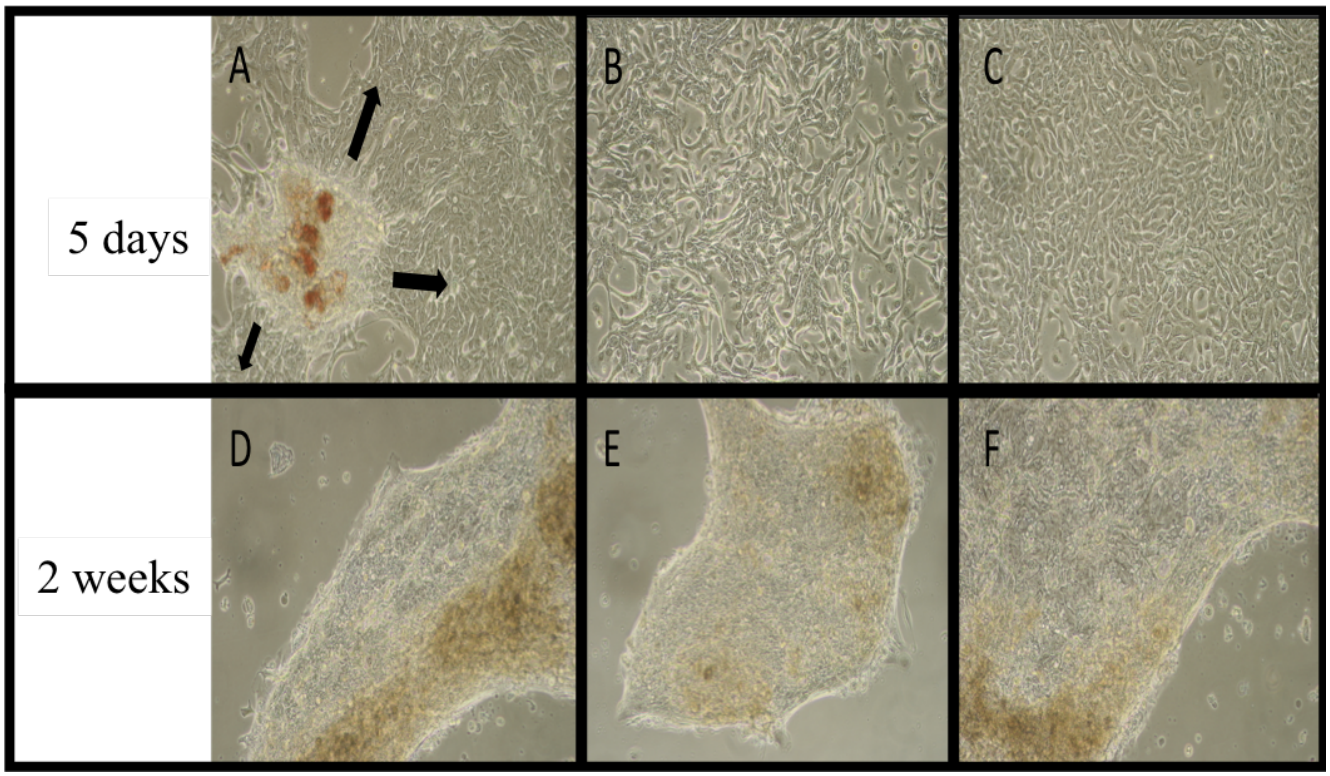

Figure 3.7 Bladder cell proliferation following explant culturing on coated plates containing StemPro® media.

(A) Cell migration ongoing from adherent bladder tissue after five days. (B, C) Cell proliferation across the plate. (D, E and F) shows that the cells stopped growing and appeared apoptotic and bloated. Images were captured at X40 magnification.

3.4.3 Divergent morphology in primary tissue culture.

Cell morphology varied depending upon whether they were cultured in StemPro, EpiLife or KSFMc. Meanwhile the addition of new StemPro media to the cultured cells helped to improve cellular contacts while enhancing cellular proliferation. However, cells started to differentiate and produced a different morphology, as shown in Figure 3.8.

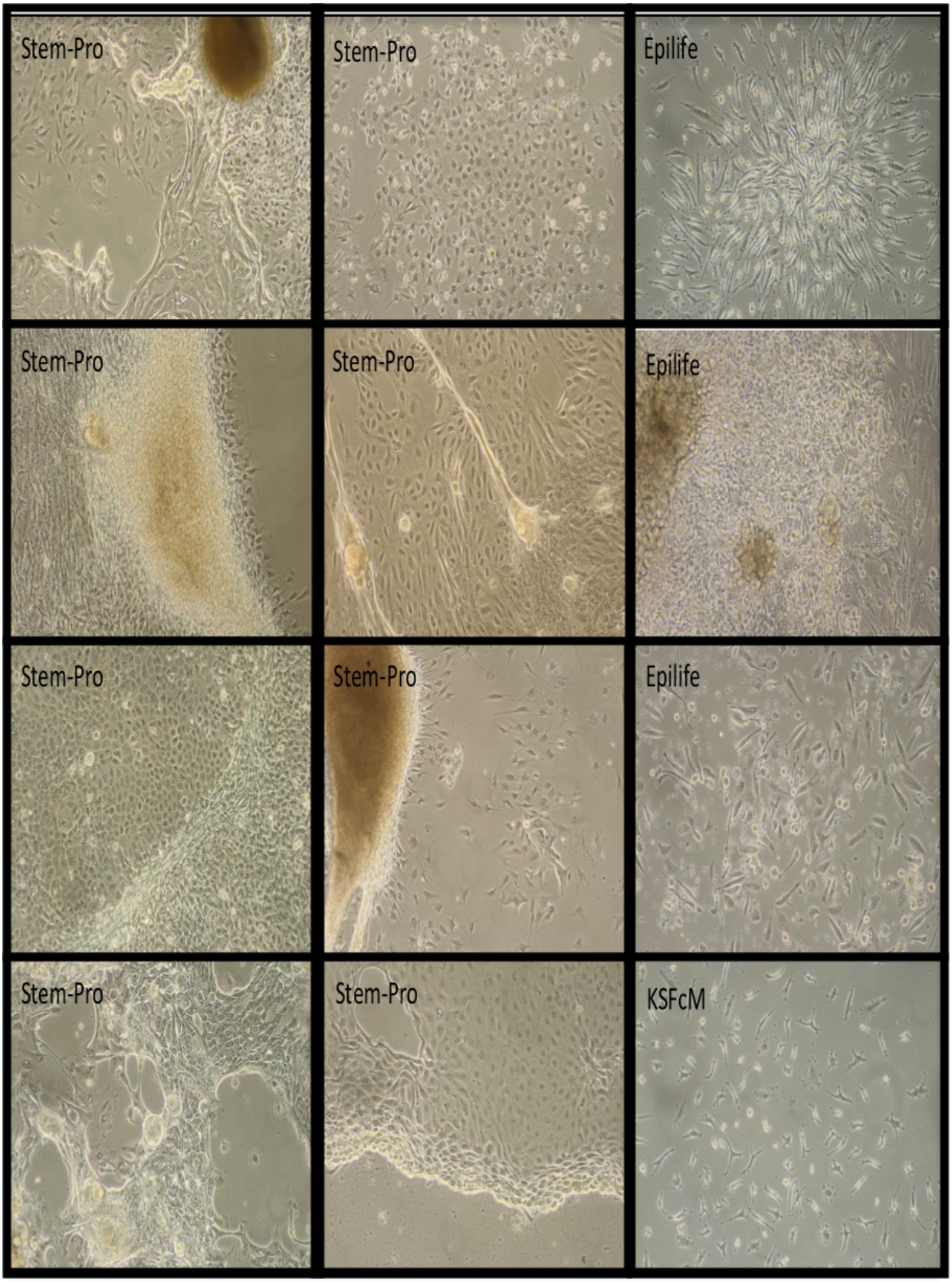

Figure 3.8 Primary tumour tissue specimens being cultured in different cell culture media

EpiLife, KSFMc and StemPro were used in this study. Images were captured at X40 magnification.

3.5 Discussion

Given that bladder cancer stem cells (CSC) are hypothesised to be present in the basal layer of the urothelium (Van Batavia et al., 2014), several *in vitro* models have previously attempted to identify and isolate the said cells (Li et al., 2017). Characterisation of these CSCs has been attempted using specific markers like Sonic hedgehog (SHH) (Papafotiou et al., 2016), SOX2 (Zhu et al., 2017), CD44 (Wasfy and El-Guindy, 2017), Cytokeratin 5 (Chan et al., 2010) and Keratin 14 (Krt14) (Papafotiou et al., 2016). The expression of some of these markers in cohesion reliably indicates the presence of at least some subpopulations of these cancer stem cells (Chan et al., 2009). Recent research has indicated the existence of a unique gene signature distinct to basal urothelial cells and to differentiated urothelial cells (Chan et al., 2009). This research has been restricted to bladder cancer cell lines, however, and has not been reliably verified in primary bladder cancer tissues or primary bladder cancer tissue explants. This study has tried to redress this omission by attempting to create a protocol for successfully culturing such primary cancer tissue biopsies for later characterisation using techniques like fluorescence associated cell sorting (refer to Chapter 4) and DNA methylation sequencing (refer to Chapter 5).

When the explant technique was used to place biopsied bladder cancer tissue in 30 ng/ml cholera toxin containing Keratinocyte Serum Free Media complete (KSFMc) additionally supplemented with 0.6 mM Ca^{2+} (refer Figure 3.4 (1)) and EpiLife media (refer Figure 3.4 (2)) on uncoated culture plates it resulted in cellular attachment but there was no growth or proliferation of the cellular material. A similar amount of the re-sectioned biopsied tissue placed subsequent to the explant technique in Dulbecco's Modified Eagles medium (DMEM) supplemented with foetal calf serum was able to attach onto the culture plates and grow out into cells with a smooth muscle-like morphology (refer Figure 3.4 (3)). The absence of cellular proliferation and differentiation of the biopsied bladder carcinoma tissue could be due to their placement in serum free media like KSFMc and EpiLife. KSFMc medium has been commonly used for culturing out normal urothelial cells, however (Southgate et al., 1994), while EpiLife medium has been

successfully used in a combinatorial approach with DMEM containing 10% foetal calf serum (FCS) to grow out carcinoma associated fibroblasts (Hatina and Schulz, 2012). The induction of cellular outgrowth and later differentiation into cells with a smooth muscle-cell-like morphology could imply that culturing in DMEM enriched with FCS is able selectively to enrich for such a subpopulation from bladder carcinoma tissue. The absence of primary urothelial carcinoma tissue in serum free media could imply that certain factors in foetal calf serum is enabling outgrowth from a select subpopulation of urothelial carcinoma stem cells. The replacement of serum of bovine origin with serum sourced from other sources has not been tested here, however. Previous research on serum sourced from bovine or human specimens has indicated that when used for cultured urinary bladder cell lines responded similarly (Rigby and Franks, 1970). In order to overcome/ or select for uniform, or at least partial epithelial/urothelial-like, outgrowth from these re-sectioned primary bladder cancer tissue; an approach using other serum free media ought to be tested, such as DH-S1, which has previously been used for culturing bladder carcinoma cell lines (Messing et al., 1982).

Additionally, the use of the stripping HBSS technique for growing out the bladder carcinoma cells in culture did not yield cellular outgrowth for the KSFMc serum free media (refer Figure 3.5 (A)). The bladder carcinoma cells survived for much longer and were able to attach themselves onto the culture plates when EpiLife media (refer Figure 3.5 (B)) was used in combination with the stripping HBSS method. Nonetheless, these cells died out, indicating that the stripping HBSS technique by itself was not sufficient to grow out these cells in the absence of serum. Other factors that might also have had a negative influence include the prolonged and harsh digestion processes associated with the stripping HBSS technique or the possibility that the re-sectioned cells might already have initiated the path towards apoptosis leading to necrosis.

The utilisation of coated matrixes on the cell plates used for tissue culturing had a positive effect on cell cultures grown in serum-free media (refer Figure 3.6). The cells were able to both attach and grow out as tumorospheres aided by the coated matrix. The replacement of the DMEM with serum free media meanwhile promoted cellular proliferation, indicating that bladder tumour cells yielded better growth rates when exposed to serum-free medium supplemented with growth factors. Although the cellular growth later stopped, this remained a good indication of the suitability of using multiple growth media with additional supplements like growth factors/ sera, to establish primary bladder carcinoma cells.

Coated matrices enhanced culture and promoted tissue attachment and some kind of growth but stopped after two weeks, and although StemPro was then used in combination with the explant technique and coating matrix (refer Figure 3.7), this approach was undermined by fibroblast contamination of the culture.

Additional approaches like Cancer Tissue Originated Spheroids (CTOS) using serum free StemPro media have been able to promote tissue attachment and induce colorectal tumorospheres to proliferate (Kondo et al., 2011); but this technique was unsuccessful when used on bladder tumour tissue in this study. This loss of cellular attachment could be because this method was originally designed/ setup for colorectal cancer cell cultures (Kondo et al., 2011). Also the bladder tissue dissociation could have resulted in damage to the bladder tissues. A combinatorial approach featuring the use of the coated matrix and the explant method together with the StemPro media meanwhile promoted better bladder tumour cell growth (refer Figure 3.8). These proliferating cells, however, also contained a subpopulation of fibroblast cells and were not just urothelial cells. This indicated the drawback of utilising biopsied tissue for growing out urothelial tumour tissue.

Although I was unable to establish a primary bladder tumour culture protocol for growing out urothelial carcinoma tissue I have been able to identify a novel method using media supplemented with sera to grow out smooth muscle like cells. The serum free StemPro media, although originally designed for colorectal cell culture, could still be utilised to promote tumour cell out growth when used with coated matrices and explant isolation techniques. These techniques would still have to be modified with other media or growth factors to induce urothelial growth and confluence, however.

CHAPTER FOUR

4 CELL SORTING OF FRESH BLADDER CANCERS

4.1 Introduction

Bladder cancer is a common malignancy (Humphrey et al., 2016) classified using pathological staging and grading (Boustead et al., 2014). Bladder cancer stem cells (BCSC) may give rise to distinct tumour cells causing tumour heterogeneity (Easwaran et al., 2014). Current data supports the concept [hierarchy model] that only a few cancer stem cells (CSC) possess such abilities (Beck and Blanpain, 2013, Kreso and Dick, 2014), as compared to the Stochastic Model in which all malignant cells possess tumorigenic potential. CSCs possess unique phenotypes, as evidenced by their expression of specific Cluster of Differentiation (CD) cell surface markers (Tarnok et al., 2010). CD surface markers are expressed when immune cells undergo differentiation. This leads to the expression of active moieties along their cell surface which later serve as markers for different immune cell subtypes (Andrews et al., 2013). These macromolecules can serve as ligands for fluorescent molecule conjugated receptors in flow cytometry (Gilbert and Ross, 2009).

Flow cytometry is a laser or impedance based approach for cell sorting (Giaretti, 1997). Fluorescence-activated cell sorting (FACS) is the most common use of flow cytometry in oncology (Cunderlikova et al., 2007). FACS enables the examination of heterogeneous cell populations while avoiding tissue shrinkage or sectioning artefacts associated with histological techniques (Herculano-Houzel et al., 2015). Moreover, the identification and purification of unique subpopulations of cells expressing particular cell surface markers is feasible without loss of cell viability (Basu et al., 2010).

Recent advances (Luchini and Cheng, 2017) have categorised bladder cancers into three groups: basal, intermediate and differentiated sub-types, with each possessing characteristic cell markers (such as keratins) (Volkmer et al., 2012). Keratins are a transcription product formed during epithelial proliferation and are usually conserved during neoplastic transformation. Bladder cancer cells expressing keratins possess unique cell surface receptors, identification of which could be utilised to

predict differentiation states. Keratin 14 (KRT14) is characteristic of the most primitive differentiation state, i.e. the basal subtype, while keratin 5 and keratin 20 are expressed in the intermediate and differentiated subtypes, respectively (Volkmer et al., 2012). Further studies performed using cell sorting have also revealed that certain tumour-initiating cells (TIC) possess cell surface markers [$CD44^{+}CK5^{+}CK20^{-}$] mirroring normal bladder basal cells. Cells sorted from these isolates have been shown to be capable of regenerating into heterogeneous tumours when implanted as xenografts (Chan et al., 2009). Additionally, the global gene expression profiling has shown that those sorted CSCs positive for $CD44^{+}$ have a phenotype similar to that of aggressive bladder cancer (Chan et al., 2010).

Knowledge of the cell cycle distribution of CSCs is ideal for identifying targets for therapeutic intervention prior to tumour initiation (Liu et al., 2016). These cell cycle distributions can also be identified using flow cytometry (Pozarowski and Darzynkiewicz, 2004) since resistant subpopulations possess autophagy-resistant characteristics unique to the G2/M phase cell block (Chappell and Dalton, 2010). Since cells in the G2/M phase are more susceptible to radiation than radio-resistant dormant (G1/0 and S phases) cells (Sinclair, 2012), further evaluation of their DNA content is necessary. Moreover, overexpression of CD44 stimulated by Interleukin-6 (IL-6) is observed in bladder cancer cells resistant to irradiation (Wu et al., 2017). Flow cytometry could serve to detect an aneuploid population of cells in high-grade urinary bladder carcinomas while sorting for cell surface markers (Melamed, 1992). A non-invasive approach using flow cytometry of urine samples while purging for the markers cytokeratin and CD45 has been proven to be useful for bladder cancer diagnosis (Barlandas-Rendon et al., 2002).

Chromatin flow cytometry can identify changes in the epigenetic makeup in response to histone acetylation and methylation (Obier and Muller, 2010), especially in drug-treated *in vivo* cultures of cancer biopsies. Sorted cells from the same could be utilised to identify characteristics unique to high-grade bladder carcinoma, like promoter hypermethylation (Catto et al., 2009). Optimised epitope

retrieval strategies have made it possible to detect 5-methylcytosine reliably using flow cytometry (Celik-Uzuner et al., 2017). Since promoter hypermethylation corresponds to advanced tumour staging and tumour progression (Catto et al., 2005), sorted tissue types with similar morphologies could be distinguished using a combinatorial approach involving both flow cytometry and bisulphite sequencing. This could also serve in identifying unique cell-signalling mechanisms which could be specifically targeted to increase response rates to therapeutic intervention (Drayton and Catto, 2012). Sorting bladder cancer tumour cells could also prevent risks associated with over- or under-staging using imaging tools. The predictive impact of epigenetic processes in bladder cancer is still unclear, however, and therefore warrants further investigation.

Hypothesis

I hypothesised that distinct bladder cancer subpopulations exist in freshly dissected bladder tissue types and in bladder cancer cell lines, and that these can be identified using FACS sorting.

I also hypothesised that these subpopulations exhibit distinct characteristics in bladder cell lines and bladder tissues.

Aim

To sort bladder cell lines and fresh tissues into distinct subpopulations using the cell surface markers CD44, CD47, CD49f and CD90.

4.2 Materials and methods

4.2.1 Patients Samples

A total of 38 tissue samples were used in this study. Both normal (n=4) and tumour (n=34) fresh bladder tissues were obtained from patients who had undergone either surgical removal of the bladder or part of the bladder, surgical removal of prostate (radical prostatectomy) at the Royal Hallamshire Hospital, Sheffield, UK. All patients underwent informed consent in an ethically approved programme (Investigation of Molecular Instability in the Pathogenesis of Urothelial Cancer, STH 15574).

The age of patients ranged from 47-94 years with a mean age of 72 years, and 28 out of 38 samples were from males. Of those samples, 24 bladder tumour tissues were subsequently excluded as they either contained too much necrotic tissue, failed tissue dissociation or straining during the sorting process. Thus, ten bladder tumour and three normal bladder biopsies were successfully disaggregated and analysed. The details of all tumour tissues stages and grades (A) as well as sorted tissue (B) are shown in table 4.1.

Table 4.1 The stage and grade of all bladder tumour tissues used in flow cytometry (A). The bladder tumour tissues sorted in this chapter.

A

Stage and Grade	Number (%)
pTa	13 (38.4%)
pT1	10 (29.4%)
≥pT2	11 (32.2%)
Total	34
G2	10 (29.4%)
G3	24 (70.6%)
Total	34

B

Sorted tissue	Grade (Stage)	Number
Intermediate grade	G2 (≤ pT1)	5
High grade	G3 (≥ pT2)	5

4.2.2 Flow cytometry

Bladder tissues were dissociated manually and strained through a filter to separate clumps and obtain a single cell suspension. Cell culture isolates were dissociated using a combination of trypsin and ethylene diamine tetra acetic acid (EDTA). Dissociated cells were washed multiple times and a lysis buffer of red blood cells (RBC) was added for the tissue samples only (RBC lysis buffer serves to remove erythrocytes which otherwise might influence the accuracy of the FACS® analysis). F_c receptor blocking was performed to prevent the immune complex from influencing the immune staining to be performed in the next step. Following the Fc receptor blockade, immune staining was performed for the cell surface markers (e.g. CD44, CD47, CD49f and CD90) and isotypes that matched the primary antibodies. The next steps involved cell sorting, which was performed using FACSAria™, following which data analysis was performed using FlowJo® software. DNA extraction was then performed on the sorted cells of both bladder tumour biopsies and normal tissues using a commercially available kit (DNeasy from Qiagen®). The extracted DNA was then used to perform downstream analysis (Figure 4.1).

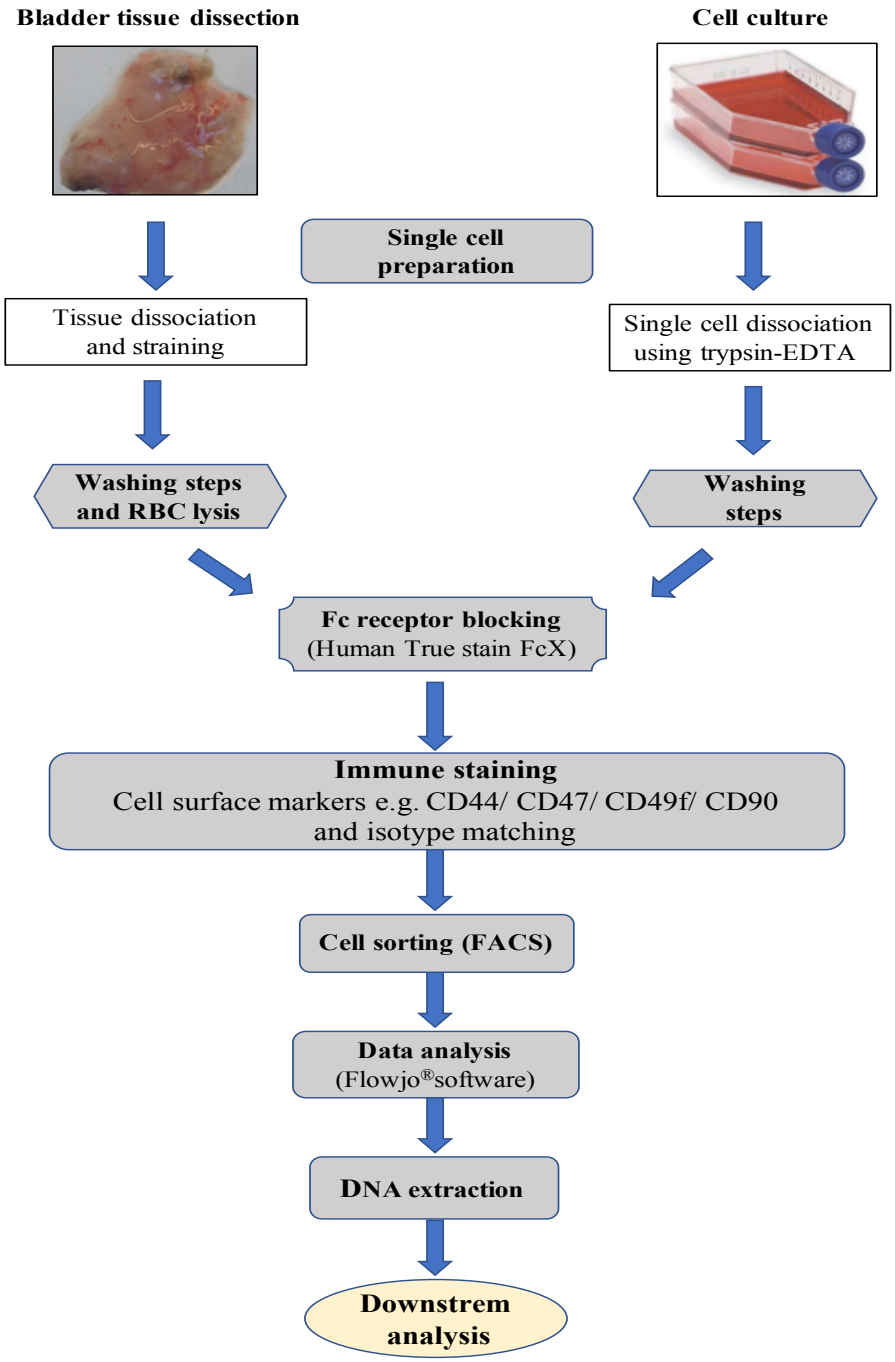

Figure 4.1 The general workflow followed in the research reported in this chapter.

Excised bladder tissues as well as bladder cell line isolates were dissociated, washed, blocked and then sorted for selected cell surface markers and their matched isotype. The data obtained was analysed using FlowJo® software prior to DNA extraction and downstream analysis.

4.2.3 Gating strategy for fluorescence activated cell sorting (FACS) analysis

For flow cytometry, specific gating was used to ensure optimal results from different tissues and cell lines (Lugli et al., 2010). Compensation and sorting procedures were performed using the BD FACSAria™ III cell sorter with the BD FACSDiva™ software. Dissociated cells were sorted in a few gating steps. First, the desired original population was gated while avoiding debris (Figure 4.2.a). Then, single cells were gated while avoiding doublets cells (Figure 4.2.b). After discrimination of the doublets cell, live cells were selected by gating the negative population that did not express the viability dye (Figure 4.2.c). The live cells obtained were pre-stained with live/dead viability dye that consisted of fluorophore-conjugated antibodies with different emission. They were then sorted into distinct live sub-populations. Cell sorting was either done for subpopulations which were specific for single cell surface markers or dual cell surface markers. After sorting, FlowJo software (version 10) was used to generate visualisation and numerical data (Figure 4.2).

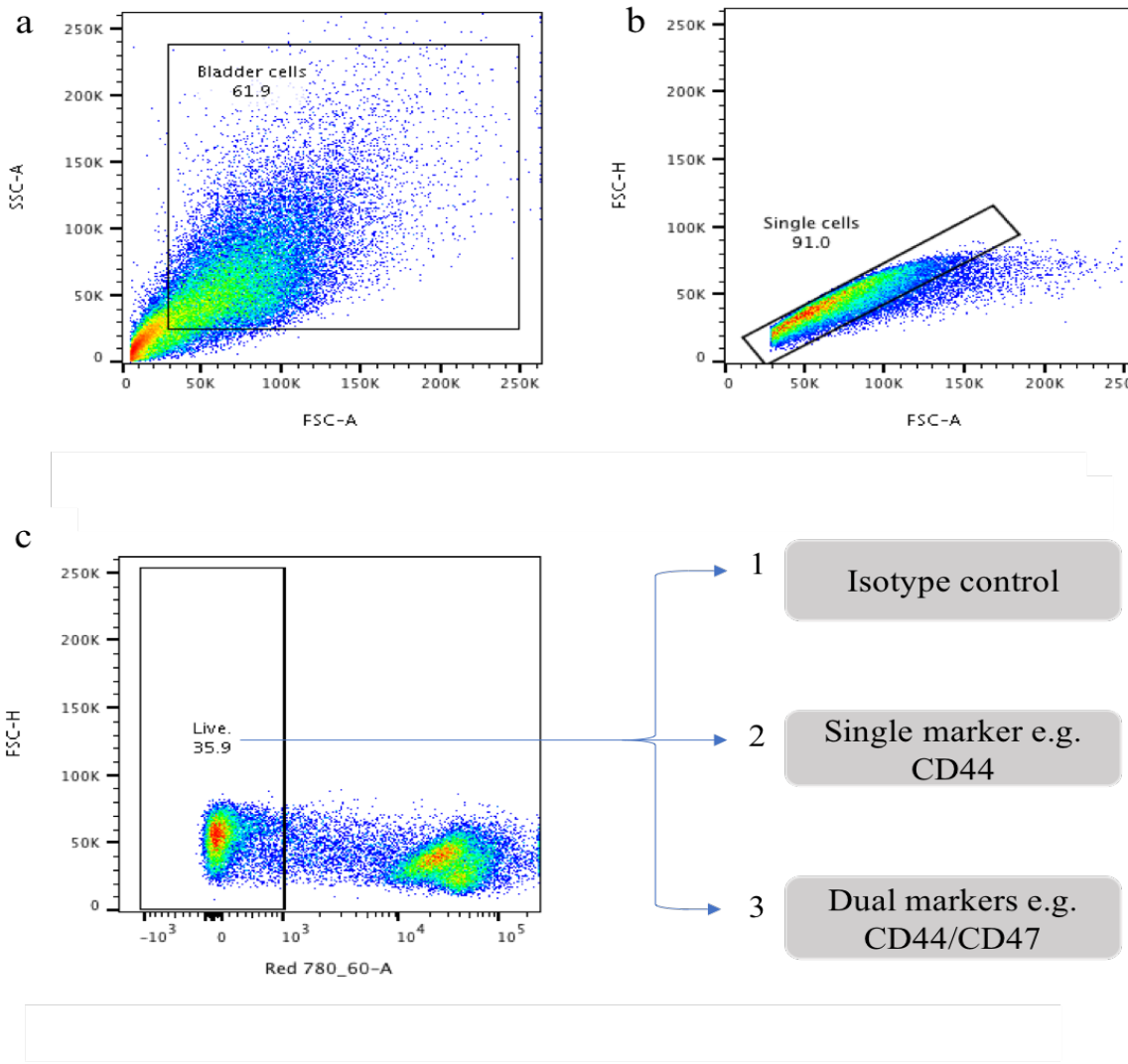

Figure 4.2 Gating strategy utilised for fluorescence activated cell sorting (FACS) analysis.

The protocol utilised sorted dissociated single cells from cell lines and aggregates or clumps of tissue samples. These were then sorted into live and dead tumour cells, following which the live cell isolates were sorted for isotype matched controls, for a single cell marker, e.g. CD44, as well as for dual markers, e.g. CD44/CD47.

4.2.4 Identification of non-specific binding in cell lines and tissue.

The primary antibody used in flow cytometry can result in non-specific binding (mainly to Fc receptors present on the cell surface). To test the non-specific binding of the primary antibody, an isotype that matched the primary antibody host species and the same conjugated fluorophore was selected. Emission spectra for all conjugated antibodies which were either conjugated to phycoerythrin (PE) or

allophycyanin (APC), as well their isotype-matched controls, were examined in order to identify whether there was any nonspecific binding reflected in the isotype emission spectra. The antibodies used were [PE anti-human/mouse CD49f, PE anti-human/ CD90 (Thy 1), APC anti-mouse/human CD44 and PE anti-human CD47]. As shown in Figure 4.3, no expression was observed in any of the isotypes used in this study.

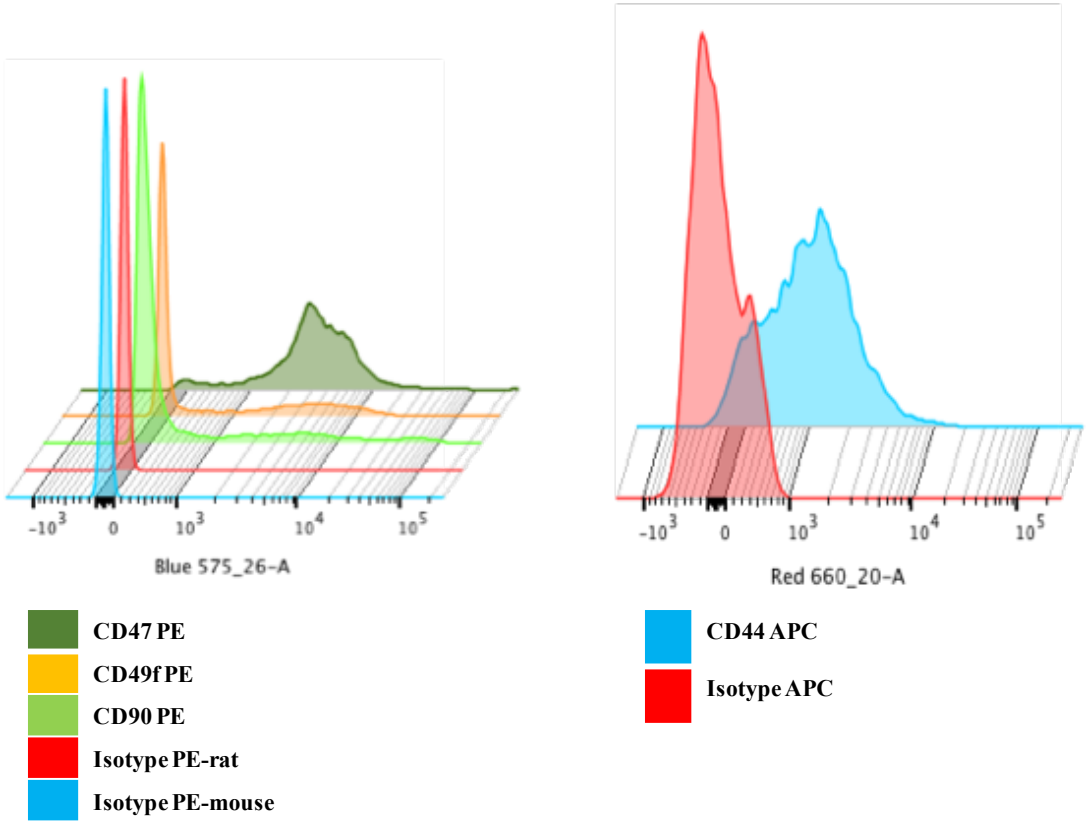

Figure 4.3 Fluorescence emission spectra for antibodies specific for the cell surface markers and isotypes.

Fluorescence emission spectra of all three cell surface markers, CD47, CD49f and CD90, together with their matched isotype, were conjugated with phycoerythrin (PE) (left side). The isotype PE-mouse (Mouse IgG1, K Isotype control) was used to check for the nonspecific binding of CD47 and CD90, while the isotype PE-rat (Rat IgG2a, K Isotype control) was used to check for the nonspecific binding for CD49f. The right side of the figure shows fluorescence emission spectra for cell surface marker CD44 and its matching isotype, both conjugated with allophycocyanin (APC) and the isotype control for this marker was (Rat IgG2b,K isotype control).

4.3 Results

4.3.1 Expression of CD44, CD47, CD49f and CD90 markers in cell lines

FACS was performed using five bladder cancer cell lines (EJ, EJ-Cisplatin Resistant (EJ-R), EJ-D4 clone, EJ-G7 clone and RT112) and a normal human urothelium cell line (NHU) with antibodies to CD44, CD90, CD47 and CD49f. The findings were compared with unstained controls. Analysis with FlowJo revealed various levels of expression for CD44, CD47 and CD49f in the cell lines, but no CD90 expression was detected in any of the bladder cell lines examined (Figure 4.4).

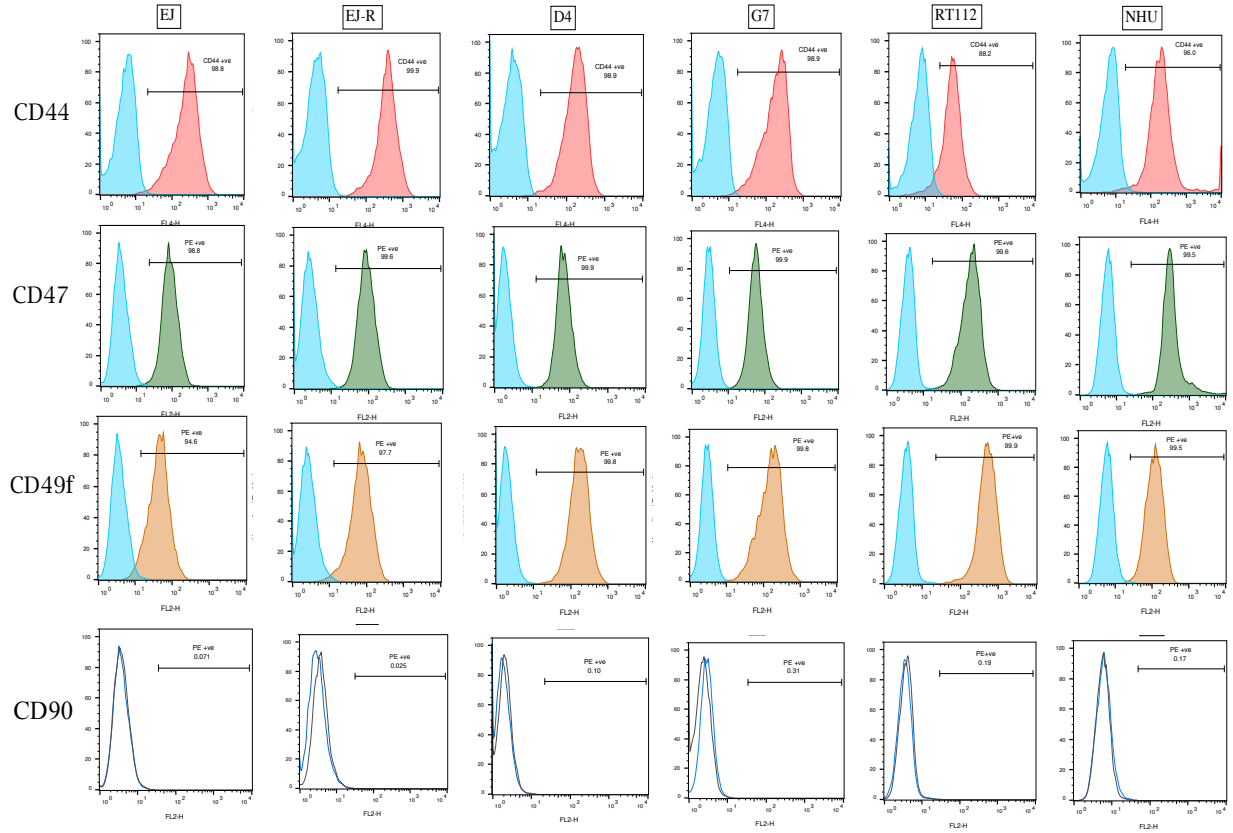

Figure 4.4 FACS® sorting analysis of bladder cell lines immune stained with the cell surface markers CD44, CD47, CD49f and CD90.

The representative histograms show the percentage of positive cells that express the cell surface marker CD44, CD47 and CD49f and their unstained control (blue histogram). Gating was applied to the unstained control sample and then to the relative sample.

There were significant differences in expression in the distribution of specific markers, like CD44 and CD49f, between the various cell lines. Post-hoc analysis performed using Tukey's honest significance

difference (HSD) test revealed significant differences in the mean expression levels of CD44 cell surface marker between the EJ-R cell line and the NHU cell line (p= 0.039) as well as between the NHU cell line and the RT112 cell line (p= 0.001). More than 99% of the cells in the EJ-R cell line expressed CD44, and just over 96% in the NHU cell line. The Among all the cell lines examined, the RT112 cell line had the lowest percentage of CD44 expression as a single marker (at just above 90%). Similarly significant expression levels were also apparent for the cell surface marker CD49f. In the EJ cell line 95% of the cells expressed this marker, and 99% in the RT112 were cell line (p= 0.041). D4 (p= 0.007) and G7 (p= 0.008) also had close to 99% expression of this marker. No significant expression levels were observed for the cell surface marker CD47, however. An analysis of variance (ANOVA) between cell lines performed on CD44 and CD49f markers revealed that the results are significant at 0.001 and 0.006 respectively; while no significance was observed for the CD47 marker (Figure 4.5).

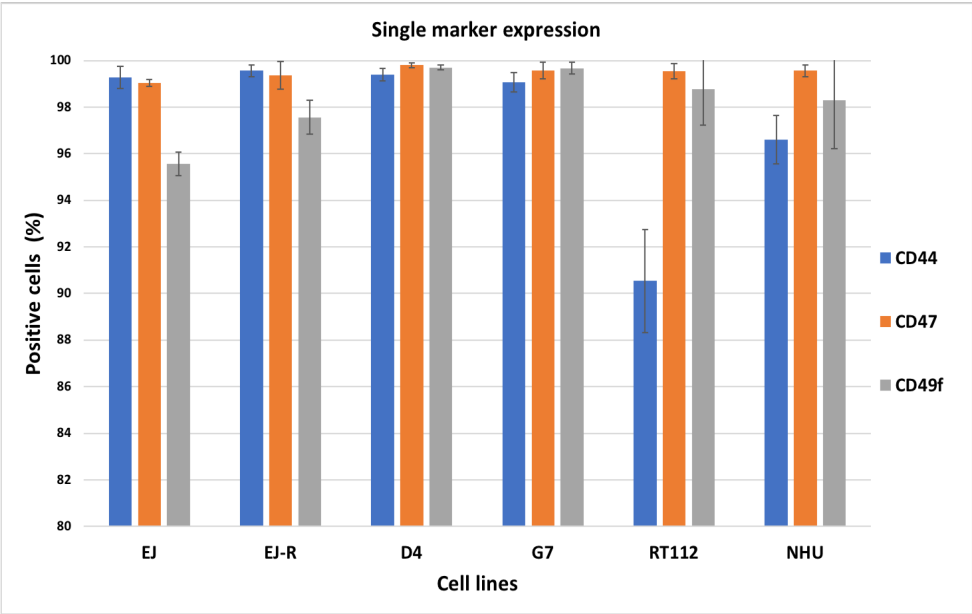

Figure 4.5 Analysis of single marker expression for all markers, CD44, CD47, CD49f and CD90, across different cell lines.

Six cell lines: EJ, EJR, EJ-D4 clone, EJ-G7 clone, RT112 and NHU were used for this investigation. The results were obtained from three independent replicates. Error bars represent ± standard deviation (± SD). Testing for the difference in the expression of cell surface markers between various cell lines was done using an analysis of variance (ANOVA). Post-hoc analysis performed using Tukey's honest significance difference (HSD) was used for multiple comparison.

4.3.2 Co-expression of CD44 and CD47 in bladder cell lines

Next, I analysed the co-expression of CD44 and CD47 in these cell lines. Once again, whilst the patterns were broadly similar, in-depth comparisons revealed the existence of distinct subpopulations of CD44 and CD47 dual positive cells (Figure 4.6).

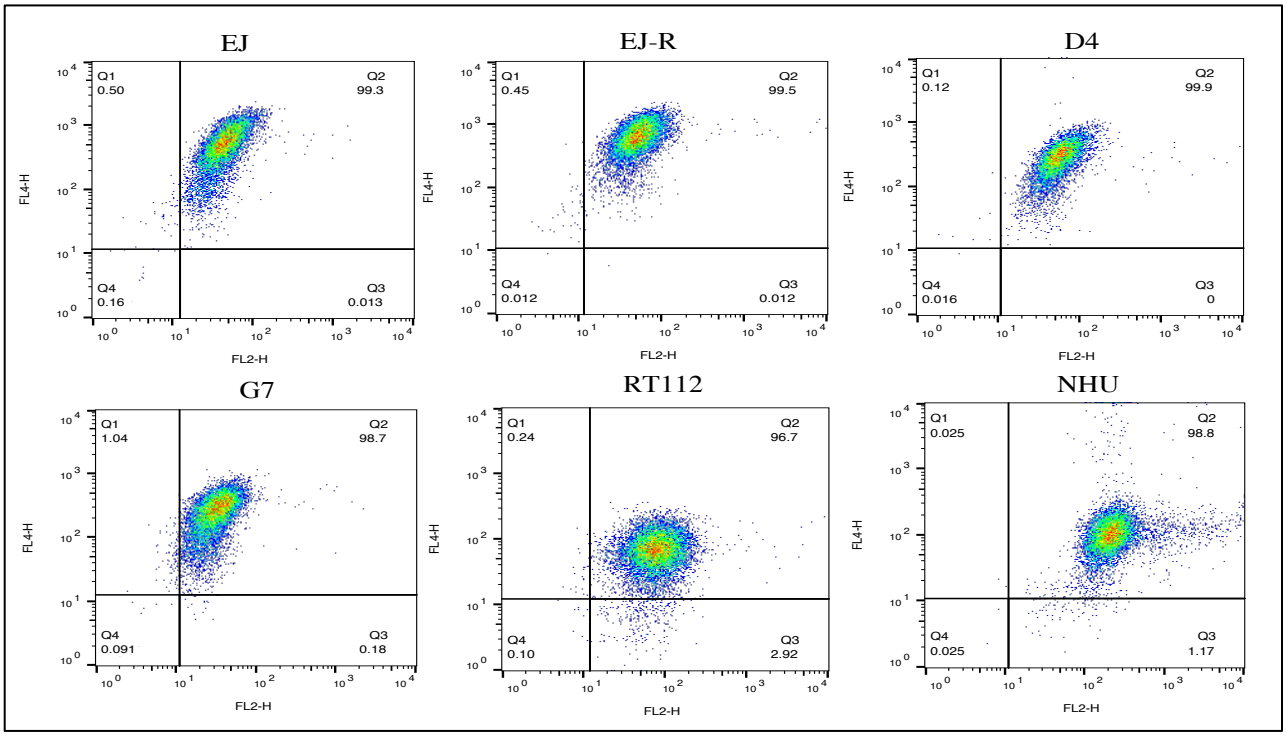

Figure 4.6 FACS® sorting analysis of different bladder cell lines using dual cell surface marker expression for CD44 and CD47.

The representative scatter plots show the percentage of positive cells that express the cell surface markers CD44 and CD47. Six cell lines were analysed: EJ, EJR, EJ-D4 clone, EJ-G7 clone, RT112 and NHU. Gating was first applied to the unstained control sample and then applied to its relative sample. The CD47 marker is represented on the X axis (FL2-H) and CD44 marker is represented on the Y axis (FL4-H).

Post-hoc analysis was performed using Tukey's honest significance difference (HSD) test and revealed differences in the mean expression levels of $CD47^{-}/CD44^{+}$ cell surface markers between the EJ-R cell line and NHU (P=0.05) and G7 (P=0.004), as well as between the EJ cell line and NHU (P=0.029) and G7 (P=0.006); also, between RT112 and NHU (P=0.013) and G7 (P=0.014), and between NHU and G7

(P=0.001). Furthermore, using Tukey's (HSD) testing, significant upregulation was observed in the expression levels of $CD47^{+}/CD44^{+}$ cell surface markers between EJ and RT112 (P=0.008), as well as between the EJ-R subpopulation and RT112 (P=0.005), and between RT112 and D4 (P=0.004). Significant upregulation of the mean expression levels were not observed for $CD47^{+}/CD44^{-}$ and $CD47^{-}/CD44^{-}$. Analysis of variance (ANOVA) was performed and revealed that the mean results were significant overall for $CD47^{+}/CD44^{+}$ cell surface markers (Figure 4.7).

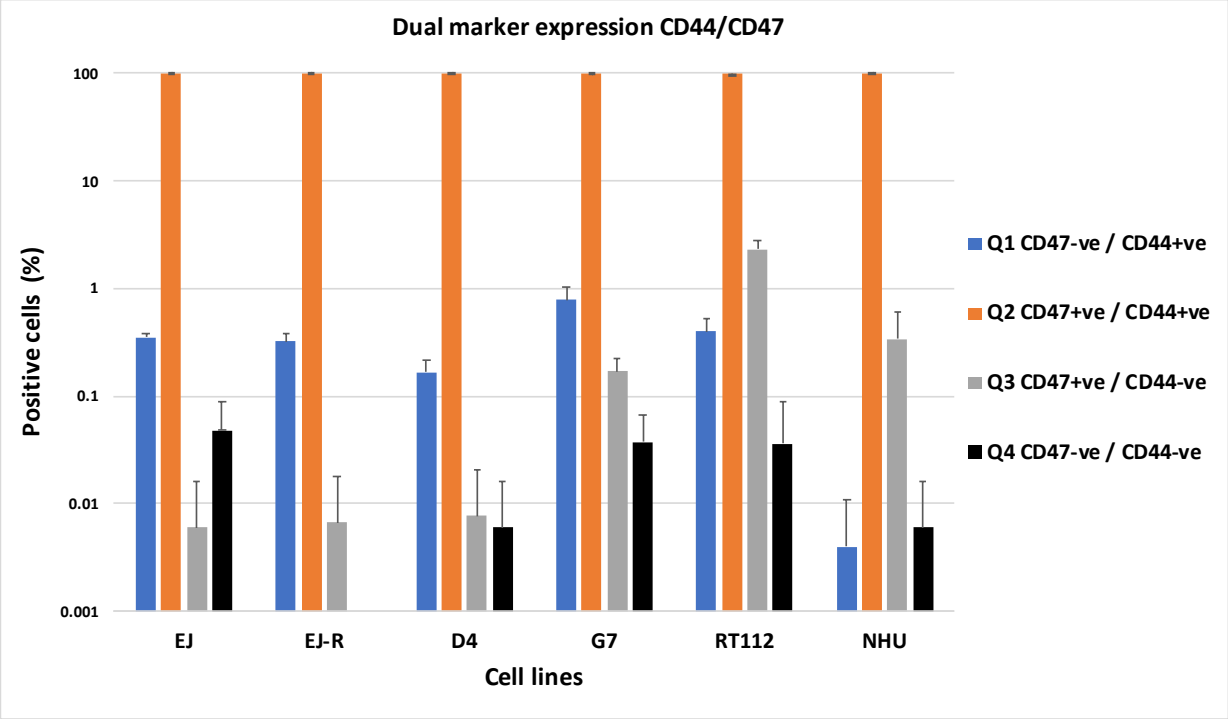

Figure 4.7 Analysis of the expression of dual cell surface markers of CD44 and CD47 for bladder cell lines.

Six cell lines were analysed: EJ, EJR, EJ-D4 clone, EJ-G7 clone, RT112 and NHU. Results are from three independent replicates. Error bars represent ± standard deviation (±SD). The data is shown in logarithmic scale. Testing for the difference in the expression of cell surface markers between various cell lines was done by using an analysis of variance (ANOVA). Post-hoc analysis performed using Tukey's honest significance difference (HSD) was used for multiple comparison. The analysis revealed elevated expression levels of $CD47^{+}/CD44^{+}$ marker in tumour cells in the cell lines examined.

4.3.3 Co-expression of CD44 and CD49f

I repeated the FACS analysis using antibodies to both CD44 and CD49f. As before, it was clear that there were distinct subpopulations positive for both CD44 and CD49f (Figure 4.8).

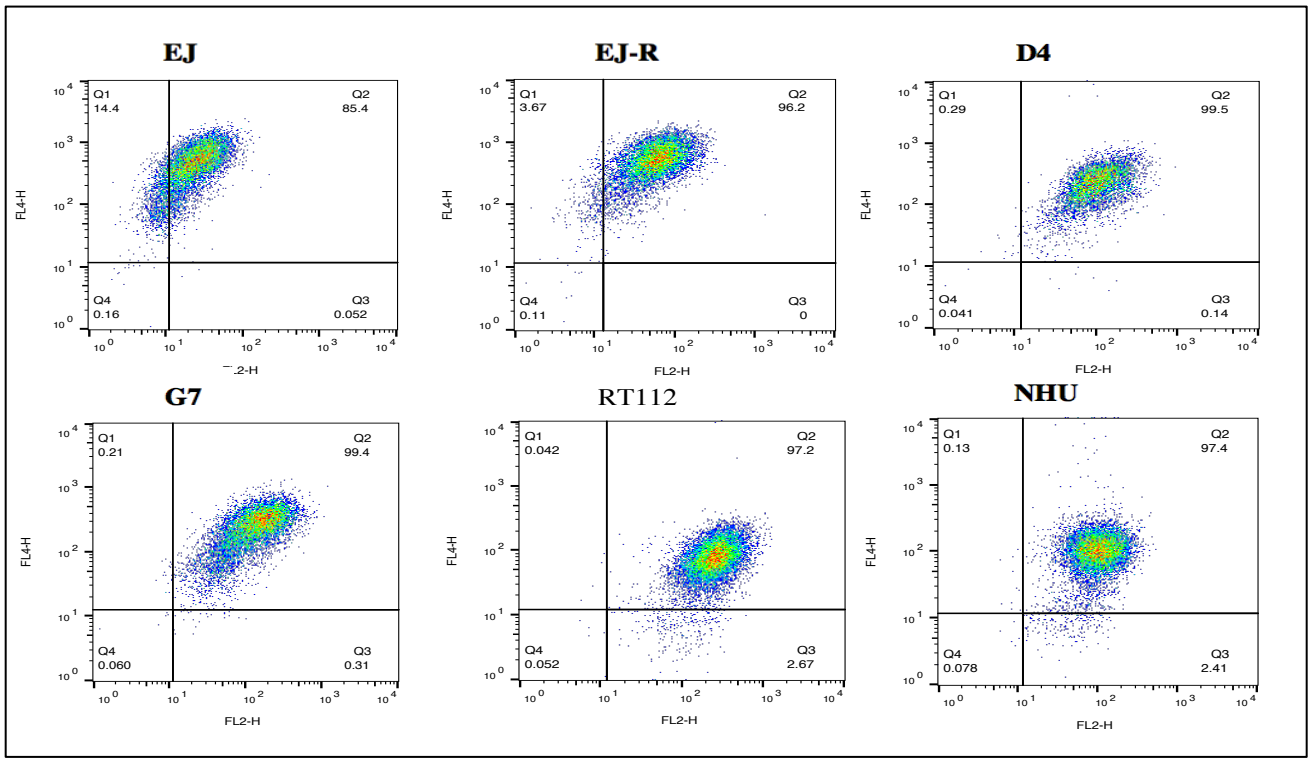

Figure 4.8 FACS® sorting analysis of different bladder cell lines using dual cell surface markers expression for CD44 and CD49f.

The representative dot plot shows the percentage of positive cells that expressed the cell surface markers CD44 and CD49f. Six cell lines were analysed: EJ, EJR, EJ-D4 clone, EJ-G7 clone, RT112 and NHU. Gating was first applied to the unstained control sample and then applied to its relative sample. The CD49f marker is represented on the X axis and the CD44 marker is represented on the Y axis.

Statistical analysis revealed significant differences in expression patterns in the distribution of cells positive for both CD49f and CD44. Post-hoc analysis performed using Tukey's honest significance difference (HSD) test revealed a significant difference in the expression levels of $CD49f^{-}/CD44^{+}$ cell surface marker between the EJ cell line and all other cell lines (P=0.001), between EJ-R and RT112 (significance level at 0.009), D4 (P=0.014), G7 (P=0.015) and NHU (P=0.012); as well as between EJ-R and RT112 (P=0.009) and NHU (P=0.012). Similarly, further post-hoc analysis performed using

Tukey's honest significance difference (HSD) test revealed a significant difference in the expression levels of $CD49f^{+}/CD44^{+}$ cell surface markers between EJ and all other cell lines (P=0.001); and between the EJ-R subpopulation and D4 (P=0.022 and P=0.049), G7 (P=0.031) and NHU (P=0.026). Significant differences in expression levels were also observed for $CD49f^{+}/CD44^{-}$ cell surface markers between the RT112 and all other cell lines (P=0.001). Significance difference in the expression levels were also observed for $CD49f^{-}/CD44^{-}$ cell surface markers between EJ and EJ-R (P=0.001), RT112 (P=0.002), G5 (P=0.001) and NHU (P=0.001). An analysis of variance (ANOVA) revealed that the results are significant overall for all quadrants examined (Figure 4.9).

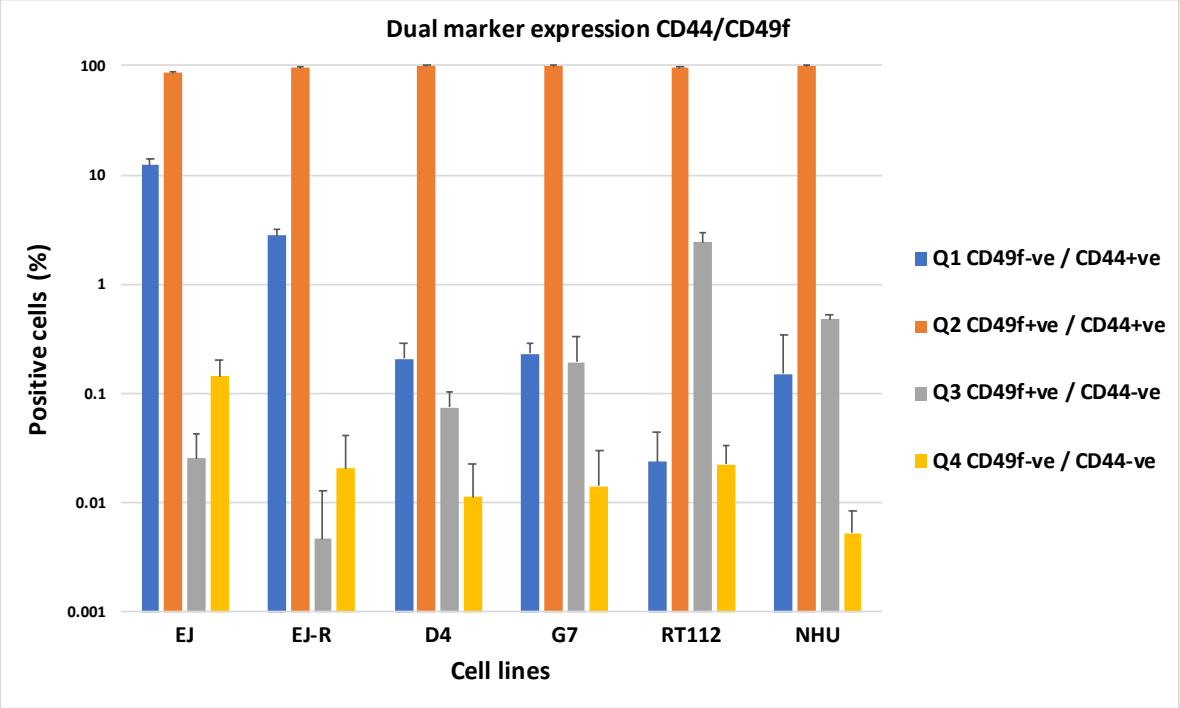

Figure 4.9 Analysis of dual cell surface markers expression of CD44 and CD49f for bladder cell lines.

The six cell lines used for this investigation included EJ, EJR, EJ-D4 clone, EJ-G7 clone, RT112 and NHU cell lines. The results were obtained from three independent replicates. The error bars represent ± standard deviation (±SD). The data is shown in logarithmic scale. Testing for the difference in cell surface markers expression between various cell lines was done by using an analysis of variance (ANOVA). Post-hoc analysis performed using Tukey's honest significance difference (HSD) was used for multiple comparison.

4.3.4 Expression of CD44, CD47, CD49f and CD90 markers in fresh tissue samples

Bladder tissue samples were tested in order to investigate the presence of the CD90 marker, as well as the expression of the other cell surface markers across different bladder tissues. FACS was performed for the three bladder tissue types available: normal, intermediate grade (WHO Grade 2) and high-grade (WHO Grade 3) tumours against their unstained controls. Analysis revealed differences in all three-tissue types examined (Fig 4.10).

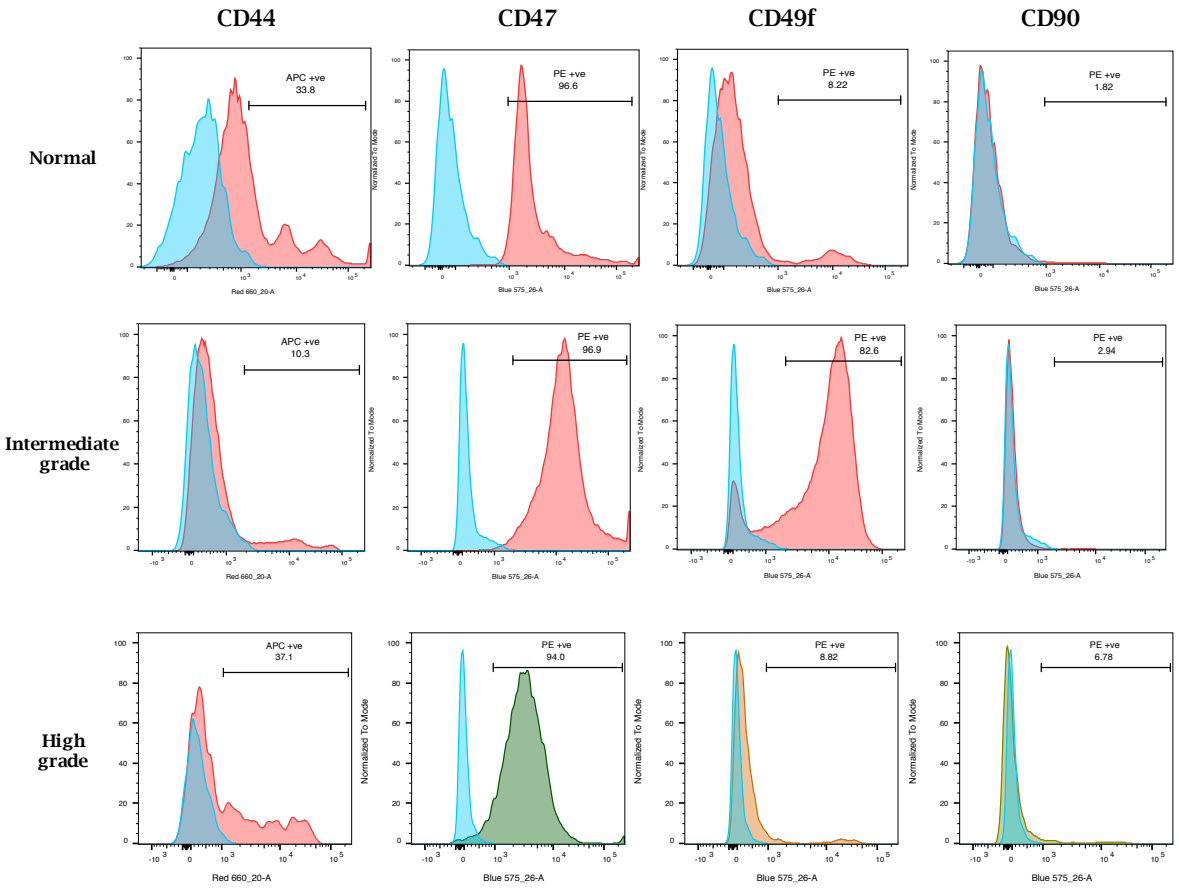

Figure 4.10 FACS® sorting analysis of bladder tumour cells stained with single cell surface markers CD44, CD47, CD49f and CD90.

The representative histograms demonstrate the percentage of positive cells that express single cell surface marker (CD44, CD47, CD49f and CD90) and their unstained control (blue). Gating was applied to the unstained control sample and then applied to the relative sample.

Post-hoc analysis performed using Tukey's honest significance difference (HSD) test revealed significant differences in the mean expression levels of each cell surface marker in each tissue type (Figure 4.11). For example, 8% of cells expressed CD49f in normal tissue, whereas 72% of cells expressed CD49f in intermediate grade tumour tissue (a difference that was significant at P= 0.001), while 21% of cells expressed CD49f in high-grade tumour tissue (P=0.001, compared to expression in intermediate grade tissue). The differences in the distribution of CD90 positive cells were also highly significant between normal tissue (with 3% of the cells expressing CD90) and high-grade bladder tumour tissue (were 9% of the cells expressed CD90) (P=0.008), and also between high-grade and intermediate grade bladder tumour tissues (were 5% of the cells expressed CD90) (P= 0.044) tumours. No significant difference was seen for the cell surface markers CD44 and CD47 in all tissues examined. An analysis of variance (ANOVA) performed revealed that the results are significant overall for CD90 (P=0.008) and for CD49f (P=0.001) (Figure 4.11).

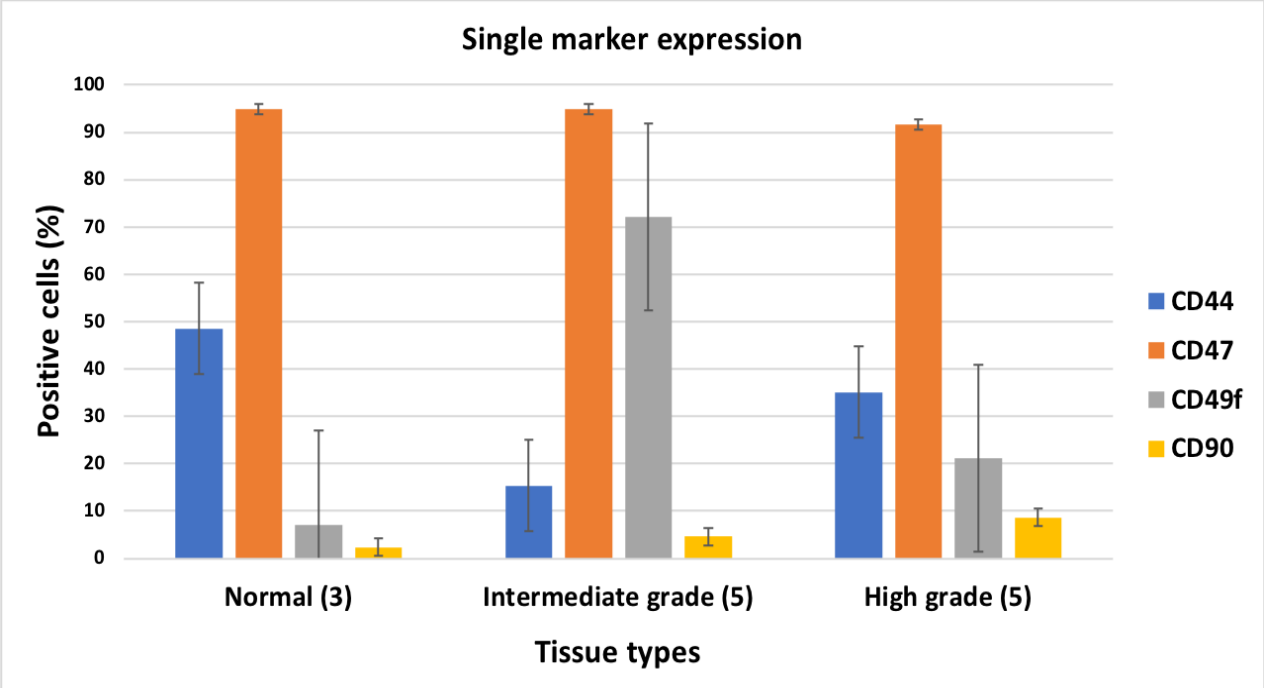

Figure 4.11 Analysis of the expression of single cell surface markers CD44, CD47, CD49f and CD90 in different bladder tissue types.

Three normal bladder tissues, five intermediate grade bladder tissue tumours and five high-grade bladder tissue tumours were used. The results were obtained from independent biological replicates. The error

bars represent ± standard deviation (± SD). Testing for the difference in the expression of cell surface markers between bladder tissue types was done using analysis of variance (ANOVA). Post-hoc analysis was performed for multiple comparison using Tukey's honest significance difference (HSD).

4.3.5 Co-expression of CD44 and CD47 in fresh bladder tissues

FACS was performed on the three bladder tissues types using antibodies to CD44 and CD47. FACS data characterisation revealed the existence of distinct subpopulations positive for dual cell surface markers CD44 and CD47 (Figure 4.12).

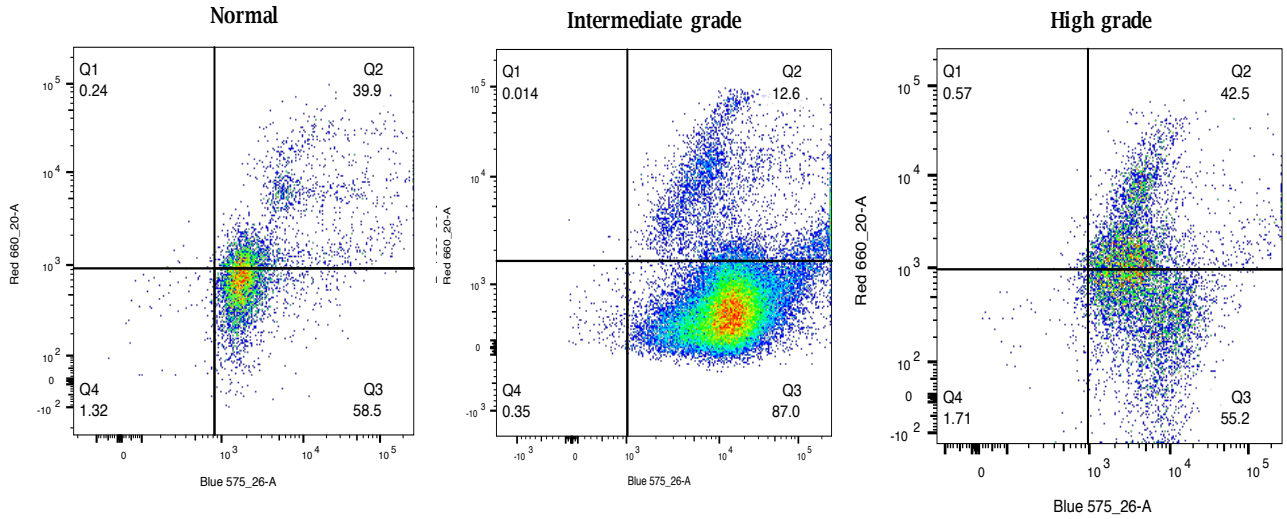

Figure 4.12 FACS ® sorting analysis of bladder tissue cells stained for dual cell surface markers CD44 and CD47.

The representative dot plot illustrates the percentage of positive cells that expressed the cell surface marker CD44 and CD47. Gating was first applied to the unstained control sample and then applied to its relative sample. The CD47 marker is represented on the X axis and the CD44 marker is represented on the Y axis.

Cells positive for both CD47 and CD44 were highest in normal bladder tissue (55%) followed by high-grade bladder tumour tissue (45%) and intermediate grade bladder tumour tissue (18%). Significant numbers of cells positive for CD47 were present in intermediate grade bladder tissue (78%), high-grade (45%) and normal urothelial tissue (42%).

Statistical analysis revealed divergent expression patterns in the distribution of cells positive for both CD44 and CD47 in different bladder tissue types. Performing analysis of variance (ANOVA) revealed that the results were significant overall between different bladder tissue types only for the $CD47^{+}/CD44^{+}$ cell surface marker (P= 0.042) and $CD47^{+}/CD44^{-}$ cell surface marker (P= 0.029). Post-hoc analysis was performed using Tukey's honest significance difference (HSD) test revealed significant mean expression levels of $CD47^{+}/CD44^{-}$ cell surface marker between the intermediate grade and high-grade bladder tumour tissues (P= 0.049) only (Figure 4.13).

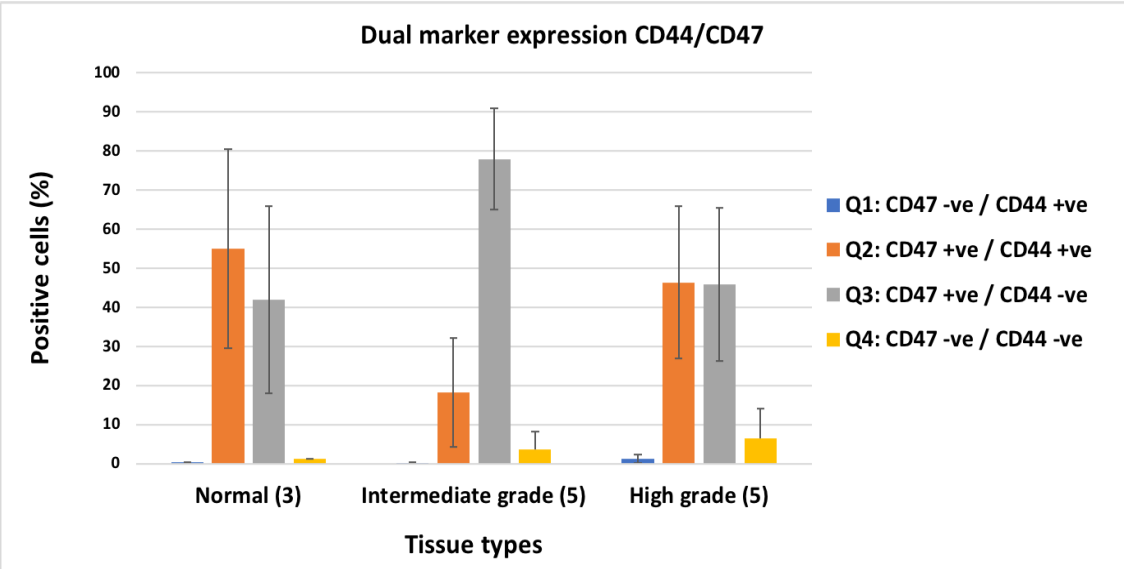

Figure 4.13 Analysis of the expression of dual cell surface markers of CD44 and CD47 for different bladder tissue types.

Three normal bladder tissues, five intermediate grade bladder tissue tumours and five high-grade bladder tissue tumours were used. The results were obtained from independent biological replicates. The error bars represent ± standard deviation (± SD). Testing for the difference in cell surface marker expression between various cell lines was done using analysis of variance (ANOVA). Post-hoc analysis was performed using Tukey's honest significance difference (HSD) for multiple comparison.

4.3.6 Co-expression of CD44 and CD49f in fresh bladder tissues

Next, FACS was performed for cells with expression of both cell surface markers CD44 and CD49f (Figure 4.14).

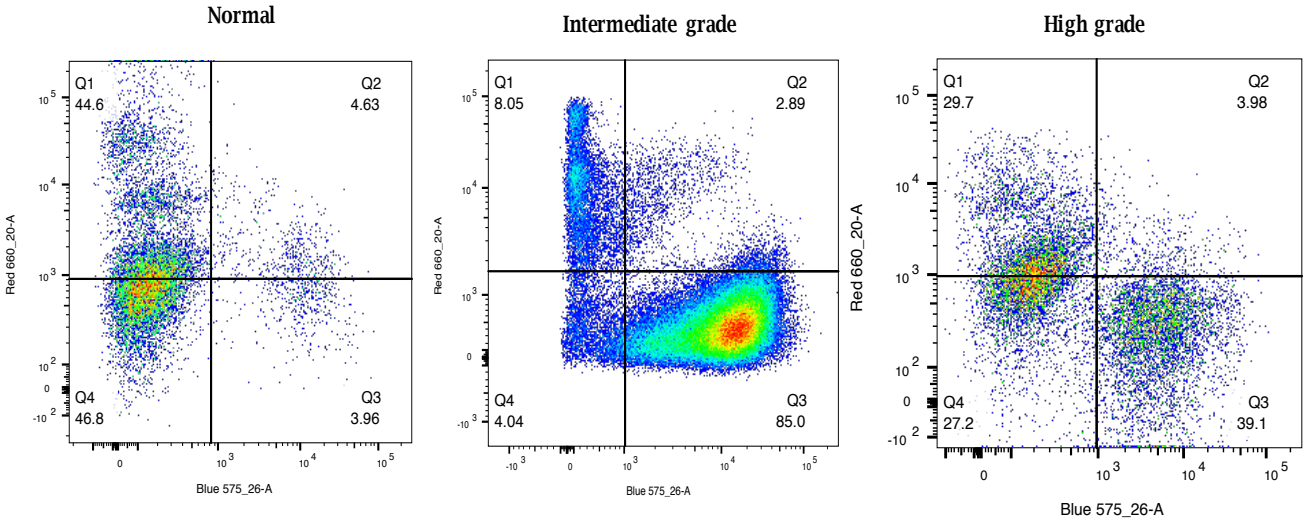

Figure 4.14 FACS ® sorting analysis of bladder tissue cells stained with dual cell surface markers CD44 and CD49f.

The representative dot plot illustrates the percentage of positive cells that expressed both cell surface marker CD44 and CD49f. Gating was first applied to the unstained control sample and then applied to its relative sample. The CD49f marker is represented on the X axis and the CD44 marker is represented on the Y axis.

Only a small proportion of cells were positive for both CD49f and CD44 expression (not more than 4% in all the graded tissue examined). Significant numbers of cells positive for CD44 were present in normal bladder tissue (58%), high grade (42%) and intermediate grade (12%) bladder tumour tissues. Cells positive for CD49f but negative for CD44 were highest in intermediate grade bladder cancer (70%) followed by high-grade bladder cancer (18%) and normal tissue (4%).

Statistical analysis revealed divergent expression patterns in the distribution of cells positive for CD44 and CD49f in the bladder tissues types (ANOVA P=0.011). Post-hoc analysis performed using Tukey's

honest significance difference (HSD) test revealed a significant difference in the expression levels of $CD49f^{-}/CD44^{+}$ cell surface markers between normal tissue and intermediate grade tumours only (P=0.012). The difference in the pattern of cells with $CD49f^{+}/CD44^{-}$ expression was significant when compared between intermediate and high-grade bladder tumours (P=0.001) (Figure 4.15).

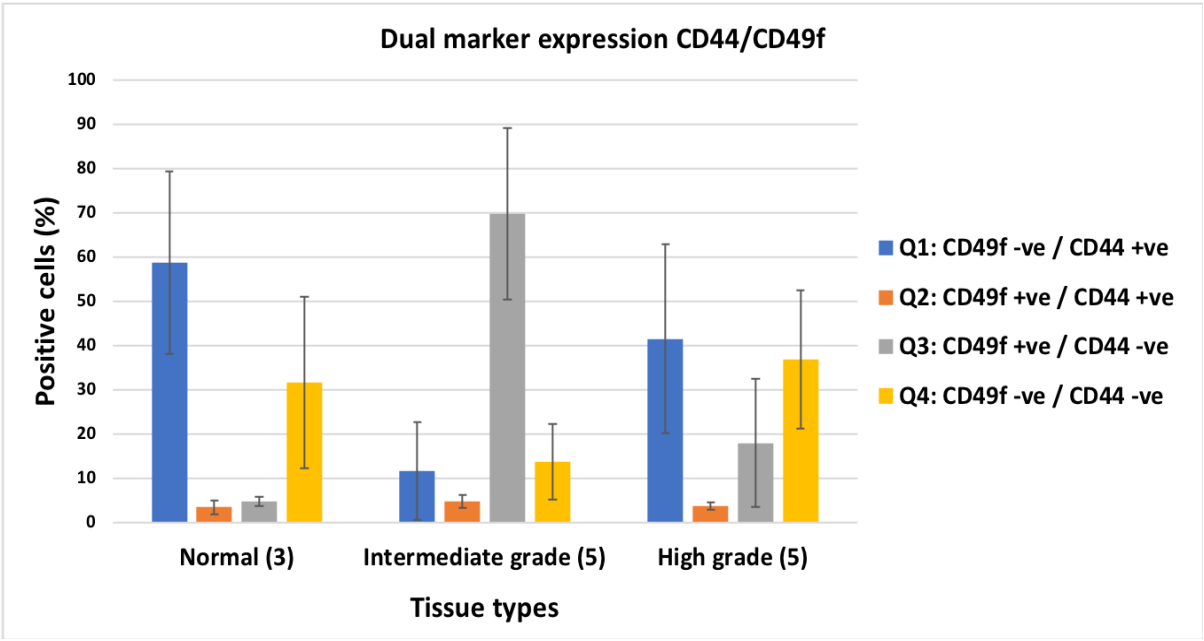

Figure 4.15 Analysis of dual cell surface markers expression of CD44 and CD49f for different bladder tissue types.

Three normal bladder tissues, five intermediate grade bladder tissue tumours and five high-grade bladder tissue tumours were used. The results were obtained from independent biological replicates. The error bars represent ± standard deviation (± SD). Testing for the difference in the expression of cell surface markers between various cell lines was done using analysis of variance (ANOVA). Post-hoc analysis was performed using Tukey's honest significance difference (HSD) for multiple comparison.

4.3.7 Co-expression of CD44 and CD90 in fresh bladder tissue

Finally, I performed FACS using CD44 and CD90 antibodies in these three bladder tissue types (Figure 4.16).

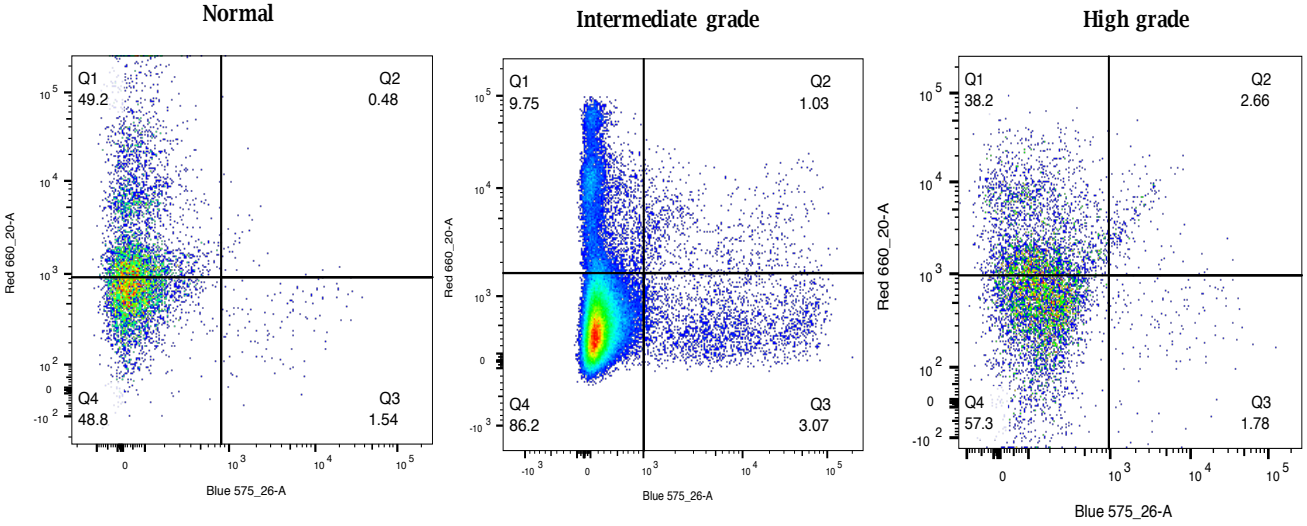

Figure 4.16 FACS® sorting analysis of bladder tissue cells stained with dual cell surface markers CD44 and CD49f.

The representative dot plot illustrates the percentage of positive cells that express the cell surface markers CD44 and CD90. Gating was first applied to the unstained control sample and then applied to its relative sample. The CD490 marker is represented on the X axis and the CD44 marker is represented on the Y axis.

The number of cells positive for both CD90 and CD44 were quite low in all the graded biopsy tissues examined. In the high-grade bladder tumour biopsy 4% of the cells expressed both these markers while intermediate grade bladder tumour tissues (2%) and normal bladder tissue (1%) were similarly lowered. Elevated numbers of the cells positive for the marker CD44 but negative for CD90 were present in normal urothelial tissue (62%), followed by high-grade bladder tumour tissue (45%) and intermediate bladder tumour tissue (15%). The number of cells negative for both these markers were highest in intermediate bladder tumour tissue biopsies (80%), high-grade bladder tumour tissues (45%) and normal bladder tissue (35%).

Analysis of variance (ANOVA) revealed divergent expression patterns in the distribution of cells positive for both CD44 and CD90 in the bladder tissues (ANOVA P=0.009) as well as between the groups for $CD90^{-}$ /$CD44^{-}$ cell surface markers (P=0.010). Post-hoc analysis performed using Tukey's honest significance difference (HSD) test revealed a significant difference in the expression levels of $CD90^{-}$ /$CD44^{+}$ cell surface marker in normal urothelial tissue compared to intermediate grade (P=0.01), and also between intermediate and high-grade (P=0.045). The differences in expression levels were also significant for $CD90^{-}$/$CD44^{-}$ in normal urothelial cells and intermediate grade (P=0.014), and also between intermediate and high-grade (P= 0.032) (Figure 4.17).

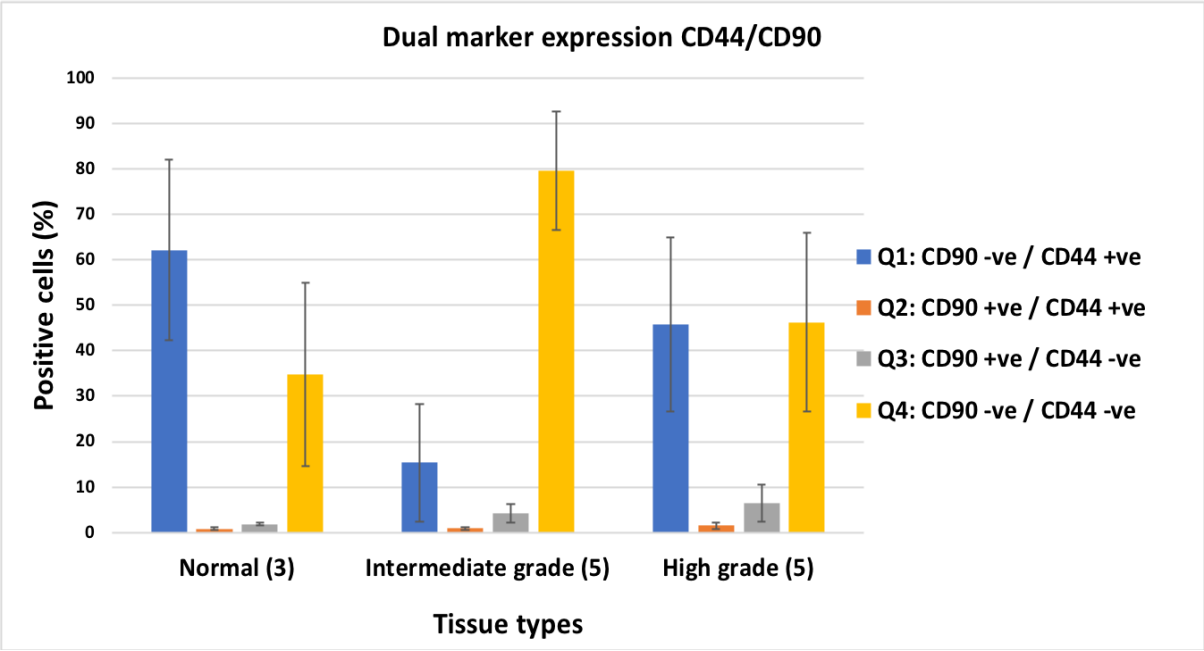

Figure 4.17 Analysis of dual cell surface markers expression of CD44 and CD49f for different bladder tissue types.

Three normal bladder tissues, five intermediate grade bladder tissue tumours and five high-grade bladder tissue tumours were used. The results were obtained from independent biological replicates. The error bars represent ± standard deviation (± SD). Testing the difference in cell surface markers expression between bladder tissue types was done by using an analysis of variance (ANOVA). Post-hoc analysis was performed using Tukey's honest significance difference (HSD) for multiple comparison.

4.3.8 Differences in the expression of cell surface markers between bladder cell lines and fresh tissues

In this chapter I have analysed the expression of various cell surface markers in cell lines and fresh tissues. Cell lines are used as dynamic, flexible, reproducible models to deliver an understanding of cancers, but little is known about how well they compare with primary tissues. To understand this comparison, I compared the expression of the cell surface markers examined in this chapter.

Statistical analysis (t-test) revealed significant differences in the distribution of expression patterns for cells positive for all the single surface markers expression examined (with the exception for the CD47 marker as a single expression, see Figure 4.18). Also, significant differences were observed in the expression of most of the dual markers between different bladder cell lines and bladder tissues types. This was observed between NHU cell line vs normal bladder tissue, the RT112 cell line vs intermediate grade bladder tumour tissue and the EJ cell line vs high-grade bladder tumour tissue (Figure 4.18, Figure 4.19 and Figure 4.20).

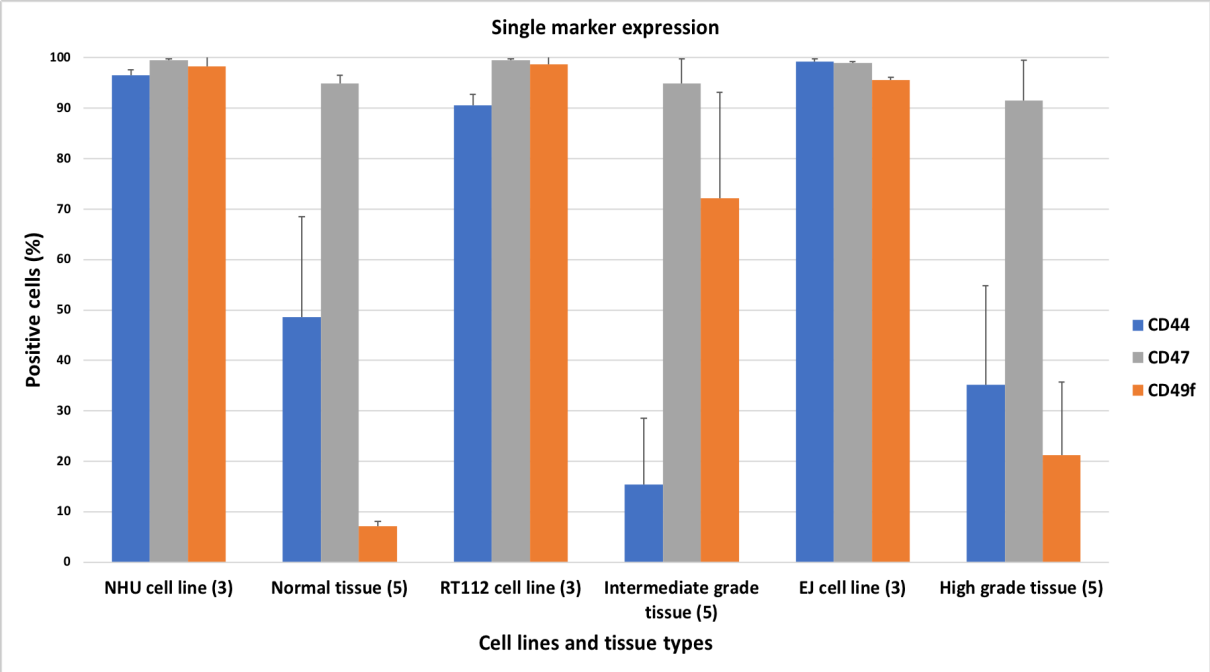

Figure 4.18 Expression of single markers in cell lines vs bladder tissue types.

The bar chart shows the percentage of various cell surface markers in bladder cancer cell lines (EJ and RT112) and a normal human urothelium cell line (NHU) as well as the bladder tissue types: normal, intermediate grade and high-grade tumours. The results were obtained from independent biological replicates of bladder tissues and three independent replicates of cell lines. The error bars represent ± standard deviation (± SD). Testing for differences in the expression of the cell surface markers between bladder tissues and cell lines was done by independent T- test.

Sorting for bladder cancer cells expressing both CD44 and CD47 revealed a very high proportion of these in the NHU, RT112 and EJ cell lines. 98% or more of the cells in these cell lines expressed these dual markers. In comparison, there was a lower expression of these markers in the normal urothelial tissue from biopsies (55%) and high-grade bladder cancer biopsies (45%). Intermediate grade bladder cancer biopsies (18%) had the lowest number of cells positive for both CD44 and CD47. This outcome was related to the higher numbers of cells that were positive for the lone cell surface marker CD47 (78%) but negative for CD44. A high proportion of cells positive for CD47 alone was also evident in normal tissue (42%) and high-grade bladder cancer biopsies (45%), while a small proportion of tissue cells

lacked both these cell surface receptors: 6% in high-grade bladder cancer biopsies, 4% in intermediate grade and 2% in normal tissue (Figure 4.19).

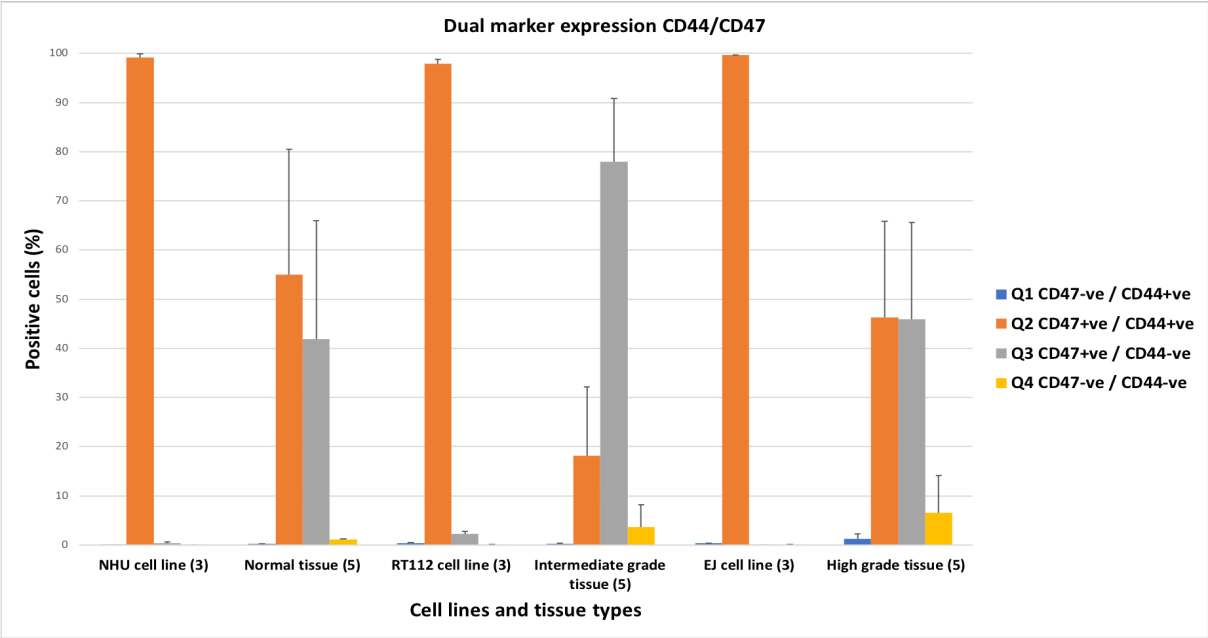

Figure 4.19 Co-expression of dual markers CD44 and CD47 in cell lines vs bladder tissue types. The bar chart shows the percentage of various cell surface markers in bladder cancer cell lines (EJ and RT112) and a normal human urothelium cell line (NHU) as well as the bladder tissue types: normal, intermediate grade and high-grade tumours. The results were obtained from independent biological replicates of bladder tissues and three independent replicates of cell lines. The error bars represent ± standard deviation (± SD). Testing for differences in the cell surface markers expression between bladder tissues and cell lines was done by independent T- test.

Sorting for bladder cancer cells revealed a very high proportion expressing both CD49f and CD44 in the NHU, RT112 and EJ cell lines. 96% or more of the cells in the NHU and RT112 cell lines were positive for these dual markers, while the EJ cell line had slightly lower expression levels of cells positive for both these markers at 88%. When these results were compared with the tissue samples from biopsies, however, the expression of both CD49f and CD44 together was much less: 4% in normal tissue, 6% in intermediate grade biopsies and 3% in high-grade bladder tumour biopsies. Bladder cells positive for the cell surface receptor CD44 but lacking CD49f, meanwhile, were elevated in the normal tissue

biopsies (59%), high-grade tissue biopsies (42%), EJ cell line (13%) and intermediate grade tissue (12%). A significant proportion of cells lacking both CD49f and CD44 receptors were apparent in high-grade biopsy tissues (36%) and normal tissue (32%) (Figure 4.20).

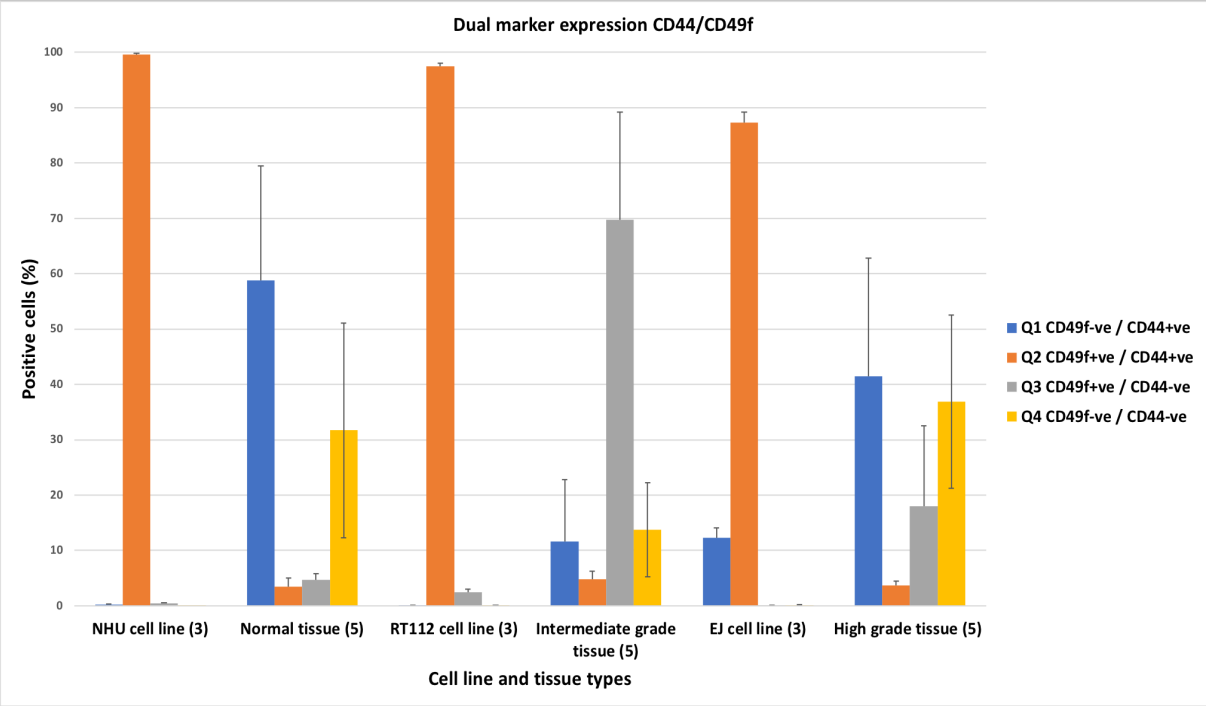

Figure 4.20 Co-expression of dual markers CD44 and CD49f in cell lines vs bladder tissue types.

The bar chart shows the percentage of various cell surface markers in bladder cancer cell lines (EJ and RT112) and a normal human urothelium cell line (NHU) as well as the bladder tissue types: normal, intermediate grade and high-grade tumours. The results were obtained from independent biological replicates of bladder tissues and three independent replicates of cell lines. The error bars represent ± standard deviation (± SD). Testing for differences in the expression of the cell surface markers n between bladder tissues and cell lines was done by independent T- test.

4.4 Discussion

Fluorescence activated cell sorting (FACS) has enabled a critical assessment of otherwise inaccessible subpopulations in bladder cancer. Here FACS was used for the identification and characterisation of subpopulations present in fresh malignant and normal bladder tissues and in bladder cancer cell lines.

It was found that the cell lines had enhanced expression of CD44, CD47 and CD49f, whilst CD90 was absent (refer Figure 4.5). The CD90 receptor is often upregulated in bladder cancer following resection (Takeuchi et al., 2016) and so its absence could indicate the loss of cell subpopulations by in vitro passage (Volkmer et al., 2012). The expression of CD44 and CD49f could imply that these cell lines constitute an intermediate bladder cancer population which lack the basal subtype observed in CD90 positive bladder cancer cells (Volkmer et al., 2012). This is contrary to recent data (Earl et al., 2015) which has suggested the existence of aggressive tumour subtypes in bladder cancer cell lines. High expression of CD44, CD47 and CD49f in both the cell lines and normal human urothelial cultures implies that these possess a more terminally differentiated subtype, as observed in urothelial carcinomas (Schulz, 2006, Tian et al., 2015). Selection of CD90(-) cells or adaption through somatic alteration, e.g. altered CpG sites (Nickerson et al., 2017), could be responsible for the absence of the CD90 surface marker in these cell lines. This finding cautions against the use of cell lines when extrapolating findings into human cancers (Dirks et al., 1999, Masters et al., 1988, Bian et al., 2017). Existing data suggests that enriched bladder cancer cells positive for CD90 did not possess cancer stem cell like characteristics but instead exhibited elevated phenotypic plasticity (Skowron et al., 2015).

The existence of cell subpopulations expressing both CD44 and CD47 (refer Figure 4.7) implies that these surface markers play a role in the survival of the examined cell lines or reflect populations capable of this growth. Although CD44 has previously been identified as unviable as a prognostic marker of bladder cancer (Hofner et al., 2014), its expression has been identified as a hallmark of tumour-initiating

cells (Chan et al., 2009). Co-expression of CD44 with CD47 (a known inhibitor of macrophage phagocytosis) (Barclay and Brown, 2006) in the examined bladder cell lines could account for the tumorigenic potential of these cells. The existence of similar subpopulations expressing both CD44 and CD47 in bladder cancer biopsies indicates that these are cells are more differentiated, pointing to a lowered tumorigenic potential (Volkmer et al., 2012). Elevated expression of CD47 in these distinct subpopulations makes these an ideal target for anti-CD47 therapy, as realised in lung cancer (Liu et al., 2017b).

Co-expression of CD49f (a characteristic marker for differentiated urothelial cells) with CD44 observed in majority of the sorted cell lines and normal human urothelial tissue (refer Figure 4.9) reflects the absence of stem cell like characteristics (Liu et al., 2012). This could imply that these cells lack tumorigenic ability but may still be able to survive, proliferate and even form organoids, as recently observed using mouse urothelium (Real et al., 2018). The co-expression of these cell surface markers could be utilised to examine/ identify differentiation states as well as cell signalling processes, however.

Cell sorting revealed subpopulations expressing just a lone cell surface marker; with CD90 receptor expression levels being the lowest of the examined four markers (refer Figure 4.11). This was in marked contrast to the bladder cancer cell lines as well as normal human urothelial cultures where CD90 expression was absent. The subpopulations expressing significant CD90 expression could resemble the most primitive/basal subtype (Volkmer et al., 2012). CD90 expression being highest in the high-grade bladder cancer specimens could signify its tumorigenic potential.

Elevated levels of cells positive for the cell surface receptors, CD44 and CD47, were evident in both high-grade bladder tumours as well as the normal human urothelial cells (refer Figure 4.13). This high expression of $CD44^{+}$ cells in high-grade tumours and normal bladder basal cells matches previously

available data from lineage tracing experiments (Chan et al., 2009). Meanwhile co-expression of the examined receptors with the CD47 receptor in these cells makes them immune to macrophage phagocytosis, thus enabling the long-term survival of such oncogenic cells (Veillette and Chen, 2018). Meanwhile low numbers of bladder cells were positive for both CD44 and CD49f in both high-grade tumour tissues and low-grade tumour tissues as well as in normal urothelial tissue (figure 4.15). This implies that these cells are at a higher differentiation state, which fits with the hierarchical differentiation model of bladder tumour organisation (Zhang et al., 2016) – with basal cells being least differentiated and luminal the most differentiated. The absence of statistically significant levels of $CD44^+$ and $CD90^+$ positive bladder cells (refer Figure 4.17) indicates the elevated differentiated states the examined tumour tissues were at.

The heterogeneity of biopsied tissues and its different differentiation states could account for the differences in the receptor expression levels observed when compared to the urothelial cell lines. The urothelial cell lines however were all sourced from the same native tissue and had been grown in a similar *in vitro* environment. These cultured urothelial cells possessed a terminal differentiation subtype similar to the biopsied urothelial tissue they however did not possess a similar tumour microenvironment or were exposed to physiological systems as the biopsied tumour urothelial cells.

With all the above results, the fact that only ten bladder tumour specimens were examined was a hindering factor in arriving at a conclusion regarding the role of CD90 and CD44 in bladder cancer progression. The long-term storage of sorted cells has affected the quality and purity of DNA extracted from these cells which prevented further downstream investigation using the array methods. Also, the tissue size varied from small to large as well as good and poor (diathermy artefact) which had an effect on cell viability during the sorting procedure.

CHAPTER FIVE

5 5-HYDROXYMETHYLCYTOSINE IN BLADDER CANCER

5.1 Introduction

Epigenetic alterations, such as DNA methylation, histone modifications, and non-coding RNA expression, affect genomic function without sequence or copy number changes. Of these, DNA methylation has been frequently studied (Chatterjee et al., 2018), with the majority of these epigenetic alterations occurring in CpG (Cytosine-phosphate-Guanine) dinucleotides. Such alterations are underrepresented in the genome and are often located in concentrated islands (Bird, 2002). Several techniques are currently used to identify changes in methylation, including sodium bisulfite conversion and sequencing (Darst et al., 2010); differential enzymatic cleavage of DNA (Piperi and Papavassiliou, 2011); and affinity capture of methylated DNA (Bogdanovic and Veenstra, 2011).

Bisulfite sequencing (BS) utilises the differences in the conversion of cytosine residues upon treatment with bisulfite to create sequence changes so as to identify 5-methyl cytosine methylation status: 5mCs are resistant to sodium bisulfite while unmethylated cytosines are converted into nucleotide uracil (Frommer et al., 1992). Subsequent sequencing or polymerase chain reaction (PCR) can then determine methylated bases at the desired gene loci (Li and Tollefsbol, 2011). A key limitation of bisulfite sequencing is its inability to examine other known base modifications like 5-hydroxymethylcytosine (5hmC) (Bachman et al., 2014); 5-formylcytosine (5fC) (Raiber et al., 2015); and 5-carboxylcytosine (5caC) (Eleftheriou et al., 2015).

Although the functional role of each of these base modifications has yet to be ascertained, the loss of 5hmC has been identified as a hallmark of cancer (Pfeifer et al., 2014). 5hmC distribution along non-coding RNAs (lncRNA) has been identified to modulate clinical outcomes in colorectal cancer (Hu et al., 2017). Catalytic oxidation of 5mC into 5hmC by dioxygenases like ten eleven translocation 1 (TET1) has been found to induce oncogenesis when TET1 is overexpressed (Ficz and Gribben, 2014). The total expression level of 5hmC in the cell free methylome has prognostic potential since it provides useful

information on tumour types and stages (Song et al., 2017). 5hmC distribution has also been found to enable lineage tracing in cancer stem cells (Tarayrah and Chen, 2013).

In bladder cancer, expression levels of 5hmC can usefully quantify global methylation levels and serve as a pointer to the activity of TET1 enzymes (Jones and Baylin, 2007). Previous analysis of urothelial tissues using immune staining has identified that low levels of 5hmC indicate the existence of further ongoing demethylation processes which could be of clinical significance (Munari et al., 2016).

Hypothesis

I hypothesised that the 5hmc level differs between normal and tumour tissues.

I hypothesised that traditional bisulfite sequencing (BS) cannot distinguish between cytosine moieties, resulting in differences between BS and oxidative bisulfite sequencing (OXBS) results.

Aims

To investigate the profile of 5hmC in normal and malignant bladder tissue.

To correlate methylation with gene expression results and ascertain differences between BS and OXBS.

5.2 Materials and methods

5.2.1 Patients and Tumour Samples

This study uses ten fresh frozen bladder biopsy specimens from different individuals. Phenotypically, 3 samples were from normal bladder tissue samples and 7 from muscle invasive tumours (See Table 5.1). All patients gave informed consent in an ethically approved programme (Investigation of Molecular Instability in the Pathogenesis of Urothelial Cancer, STH 15574).

Table 5.1 Bladder tissue samples used in this investigation, including normal and tumour sources

Bladder tissue	Gender
Normal bladder tissue	
Normal tissue (NT) 1, NT 2 and NT 3	Male (M)
Total	3
Bladder tumour tissue	
Bladder cancer (BC) 1, BC 2, BC 4, BC 5 and BC 9	Male (M)
BC 3 and BC 6	Female (F)
Total	7

5.2.2 Oxidative bisulfite sequencing (OXBS) assay

Traditional bisulifte sequencing (BS) assays have only limited ability to distinguish 5-methylcytosine from 5-hydroxymethylcytosine. OXBS treatment can distinguish between 5-mC and 5hmC, by removing the hydroxy group from 5hmC by oxidation treatment, thus converting it to 5-formylcytosine (5-fC). Following bisulfite treatment of 5-fC, and amplification, the base is converted to thymine (Figure 5.1). A commercial kit can be used to treat DNA with BS and OXBS (TrueMethyl^{TM} Array kit) (Booth et al., 2012), requiring high concentration of genomic DNA (not less than 2-µg), thus limiting its application to human cancer samples.

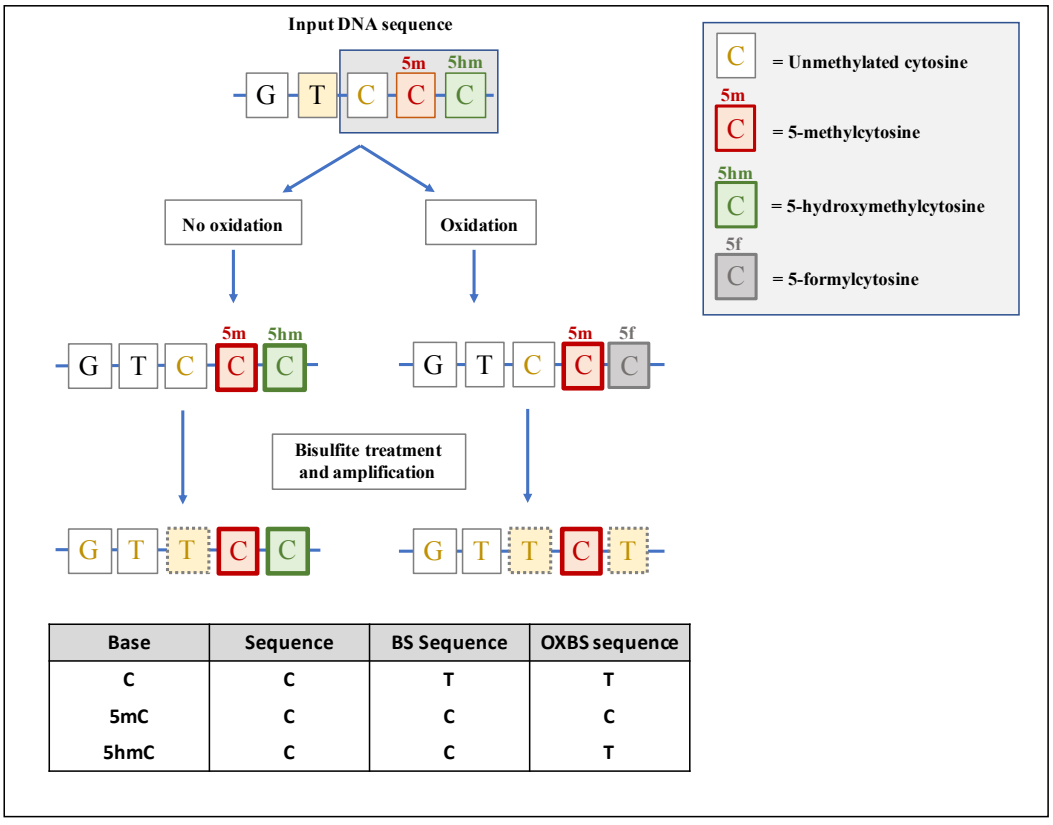

Base	Sequence	BS Sequence	OXBS sequence
C	C	T	T
5mC	C	C	C
5hmC	C	C	T

Figure 5.1 Illustration for the modified bisulfite sequence assay

Input DNA sequence containing unmethylated cytosine (C), 5-methylecytosine (5mC) and 5-hydroxymethylcytosine (5hmC). The oxidation step converts 5hmC into 5fC, while the lack of an oxidation step will keep 5hmC unchanged. After bisulfite treatment and an amplification step, both C and 5fC will be read as thymine (T) while 5mC will be read as cytosine (C) for the oxidised samples. On the other hand, the non-oxidised samples after bisulfite treatment and amplification will only read (C) as (T) while both 5mC and 5hmC will be read as (C).

This study quantified Genomic DNA isolates with Thermo Fischer Scientific Qubit™ dsDNA BR Assay kit. Following DNA quantification, 1-µl of spike-in digestion control provided in the true methyl array kit was added to 49-µl of the requisite quantified DNA sample. The spike-in of digestion control help ensure a successful oxidation measurement and is ideal for presenting a go/no go decision before proceeding with the samples towards array sequencing (Figure 5.2). Quantified DNA samples purified by magnetic beads were then denatured and split into two tubes for BS and OXBS sequencing. Following denaturation, oxidative solution was added to the OXBS samples while ultra-pure water was added to the BS samples and incubated for 30 minutes at 40 ^{0}C. Resultant OXBS and BS samples were bisulfite treated and quantified using the Qubit™ ssDNA assay kit. Samples were then prepared for Illumina 450K array sequencing by following the manufacturer protocol with minor changes (see Section 2.3.8, Materials and Methods) in parallel.

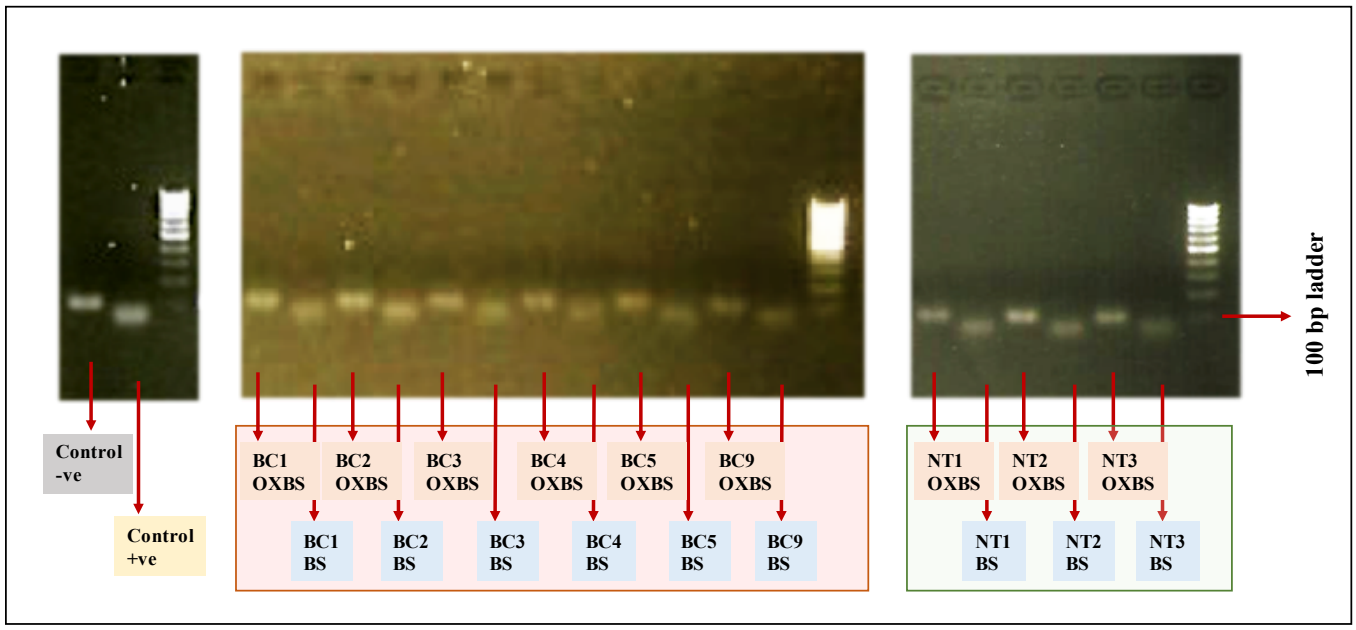

Figure 5.2 Confirmation of successful oxidation using gel electrophoresis.

The figure demonstrates the amplification of the 100bp band of the spike-in control after Taq1 digestion. DNA from samples were obtained at the end of bisulfite treatment and amplification and were run on 1.5% agarose gel, which 100bp DNA ladder was used. The left panel shows the amplification band of digestion control after Taq1 restriction enzyme digestion in both the positive and negative cutting control, provided in the TrueMethyl^{TM} array kit. The middle panel shows the amplification band of digestion control after Taq1 restriction enzyme digestion in the six bladder tumour tissue samples (OXBS and BS) used in this study. The right panel shows the amplification band of spike-in control after Taq1 restriction enzyme digestion in the three normal bladder tissue samples (OXBS and BS) used in this study.

5.2.3 DNA methylation 450K array analysis

As detailed in the Methods section, I used Illumina Infinium HumanMethylation450K Assay, which can measure around 480,000 cytosine sites, genome wide and cover 99% RefSeq genes. I used three normal and seven bladder tumour tissues from different donors, which served as biological replicates. To analyse the BS and OXBS treated genomic DNA in parallel, microarray files, in both green and red IDAT formats, were analysed using the R (version 3.4.1) software (Figure 5.3). A quality control check was performed prior statistical analysis, to eliminate outlier samples that could have failed hybridisation, or other technical failures. Identification and removal of these samples is critical to get a true molecular picture, and avoid data skewed by bad samples e.g. BC6 as it clustered with the normal.

Raw data was read and decrypted via the mini library from Bioconductor. Raw channel intensities were then normalised via the FunctionalNormalisation method from Minfi (Fortin Jp Fau - Labbe et al., 2014). Functional Normalisation is an advantageous method, particularly with cancer samples as it preserves global methylation differences, which can vary significantly. The normalisation method also uses the first two principal components, from the control probes, to regress out technical variation. Once normalisation is complete, it's important to filter at the probe level to remove any uninformative, or misleading observations, which also has the added benefit of reducing the multiple testing burdens on the experiment. The probe level filtering strategy is twofold; remove probes with SNPs in the probe's single base extension (SBE), probe sequence, or CpG site, and remove probes where its detection p value is >0.01. An additional note is that sex chromosomes were excluded from this analysis, due to the distinct methylation differences between males and females.

Post normalisation and probe filtering, Principal Components Analysis (PCA), was performed on M-Values to gain an experiment wide view of methylation variability. It is key to note that M-Values are log-like values that adhere to the underlying assumptions of linear modelling, i.e. the data is heteroskedastic. This means that beta values are unsuitable for statistical tests, however they are provided for the sake of interpretation, as the beta scale is simply between 0 and 1.

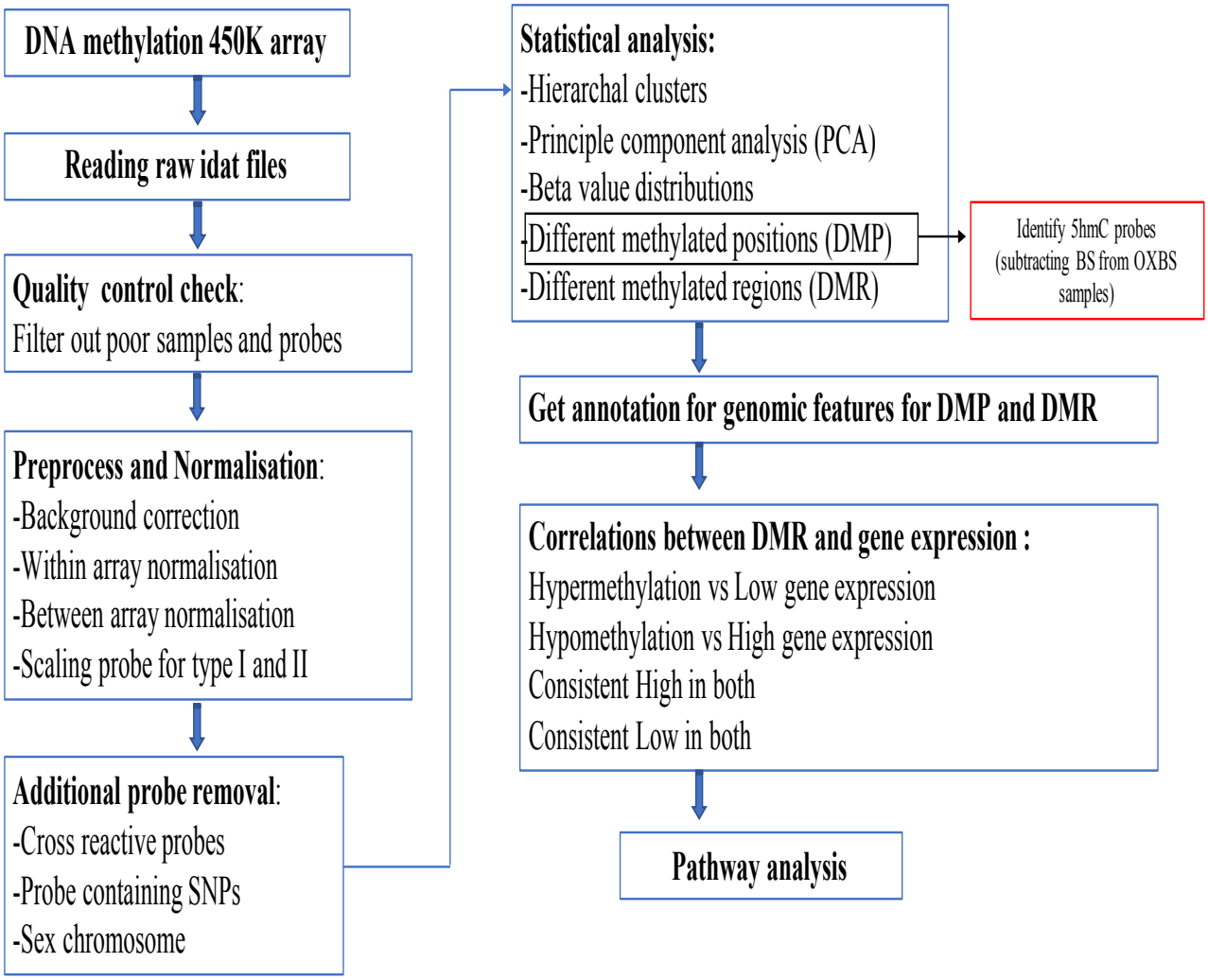

Figure 5.3 Infinium HumanMethylation450K array analysis workflow

Detection of 5hmC

To detect 5hmC status at CpGs, differently methylated CpG sites were localised via the conversion BS and OXBS. For each microarray probe, beta values between 0-1 were generated to identify the methylation level at specific locus (1 represents 100% methylation while 0 represents 0% methylation (i.e., unmethylated)). In bisulfite conversion, beta values generated represent the total methylation levels for both cytosine modifications in 5mC and 5hmC; while in oxidative bisulfite conversion, beta values represent the methylation score only for 5mC cytosine modification. To estimate the 5hmC levels for a specific probe, the average beta values of the normalised data of BS treated samples were subtracted

from the average beta values of OXBS treated samples at each particular probe. This was separately done for each tissue type (normal and tumour), and the delta beta value represented the differing 5hmC positions (Figure 5.4).

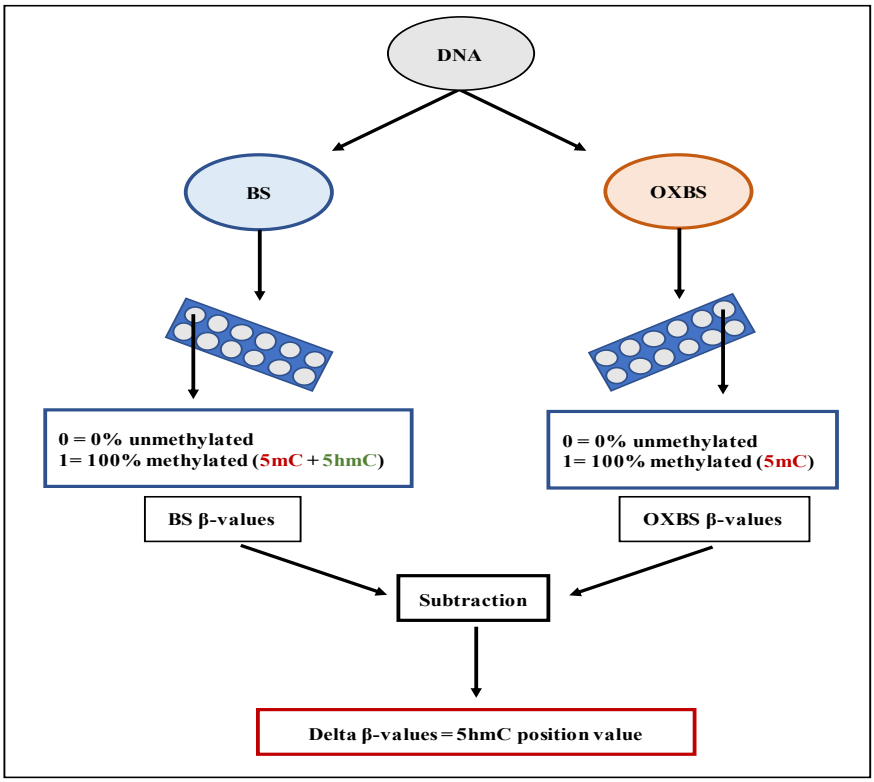

Figure 5.4 Detection of 5hmC positions value

Beta values generated from the bisulfite conversion (BS) represent the total methylation levels for both cytosine modifications in 5mC and 5hmC; while beta values from the oxidative bisulfite conversion (OXBS) represent the methylation score only for 5mC cytosine modification. The average beta values of BS treated samples were subtracted from the average beta values of OXBS treated samples in order to estimate the 5hmC levels for a specific probe at each particular position.

Validation of 5hmC sites

CpG positions with 5hmC positive sites in either normal or tumour tissues (and both) were selected based on the availability of CCGG motif for validation using specific qPCR assay (Quest 5-hmc qPCR detection kit). This assay uses glucosylation of 5hmC position in order to create a protection to this position. Then followed by digestion using the MspI restriction enzyme, which is used to digest specific

CCGG sites. Then, qPCR was performed on three tubes of the same sample: glucosylated-digested DNA (5hmC protected), unglucosylated-digested DNA (5hmC unprotected), and no treatment DNA. (Figure 5.3). Thus, determining the level of 5hmC at a given locus is applicable using this equation:

[(0% control) – (+5hmC) / (0% control) - (100% no treatment control)] x 100 = % 5hmC

Key: (***0% control)*** = digested unglucosylated DNA

(+ 5hmC) = digested glucosylated DNA

(100% no treatment control) = untreated original sample DNA

Different methylation positions DMPs and Different methylation regions DMRs

A statistical analysis was performed using moderated T-testing from a linear model, created using the Limma - Bioconductor package of R software, which was then applied to either paired or grouped design models to obtain different methylated positions (DMPs). This was separately done for each type of conversion BS and OXBS. Statistical significance was defined as false discovery rate values <0.01 (Benjamini and Hochberg, 1995). DMPs were obtained between normal and tumour samples with the conversion mechanism either the BS or the OXBS. Following this, the different methylated regions (DMRs) were obtained between normal and tumour samples with the conversion mechanism being either BS or OXBS. To identify continuous regions of differential methylation, DMRcate (Bioconductor package) was leveraged to make these identifications. DMRcate is based on the fundamentals of the BumpHunter methodology / package, but orientated to molecular biology and optimised to take Limma design matrices as input (Peters et al., 2015). Statistical analysis was performed with a false discovery rate at <0.01.

DMR and gene expression correlation

Correlation between the DMRs results and the publicly available normal bladder and matched bladder tumour gene expression data from the cancer genomic atlas (TCGA) repository was then performed (https://portal.gdc.cancer.gov/). Raw gene expression data files were not accessible, only gene summary counts were available for both normal bladder and high-grade tumour tissues. As this data was quantified against hg38/ GRCh38, the LiftOver package from Bioconductor was used with the respective chain file from UCSC to convert the coordinate systems. These mappings were applied to the DMR results to approximately map to the TCGA gene expression results.

Pathway analysis and protein-protein interaction

The Enricher analysis tool was used (http://amp.pharm.mssm.edu/Enrichr/) to identify functional pathways involved in gene annotation of 5hmC positions identified in each tissue type (normal and tumour). For pathway analysis and the protein-protein interaction of gene list obtained after DMRs and gene expression correlation, the String database (https://string-db.org/) was used.

5.3 Results

5.3.1 Statistical analysis of Illumina Infinium HumanMethylation450K

Unsupervised clustering of M-values at each probe were compared across all samples. A clear separation was observed between the two types of bladder tissues used (normal and tumour) when the cluster dendrogram was generated for the array dataset. A distinct separation was also observed between the two types of conversion, BS and OXBS, within the same sample (Figure 5.5), which was mostly expected, and reassuring that no technical variation was dominating the expected signal.

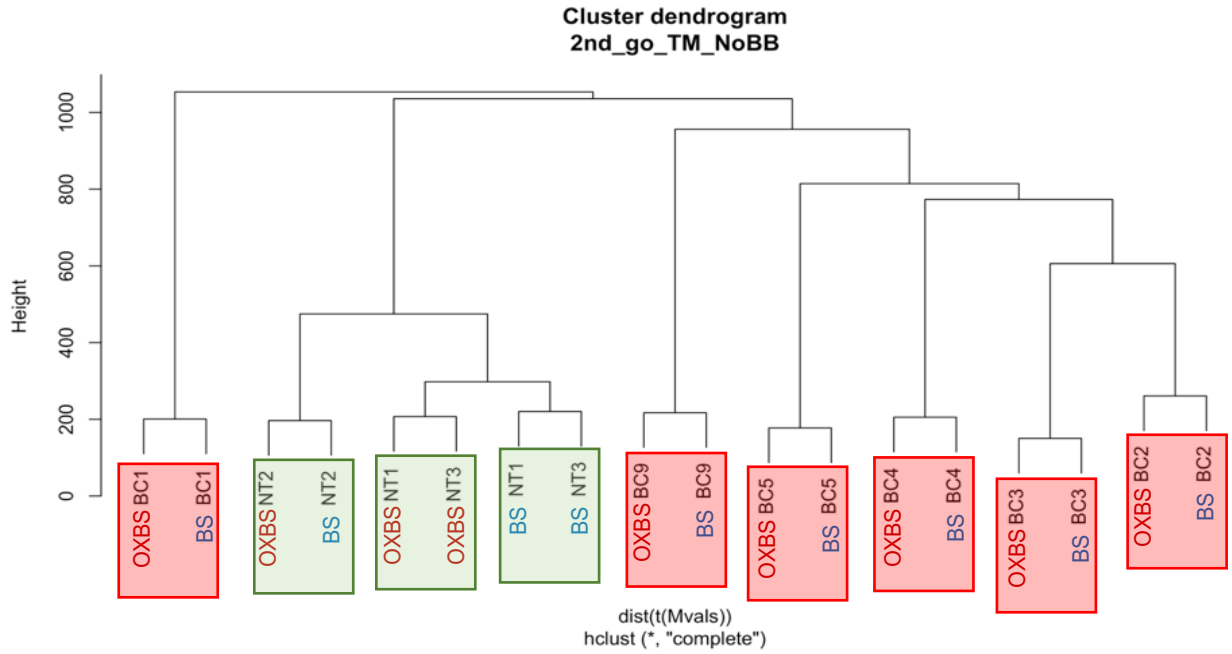

Figure 5.5 Hierarchical clusters for OXBS and BS samples.

Unsupervised hierarchical clustering of M-values of normalised data with p-value of < 0.01 for all 9 tissue samples. The green boxes represent the normal bladder tissues, NT1, NT2 and NT3; and the red boxes represent bladder cancer tissues BC1, BC2, BC3, BC4, BC5 and BC9.

Principal component analysis (PCA) of M-values of the dataset shows a clear explanation of primary variation between the normal bladder and tumour samples for the first principal component analysis at 36.47%. The 2nd principal component analysis showed a separation between samples using BS and those using OXBS for each tissue type at 18.41%. In addition, the second PCA showed a clear variation between the bladder tumour samples (Figure 5.6).

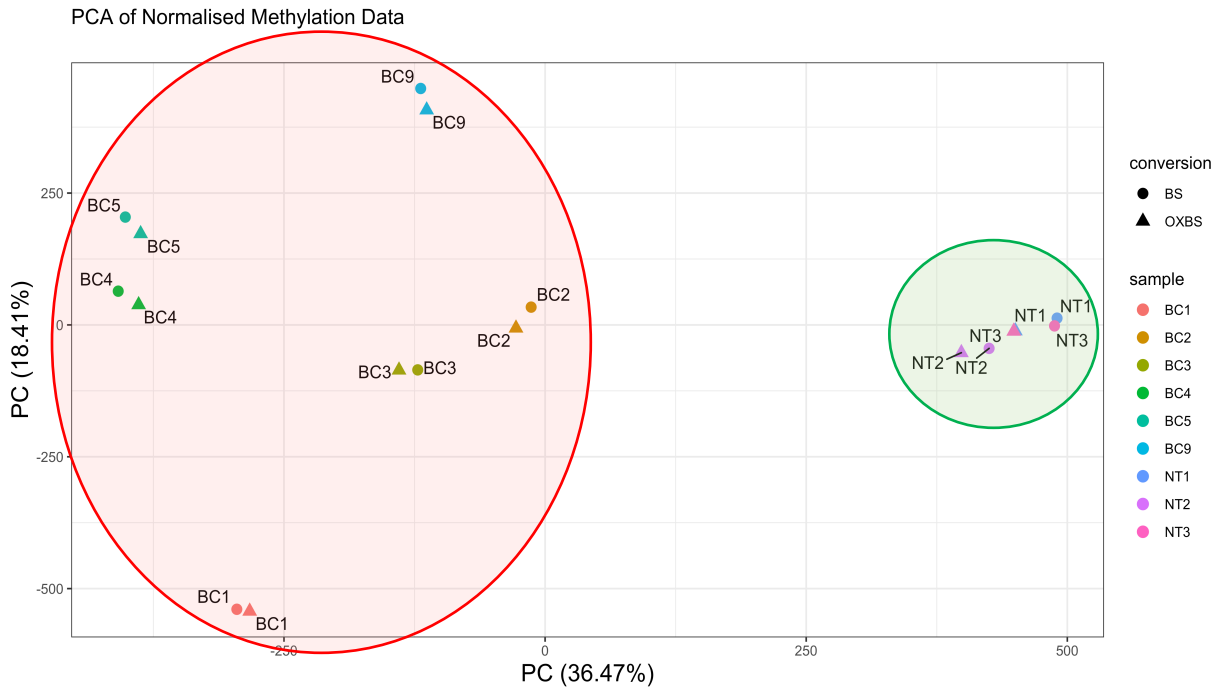

Figure 5.6 Principal component analysis (PCA) for all bladder tissue types.

PCA of normalised data set detected using P value <0.01. The small circles represent BS conversion, while the small triangles represent OXBS conversion. Tissue types are represented in different colours (normal = green circle on the right; tumour = red circle on the left).

Density profiling of beta values of the dataset showed a reduction in global methylation levels for OXBS samples when compared to BS samples. This was observed in the beta distribution profile of both normal and tumour tissues between samples using BS and those using OXBS (Figure 5.7).

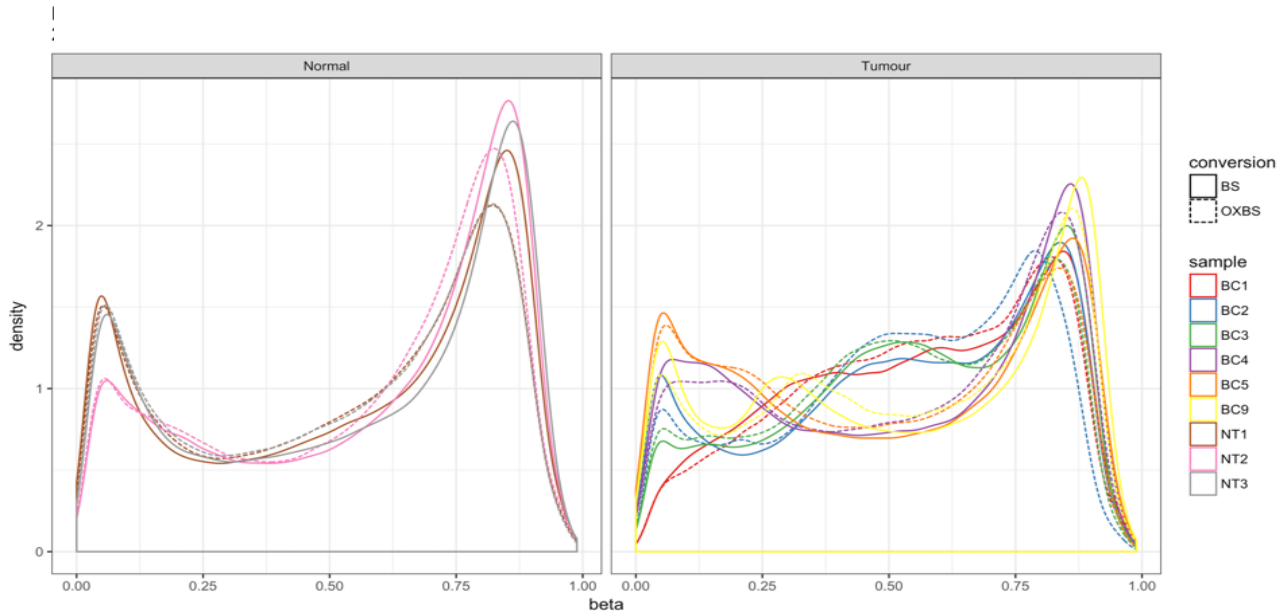

Figure 5.7 Density plot for beta distribution for normal and tumour samples.

Density plot showing the beta values distribution of normalised beta values with p-value of <0.01 for all three normal bladder tissue samples (box on the left) and all six-bladder tumour tissue samples (box on the right). Solid lines represent BS conversion while the dashed lines represent OXBS conversion.

5.3.2 Identification of 5hmC sites

Normal tissues contained more 5hmC positive probes than malignant tissues. The total number of 5hmC positive sites identified in bladder normal samples was 7,576 CpG sites, while 1,877 CpG sites were identified for tumour tissue samples. Only 6,814 5hmC probes were found specific for normal tissue samples, and 1,115 5hmC probes were identified in tumour tissue samples. 762 similar 5hmC positions were found in both normal and tumour samples (Figure 5.8). These significant probes were identified with a relative p-value of <0.01. Positive values obtained represented potential sites of 5hmC, while negative values were discarded since they reflected technical background error.

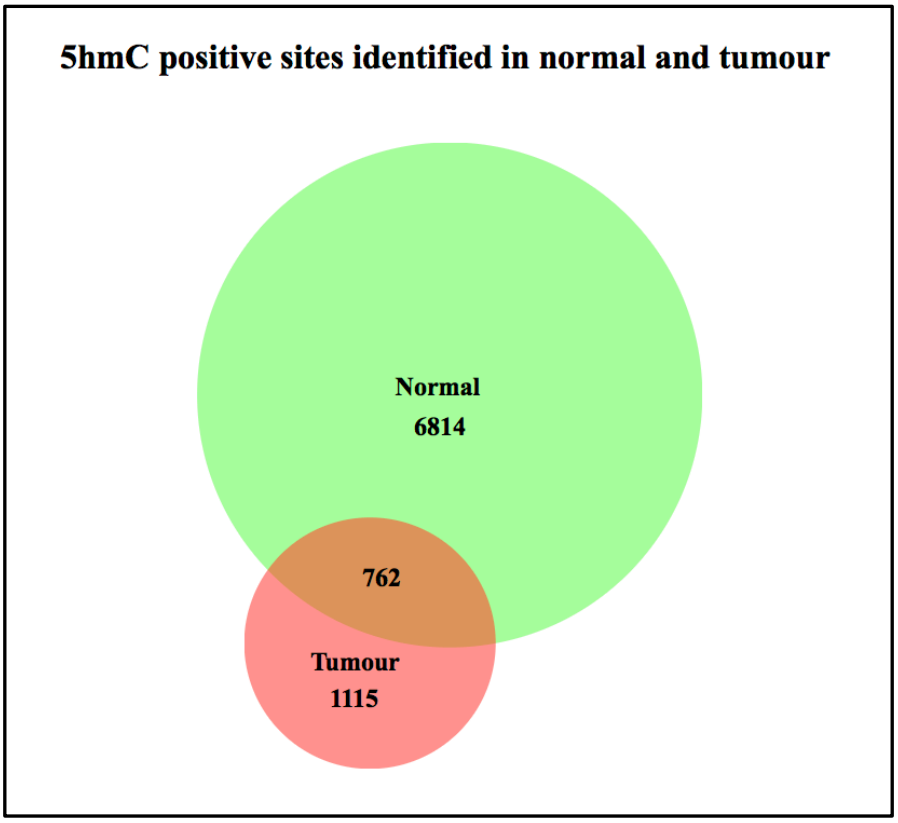

Figure 5.8 Different 5hmC positions identified in normal and tumour tissues.

The Venn diagram shows the area-proportional of the number of 5hmC positions identified in normal and tumour tissues as well as the shared 5hmC positions common to both normal and tumour urothelium. Figure 5.8 was produced using the web application BioVenn (Hulsen et al., 2008).

5.3.3 Distribution of 5hmC sites

The normal tissues contained more 5hmC positive probes than the malignant tissues in all genomic regions. The highest proportion of 5hmC probes in normal urothelium were intronic, intergenic and upstream; whereas, in the tumour tissues the highest proportions were intronic, intergenic and exonic (Figure 5.9).

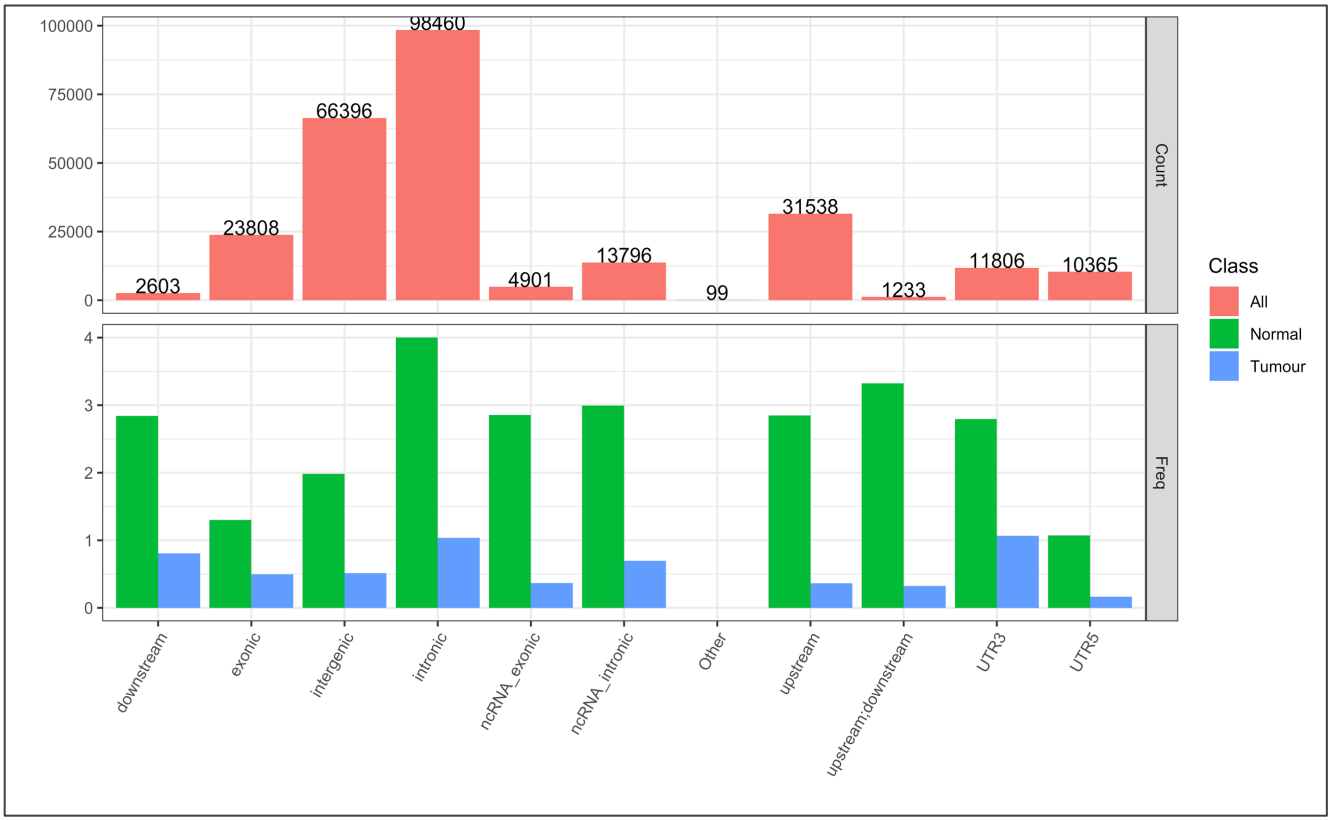

Figure 5.9 Number of probes found to have 5hmC signal in normal and tumour tissues.

The upper bar chart indicates the number of probes within the 450K array region; the lower bar chart indicates the frequency of 5hmC probe signal found in normal (green bars) and tumour (red bars) tissues relative to the total probes in each region in the 450K array.

CpG sites that had positive 5hmC probes were further investigated on the basis of CpG relation to island (a CpG rich region). It was clearly observed that, in both normal and tumour tissues, these identified 5hmC sites were mostly located on CpG sites in the open sea (far isolated manner from CpG island) at similar rates of 48% and 51%, respectively. Similarly, the CpG sites on islands with 5% for both normal and tumour samples. Different rates were apparent for 5hmC positions found in CpG content shores (>2kb flanking CpG island) and shelf (>2kb flanking CpG shores), however. CpG sites located in the shelf were 14% for normal tissues and 22% for tumour tissues, while 5hmC probes located in the CpG shore were 33% in normal and 22% in the tumour tissues (Figure 5.10).

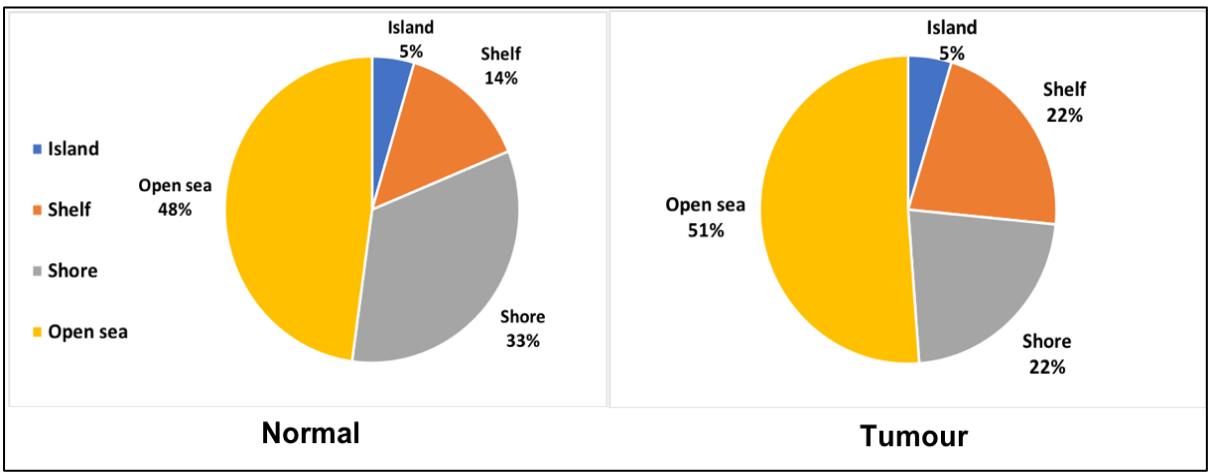

Figure 5.10 CpG distribution of 5hmC positive sites.

The pie charts show CpG content distribution of 5hmC positive sites in normal (left) and tumour (right) samples.

5.3.4 Validation of 5hmC specific loci

Similar results were observed between the 450K array results and the qPCR results at different 5hmC sites. Positive 5hmC sites were found only in normal tissue and were cg12068908, cg20340596 and cg10967023, while 5hmC sites were found only in tumour tissue, namely cg09307193, cg24092939 and cg06044662. The cg24327132 site, however, was found to be positive in both normal and tumour tissue. The details of the primers for these 5hmC sites can be found in Appendix 2.

Table 5.2 Validation of 5hmC loci found in each of tissue types

5hmC position found in normal tissue samples was confirmed to have positive delta-beta value in normal tissue only (Table 5.2 (A)).

(A) CpG loci found to contain 5hmC sites only in normal samples			
Probe ID	**450K array (%)**	**qPCR normal (%)**	**qPCR tumour (%)**
cg12068908	**20**	**21**	**-16**
cg20340596	**18**	**21**	**-3**
cg10967023	**18**	**22**	**-16**

On the contrary, 5hmC position found in tumour tissue samples was confirmed to have positive delta-beta value in tumour only (Table 5.2 (B)).

(B) CpG loci found to contain 5hmC sites only in tumour samples			
Probe ID	**450K array (%)**	**qPCR tumour (%)**	**qPCR normal (%)**
cg09307193	**13**	**17**	**-31**
cg24092939	**14**	**14**	**-12**
cg06044662	**13**	**12**	**-9**

5hmC sites were present in both normal bladder and tumour bladder tissue, showing similar delta-beta values corresponding to each tissue type both the 450K and qPCR results (Table 5.2 (C)).

(C) CpG locus found to contain 5hmC sites in both normal and tumour samples			
Probe ID	**450K array (%)**	**qPCR normal (%)**	**qPCR tumour (%)**
cg24327132	**18% (Normal) 5% (Tumour)**	**16**	**7**

5.3.5 Functional annotation analysis of 5hmC sites

5hmC sites located in the promotor region were selected for pathway analysis. Enrichr analysis tools was used (http://amp.pharm.mssm.edu/Enrichr/). The top 5 pathways identified (p-value of <0.01) for the genes related to the 5hmC position of normal tissue were chronic myeloid leukaemia, non-small cell lung cancer, endocytosis, cell cycle and viral carcinogenesis pathways. Different pathways were identified from the genes related to the 5hmC position found in the tumour tissues, however; the top five are the TNF signalling pathway, Toll-like receptor signalling pathway, Chagas disease (American trypanosomiasis), Epstein-Barr virus infection, and neurotrophin signalling pathways (Figure 5.11).

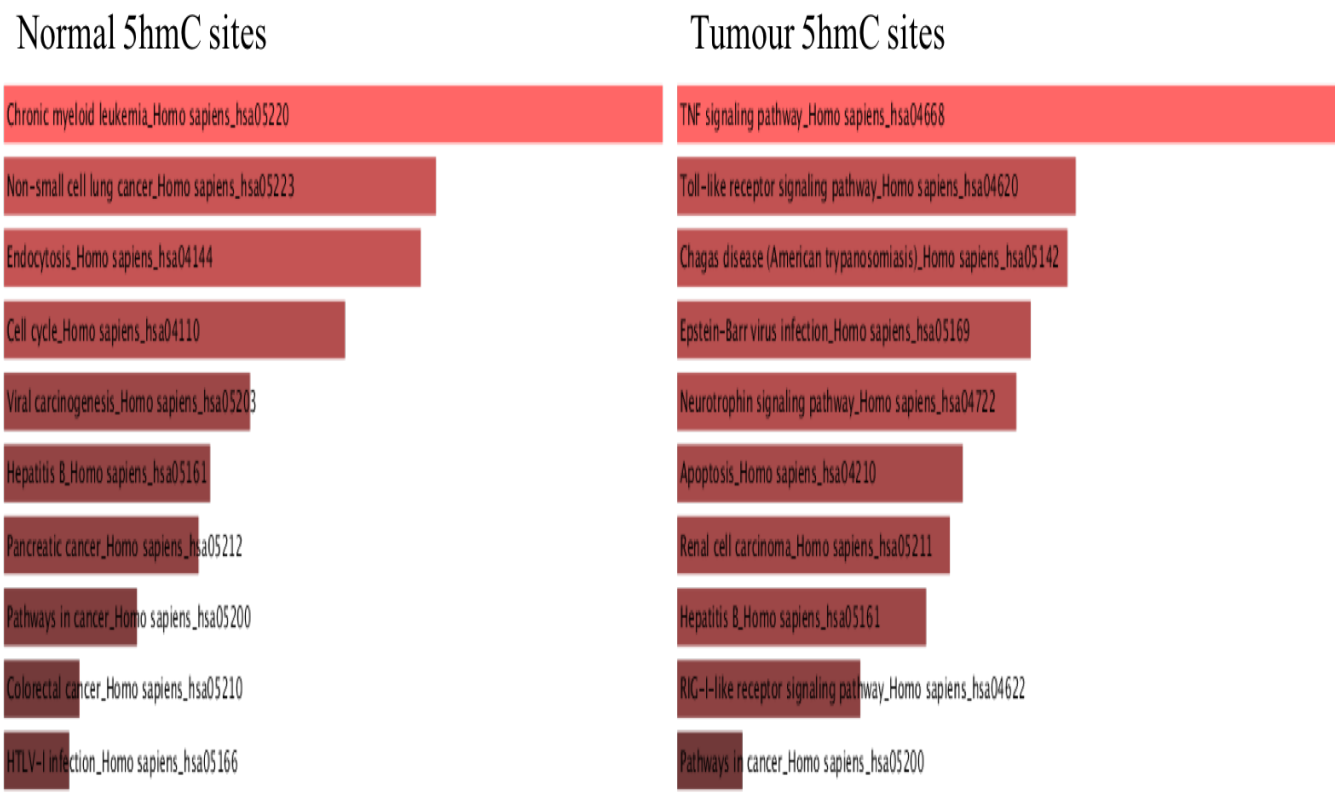

Figure 5.11 Pathway analysis of genes found to have 5hmC positive sites in normal bladder and bladder tumour samples.

5.3.6 Identification of DMPs found in BS and OXBS samples

BS treated samples contained high numbers of DMPs compared to OXBS treated samples. 25, 419 different methylated CpG sites were found in normal and tumour samples of BS conversion; 9,832 CpG sites were hypermethylated and 15,587 CpG sites hypomethylated. 17,754 CpG sites were identified for OXBS samples, with only 8,724 being hypermethylated and 9,030 being hypomethylated (Figure 5.12).

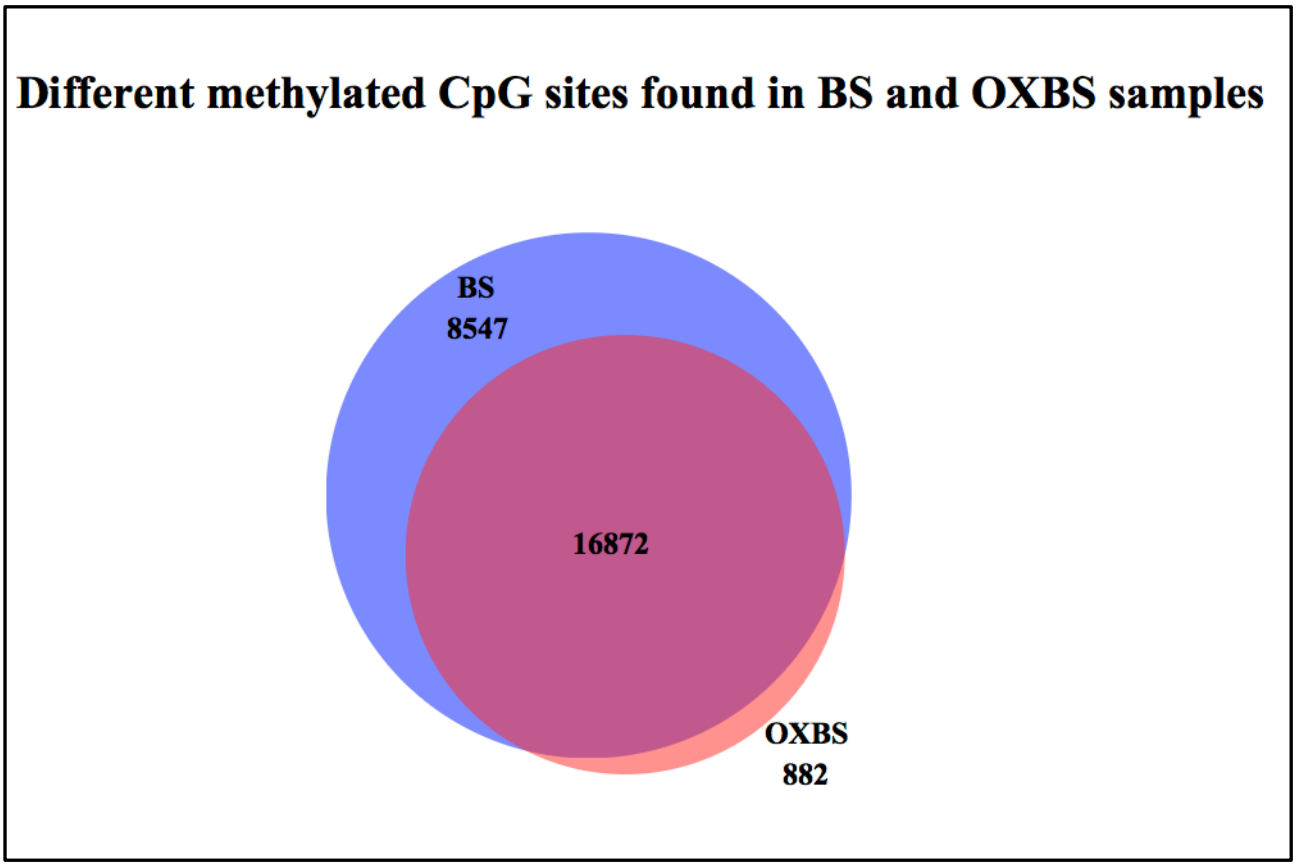

Figure 5.12 Different methylated CpG sites found between normal and tumour samples.

The Venn diagram shows the area-proportional of the numbers of significantly different methylated CpG sites (between normal and tumour) found in both BS and OXBS samples as well as the shared different methylated positions common to both BS and OXBS samples. Figure was produced using a web application called BioVenn (Hulsen et al., 2008).

Analysis of CpG content distribution showed that hypermethylated CpG sites were located at CpG islands in both types of conversion: 64% and 63% for BS and OXBS, respectively. Hypomethylated CpG sites were distributed mostly on the open sea, however: 58% and 62% for BS and OXBS, respectively (Figure 5.13).

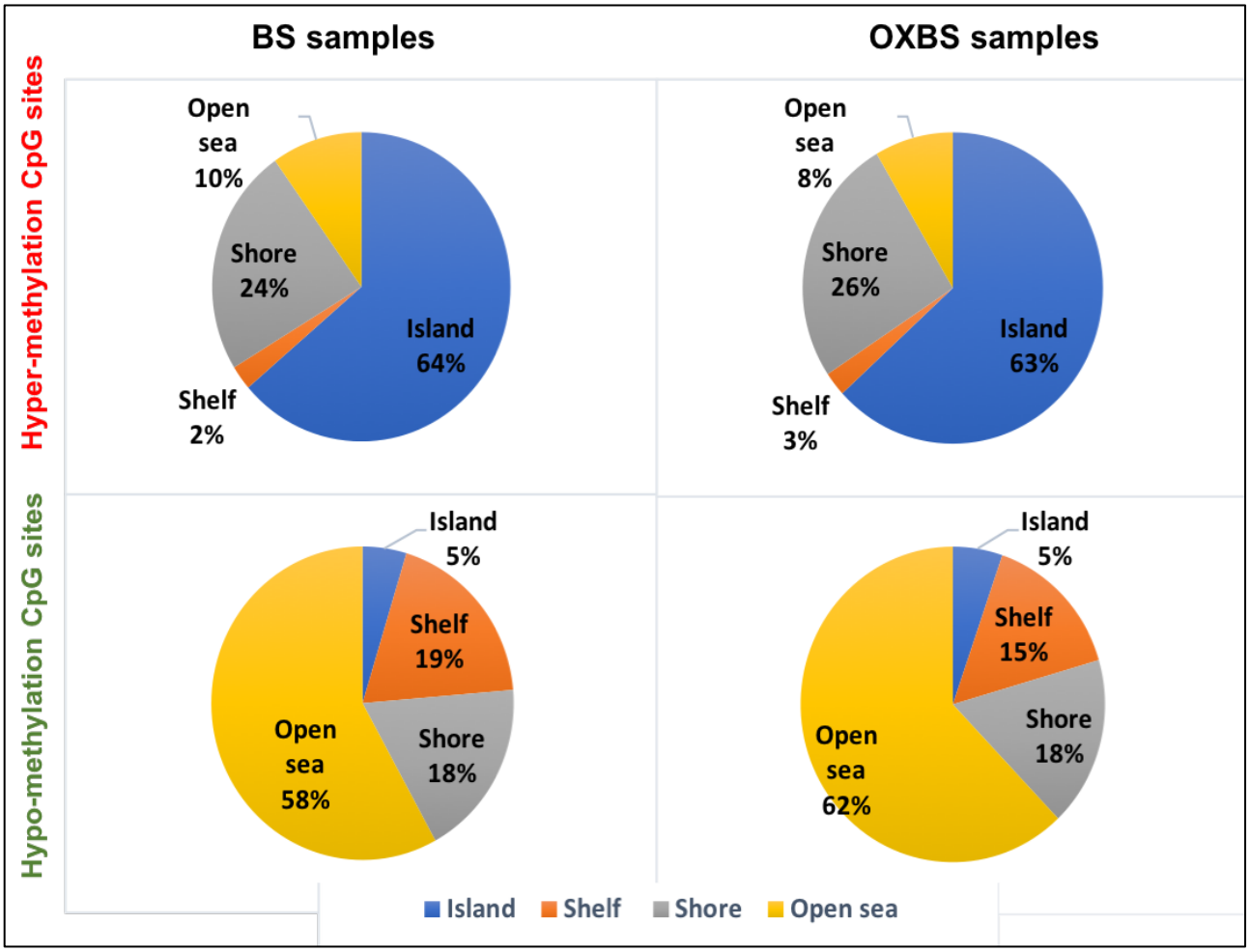

Figure 5.13 CpG distribution of DMPs of BS and OXBS.

The pie charts indicate the CpG content distribution of DMPs in BS (left) and OXBS (right) conversion. The upper pie charts indicate the hypermethylated CpG sites found in both BS and OXBS conversion; while the bottom pie charts show the CpG content of hypomethylated CpG sites found in BS and OXBS conversion.

5.3.7 Identification of DMRs found in BS and OXBS samples

It was clearly observed that BS treated samples contained higher numbers of DMRs than the OXBS treated samples. 3,775 different methylated regions were found with the BS conversion type. Of these, 2009 regions were found to be hypermethylated and 1766 regions were hypomethylated. For OXBS conversion, 2,456 regions were identified of which 1682 were hypermethylated and 774 were hypomethylated (Figure 5.14).

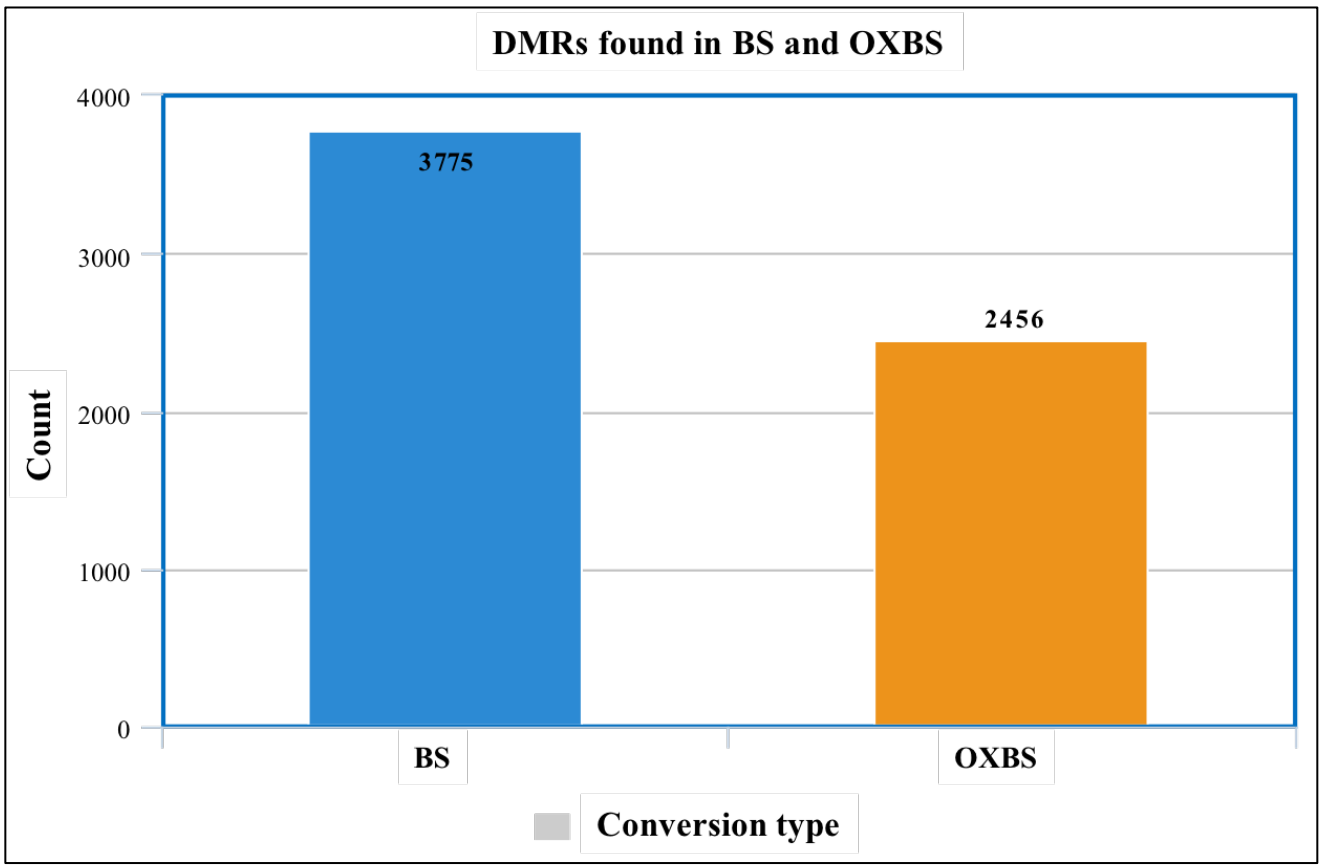

Figure 5.14 Differentially methylated regions found between normal and tumour samples.

The bar graph shows the number of different methylated regions found in both BS (blue) and OXBS (orange) samples. X-axis shows conversion type and Y-axis shows the number of regions found.

5.3.8 Correlation of DMRs and gene expression data with TCGA data

Results were characterised from DMRs between normal and tumour tissue. All gene expression data available from the ATLAS website was downloaded and used as a reference. Data was classified based on methylation level and gene expression relations. Results indicate variation between samples using BS and those using OXBS (Figure 5.15). Four categories of DMRs were identified: DMRs with decreased gene expression-increased methylation; DMRs consistently high in both gene expression and methylation; DMRs consistently low in both gene expression and methylation; and DMRs with increased gene expression-decreased methylation. The highest numbers were observed using BS samples high in both methylation level and gene expression, with 265 regions identified; however this was significantly reduced to 77 regions for OXBS samples of the same category. The lowest numbers

of DMRs were observed when gene expression increased while methylation levels decreased in both BS and OXBS samples.

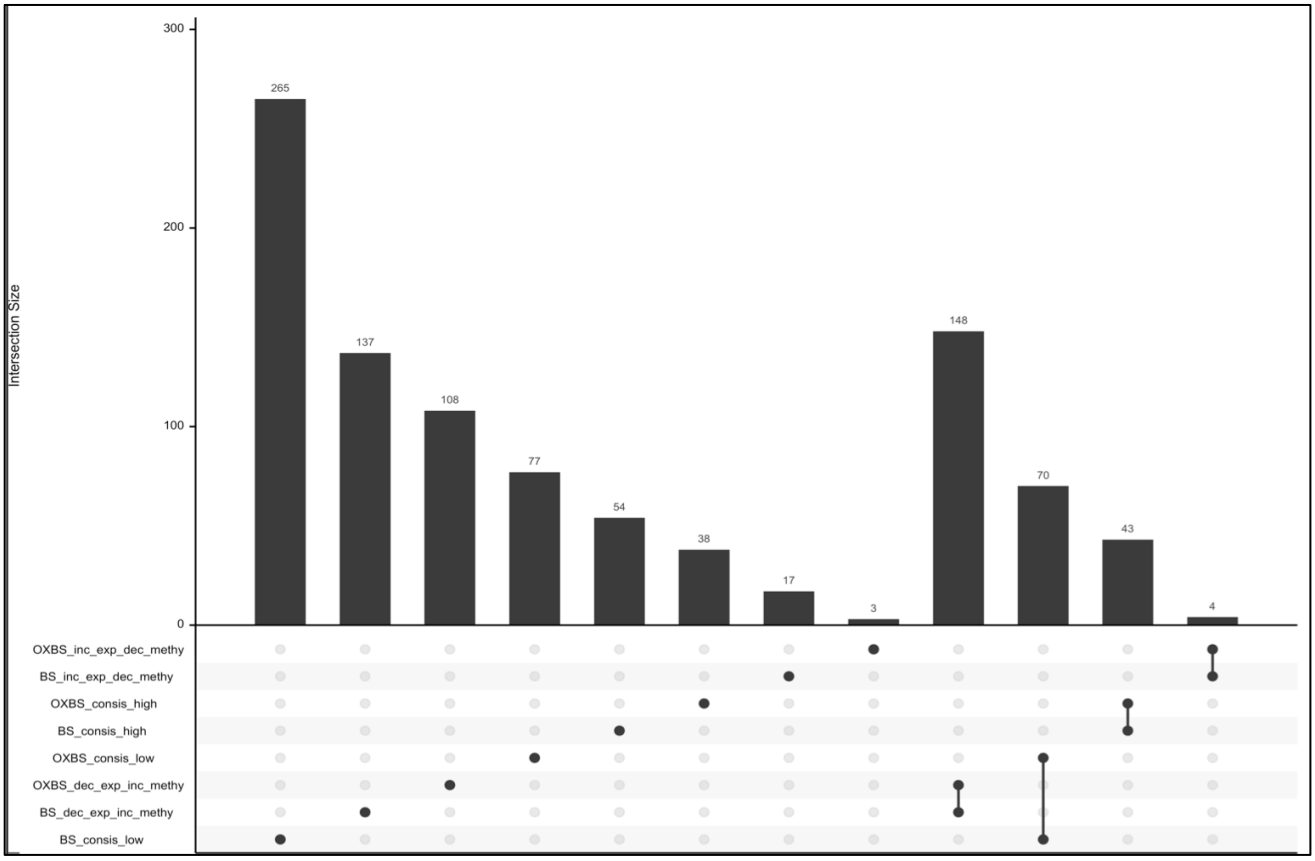

Figure 5.15 DMRs and gene expression correlation.

The X-axis shows the following categories present for both BS and OXBS conversion samples: increased gene expression vs decreased methylation (inc_exp_dec_methy); consistently high in both gene expression and methylation (consis_high); consistently low in both gene expression and methylation (consis_low); and decreased gene expression vs increased methylation (dec_exp_inc_methy). The Y-axis indicates the numbers found. A single dot represents the DMRs found in relative categories, and connected dots represent the matched DMRs between BS and OXBS of the same category.

5.3.9 Functional annotation analysis of OXBS data

Hyper-methylation and decreased gene expression show the higher number of genes found to have similarities in both OXBS and BS samples. String database (https://string-db.org/) was used to investigate the pathways and protein-protein interaction of the genes that shows hyper-methylation and decreased gene expression. Based on earlier observations in this Chapter, I selected the OXBS list for pathway analysis since it reflects accurate measurement in OXBS samples compared to BS samples (Figure 5.16).

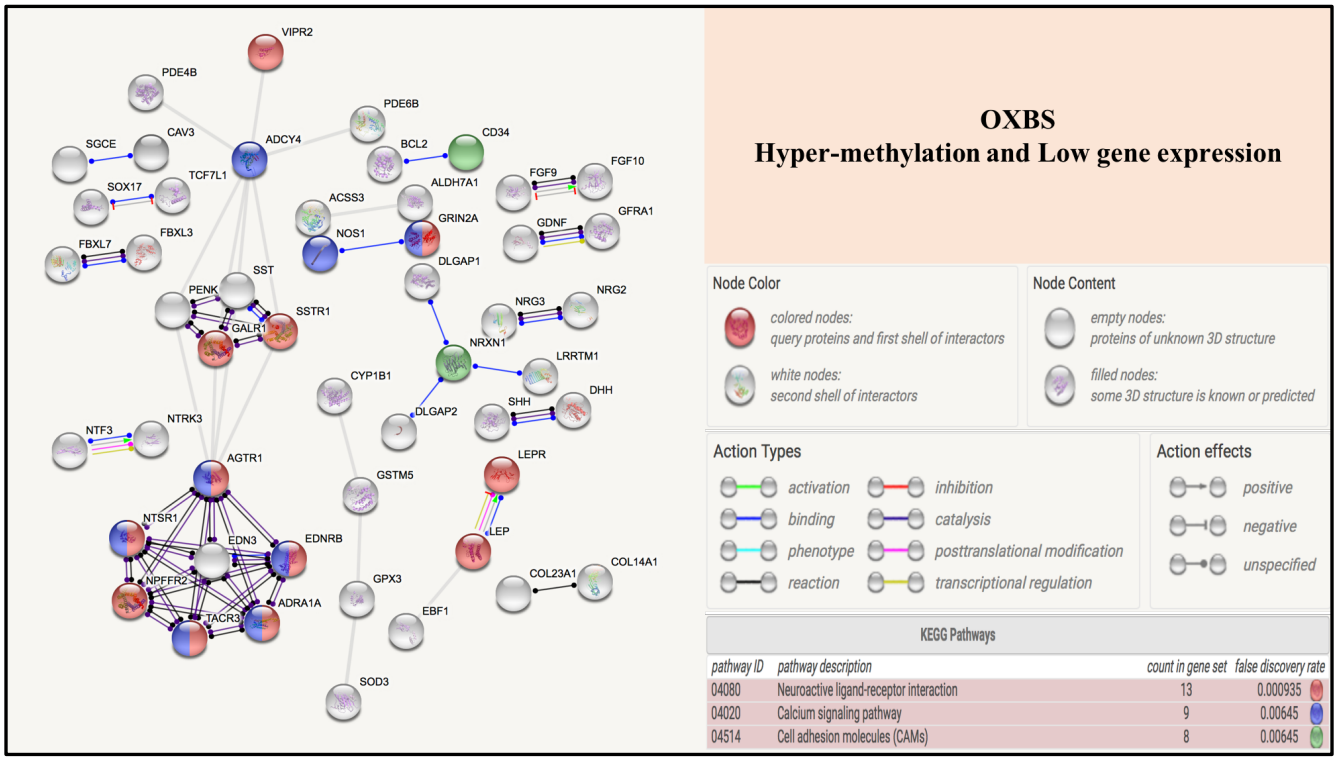

Figure 5.16 Pathway analysis and protein-protein interaction of genes found to be hyper-methylated and decreased gene expression for OXBS samples.

5.4 Discussion

The perturbation of 5-hydroxymethylcytosine (5hmC) in bladder cancer, offers the potential for cytosine demethylation products to serve as biomarkers (Dedeurwaerder and Fuks, 2012, Strand et al., 2014). Demethylation occurs following rapid and successive oxidative insults to cytosine moieties (Kulis and Esteller, 2010), causing the breakdown into 5hmC (Pfeifer et al., 2013) and 5-formylcytosine (5fC) (Raiber et al., 2015). Previous research using sodium bisulfite sequencing was unable to detect these breakdown moieties (Wu et al., 2016).

In this study, I identified the breakdown products of cytosine demethylation and compared their presence in normal and malignant bladder tissues. Oxidative bisulfite sequencing allows for discrimination of demethylation products by modifying 5hmC into 5fC, which is then converted into the ribose sugar Uracil (Booth et al., 2013). I utilised both BS and OXBS sequencing (Aijo et al., 2016) using two halves of the extracted DNA from the same biopsy to compare patterns of 5mC and 5hmC. These findings support and inform in more detail the existence of 5hmC expression in urothelial carcinoma tissues (Munari et al., 2016).

The distribution of 5hmC in human cells is dependent both on the tissue type as well as the disease characteristics (Li and Liu, 2011). I observed differences between normal urothelial tissues and bladder carcinoma specimens. High level comparisons clearly distinguished malignant and normal tissues as inferred from the principal component analysis (refer Figure 5.6) and the M-values (meaning that the log2 ratio of the intensities of the probe that is methylated versus the probe that is unmethylated) (Du et al., 2010). Quantitative counting of 5hmC sites revealed similar patterns (including intronic, intergenic and exonic sequences), although more 5hmC sites were found in the normal tissues (refer Figure 5.8 and 5.9). The exact significance of such distribution is still not yet clear. Changes in intronic sites could disrupt protein expression levels, transcription regulating motifs and non-coding RNA genes (Vaz-

Drago et al., 2017); or they could impact the genes closest to them, (Macintyre et al., 2014) changes in the exonic sites could impact splicing mRNA mechanisms (Sterne-Weiler and Sanford, 2014). The existence of unique sites where 5hmC was localised, however, indicates the role these cytosine residues play in the evolution of unique bladder cancer subtypes and pathologies. Of the several examined CpG loci only one locus (cg24327132) was identified to be common to both urothelial carcinoma tissues and normal bladder urothelium (refer Table 5.2).

Overall methylation levels were low for the oxidative bisulfite sequenced specimens compared to the bisulfite sequenced samples (refer Figure 5.7). Low beta values in the oxidative bisulfite sequenced specimens indicate the absence of 5hmC levels in both the normal and carcinoma specimens. This comports with previous research performed on normal brain and blood samples (Stewart et al., 2015). Low beta values could also indicate low demethylation activity in the tumour specimens, resulting in low levels of the TET1 [Ten-eleven translocation methylcytosine dioxygenase 1] enzyme activity.

Functional pathway analysis revealed significant differences in the localisation of the 5hmC sites between normal and malignant tissues (refer Figure 5.11). The expression of 5hmC in normal urothelial tissues in sites specific for genes implicated in a myriad of diseases (e.g., chronic myeloid leukaemia) could be because these residues create small nuclear polymorphisms (SNP) leading to a diseased state (Andrew et al., 2015). However, a non-parallel localisation in gene loci specific for signalling pathways (e.g., Tumour Necrosis Factor (TNF), and Toll-like receptor) suggest these residues could generate unique urothelial carcinoma subtypes.

Previous research has implicated the TNF polymorphisms in driving bladder cancer development (Marsh et al., 2003); although enhanced TNF production has also been associated with anti-tumour activity (Kim et al., 1993). The enhanced localisation of these cytosine residues on the loci for Toll-like receptors

could imply they are part of the sustained anti-tumour expression (LaRue et al., 2013). The localisation of 5hmC moieties in loci specific for Chagas disease is uncertain, but it could imply that these causative mechanisms/factors driving urothelial carcinoma and Chagas disease could be similar. The protracted localisation of 5hmC along loci specific for Epstein-Barr virus could indicate that the examined tumour tissue was infiltrated by lymphocytes positive for this virus (Abe et al., 2008). Other pathways could transactivate other moieties like Epidermal Growth Factor (EGF) (Mitre et al., 2017); a known factor behind urothelial oncogenesis. One such example would be the neurotrophin signalling pathway, regulating the expression of neurotrophins, like Brain-derived neurotrophic factor (BDNF), via the receptors Tropomyosin receptor kinase B (TrkB) and Low-affinity nerve growth factor (LNGFR/p75NTR).

Microarray findings include the higher numbers of DMPs in the BS (i.e. 5mC) than in the OXBS samples (i.e. 5hmC) (refer Figure 5.12). The reasons for this are unclear, but may reflect the role of 5hmC in urothelial development, metabolism in cancer, or rates of repair of cytosine damage. Most of the DMPs appear to be tissue-specific DMPs. The urothelial carcinoma specific DMPs were examined in closer detail (refer Figure 5.13). Side-by-side comparison of normal and carcinoma afflicted urothelial tissues using both bisulfite sequencing and oxidative bisulfite sequencing revealed higher numbers of CpG sites in the BS specimens than in the OXBS specimens. This might suggest the technical accuracy of the oxidative bisulfite technique. The oxidative bisulfite sequencing also revealed DMPs, which were either hypermethylated or hypomethylated. Analysis of these DMPs revealed that the hypermethylated regions were localised in specific islets/islands in both bisulfite sequenced and oxidative bisulfite sequenced specimens while the hypomethylated regions occurred in a far more isolated manner than in open seas. The implication of this finding is still not yet clear but has to be investigated further.

Estimation of different methylation regions (DMRs) in both the normal urothelial and muscle invasive bladder carcinoma specimens (with reference data from The Cancer Genome Atlas (TCGA) site) made possible the sorting of the diverse datasets (refer Figure 5.15). The differentiation analysis benchmark was realised using an FDR cut-off <0.01 as the significance threshold. Such sorting of the methylome data enabled identification of genes common to both the bisulfite and oxidative bisulfite sequenced specimens, which were however expressed in consistently lower numbers relative to the normative TCGA data. Also revealed was hypomethylated genes with increased gene expression profiles unique to either bisulfite or oxidative bisulfite sequenced specimens (unfortunately, these were excluded from further functional annotation analysis due to the strict statistical selection criteria). This hypomethylated data, however, needs to be examined in detail in future research.

Functional annotation analysis performed using STRING database identified genes from similar biochemical pathways and new oncogenic patterns (unique to the urothelial carcinoma) (refer Figure 5.16). Annotated data was selected for functional analysis using the Kyoto Encyclopedia of Genes and Genomes (KEGG) pathway enrichment analysis; then the protein-protein interaction of these molecules/genes was explored. Such analysis revealed that 30 genes specific for 3 biochemical pathways: Neuroactive ligand receptor interaction; Calcium signalling pathway; and Cell adhesion molecules (CAMs), were affected by epigenetic cytosine modifications. These genes and their associated pathways could serve as possible markers in the identification and characterisation of muscle invasive bladder cancer, although this needs to be examined more closely.

Role of Neuroactive ligand receptor interaction pathway in MIBC

Prime among the identified pathways was the Neuroactive ligand receptor interaction pathway; with 13 genes possessing low expression profiles but consistently hypermethylated – implying heavy suppression of gene expression. Only 12 genes showed a connected action when the list was uploaded

to explore the protein-protein interaction: Vasoactive intestinal peptide receptor 2 (VIPR2); Glutamate Ionotropic receptor NMDA Type subunit 2A (GRIN2A); Somatostatin receptor 1 (SSTR1); Galanin receptor 1 (GALR1); Leptin (LEP); Leptin receptor (LEPR); Angiotensin II receptor type 1 (AGTR1); Endothelin receptor type B (EDNRB); Alpha 1-A adrenergic receptor (ADRA1A); Tachykinin receptor 3 (TACR3); Neuropeptide FF receptor 2 (NPFFR2); and Neurotensin receptor type 1 (NTSR1).

The lack of expression of VIPR2 could in turn lead to the absence or insufficiency of the vasoactive intestinal peptide (VIP). This absence of the VIP protein has been previously identified to enhance susceptibility of death from metastatic bladder cancer in a murine model (Mirsaidi et al., 2017). In contrast, an overexpression of this protein has also been reported in bladder tumours (Moody et al., 2016a) and could suggest its role in the transactivation of the Epidermal Growth Factor (EGF) and its associated receptor, i.e., EGFR (Moody et al., 2016b). The GRIN2A gene has been previously identified as a tumour suppressor in melanomas (Wei et al., 2011); it is also a known target for methylation in breast cancer (Kim et al., 2008b). Although its expression has been deemed to be low in both normal urothelial samples as well as in bladder tumours (Hurst et al., 2012), characterisation of GRIN2A mutation could be suitable for identifying novel subtypes of muscle invasive bladder cancer. Low expression and hypermethylation of the SSTR1 moiety previously localised in both normal and bladder cancer specimens (Karavitakis et al., 2014) could be of prognostic and therapeutic significance in the treatment of muscle invasive bladder cancer. Hypermethylation of the GALR1 gene comports with previous data where the CpG islands along the promoter region of the same gene were methylated in muscle invasive bladder cancer specimens (Li et al., 2016).

Both leptin and its receptor, belonging to the Neuroactive ligand receptor interaction family, have previously been suggested in bladder cancer development. The elevated significance I observed for both these genes matches other data especially from histochemistry where the leptin receptor was identified

to prevent aberrant cancer cells from entering the S phase during the cell cycle (Yuan et al., 2004). This hunger-regulating hormone has also been identified to promote the vascular endothelial growth factor-C (VEGF-C) by mediating other signalling pathways like Phosphatidyl Inositol 3 kinase (PI3K) and Akt (Yang et al., 2016). The hypermethylation of these molecules could therefore significantly impact muscle invasive bladder tissue proliferation via its regulation of cell cycle as well as lymphangiogenesis. In contrast to the angiogenesis promoting function of the leptin receptor, the AGTR1 gene identified by the pathway analysis is a known angiogenesis inhibitor and a known apoptosis promoter in bladder cancer (Pei et al., 2017). A similar study has previously postulated its role as a diagnostic moiety with a possible tumour suppressive role (Dolley-Hitze et al., 2010).

Hypermethylation of CpG rich promoter regions of the EDNRB gene (Zuiverloon et al., 2012) could cause a decline in transcriptional expression of the EDNRB protein; this has been identified to modify the Endothelin-1 (ET1) signalling system (Mousavi Ardehaie et al., 2017); and to promote the proliferation, angiogenesis and metastasis of bladder tumours. Similar to its applicability as a prognostic marker for non-muscle invasive bladder cancer (Zuiverloon et al., 2012), the presence of this gene can be utilized also for detecting muscle-invasive bladder tumours. The ADRA1A gene, a member of the G protein-coupled receptor superfamily, was also identified. This protein has been identified to be involved in the activation of several mitogenic responses, and as a regulator of cellular proliferation (Gao et al., 2000). The role of this gene in BC is not known (Owaki et al., 2015). The effect of hypermethylation of TACR3 gene situated on chromosome 4 in bladder cancer is currently unclear although this gene has been identified in bladder tumour specimens (Zaravinos et al., 2011). The role of NPFFR2, also a member of the G-protein coupled receptor family, in bladder cancer is uncertain and warrants further investigation. Although the role of the NTSR1 gene in bladder cancer is uncertain, epigenetic silencing of this gene has been implicated in the development of lateral and non-invasive colorectal tumours (Kamimae et al., 2015).

Role of Calcium signalling pathway in MIBC

This pathway is primarily involved in the maintenance of intercellular communication in normal urothelial cells. Impaired gap junction formation and a resultant deviant intercellular calcium signalling have been reported in urinary bladder cancer cells (Leinonen et al., 2007). My analysis of microarray data revealed nine genes associated with this pathway to be hypermethylated as well as being low expression in muscle invasive bladder tumour tissues. Only eight genes showed a connected action when the list was uploaded to explore the protein-protein interaction: Adenyl cyclase type 4 (ADCY4); Nitric oxide synthase 1 (NOS1); Glutamate Ionotropic receptor NMDA Type subunit 2A (GRIN2A); Angiotensin II receptor type 1 (AGTR1); Endothelin receptor type B (EDNRB); Alpha 1-A adrenergic receptor (ADRA1A); Tachykinin receptor 3 (TACR3); and Neurotensin receptor type 1 (NTSR1). Of these eight, all were common to the Neuroactive ligand receptor interaction pathway (with their respective roles in bladder cancer previously discussed) except for ADCY4 and NOS1. The expression of NOS1 protein by macrophages in tumorigenic cells has been identified to confer the said cells resistance to chemotherapeutic agents like cisplatin (Perrotta et al., 2018). Very little information currently exists on the role of ADCY4 in bladder cancer, making it difficult to draw conclusions; thus, further research into its role in MIBC genesis is warranted. Hypermethylation of the NOS1 gene observed here could imply that the examined MIBC tissues were not resistant to the platinum complex cisplatin, although this must be examined more closely.

Role of Cell adhesion molecules (CAMs) in MIBC

These molecules are primarily involved in cell adhesion as the name implies, with their associated molecules either calcium dependent or calcium independent. Dysfunction of calcium dependent molecules (primarily various Cadherins, e.g., E-cadherin) has been identified to promote tumour invasion in cultured urothelial cells (Davies et al., 1999), while other Cadherins (e.g., P-Cadherin, N-Cadherin) abnormal expression promoted invasive urothelial phenotype (Bryan, 2015). Microarray

analysis has revealed the identities of CAM family genes like CD34, and Neurexin-1 alpha (NRXN1) to be hypermethylated. CD34, previously identified as a prognostic marker for non-muscle invasive bladder cancer could serve in a similar role in the detection of MIBC (Ajili et al., 2012). Its significance in tumour angiogenesis in MIBC must be examined in further detail. The role of NRXN1 in MIBC is currently not clear with scant information regarding its functionality in urothelial tissues.

The fact that the gene expression data was not readily accessible made it difficult to apply the preferred statistical criteria when correlating changes in methylation level and RNA expression. Moreover, the gene expression data of regions containing high numbers of contiguous 5hmC sites could aid in identifying region specific 5hmC involvement. This would help in identifying the role entire gene transcripts could have in bladder cancer genesis while not being limited to identifying novel CpG sites. Additionally, it would also be beneficial to examine TET enzyme activity using immunohistochemistry (IHC). This would enable differentiation of TET enzyme activity levels in normal urothelium and bladder tumour. Meanwhile the limited numbers of tumour tissues analysed (six tumours and three normal samples) analysed made it difficult to arrive at more definitive conclusions.

CHAPTER SIX

6 EPIGENETIC CHANGES IN UROTHELIAL CELL POPULATIONS WITH DIFFERENT CELL SURFACE MARKERS

6.1 Introduction

So far in this thesis I have pursued two approaches to better understand bladder cancer: namely cell sorting to explore tumour components and profiling of 5hmC across the epigenome. In this chapter, I combine these approaches to understand epigenetic profiles of the different sorted cellular components. Little is known about epigenetic alterations in cell specific fraction and I hope to understand whether urothelial cells share common changes or show distinct differences. An integrated analysis using specific bladder cancer subpopulations specific for the cell surface markers CD44, CD47, CD49f and CD90 could be helpful in determining the nature of the variability guiding the emergence of these subpopulations.

Hypothesis

I hypothesised that FACS sorted urothelial cell subpopulations possess distinct epigenetic profiles and that these can be detected by qPCR.

Aims

To explore Cytosine methylation and hydroxymethylation in CD44/CD47, CD44/CD49f and CD44/CD90 urothelial cells.

6.2 Materials and Methods

6.2.1 Patient and Tissue Samples

A total of seven tissue samples were used in this chapter. Both normal urothelium (n=3) and high-grade tumour (n=5) bladder tissues were obtained from patients who had undergone surgical removal of the bladder, or part of the bladder, at the Royal Hallamshire Hospital, Sheffield. Details of these samples are provided in Appendix 1. Fresh tissue was homogenised and FACS sorted using a panel of antibodies to obtain cells expressing CD44/CD47, CD44/CD49f and CD44/CD90 (see chapter 4 for full details).

6.2.2 5hmC Detection qPCR Assay

Whilst a whole epigenome approach is best for profiling changes in cells, it requires higher quantities of DNA than available to me after FACS sorting cells. The amount of DNA obtained after FACS reflects the relative abundance of the selected cells and the total amount of starting tissue. I used qPCR to detect 5hmc (see Chapter two, Section 2.3.9). This assay requires a DNA concentration of 100 ng per reaction and a purity of 1.8). Due to the low-sorted cell numbers, sorted urothelial (normal or tumour) cells were pooled together to have sufficient DNA concentration for analysis. For example, sorted cells that were positive for the dual cell surface markers $CD44^{+}/CD47^{+}$ of all high-grade tumour patients were pooled together into one tube while sorted cells of the same tumour patients for the other three coordinates ($CD44^{-}/CD47^{+}$, $CD44^{+}/CD47^{-}$, $CD44^{-}/CD47^{-}$) were pooled together into a different tube. This pooling was similarly applied to the other dual cell surface markers examined (i.e. CD44/CD49f and CD44/CD90) and might have smoothed out inter-individual heterogeneity.

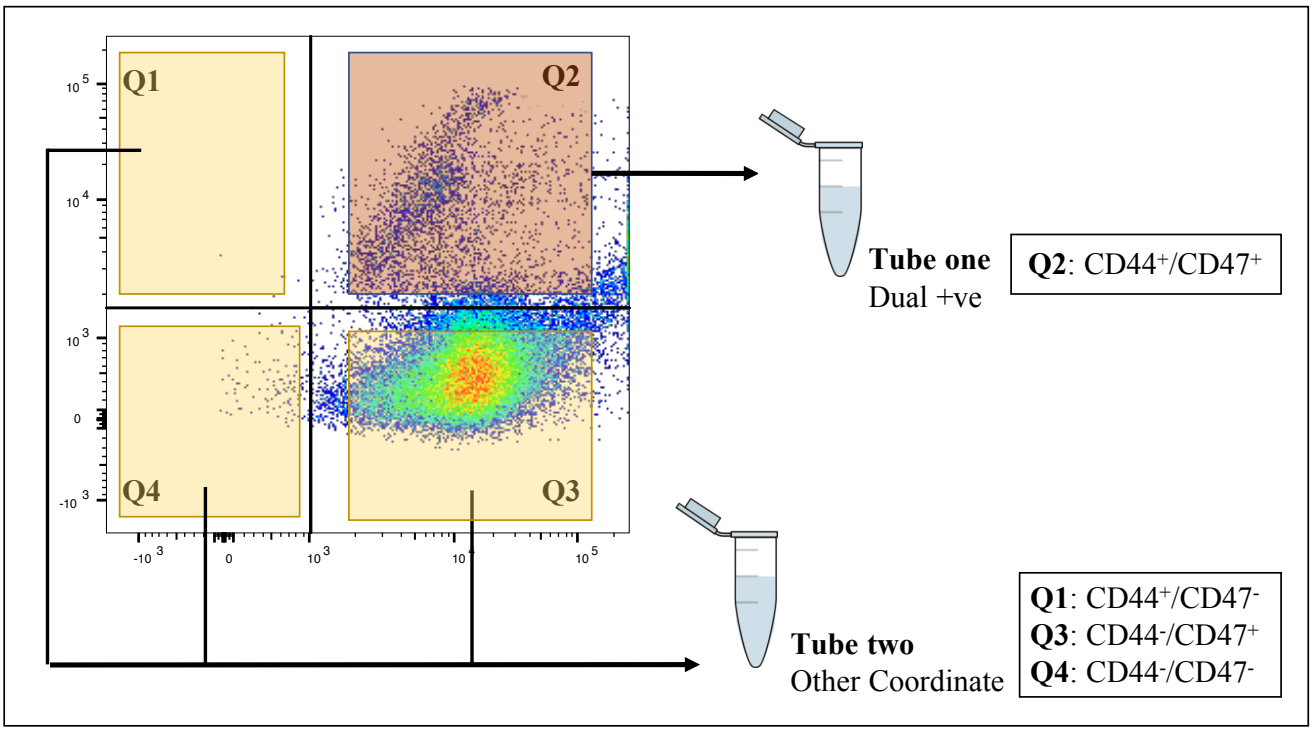

Figure 6.1 Illustration of samples used for qPCR

6.3 Results

Sorted cells from both fresh tumours and normal urothelial tissues were examined using specifically designed qPCR probes. These regions were identified in Chapter 5. 5hmC levels for the locus cg24327132 were examined in the normal urothelial and high-grade urothelial carcinoma tissue (Table 6.1, 6.2 and 6.3). The 5hmC levels from the 450K methylation assay were found to be elevated in the probe examined from the normal urothelial tissue, at 18% compared to the 5% observed for the bladder carcinoma tissue. Closer inspection of the 5hmC locus cg24327132 was then performed for the specimens irrespective of their dual cell surface receptor populations (CD44/CD47, CD44/CD49f and CD44/90). This revealed variability in the 5hmC levels in the examined tissues.

In the normal urothelial cells sorted for the dual cell surface receptors $CD44^+/CD47^+$, the 5hmC levels were undetectable (-20%) while the 5hmC levels were high (90%) in the cells of the other coordinates. In the high-grade urothelial carcinoma cells sorted for the dual positive $CD44^+/CD47^+$ receptors the 5hmC levels were above 100% (324%). The cells along the other coordinates meanwhile had undetectable 5hmC levels (-105%) (table 6.1).

Probe id: cg24327132	**450K (**18% normal**)**	**450K (**5% tumour**)**

Table 6.1 qPCR result for dual surface markers CD44/CD47

NORMAL				**HIGH-GRADE**		
(CD44/CD47) other	**Ct value**	**5hmC (%)**		**(CD44/CD47) other**	**Ct value**	**5hmC (%)**
5hmC protected	31.722181			5hmC protected	33.3667	
5hmC unprotected	30.755924	91		5hmC unprotected	32.359	-105
Untreated DNA	31.822933			Untreated DNA	31.39857	
($CD44^+/CD47^+$) dual +ve				**($CD44^+/CD47^+$) dual +ve**		
5hmC protected	33.423992			5hmC protected	35.824017	
5hmC unprotected	32.080208	-20		5hmC unprotected	33.819828	324
Untreated DNA	25.445518			Untreated DNA	34.43775	

In addition, the 5hmC levels in the normal urothelial cells positive for the dual cell surface receptors $CD44^{+}/CD49f^{+}$and the cells along the other coordinates were above 100% (211% and 220% respectively). High-grade urothelial carcinoma cells positive for the $CD44^{+}/CD49f^{+}$ cell surface receptors had low 5hmC levels (7%) while the other cells of the other coordinates had a 5hmc level above 100% (619%) (table 6.2).

Probe id: cg24327132	**450K (**18% normal**)**	**450K (**5% tumour**)**

Table 6.2 qPCR result for dual surface markers CD44/CD49f

NORMAL				**HIGH-GRADE**		
(CD44/CD49f) other	**Ct value**	**5hmC (%)**		**(CD44/CD49f) other**	**Ct value**	**5hmC (%)**
5hmC protected	33.637917			5hmC protected	34.421894	
5hmC unprotected	29.42601	220		5hmC unprotected	30.406303	619
Untreated DNA	31.342716			Untreated DNA	31.05499	
($CD44^{+}/CD49f^{+}$) dual +ve				**($CD44^{+}/CD49f^{+}$) dual +ve**		
5hmC protected	24.177757			5hmC protected	34.607143	
5hmC unprotected	30.670734	211		5hmC unprotected	34.632214	7
Untreated DNA	27.591448			Untreated DNA	34.280983	

The normal urothelial cells positive for cell surface receptors $CD44^+/CD90^+$ as well as the other cells of the other coordinates had an undetectable 5hmC level (-165% and -10% respectively). 5hmC was detected only in the high-grade bladder carcinoma cells sorted for the $CD44^+/CD90^+$ cell surface receptors (92%). The other high-grade urothelial carcinoma cells from the other coordinates had undetectable 5hmC level (-152%) (table 6.3).

Probe id: cg24327132	**450K (**18% normal**)**	**450K (**5% tumour**)**

Table 6.3 qPCR result for dual surface markers CD44/CD90

NORMAL				**HIGH-GRADE**		
(CD44/CD90) other	**Ct value**	**5hmC (%)**		**(CD44/CD90) other**	**Ct value**	**5hmC (%)**
5hmC protected	31.842625			5hmC protected	34.626858	
5hmC unprotected	31.591469	-10		5hmC unprotected	31.868376	-152
Untreated DNA	29.180336			Untreated DNA	30.051004	
($CD44^+/CD90^+$) dual +ve				**($CD44^+/CD90^+$) dual +ve**		
5hmC protected	27.319859			5hmC protected	33.79121	
5hmC unprotected	29.301416	-165		5hmC unprotected	34.254524	92
Untreated DNA	30.504015			Untreated DNA	33.750553	

6.4 Discussion

In-depth analysis of 5hmC levels using both 450K methylation assays and qPCR analysis revealed variations in both normal urothelial and high-grade tumour tissues. Specifically, the genomic analysis of the sorted dual cell populations revealed subtle differences in 5hmC levels at specific genomic locus, which were unidentified in the methylation array. With the locus cg24327132, the qPCR evaluation showed that dual cell surface receptor populations in normal urothelium positive for both $CD44^{+}/CD47^{+}$ lacked 5hmC. The opposite was observed, however, for cells from the other coordinates of this dual cell surface receptor. The higher 5hmC levels in these cells (the cells along the other coordinates), however, were probably erroneous readings since the untreated DNA had elevated cycle threshold (Ct) values. This could be an aftereffect of the low concentration and quality of the DNA. In addition, the very high levels of 5hmC in high-grade urothelial carcinoma cells positive for the dual markers $CD44^{+}/CD47^{+}$ were also probably not reliable since these readouts were above the maximum prescribed in the Quest 5hmC detection kit. Readouts >100 were deemed to be technically unreliable while readouts <0 were deemed to denote an absence of 5hmC detection site. These unreliable values could also be a result of the deteriorating quality of the DNA being evaluated. Meanwhile, the sorted cells along the other coordinates lacked detectable levels of 5hmC.

The 5hmC levels in the normal urothelial cells positive for the dual cell surface receptors $CD44^{+}/CD49f^{+}$ and the cells along the other coordinates had technically unreliable levels of 5hmC. The 5hmC levels in the high-grade urothelial carcinoma cells positive for $CD44^{+}/CD49f^{+}$ were significant, albeit low but the carcinoma cells from the other coordinates were technically unreliable. The unreliable levels of 5hmC seen for the CD49f/CD44 in the normal urothelial cells and some of the high-grade urothelial carcinoma cells could be due to the low DNA concentration used as well as the deteriorating quality of the DNA in these sorted cells.

The 5hmC levels in normal urothelial cells positive for the dual cell surface receptors $CD44^+/CD90^+$ were undetectable. The same was observed for the cells along the other coordinates for these receptors. The dual positive high-grade bladder carcinoma cells for the same receptors had elevated and significant levels of 5hmC. The cells from the other coordinates, however, had undetectable levels of 5hmC.

The majority of urothelial tissue types examined using different cell surface markers therefore had 5hmC levels being insignificant or technically unreliable. This could be because of the low DNA content being made available for the genomic analysis. Further to this the DNA quality could have deteriorated, either due to the digestion process or due to the prolonged storage of sorted cells in flow cytometry buffer. This could have meant that the qPCR evaluation was not replicable. A similar number of artefacts was however not observed in the array data (see Chapter 5) due probably to the better DNA concentration and quality attained from the urothelial tissues.

CHAPTER SEVEN

7 FINAL DISCUSSION

7.1 Discussion

Bladder cancer is a common malignancy and one of the most expensive to manage. Molecular analysis suggests the cancer contains a variety of heterogeneous clones and can be assigned to one of several genomic subgroups. These subgroups are characterised by unique cell surface receptors and may have distinct sensitivities to chemo and radiation therapy. Previous research has characterised some of the markers specific for various differentiation states in bladder cancer (Volkmer et al., 2012), but little is known of the underlying events in individual cancers. To address this situation, I investigated epigenetic changes in individual cancers using tissue culture, flow cytometry and DNA methylation arrays.

To identify subpopulations in MIBC, I attempted to grow biopsy cells in the laboratory. Researchers, such as (Van Batavia et al., 2014), hypothesised that the basal layer of MIBC tissue includes cancer stem cells (CSC) that, in turn, are the progenitors of cancer subtypes. Studies performed previously using *in vitro* models have suggested the existence of gene signatures that distinguish basal urothelial cells from differentiated urothelial cells (Chan et al., 2009). I attempted to validate this hypothesis using primary tissue culture techniques on biopsied tissues. However, my research was hindered by the biopsied cells failing to grow in various serum-free media or being overgrown by fibroblasts or smooth muscle cells e.g. in Dulbecco's Modified Eagle's media (DMEM) supplemented with foetal calf serum (FCS). I was more successful, in the short term, with coated matrices and serum containing media. However, the cells later failed to establish as primary cultures.

Parallel to my work with primary tissue culture, I attempted to characterise bladder cancer subpopulations using the cell surface markers CD44, CD47, CD49f and CD90. Such a characterisation would identify cell subpopulations. To accomplish this, fresh biopsies of malignant urothelial tissues and normal bladder urothelium were sorted using fluorescence-activated cell sorting (FACS). These experiments revealed few cells expressing the CD90 cell surface receptor, suggesting the biopsied

tissues lacked the basal subtype bladder cancer cells. In contrast, I found many cells with high expression of the other markers, such as CD44 and CD47, indicative of terminally differentiated luminal subtype (Chan et al., 2009). This finding is in stark contrast to previous research from *in vitro* models, which had suggested CD90-positive bladder cancer cells were common and a rich repository for CSCs. The identification of enhanced levels of CD47 in certain subpopulations could be of clinical significance, as these could be viable targets for anti-CD47 therapy. I found that the expression of the CD49f receptor occurred with the CD44 receptor. A Study using mouse urothelium have previously identified these subpopulations to be lacking in tumorigenic potential, although they still could serve as models to identify differentiation states (Real et al., 2018). Although I was unable to isolate subpopulations with a basal phenotype, the presence of many differentiation states in the biopsied tissues is reflective of the hierarchical differentiation model of bladder tumour organisation.

My next experiments focused on changes in DNA methylation in bladder cancer. It has been known for many years that aberrant cytosine hypermethylation is associated with silencing of tumour suppressor genes and/or activation of oncogenes (Herman, 1999, Jarmalaite et al., 2008, Cabello et al., 2011). Recent advances in epigenetic understanding have identified different methyl states for the 5- residue of cytosine DNA bases, such as hydroxymethyl cytosine (Booth et al., 2012, Booth et al., 2013). These epigenetic residues have not been previously investigated in MIBC in detail. I used bisulfite (BS) and oxidative bisulfite (OXBS) treatment to examine changes in malignant and normal urothelial tissues (see figure 5.1 in Chapter 5). My main finding was that broadly lower levels of 5hmC were seen in malignant tissues, when compared to normal urothelium. Many genes with lower 5hmC concentrations in cancer are implicated in carcinogenesis (see figure 5.11), suggesting these epigenetic traits may play a role in this process. Importantly, differences in 5hmC (between normal and malignant tissues) were seen in all genomic loci, including introns (and other non-gene coding regions) and in non-coding RNA genomic regions (see figure 5.9). Functional pathway analysis using the genes with higher concentrations of

5hmC in normal tissues revealed enrichment for those involved in many cancers (e.g. leukaemia, lung cancer (see figure 5.11). The exact mechanism of this involvement is currently unclear.

7.2 Study Limitations

There are several key limitations that affected this work;

1. Firstly, I was unable to grow primary tumours in vitro. It was hard to obtain a regular supply of fresh tissue and the quality varied from good to poor (diathermy artefact). In the samples that did grow, I saw observed overgrowth of fibroblasts and smooth muscle cells after 2 weeks. This is despite a successful programme of normal urothelial cells growth (NHU cell lines).
2. Secondly, the number and quality of fresh samples limited FACS sorting. I was unable to find enough $CD90^{+}$ cells and so I could not explore stem cell fractions.
3. Thirdly, my methylation analysis was limited by the lack of raw RNA sequencing data available from ATLAS website. Whilst the tumours I studied were from the original TCGA cases, I was unable to directly compare 5hmC and gene expression in individual cancers.

7.3 Future Work

With several bladder cancer differentiation states being identified in MIBC biopsies, focus on identifying new cell surface markers specific to the tumour initiating cells is of prime importance. Precise knowledge of such marker populations could have positive translational impact e.g. in devising new drug molecules. The genes and pathways identified using the 450K array should be investigated further using gene knockout/ knock down model organisms e.g. mice, rat. Subpopulations positive for specific cell surface receptors should be evaluated using xenograft models. Also the primary tissue culture work I have initiated should be continued further using 3D cell culture models. A varied approach using several different cell culture media both containing serum and lacking it should be utilised to evaluate

primary urothelial carcinoma proliferation as well as standardising a protocol for primary cell culture of urothelial carcinoma.

7.4 Summary

I identified several limiting factors surmounting this bladder cancer research while addressing several queries raised by epigenetic alteration. Nonetheless, this research can still serve as groundwork for future bladder cancer research. Protocols developed here include a primary tissue culture technique for malignant urothelial tissues, which was successful in inducing cellular attachment and proliferation. This technique was, however, limited by the difficulty involved in getting these cells to expand upon further culturing. Although the protocol used for sorting cells into distinct subpopulations of basal and terminally differentiated bladder subpopulations was realised from previous research, the technique itself was limited by cell numbers, which prevented further downstream investigation.

For the first time, different 5hmC CpG sites were identified between normal and tumour bladder samples, which could serve as a basis for future research. Their presence in a more condensed manner i.e. 5hmC rich regions in bladder tumour tissue could be correlated with the gene expression data specific for these regions. Further investigation of the genes and pathways identified in the methylation/RNA expression data could be done using gene knockout models both in bladder cancer cell lines/ or murine mice. This could greatly assist the understanding of the normative role of epigenetic alterations, making it possible to distinguish these from their deleterious effects, which induce bladder carcinoma.

REFERENCES

ABE, T., SHINOHARA, N., TADA, M., HARABAYASHI, T., SAZAWA, A., MARUYAMA, S., MORIUCHI, T., TAKADA, K. & NONOMURA, K. 2008. Infiltration of Epstein-Barr virus-harboring lymphocytes occurs in a large subset of bladder cancers. *Int J Urol,* 15**,** 429-34.

ABOL-ENEIN, H. 2008. Infection: is it a cause of bladder cancer? *Scand J Urol Nephrol Suppl***,** 79-84.

AIJO, T., HUANG, Y., MANNERSTROM, H., CHAVEZ, L., TSAGARATOU, A., RAO, A. & LAHDESMAKI, H. 2016. A probabilistic generative model for quantification of DNA modifications enables analysis of demethylation pathways. *Genome Biol,* 17**,** 49.

AJILI, F., KACEM, M., TOUNSI, H., DAROUICHE, A., ENAYFER, E., CHEBI, M., MANAI, M. & BOUBAKER, S. 2012. Prognostic impact of angiogenesis in nonmuscle invasive bladder cancer as defined by microvessel density after immunohistochemical staining for CD34. *Ultrastruct Pathol,* 36**,** 336-42.

ANDREW, A. S., GUI, J., HU, T., WYSZYNSKI, A., MARSIT, C. J., KELSEY, K. T., SCHNED, A. R., TANYOS, S. A., PENDLETON, E. M., EKSTROM, R. M., LI, Z., ZENS, M. S., BORSUK, M., MOORE, J. H. & KARAGAS, M. R. 2015. Genetic polymorphisms modify bladder cancer recurrence and survival in a USA population-based prognostic study. *BJU Int,* 115**,** 238-47.

ANDREWS, T. E., WANG, D. & HARKI, D. A. 2013. Cell surface markers of cancer stem cells: diagnostic macromolecules and targets for drug delivery. *Drug Deliv Transl Res,* 3**,** 121-42.

ANTONI, S., FERLAY, J., SOERJOMATARAM, I., ZNAOR, A., JEMAL, A. & BRAY, F. 2017. Bladder Cancer Incidence and Mortality: A Global Overview and Recent Trends. *Eur Urol,* 71**,** 96-108.

AUGURIO, A., BASILICO, N. F., FILIPPONE, A. & SANPAOLO, P. 2008. Pelvic Lymph Nodes. *A Guide for Delineation of Lymph Nodal Clinical Target Volume in Radiation Therapy.* Berlin, Heidelberg: Springer Berlin Heidelberg.

AYAN, S., GOKCE, G., KILICARSLAN, H., OZDEMIR, O., YILDIZ, E. & GULTEKIN, E. Y. 2001. K-RAS mutation in transitional cell carcinoma of urinary bladder. *Int Urol Nephrol,* 33**,** 363-7.

BACHMAN, M., URIBE-LEWIS, S., YANG, X., WILLIAMS, M., MURRELL, A. & BALASUBRAMANIAN, S. 2014. 5-Hydroxymethylcytosine is a predominantly stable DNA modification. *Nat Chem,* 6**,** 1049-55.

BADAWI, H., AHMED, H., ABOUL FADL, L., HELMI, A., FAM, N., DIAB, M., ISMAIL, A., BADAWI, A. & SABER, M. 2010. Herpes simplex virus type-2 in Egyptian patients with bladder cancer or cystitis. *APMIS,* 118**,** 37-44.

BALBÁS-MARTÍNEZ, C., SAGRERA, A., CARRILLO-DE-SANTA-PAU, E., EARL, J., MÁRQUEZ, M., VAZQUEZ, M., LAPI, E., CASTRO-GINER, F., BELTRAN, S., BAYES, M., CARRATO, A., CIGUDOSA, J., DOMINGUEZ, O., GUT, M., HERRANZ, J., JUANPERE-RODERO, N., KOGEVINAS, M., LANGA OLIVA, X., LOPEZ-KNOWLES, E. & REAL, F. 2013. *Recurrent inactivation of STAG2 in bladder cancer is not associated with aneuploidy*.

BANGMA, C. H., LOEB, S., BUSSTRA, M., ZHU, X., EL BOUAZZAOUI, S., REFOS, J., VAN DER KEUR, K. A., TJIN, S., FRANKEN, C. G., VAN LEENDERS, G. J., ZWARTHOFF, E. C. & ROOBOL, M. J. 2013. Outcomes of a bladder cancer screening program using home hematuria testing and molecular markers. *Eur Urol,* 64**,** 41-7.

BARCLAY, A. N. & BROWN, M. H. 2006. The SIRP family of receptors and immune regulation. *Nat Rev Immunol,* 6**,** 457-64.

BARLANDAS-RENDON, E., MULLER, M. M., GARCIA-LATORRE, E. & HEINSCHINK, A. 2002. Comparison of urine cell characteristics by flow cytometry and cytology in patients suspected of having bladder cancer. *Clin Chem Lab Med,* 40**,** 817-23.

BASU, S., CAMPBELL, H. M., DITTEL, B. N. & RAY, A. 2010. Purification of specific cell population by fluorescence activated cell sorting (FACS). *J Vis Exp*.

BAUER, C., STEC, K., GLINTSCHERT, A., GRUDEN, K., SCHICHOR, C., OR-GUIL, M., SELBIG, J. & SCHUCHHARDT, J. 2015. BioMiner: Paving the Way for Personalized Medicine. *Cancer Inform,* 14**,** 55-63.

BECK, B. & BLANPAIN, C. 2013. Unravelling cancer stem cell potential. *Nat Rev Cancer,* 13**,** 727-38.

BENBROOK, D. M. 2006. Organotypic cultures represent tumor microenvironment for drug testing. *Drug Discovery Today: Disease Models,* 3**,** 143-148.

BENJAMINI, Y. & HOCHBERG, Y. 1995. Controlling the False Discovery Rate: A Practical and Powerful Approach to Multiple Testing. *Journal of the Royal Statistical Society. Series B (Methodological),* 57**,** 289-300.

BERTZ, S., ABEE, C., SCHWARZ-FURLAN, S., ALFER, J., HOFSTADTER, F., STOEHR, R., HARTMANN, A. & GAUMANN, A. K. 2014. Increased angiogenesis and FGFR protein expression indicate a favourable prognosis in bladder cancer. *Virchows Arch,* 465**,** 687-95.

BIAN, X., YANG, Z., FENG, H., SUN, H. & LIU, Y. 2017. A Combination of Species Identification and STR Profiling Identifies Cross-contaminated Cells from 482 Human Tumor Cell Lines. *Sci Rep,* 7**,** 9774.

BIRD, A. 2002. DNA methylation patterns and epigenetic memory. *Genes Dev,* 16**,** 6-21.

BLAVERI, E., SIMKO, J. P., KORKOLA, J. E., BREWER, J. L., BAEHNER, F., MEHTA, K., DEVRIES, S., KOPPIE, T., PEJAVAR, S., CARROLL, P. & WALDMAN, F. M. 2005.

Bladder cancer outcome and subtype classification by gene expression. *Clin Cancer Res,* 11**,** 4044-55.

BOCK, C., BEERMAN, I., LIEN, W. H., SMITH, Z. D., GU, H., BOYLE, P., GNIRKE, A., FUCHS, E., ROSSI, D. J. & MEISSNER, A. 2012. DNA methylation dynamics during in vivo differentiation of blood and skin stem cells. *Mol Cell,* 47**,** 633-47.

BOFFETTA, P. 2006. Human cancer from environmental pollutants: the epidemiological evidence. *Mutat Res,* 608**,** 157-62.

BOGDANOVIC, O. & VEENSTRA, G. J. 2011. Affinity-based enrichment strategies to assay methyl-CpG binding activity and DNA methylation in early Xenopus embryos. *BMC Res Notes,* 4**,** 300.

BONAZZA, C., ANDRADE, S. S., SUMIKAWA, J. T., BATISTA, F. P., PAREDES-GAMERO, E. J., GIRAO, M. J., OLIVA, M. L. & CASTRO, R. A. 2016. Primary Human Uterine Leiomyoma Cell Culture Quality Control: Some Properties of Myometrial Cells Cultured under Serum Deprivation Conditions in the Presence of Ovarian Steroids. *PLoS One,* 11**,** e0158578.

BOOTH, M. J., BRANCO, M. R., FICZ, G., OXLEY, D., KRUEGER, F., REIK, W. & BALASUBRAMANIAN, S. 2012. Quantitative sequencing of 5-methylcytosine and 5-hydroxymethylcytosine at single-base resolution. *Science,* 336**,** 934-7.

BOOTH, M. J., OST, T. W., BERALDI, D., BELL, N. M., BRANCO, M. R., REIK, W. & BALASUBRAMANIAN, S. 2013. Oxidative bisulfite sequencing of 5-methylcytosine and 5-hydroxymethylcytosine. *Nat Protoc,* 8**,** 1841-51.

BOURKE, L., BAULD, L., BULLEN, C., CUMBERBATCH, M., GIOVANNUCCI, E., ISLAMI, F., MCROBBIE, H., SILVERMAN, D. T. & CATTO, J. W. F. 2017. E-cigarettes and Urologic Health: A Collaborative Review of Toxicology, Epidemiology, and Potential Risks. *Eur Urol,* 71**,** 915-923.

BOUSTEAD, G. B., FOWLER, S., SWAMY, R., KOCKLEBERGH, R., HOUNSOME, L. & SECTION OF ONCOLOGY, B. 2014. Stage, grade and pathological characteristics of bladder cancer in the UK: British Association of Urological Surgeons (BAUS) urological tumour registry. *BJU Int,* 113**,** 924-30.

BRINKMAN, M. T., BUNTINX, F., KELLEN, E., VAN DONGEN, M. C., DAGNELIE, P. C., MULS, E. & ZEEGERS, M. P. 2011. Consumption of animal products, olive oil and dietary fat and results from the Belgian case-control study on bladder cancer risk. *Eur J Cancer,* 47**,** 436-42.

BRYAN, R. T. 2015. Cell adhesion and urothelial bladder cancer: the role of cadherin switching and related phenomena. *Philos Trans R Soc Lond B Biol Sci,* 370**,** 20140042.

BULL, N. D., JOHNSON, T. V., WELSAPAR, G., DEKORVER, N. W., TOMAREV, S. I. & MARTIN, K. R. 2011. Use of an adult rat retinal explant model for screening of potential retinal ganglion cell neuroprotective therapies. *Invest Ophthalmol Vis Sci,* 52**,** 3309-20.

BURCHILL, S. A., NEAL, D. E. & LUNEC, J. 1994. Frequency of H-ras mutations in human bladder cancer detected by direct sequencing. *Br J Urol,* 73**,** 516-21.

CABELLO, M. J., GRAU, L., FRANCO, N., ORENES, E., ALVAREZ, M., BLANCA, A., HEREDERO, O., PALACIOS, A., URRUTIA, M., FERNANDEZ, J. M., LOPEZ-BELTRAN, A. & SANCHEZ-CARBAYO, M. 2011. Multiplexed methylation profiles of tumor suppressor genes in bladder cancer. *J Mol Diagn,* 13**,** 29-40.

CALVET, C. Y., ANDRE, F. M. & MIR, L. M. 2014. The culture of cancer cell lines as tumorspheres does not systematically result in cancer stem cell enrichment. *PLoS One,* 9**,** e89644.

CANCER GENOME ATLAS RESEARCH, N. 2014. Comprehensive molecular characterization of urothelial bladder carcinoma. *Nature,* 507**,** 315-22.

CAO, J. & YAN, Q. 2012. Histone ubiquitination and deubiquitination in transcription, DNA damage response, and cancer. *Front Oncol,* 2**,** 26.

CARDIS, E., GILBERT, E. S., CARPENTER, L., HOWE, G., KATO, I., ARMSTRONG, B. K., BERAL, V., COWPER, G., DOUGLAS, A., FIX, J. & ET AL. 1995. Effects of low doses and low dose rates of external ionizing radiation: cancer mortality among nuclear industry workers in three countries. *Radiat Res,* 142**,** 117-32.

CARREON, T., RUDER, A. M., SCHULTE, P. A., HAYES, R. B., ROTHMAN, N., WATERS, M., GRANT, D. J., BOISSY, R., BELL, D. A., KADLUBAR, F. F., HEMSTREET, G. P., 3RD, YIN, S. & LEMASTERS, G. K. 2006. NAT2 slow acetylation and bladder cancer in workers exposed to benzidine. *Int J Cancer,* 118**,** 161-8.

CATTO, J. W., AZZOUZI, A. R., REHMAN, I., FEELEY, K. M., CROSS, S. S., AMIRA, N., FROMONT, G., SIBONY, M., CUSSENOT, O., MEUTH, M. & HAMDY, F. C. 2005. Promoter hypermethylation is associated with tumor location, stage, and subsequent progression in transitional cell carcinoma. *J Clin Oncol,* 23**,** 2903-10.

CATTO, J. W., MIAH, S., OWEN, H. C., BRYANT, H., MYERS, K., DUDZIEC, E., LARRE, S., MILO, M., REHMAN, I., ROSARIO, D. J., DI MARTINO, E., KNOWLES, M. A., MEUTH, M., HARRIS, A. L. & HAMDY, F. C. 2009. Distinct microRNA alterations characterize high- and low-grade bladder cancer. *Cancer Res,* 69**,** 8472-81.

CAZIER, J. B., RAO, S. R., MCLEAN, C. M., WALKER, A. K., WRIGHT, B. J., JAEGER, E. E., KARTSONAKI, C., MARSDEN, L., YAU, C., CAMPS, C., KAISAKI, P., OXFORD-ILLUMINA, W. G. S. C., TAYLOR, J., CATTO, J. W., TOMLINSON, I. P., KILTIE, A. E. & HAMDY, F. C. 2014. Whole-genome sequencing of bladder cancers reveals somatic CDKN1A mutations and clinicopathological associations with mutation burden. *Nat Commun,* 5**,** 3756.

CELIK-UZUNER, S., LI, Y., PETERS, L. & O'NEILL, C. 2017. Measurement of global DNA methylation levels by flow cytometry in mouse fibroblasts. *In Vitro Cell Dev Biol Anim,* 53**,** 1-6.

CÉZAR, D., BIZARI, L., MESQUITA, J. C., DENADAI, E. & SILVA, A. E. 2002. Chromosomal aneuploidies in bladder cancer, chronic cystitis and normal urothelium detected by fluorescence in situ hybridization. *Rev. bras. cancerol,* 48**,** 517-522.

CHAE, Y. K., RANGANATH, K., HAMMERMAN, P. S., VAKLAVAS, C., MOHINDRA, N., KALYAN, A., MATSANGOU, M., COSTA, R., CARNEIRO, B., VILLAFLOR, V. M., CRISTOFANILLI, M. & GILES, F. J. 2017. Inhibition of the fibroblast growth factor receptor (FGFR) pathway: the current landscape and barriers to clinical application. *Oncotarget,* 8**,** 16052-16074.

CHALASANI, V., CHIN, J. L. & IZAWA, J. I. 2009. Histologic variants of urothelial bladder cancer and nonurothelial histology in bladder cancer. *Can Urol Assoc J,* 3**,** S193-8.

CHAMIE, K., LITWIN, M. S., BASSETT, J. C., DASKIVICH, T. J., LAI, J., HANLEY, J. M., KONETY, B. R. & SAIGAL, C. S. 2013. Recurrence of high-risk bladder cancer: a population-based analysis. *Cancer,* 119**,** 3219-27.

CHAN, K. S., ESPINOSA, I., CHAO, M., WONG, D., AILLES, L., DIEHN, M., GILL, H., PRESTI, J., JR., CHANG, H. Y., VAN DE RIJN, M., SHORTLIFFE, L. & WEISSMAN, I. L. 2009. Identification, molecular characterization, clinical prognosis, and therapeutic targeting of human bladder tumor-initiating cells. *Proc Natl Acad Sci U S A,* 106**,** 14016-21.

CHAN, K. S., VOLKMER, J. P. & WEISSMAN, I. 2010. Cancer stem cells in bladder cancer: a revisited and evolving concept. *Curr Opin Urol,* 20**,** 393-7.

CHAN, M. W., CHAN, L. W., TANG, N. L., LO, K. W., TONG, J. H., CHAN, A. W., CHEUNG, H. Y., WONG, W. S., CHAN, P. S., LAI, F. M. & TO, K. F. 2003. Frequent hypermethylation of promoter region of RASSF1A in tumor tissues and voided urine of urinary bladder cancer patients. *Int J Cancer,* 104**,** 611-6.

CHAPPELL, J. & DALTON, S. 2010. Altered cell cycle regulation helps stem-like carcinoma cells resist apoptosis. *BMC Biol,* 8**,** 63.

CHATTERJEE, A., RODGER, E. J. & ECCLES, M. R. 2018. Epigenetic drivers of tumourigenesis and cancer metastasis. *Semin Cancer Biol,* 51**,** 149-159.

CHAVAN, S., BRAY, F., LORTET-TIEULENT, J., GOODMAN, M. & JEMAL, A. 2014. International variations in bladder cancer incidence and mortality. *Eur Urol,* 66**,** 59-73.

CHEN, T., HEVI, S., GAY, F., TSUJIMOTO, N., HE, T., ZHANG, B., UEDA, Y. & LI, E. 2007. Complete inactivation of DNMT1 leads to mitotic catastrophe in human cancer cells. *Nat Genet,* 39**,** 391-6.

CHEN, Z., LI, S., SUBRAMANIAM, S., SHYY, J. Y. & CHIEN, S. 2017. Epigenetic Regulation: A New Frontier for Biomedical Engineers. *Annu Rev Biomed Eng,* 19**,** 195-219.

CHENG, J. C., WEISENBERGER, D. J., GONZALES, F. A., LIANG, G., XU, G. L., HU, Y. G., MARQUEZ, V. E. & JONES, P. A. 2004. Continuous zebularine treatment effectively sustains demethylation in human bladder cancer cells. *Mol Cell Biol,* 24**,** 1270-8.

CHOI, W., PORTEN, S., KIM, S., WILLIS, D., PLIMACK, E. R., HOFFMAN-CENSITS, J., ROTH, B., CHENG, T., TRAN, M., LEE, I. L., MELQUIST, J., BONDARUK, J., MAJEWSKI, T., ZHANG, S., PRETZSCH, S., BAGGERLY, K., SIEFKER-RADTKE, A., CZERNIAK, B., DINNEY, C. P. & MCCONKEY, D. J. 2014. Identification of distinct basal and luminal subtypes of muscle-invasive bladder cancer with different sensitivities to frontline chemotherapy. *Cancer Cell,* 25**,** 152-65.

CHOUDHURY, N. J., KIYOTANI, K., YAP, K. L., CAMPANILE, A., ANTIC, T., YEW, P. Y., STEINBERG, G., PARK, J. H., NAKAMURA, Y. & O'DONNELL, P. H. 2016. Low T-cell Receptor Diversity, High Somatic Mutation Burden, and High Neoantigen Load as Predictors of Clinical Outcome in Muscle-invasive Bladder Cancer. *Eur Urol Focus,* 2**,** 445-452.

CHRISTOFORIDOU, E. P., RIZA, E., KALES, S. N., HADJISTAVROU, K., STOLTIDI, M., KASTANIA, A. N. & LINOS, A. 2013. Bladder cancer and arsenic through drinking water: a

systematic review of epidemiologic evidence. *J Environ Sci Health A Tox Hazard Subst Environ Eng,* 48**,** 1764-75.

CHRISTOPH, F., WEIKERT, S., KEMPKENSTEFFEN, C., KRAUSE, H., SCHOSTAK, M., MILLER, K. & SCHRADER, M. 2006. Regularly methylated novel pro-apoptotic genes associated with recurrence in transitional cell carcinoma of the bladder. *Int J Cancer,* 119**,** 1396-402.

CORDON-CARDO, C., DALBAGNI, G., SAEZ, G. T., OLIVA, M. R., ZHANG, Z. F., ROSAI, J., REUTER, V. E. & PELLICER, A. 1994. p53 mutations in human bladder cancer: genotypic versus phenotypic patterns. *Int J Cancer,* 56**,** 347-53.

COWAN, M., SPRINGER, S., NGUYEN, D., TAHERI, D., GUNER, G., RODRIGUEZ, M. A., WANG, Y., KINDE, I., VANDENBUSSCHE, C. J., OLSON, M. T., CUNHA, I., FUJITA, K., ERTOY, D., BIVALACQUA, T. J., KINZLER, K., VOGELSTEIN, B., NETTO, G. J. & PAPADOPOULOS, N. 2016. High prevalence of TERT promoter mutations in primary squamous cell carcinoma of the urinary bladder. *Mod Pathol,* 29**,** 511-5.

CUMBERBATCH, M. G., COX, A., TEARE, D. & CATTO, J. W. 2015. Contemporary Occupational Carcinogen Exposure and Bladder Cancer: A Systematic Review and Meta-analysis. *JAMA Oncol,* 1**,** 1282-90.

CUNDERLIKOVA, B., WAHLQVIST, R., BERNER, A., VASOVIC, V., WARLOE, T., NESLAND, J. M. & PENG, Q. 2007. Detection of urinary bladder cancer with flow cytometry and hexaminolevulinate in urine samples. *Cytopathology,* 18**,** 87-95.

DADHANIA, V., CZERNIAK, B. & GUO, C. C. 2015. Adenocarcinoma of the urinary bladder. *Am J Clin Exp Urol,* 3**,** 51-63.

DAMMANN, R., SCHAGDARSURENGIN, U., STRUNNIKOVA, M., RASTETTER, M., SEIDEL, C., LIU, L., TOMMASI, S. & PFEIFER, G. P. 2003. Epigenetic inactivation of the Ras-

association domain family 1 (RASSF1A) gene and its function in human carcinogenesis. *Histol Histopathol,* 18**,** 665-77.

DAMRAUER, J. S., HOADLEY, K. A., CHISM, D. D., FAN, C., TIGANELLI, C. J., WOBKER, S. E., YEH, J. J., MILOWSKY, M. I., IYER, G., PARKER, J. S. & KIM, W. Y. 2014. Intrinsic subtypes of high-grade bladder cancer reflect the hallmarks of breast cancer biology. *Proc Natl Acad Sci U S A,* 111**,** 3110-5.

DANGLE, P. P., ZAHARIEVA, B., JIA, H. & POHAR, K. S. 2009. Ras-MAPK pathway as a therapeutic target in cancer--emphasis on bladder cancer. *Recent Pat Anticancer Drug Discov,* 4**,** 125-36.

DARST, R. P., PARDO, C. E., AI, L., BROWN, K. D. & KLADDE, M. P. 2010. Bisulfite sequencing of DNA. *Curr Protoc Mol Biol,* Chapter 7**,** Unit 7.9.1-17.

DAVIES, G., JIANG, W. G. & MASON, M. D. 1999. Cell-cell adhesion molecules and their associated proteins in bladder cancer cells and their role in mitogen induced cell-cell dissociation and invasion. *Anticancer Res,* 19**,** 547-52.

DE CARVALHO, D. D., SHARMA, S., YOU, J. S., SU, S. F., TABERLAY, P. C., KELLY, T. K., YANG, X., LIANG, G. & JONES, P. A. 2012. DNA methylation screening identifies driver epigenetic events of cancer cell survival. *Cancer Cell,* 21**,** 655-67.

DEAK, M., CLIFTON, A. D., LUCOCQ, L. M. & ALESSI, D. R. 1998. Mitogen- and stress-activated protein kinase-1 (MSK1) is directly activated by MAPK and SAPK2/p38, and may mediate activation of CREB. *EMBO J,* 17**,** 4426-41.

DEDEURWAERDER, S. & FUKS, F. 2012. DNA methylation markers for breast cancer prognosis: Unmasking the immune component. *Oncoimmunology,* 1**,** 962-964.

DEGEORGE, K. C., HOLT, H. R. & HODGES, S. C. 2017. Bladder Cancer: Diagnosis and Treatment. *Am Fam Physician,* 96**,** 507-514.

DEVANAND, P., KIM, S. I., CHOI, Y. W., SHEEN, S. S., YIM, H., RYU, M. S., KIM, S. J., KIM, W. J. & LIM, I. K. 2014. Inhibition of bladder cancer invasion by Sp1-mediated BTG2 expression via inhibition of DNA methyltransferase 1. *FEBS J,* 281**,** 5581-601.

DICKINSON, A. J., FOX, S. B., PERSAD, R. A., HOLLYER, J., SIBLEY, G. N. & HARRIS, A. L. 1994. Quantification of angiogenesis as an independent predictor of prognosis in invasive bladder carcinomas. *Br J Urol,* 74**,** 762-6.

DIDIANO, D. & HOBERT, O. 2008. Molecular architecture of a miRNA-regulated 3' UTR. *RNA,* 14**,** 1297-317.

DIMOV, I., VISNJIC, M. & STEFANOVIC, V. 2010. Urothelial cancer stem cells. *ScientificWorldJournal,* 10**,** 1400-15.

DIRKS, W. G., MACLEOD, R. A. & DREXLER, H. G. 1999. ECV304 (endothelial) is really T24 (bladder carcinoma): cell line cross- contamination at source. *In Vitro Cell Dev Biol Anim,* 35**,** 558-9.

DODURGA, Y., TATAROGLU, C., KESEN, Z. & SATIROGLU-TUFAN, N. L. 2011. Incidence of fibroblast growth factor receptor 3 gene (FGFR3) A248C, S249C, G372C, and T375C mutations in bladder cancer. *Genet Mol Res,* 10**,** 86-95.

DOLLEY-HITZE, T., JOUAN, F., MARTIN, B., MOTTIER, S., EDELINE, J., MORANNE, O., LE POGAMP, P., BELAUD-ROTUREAU, M. A., PATARD, J. J., RIOUX-LECLERCQ, N. & VIGNEAU, C. 2010. Angiotensin-2 receptors (AT1-R and AT2-R), new prognostic factors for renal clear-cell carcinoma? *Br J Cancer,* 103**,** 1698-705.

DONOGHUE, A. M. 2004. Occupational health hazards in mining: an overview. *Occup Med (Lond),* 54**,** 283-9.

DRAYTON, R. M. & CATTO, J. W. 2012. Molecular mechanisms of cisplatin resistance in bladder cancer. *Expert Rev Anticancer Ther,* 12**,** 271-81.

DU, P., ZHANG, X., HUANG, C. C., JAFARI, N., KIBBE, W. A., HOU, L. & LIN, S. M. 2010. Comparison of Beta-value and M-value methods for quantifying methylation levels by microarray analysis. *BMC Bioinformatics,* 11**,** 587.

DUNN, K. L., ESPINO, P. S., DROBIC, B., HE, S. & DAVIE, J. R. 2005. The Ras-MAPK signal transduction pathway, cancer and chromatin remodeling. *Biochem Cell Biol,* 83**,** 1-14.

DWEEP, H., STICHT, C., PANDEY, P. & GRETZ, N. 2011. miRWalk--database: prediction of possible miRNA binding sites by "walking" the genes of three genomes. *J Biomed Inform,* 44**,** 839-47.

DYRSKJOT, L., KRUHOFFER, M., THYKJAER, T., MARCUSSEN, N., JENSEN, J. L., MOLLER, K. & ORNTOFT, T. F. 2004. Gene expression in the urinary bladder: a common carcinoma in situ gene expression signature exists disregarding histopathological classification. *Cancer Res,* 64**,** 4040-8.

EARL, J., RICO, D., CARRILLO-DE-SANTA-PAU, E., RODRIGUEZ-SANTIAGO, B., MENDEZ-PERTUZ, M., AUER, H., GOMEZ, G., GROSSMAN, H. B., PISANO, D. G., SCHULZ, W. A., PEREZ-JURADO, L. A., CARRATO, A., THEODORESCU, D., CHANOCK, S., VALENCIA, A. & REAL, F. X. 2015. The UBC-40 Urothelial Bladder Cancer cell line index: a genomic resource for functional studies. *BMC Genomics,* 16**,** 403.

EASWARAN, H., TSAI, H. C. & BAYLIN, S. B. 2014. Cancer epigenetics: tumor heterogeneity, plasticity of stem-like states, and drug resistance. *Mol Cell,* 54**,** 716-27.

ECKE, T. H., SACHS, M. D., LENK, S. V., LOENING, S. A. & SCHLECHTE, H. H. 2008. TP53 gene mutations as an independent marker for urinary bladder cancer progression. *Int J Mol Med,* 21**,** 655-61.

ELEFTHERIOU, M., PASCUAL, A. J., WHELDON, L. M., PERRY, C., ABAKIR, A., ARORA, A., JOHNSON, A. D., AUER, D. T., ELLIS, I. O., MADHUSUDAN, S. & RUZOV, A. 2015. 5-

Carboxylcytosine levels are elevated in human breast cancers and gliomas. *Clin Epigenetics,* 7**,** 88.

ELLINGER, J., BACHMANN, A., GOKE, F., BEHBAHANI, T. E., BAUMANN, C., HEUKAMP, L. C., ROGENHOFER, S. & MULLER, S. C. 2014. Alterations of global histone H3K9 and H3K27 methylation levels in bladder cancer. *Urol Int,* 93**,** 113-8.

ELLIS, H. 2005. Anatomy of the urinary bladder, prostate and male urethra. *Surgery (Oxford),* 23**,** 97-98.

EPSTEIN, J. I., AMIN, M. B., REUTER, V. R. & MOSTOFI, F. K. 1998. The World Health Organization/International Society of Urological Pathology consensus classification of urothelial (transitional cell) neoplasms of the urinary bladder. Bladder Consensus Conference Committee. *Am J Surg Pathol,* 22**,** 1435-48.

ESPEJO-HERRERA, N., CANTOR, K. P., MALATS, N., SILVERMAN, D. T., TARDON, A., GARCIA-CLOSAS, R., SERRA, C., KOGEVINAS, M. & VILLANUEVA, C. M. 2015. Nitrate in drinking water and bladder cancer risk in Spain. *Environ Res,* 137**,** 299-307.

EZPONDA, T., DUPERE-RICHER, D., WILL, C. M., SMALL, E. C., VARGHESE, N., PATEL, T., NABET, B., POPOVIC, R., OYER, J., BULIC, M., ZHENG, Y., HUANG, X., SHAH, M. Y., MAJI, S., RIVA, A., OCCHIONORELLI, M., TONON, G., KELLEHER, N., KEATS, J. & LICHT, J. D. 2017. UTX/KDM6A Loss Enhances the Malignant Phenotype of Multiple Myeloma and Sensitizes Cells to EZH2 inhibition. *Cell Rep,* 21**,** 628-640.

FALSO, M. J., BUCHHOLZ, B. A. & WHITE, R. W. 2012. Stem-like cells in bladder cancer cell lines with differential sensitivity to cisplatin. *Anticancer Res,* 32**,** 733-8.

FANG, H., YAO, B., YAN, Y., XU, H., LIU, Y., TANG, H., ZHOU, J., CAO, L., WANG, W., ZHANG, J., ZHAO, L., CHEN, X., ZHANG, F. & ZHAO, Y. 2013. Diabetes mellitus increases the risk of bladder cancer: an updated meta-analysis of observational studies. *Diabetes Technol Ther,* 15**,** 914-22.

FERLAY, J., SOERJOMATARAM, I., DIKSHIT, R., ESER, S., MATHERS, C., REBELO, M., PARKIN, D. M., FORMAN, D. & BRAY, F. 2015. Cancer incidence and mortality worldwide: sources, methods and major patterns in GLOBOCAN 2012. *Int J Cancer,* 136**,** E359-86.

FERRIS, J., BERBEL, O., ALONSO-LOPEZ, J., GARCIA, J. & ORTEGA, J. A. 2013. Environmental non-occupational risk factors associated with bladder cancer. *Actas Urol Esp,* 37**,** 579-86.

FICZ, G. & GRIBBEN, J. G. 2014. Loss of 5-hydroxymethylcytosine in cancer: cause or consequence? *Genomics,* 104**,** 352-7.

FIORITI, D., PIETROPAOLO, V., DAL FORNO, S., LAURENTI, C., CHIARINI, F. & DEGENER, A. M. 2003. Urothelial bladder carcinoma and viral infections: different association with human polyomaviruses and papillomaviruses. *Int J Immunopathol Pharmacol,* 16**,** 283-8.

FLIEGER, A., GOLKA, K., SCHULZE, H. & FOLLMANN, W. 2008. Primary cultures of human urothelial cells for genotoxicity testing. *J Toxicol Environ Health A,* 71**,** 930-5.

FORTIN JP FAU - LABBE, A., LABBE A FAU - LEMIRE, M., LEMIRE M FAU - ZANKE, B. W., ZANKE BW FAU - HUDSON, T. J., HUDSON TJ FAU - FERTIG, E. J., FERTIG EJ FAU - GREENWOOD, C. M., GREENWOOD CM FAU - HANSEN, K. D. & HANSEN, K. D. 2014. Functional normalization of 450k methylation array data improves replication in large cancer studies.

FORTUNY, J., KOGEVINAS, M., ZENS, M. S., SCHNED, A., ANDREW, A. S., HEANEY, J., KELSEY, K. T. & KARAGAS, M. R. 2007. Analgesic and anti-inflammatory drug use and risk of bladder cancer: a population based case control study. *BMC Urology,* 7**,** 13.

FOWLER, C. J., GRIFFITHS, D. & DE GROAT, W. C. 2008. The neural control of micturition. *Nat Rev Neurosci,* 9**,** 453-66.

FREEDMAN, N. D., SILVERMAN, D. T., HOLLENBECK, A. R., SCHATZKIN, A. & ABNET, C. C. 2011. Association between smoking and risk of bladder cancer among men and women. *JAMA,* 306**,** 737-45.

FROMMER, M., MCDONALD, L. E., MILLAR, D. S., COLLIS, C. M., WATT, F., GRIGG, G. W., MOLLOY, P. L. & PAUL, C. L. 1992. A genomic sequencing protocol that yields a positive display of 5-methylcytosine residues in individual DNA strands. *Proc Natl Acad Sci U S A,* 89**,** 1827-31.

FUGE, O., VASDEV, N., ALLCHORNE, P. & GREEN, J. S. 2015. Immunotherapy for bladder cancer. *Res Rep Urol,* 7**,** 65-79.

FURUSE, H. & OZONO, S. 2010. Transurethral resection of the bladder tumour (TURBT) for non-muscle invasive bladder cancer: basic skills. *Int J Urol,* 17**,** 698-9.

GAO, B. B., LEI, B. L., ZHANG, Y. Y. & HAN, Q. D. 2000. Cell proliferation and Ca(2+)-calmodulin dependent protein kinase activation mediated by alpha 1A- and alpha 1B-adrenergic receptor in HEK293 cells. *Acta Pharmacol Sin,* 21**,** 55-9.

GARCIA-GIMENEZ, J. L., LEDESMA, A. M., ESMORIS, I., ROMA-MATEO, C., SANZ, P., VINA, J. & PALLARDO, F. V. 2012. Histone carbonylation occurs in proliferating cells. *Free Radic Biol Med,* 52**,** 1453-64.

GHERVAN, L., ZAHARIE, A., ENE, B. & ELEC, F. I. 2017. Small-cell carcinoma of the urinary bladder: where do we stand? *Clujul Med,* 90**,** 13-17.

GIARETTI, W. 1997. Origins of ... flow cytometry and applications in oncology. *J Clin Pathol,* 50**,** 275-7.

GILBERT, C. A. & ROSS, A. H. 2009. Cancer stem cells: cell culture, markers, and targets for new therapies. *J Cell Biochem,* 108**,** 1031-8.

GILLIGAN, T. D., STEELE, G. S., ZIETMAN, A. L. & KANTOFF, P. W. 2003. Muscle-invasive bladder cancer.

GODWIN, J. T. & HANASH, K. 1984. Pathology of bilharzial bladder cancer. *Prog Clin Biol Res,* 162A**,** 95-143.

GOLABEK, T., SOCHA, K., KUDELSKI, J., DAREWICZ, B., MARKIEWICZ-ZUKOWSKA, R., CHLOSTA, P. & BORAWSKA, M. 2017. Chromium in urothelial carcinoma of the bladder. *Annals of Agricultural and Environmental Medicine,* 24**,** 602-605.

GOODWIN JINESH, G., WILLIS, D. L. & KAMAT, A. M. 2014. Bladder cancer stem cells: biological and therapeutic perspectives. *Curr Stem Cell Res Ther,* 9**,** 89-101.

GORE, J. L. & GILBERT, S. M. 2013. Improving bladder cancer patient care: a pharmacoeconomic perspective. *Expert Rev Anticancer Ther,* 13**,** 661-8.

GOSLING, J. A. 1985. Structure of the lower urinary tract and pelvic floor. *Clin Obstet Gynaecol,* 12**,** 285-94.

GRAHAM, D. Y. 1997. Helicobacter pylori infection in the pathogenesis of duodenal ulcer and gastric cancer: a model. *Gastroenterology,* 113**,** 1983-91.

GROENENDIJK, F. H., DE JONG, J., FRANSEN VAN DE PUTTE, E. E., MICHAUT, M., SCHLICKER, A., PETERS, D., VELDS, A., NIEUWLAND, M., VAN DEN HEUVEL, M. M., KERKHOVEN, R. M., WESSELS, L. F., BROEKS, A., VAN RHIJN, B. W., BERNARDS, R. & VAN DER HEIJDEN, M. S. 2016. ERBB2 Mutations Characterize a Subgroup of Muscle-invasive Bladder Cancers with Excellent Response to Neoadjuvant Chemotherapy. *Eur Urol,* 69**,** 384-8.

GROVER, S., SRIVASTAVA, A., LEE, R., TEWARI, A. K. & TE, A. E. 2011. Role of inflammation in bladder function and interstitial cystitis. *Ther Adv Urol,* 3**,** 19-33.

GUANCIAL, E. A., WERNER, L., BELLMUNT, J., BAMIAS, A., CHOUEIRI, T. K., ROSS, R., SCHUTZ, F. A., PARK, R. S., O'BRIEN, R. J., HIRSCH, M. S., BARLETTA, J. A., BERMAN, D. M., LIS, R., LODA, M., STACK, E. C., GARRAWAY, L. A., RIESTER, M.,

MICHOR, F., KANTOFF, P. W. & ROSENBERG, J. E. 2014. FGFR3 expression in primary and metastatic urothelial carcinoma of the bladder. *Cancer Med,* 3**,** 835-44.

GUI, Y., GUO, G., HUANG, Y., HU, X., TANG, A., GAO, S., WU, R., CHEN, C., LI, X., ZHOU, L., HE, M., LI, Z., SUN, X., JIA, W., CHEN, J., YANG, S., ZHOU, F., ZHAO, X., WAN, S., YE, R., LIANG, C., LIU, Z., HUANG, P., LIU, C., JIANG, H., WANG, Y., ZHENG, H., SUN, L., LIU, X., JIANG, Z., FENG, D., CHEN, J., WU, S., ZOU, J., ZHANG, Z., YANG, R., ZHAO, J., XU, C., YIN, W., GUAN, Z., YE, J., ZHANG, H., LI, J., KRISTIANSEN, K., NICKERSON, M. L., THEODORESCU, D., LI, Y., ZHANG, X., LI, S., WANG, J., YANG, H., WANG, J. & CAI, Z. 2011. Frequent mutations of chromatin remodeling genes in transitional cell carcinoma of the bladder. *Nat Genet,* 43**,** 875-8.

GUIBERT, S. & WEBER, M. 2013. Functions of DNA methylation and hydroxymethylation in mammalian development. *Curr Top Dev Biol,* 104**,** 47-83.

GUO, Y., CHEKALUK, Y., ZHANG, J., DU, J., GRAY, N. S., WU, C. L. & KWIATKOWSKI, D. J. 2013. TSC1 involvement in bladder cancer: diverse effects and therapeutic implications. *J Pathol,* 230**,** 17-27.

GUST, K. M., MCCONKEY, D. J., AWREY, S., HEGARTY, P. K., QING, J., BONDARUK, J., ASHKENAZI, A., CZERNIAK, B., DINNEY, C. P. & BLACK, P. C. 2013. Fibroblast growth factor receptor 3 is a rational therapeutic target in bladder cancer. *Mol Cancer Ther,* 12**,** 1245-54.

HAN, A. L., VEENEMAN, B. A., EL-SAWY, L., DAY, K. C., DAY, M. L., TOMLINS, S. A. & KELLER, E. T. 2017. Fibulin-3 promotes muscle-invasive bladder cancer. *Oncogene,* 36**,** 5243.

HAN, J., LEE, Y., YEOM, K. H., KIM, Y. K., JIN, H. & KIM, V. N. 2004. The Drosha-DGCR8 complex in primary microRNA processing. *Genes Dev,* 18**,** 3016-27.

HANAHAN, D. & WEINBERG, R. A. 2000. The hallmarks of cancer. *Cell,* 100**,** 57-70.

HANAHAN, D. & WEINBERG, R. A. 2011. Hallmarks of cancer: the next generation. *Cell,* 144**,** 646-74.

HARLING, M., SCHABLON, A., SCHEDLBAUER, G., DULON, M. & NIENHAUS, A. 2010. Bladder cancer among hairdressers: a meta-analysis. *Occup Environ Med,* 67**,** 351-8.

HATINA, J. & SCHULZ, W. A. 2012. Stem cells in the biology of normal urothelium and urothelial carcinoma. *Neoplasma,* 59**,** 728-36.

HAUGSTEN, E. M., WIEDLOCHA, A., OLSNES, S. & WESCHE, J. 2010. Roles of fibroblast growth factor receptors in carcinogenesis. *Mol Cancer Res,* 8**,** 1439-52.

HENDIJANI, F. 2017. Explant culture: An advantageous method for isolation of mesenchymal stem cells from human tissues. *Cell Prolif,* 50.

HERCULANO-HOUZEL, S., VON BARTHELD, C. S., MILLER, D. J. & KAAS, J. H. 2015. How to count cells: the advantages and disadvantages of the isotropic fractionator compared with stereology. *Cell Tissue Res,* 360**,** 29-42.

HERMAN, J. G. 1999. Hypermethylation of tumor suppressor genes in cancer. *Semin Cancer Biol,* 9**,** 359-67.

HICKLING, D. R., SUN, T. T. & WU, X. R. 2015. Anatomy and Physiology of the Urinary Tract: Relation to Host Defense and Microbial Infection. *Microbiol Spectr,* 3.

HILL, W. G. 2015. Control of urinary drainage and voiding. *Clin J Am Soc Nephrol,* 10**,** 480-92.

HOFMANN, C., OBERMEIER, F., ARTINGER, M., HAUSMANN, M., FALK, W., SCHOELMERICH, J., ROGLER, G. & GROSSMANN, J. 2007. Cell-cell contacts prevent anoikis in primary human colonic epithelial cells. *Gastroenterology,* 132**,** 587-600.

HOFNER, T., MACHER-GOEPPINGER, S., KLEIN, C., SCHILLERT, A., EISEN, C., WAGNER, S., RIGO-WATERMEIER, T., BACCELLI, I., VOGEL, V., TRUMPP, A. & SPRICK, M. R. 2014. Expression and prognostic significance of cancer stem cell markers CD24 and CD44 in

urothelial bladder cancer xenografts and patients undergoing radical cystectomy. *Urol Oncol,* 32**,** 678-86.

HOQUE, M. O., BEGUM, S., TOPALOGLU, O., CHATTERJEE, A., ROSENBAUM, E., VAN CRIEKINGE, W., WESTRA, W. H., SCHOENBERG, M., ZAHURAK, M., GOODMAN, S. N. & SIDRANSKY, D. 2006. Quantitation of promoter methylation of multiple genes in urine DNA and bladder cancer detection. *J Natl Cancer Inst,* 98**,** 996-1004.

HU, C., LIU, Y., LIN, Y., LIANG, J. K., ZHONG, W. W., LI, K., HUANG, W. T., WANG, D. J., YAN, G. M., ZHU, W. B., QIU, J. G. & GAO, X. 2018. Intravenous injections of the oncolytic virus M1 as a novel therapy for muscle-invasive bladder cancer. *Cell Death Dis,* 9**,** 274.

HU, H., SHU, M., HE, L., YU, X., LIU, X., LU, Y., CHEN, Y., MIAO, X. & CHEN, X. 2017. Epigenomic landscape of 5-hydroxymethylcytosine reveals its transcriptional regulation of lncRNAs in colorectal cancer. *Br J Cancer,* 116**,** 658-668.

HULSEN, T., DE VLIEG, J. & ALKEMA, W. 2008. BioVenn – a web application for the comparison and visualization of biological lists using area-proportional Venn diagrams. *BMC Genomics,* 9**,** 488.

HUMPHREY, P. A., MOCH, H., CUBILLA, A. L., ULBRIGHT, T. M. & REUTER, V. E. 2016. The 2016 WHO Classification of Tumours of the Urinary System and Male Genital Organs-Part B: Prostate and Bladder Tumours. *Eur Urol,* 70**,** 106-119.

HURST, C. D., ALDER, O., PLATT, F. M., DROOP, A., STEAD, L. F., BURNS, J. E., BURGHEL, G. J., JAIN, S., KLIMCZAK, L. J., LINDSAY, H., ROULSON, J. A., TAYLOR, C. F., THYGESEN, H., CAMERON, A. J., RIDLEY, A. J., MOTT, H. R., GORDENIN, D. A. & KNOWLES, M. A. 2017. Genomic Subtypes of Non-invasive Bladder Cancer with Distinct Metabolic Profile and Female Gender Bias in KDM6A Mutation Frequency. *Cancer Cell,* 32**,** 701-715 e7.

HURST, C. D. & KNOWLES, M. A. 2014. Molecular subtyping of invasive bladder cancer: time to divide and rule? *Cancer Cell,* 25**,** 135-6.

HURST, C. D., PLATT, F. M., TAYLOR, C. F. & KNOWLES, M. A. 2012. Novel tumor subgroups of urothelial carcinoma of the bladder defined by integrated genomic analysis. *Clin Cancer Res,* 18**,** 5865-5877.

ISMAILI, N. 2011. A rare bladder cancer--small cell carcinoma: review and update. *Orphanet J Rare Dis,* 6**,** 75.

ITO, S., SHEN, L., DAI, Q., WU, S. C., COLLINS, L. B., SWENBERG, J. A., HE, C. & ZHANG, Y. 2011. Tet proteins can convert 5-methylcytosine to 5-formylcytosine and 5-carboxylcytosine. *Science,* 333**,** 1300-3.

IWAN, K., RAHIMOFF, R., KIRCHNER, A., SPADA, F., SCHRODER, A. S., KOSMATCHEV, O., FERIZAJ, S., STEINBACHER, J., PARSA, E., MULLER, M. & CARELL, T. 2018. 5-Formylcytosine to cytosine conversion by C-C bond cleavage in vivo. *Nat Chem Biol,* 14**,** 72-78.

JANKOVIC, S. & RADOSAVLJEVIC, V. 2007. Risk factors for bladder cancer. *Tumori,* 93**,** 4-12.

JARMALAITE, S., JANKEVICIUS, F., KURGONAITE, K., SUZIEDELIS, K., MUTANEN, P. & HUSGAFVEL-PURSIAINEN, K. 2008. Promoter hypermethylation in tumour suppressor genes shows association with stage, grade and invasiveness of bladder cancer. *Oncology,* 75**,** 145-51.

JEBAR, A. H., HURST, C. D., TOMLINSON, D. C., JOHNSTON, C., TAYLOR, C. F. & KNOWLES, M. A. 2005. FGFR3 and Ras gene mutations are mutually exclusive genetic events in urothelial cell carcinoma. *Oncogene,* 24**,** 5218-25.

JEMAL, A., BRAY, F., CENTER, M. M., FERLAY, J., WARD, E. & FORMAN, D. 2011. Global cancer statistics. *CA Cancer J Clin,* 61**,** 69-90.

JEWETT, H. J. 1973. Proceedings: Cancer of the bladder. Diagnosis and staging. *Cancer,* 32**,** 1072-4.

JIN, B. & ROBERTSON, K. D. 2013. DNA methyltransferases, DNA damage repair, and cancer. *Adv Exp Med Biol,* 754**,** 3-29.

JOBCZYK, M., PIKALA, M., ROZANSKI, W. & MANIECKA-BRYLA, I. 2017. Years of life lost due to bladder cancer among the inhabitants of Poland in the years 2000 to 2014. *Cent European J Urol,* 70**,** 338-343.

JOHNSON, G. L. & LAPADAT, R. 2002. Mitogen-activated protein kinase pathways mediated by ERK, JNK, and p38 protein kinases. *Science,* 298**,** 1911-2.

JONES, P. A. & BAYLIN, S. B. 2007. The epigenomics of cancer. *Cell,* 128**,** 683-92.

JONES, P. A. & LIANG, G. 2009. Rethinking how DNA methylation patterns are maintained. *Nat Rev Genet,* 10**,** 805-11.

JUNKER, K., VAN OERS, J. M., ZWARTHOFF, E. C., KANIA, I., SCHUBERT, J. & HARTMANN, A. 2008. Fibroblast growth factor receptor 3 mutations in bladder tumors correlate with low frequency of chromosome alterations. *Neoplasia,* 10**,** 1-7.

KAMIMAE, S., YAMAMOTO, E., KAI, M., NIINUMA, T., YAMANO, H. O., NOJIMA, M., YOSHIKAWA, K., KIMURA, T., TAKAGI, R., HARADA, E., HARADA, T., MARUYAMA, R., SASAKI, Y., TOKINO, T., SHINOMURA, Y., SUGAI, T., IMAI, K. & SUZUKI, H. 2015. Epigenetic silencing of NTSR1 is associated with lateral and noninvasive growth of colorectal tumors. *Oncotarget,* 6**,** 29975-90.

KANWAL, R. & GUPTA, S. 2012. Epigenetic modifications in cancer. *Clin Genet,* 81**,** 303-11.

KARAVITAKIS, M., MSAOUEL, P., MICHALOPOULOS, V. & KOUTSILIERIS, M. 2014. Pattern of somatostatin receptors expression in normal and bladder cancer tissue samples. *Anticancer Res,* 34**,** 2937-42.

KASTRITIS, E., MURRAY, S., KYRIAKOU, F., HORTI, M., TAMVAKIS, N., KAVANTZAS, N., PATSOURIS, E. S., NONI, A., LEGAKI, S., DIMOPOULOS, M. A. & BAMIAS, A. 2009. Somatic mutations of adenomatous polyposis coli gene and nuclear b-catenin accumulation

have prognostic significance in invasive urothelial carcinomas: evidence for Wnt pathway implication. *Int J Cancer,* 124**,** 103-8.

KIM, C. I., SHIN, J. S., KIM, H. I., LEE, J. M. & KIM, S. J. 1993. Production of tumor necrosis factor by intravesical administration of bacillus Calmette Guerin in patients with superficial bladder cancer. *Yonsei Med J,* 34**,** 356-64.

KIM, H. G., LEE, K. W., CHO, Y. Y., KANG, N. J., OH, S. M., BODE, A. M. & DONG, Z. 2008a. Mitogen- and stress-activated kinase 1-mediated histone H3 phosphorylation is crucial for cell transformation. *Cancer Res,* 68**,** 2538-47.

KIM, K. H. & ROBERTS, C. W. 2016. Targeting EZH2 in cancer. *Nat Med,* 22**,** 128-34.

KIM, M. S., LEBRON, C., NAGPAL, J. K., CHAE, Y. K., CHANG, X., HUANG, Y., CHUANG, T., YAMASHITA, K., TRINK, B., RATOVITSKI, E. A., CALIFANO, J. A. & SIDRANSKY, D. 2008b. Methylation of the DFNA5 increases risk of lymph node metastasis in human breast cancer. *Biochem Biophys Res Commun,* 370**,** 38-43.

KIRKALI, Z., CHAN, T., MANOHARAN, M., ALGABA, F., BUSCH, C., CHENG, L., KIEMENEY, L., KRIEGMAIR, M., MONTIRONI, R., MURPHY, W. M., SESTERHENN, I. A., TACHIBANA, M. & WEIDER, J. 2005. Bladder cancer: epidemiology, staging and grading, and diagnosis. *Urology,* 66**,** 4-34.

KLEINOVINK, J. W., VAN HALL, T., OSSENDORP, F. & FRANSEN, M. F. 2017. PD-L1 immune suppression in cancer: Tumor cells or host cells? *Oncoimmunology,* 6**,** e1325982.

KNOWLES, M. A. 2007. Role of FGFR3 in urothelial cell carcinoma: biomarker and potential therapeutic target. *World J Urol,* 25**,** 581-93.

KOMPIER, L. C., LURKIN, I., VAN DER AA, M. N., VAN RHIJN, B. W., VAN DER KWAST, T. H. & ZWARTHOFF, E. C. 2010. FGFR3, HRAS, KRAS, NRAS and PIK3CA mutations in bladder cancer and their potential as biomarkers for surveillance and therapy. *PLoS One,* 5**,** e13821.

KONDO, J., ENDO, H., OKUYAMA, H., ISHIKAWA, O., IISHI, H., TSUJII, M., OHUE, M. & INOUE, M. 2011. Retaining cell-cell contact enables preparation and culture of spheroids composed of pure primary cancer cells from colorectal cancer. *Proc Natl Acad Sci U S A,* 108**,** 6235-40.

KOSCIANSKA, E., STAREGA-ROSLAN, J. & KRZYZOSIAK, W. J. 2011. The role of Dicer protein partners in the processing of microRNA precursors. *PLoS One,* 6**,** e28548.

KRESO, A. & DICK, J. E. 2014. Evolution of the cancer stem cell model. *Cell Stem Cell,* 14**,** 275-91.

KRIAUCIONIS, S. & HEINTZ, N. 2009. The nuclear DNA base 5-hydroxymethylcytosine is present in Purkinje neurons and the brain. *Science,* 324**,** 929-30.

KULIS, M. & ESTELLER, M. 2010. DNA methylation and cancer. *Adv Genet,* 70**,** 27-56.

LAKATOS, A. & JOBST, K. 1989. Histone glycosylation. *Acta Biochim Biophys Hung,* 24**,** 355-9.

LARRE, S., CATTO, J. W., COOKSON, M. S., MESSING, E. M., SHARIAT, S. F., SOLOWAY, M. S., SVATEK, R. S., LOTAN, Y., ZLOTTA, A. R. & GROSSMAN, H. B. 2013. Screening for bladder cancer: rationale, limitations, whom to target, and perspectives. *Eur Urol,* 63**,** 1049-58.

LARUE, H., AYARI, C., BERGERON, A. & FRADET, Y. 2013. Toll-like receptors in urothelial cells--targets for cancer immunotherapy. *Nat Rev Urol,* 10**,** 537-45.

LAURSEN, B. 1970. Cancer of the bladder in patients treated with chlornaphazine. *Br Med J,* 3**,** 684-5.

LEAL, J., LUENGO-FERNANDEZ, R., SULLIVAN, R. & WITJES, J. A. 2016. Economic Burden of Bladder Cancer Across the European Union. *Eur Urol,* 69**,** 438-47.

LEE, H.-W., PARK, S.-H., WENG, M.-W., WANG, H.-T., HUANG, W. C., LEPOR, H., WU, X.-R., CHEN, L.-C. & TANG, M.-S. 2018. E-cigarette smoke damages DNA and reduces repair activity in mouse lung, heart, and bladder as well as in human lung and bladder cells. *Proceedings of the National Academy of Sciences*.

LEINONEN, P., AALTONEN, V., KOSKELA, S., LEHENKARI, P., KORKIAMAKI, T. & PELTONEN, J. 2007. Impaired gap junction formation and intercellular calcium signaling in urinary bladder cancer cells can be improved by Go6976. *Cell Commun Adhes,* 14**,** 125-36.

LER, L. D., GHOSH, S., CHAI, X., THIKE, A. A., HENG, H. L., SIEW, E. Y., DEY, S., KOH, L. K., LIM, J. Q., LIM, W. K., MYINT, S. S., LOH, J. L., ONG, P., SAM, X. X., HUANG, D., LIM, T., TAN, P. H., NAGARAJAN, S., CHENG, C. W., HO, H., NG, L. G., YUEN, J., LIN, P. H., CHUANG, C. K., CHANG, Y. H., WENG, W. H., ROZEN, S. G., TAN, P., CREASY, C. L., PANG, S. T., MCCABE, M. T., POON, S. L. & TEH, B. T. 2017. Loss of tumor suppressor KDM6A amplifies PRC2-regulated transcriptional repression in bladder cancer and can be targeted through inhibition of EZH2. *Sci Transl Med,* 9.

LERNER, S. P. 2015. Update on The Cancer Genome Atlas Project on Muscle-invasive Bladder Cancer. *Eur Urol Focus,* 1**,** 94-95.

LERNER, S. P., WEINSTEIN, J., KWIATKOWSKI, D., KIM, J., ROBERTSON, G., HOADLEY, K. A., AKBANI, R., CREIGHTON, C. & GROUP, T. M. I. B. C. A. W. 2015. The Cancer Genome Atlas Project on Muscle-invasive Bladder Cancer. *Eur Urol Focus,* 1**,** 94-95.

LETASIOVA, S., MEDVE'OVA, A., SOVCIKOVA, A., DUSINSKA, M., VOLKOVOVA, K., MOSOIU, C. & BARTONOVA, A. 2012. Bladder cancer, a review of the environmental risk factors. *Environ Health,* 11 Suppl 1**,** S11.

LI, F., AN, S., HOU, L., CHEN, P., LEI, C. & TAN, W. 2014. Red and processed meat intake and risk of bladder cancer: a meta-analysis. *Int J Clin Exp Med,* 7**,** 2100-10.

LI, H. T., DUYMICH, C. E., WEISENBERGER, D. J. & LIANG, G. 2016. Genetic and Epigenetic Alterations in Bladder Cancer. *Int Neurourol J,* 20**,** S84-94.

LI, W. & LIU, M. 2011. Distribution of 5-hydroxymethylcytosine in different human tissues. *J Nucleic Acids,* 2011**,** 870726.

LI, Y., LIN, K., YANG, Z., HAN, N., QUAN, X., GUO, X. & LI, C. 2017. Bladder cancer stem cells: clonal origin and therapeutic perspectives. *Oncotarget,* 8**,** 66668-66679.

LI, Y. & TOLLEFSBOL, T. O. 2011. DNA methylation detection: bisulfite genomic sequencing analysis. *Methods Mol Biol,* 791**,** 11-21.

LI, Y., XU, X., SONG, L., HOU, Y., LI, Z., TSANG, S., LI, F., IM, K. M., WU, K., WU, H., YE, X., LI, G., WANG, L., ZHANG, B., LIANG, J., XIE, W., WU, R., JIANG, H., LIU, X., YU, C., ZHENG, H., JIAN, M., NIE, L., WAN, L., SHI, M., SUN, X., TANG, A., GUO, G., GUI, Y., CAI, Z., LI, J., WANG, W., LU, Z., ZHANG, X., BOLUND, L., KRISTIANSEN, K., WANG, J., YANG, H., DEAN, M. & WANG, J. 2012. Single-cell sequencing analysis characterizes common and cell-lineage-specific mutations in a muscle-invasive bladder cancer. *Gigascience,* 1**,** 12.

LIANG, G., CHAN, M. F., TOMIGAHARA, Y., TSAI, Y. C., GONZALES, F. A., LI, E., LAIRD, P. W. & JONES, P. A. 2002. Cooperativity between DNA methyltransferases in the maintenance methylation of repetitive elements. *Mol Cell Biol,* 22**,** 480-91.

LIGGETT, W. H., JR. & SIDRANSKY, D. 1998. Role of the p16 tumor suppressor gene in cancer. *J Clin Oncol,* 16**,** 1197-206.

LISTER, R., PELIZZOLA, M., DOWEN, R. H., HAWKINS, R. D., HON, G., TONTI-FILIPPINI, J., NERY, J. R., LEE, L., YE, Z., NGO, Q. M., EDSALL, L., ANTOSIEWICZ-BOURGET, J., STEWART, R., RUOTTI, V., MILLAR, A. H., THOMSON, J. A., REN, B. & ECKER, J. R. 2009. Human DNA methylomes at base resolution show widespread epigenomic differences. *Nature,* 462**,** 315-22.

LIU, A. Y., VENCIO, R. Z., PAGE, L. S., HO, M. E., LOPRIENO, M. A. & TRUE, L. D. 2012. Bladder expression of CD cell surface antigens and cell-type-specific transcriptomes. *Cell Tissue Res,* 348**,** 589-600.

LIU, D., ABBOSH, P., KELIHER, D., REARDON, B., MIAO, D., MOUW, K., WEINER-TAYLOR, A., WANKOWICZ, S., HAN, G., TEO, M. Y., CIPOLLA, C., KIM, J., IYER, G., AL-AHMADIE, H., DULAIMI, E., CHEN, D. Y. T., ALPAUGH, R. K., HOFFMAN-CENSITS, J., GARRAWAY, L. A., GETZ, G., CARTER, S. L., BELLMUNT, J., PLIMACK, E. R., ROSENBERG, J. E. & VAN ALLEN, E. M. 2017a. Mutational patterns in chemotherapy resistant muscle-invasive bladder cancer. *Nat Commun,* 8**,** 2193.

LIU, L., ZHANG, L., YANG, L., LI, H., LI, R., YU, J., YANG, L., WEI, F., YAN, C., SUN, Q., ZHAO, H., YANG, F., JIN, H., WANG, J., WANG, S. E. & REN, X. 2017b. Anti-CD47 Antibody As a Targeted Therapeutic Agent for Human Lung Cancer and Cancer Stem Cells. *Front Immunol,* 8**,** 404.

LIU, Q., YUAN, W., TONG, D., LIU, G., LAN, W., ZHANG, D., XIAO, H., ZHANG, Y., HUANG, Z., YANG, J., ZHANG, J. & JIANG, J. 2016. Metformin represses bladder cancer progression by inhibiting stem cell repopulation via COX2/PGE2/STAT3 axis. *Oncotarget,* 7**,** 28235-46.

LOCKE, M., HEYWOOD, M., FAWELL, S. & MACKENZIE, I. C. 2005. Retention of intrinsic stem cell hierarchies in carcinoma-derived cell lines. *Cancer Res,* 65**,** 8944-50.

LOPEZ-BELTRAN, A. & ESCUDERO, A. L. 1997. Human papillomavirus and bladder cancer. *Biomed Pharmacother,* 51**,** 252-7.

LU, T. J., LU, T. L., SU, I. J. & LAI, M. D. 1997. Tyrosine kinase expression profile in bladder cancer. *Anticancer Res,* 17**,** 2635-7.

LUCHINI, C. & CHENG, L. 2017. Predicting the biological behavior of non-muscle-invasive bladder cancer: from histology to molecular taxonomy. *Transl Androl Urol,* 6**,** 987-990.

LUGER, K., MADER, A. W., RICHMOND, R. K., SARGENT, D. F. & RICHMOND, T. J. 1997. Crystal structure of the nucleosome core particle at 2.8 A resolution. *Nature,* 389**,** 251-60.

LUGLI, E., ROEDERER, M. & COSSARIZZA, A. 2010. Data analysis in flow cytometry: the future just started. *Cytometry A,* 77**,** 705-13.

LUNNING, M. A. & GREEN, M. R. 2015. Mutation of chromatin modifiers; an emerging hallmark of germinal center B-cell lymphomas. *Blood Cancer J,* 5**,** e361.

MACARAK, E. J. & HOWARD, P. S. 1999. The role of collagen in bladder filling. *Adv Exp Med Biol,* 462**,** 215-23; discussion 225-33.

MACINTYRE, G., JIMENO YEPES, A., ONG, C. S. & VERSPOOR, K. 2014. Associating disease-related genetic variants in intergenic regions to the genes they impact. *PeerJ,* 2**,** e639.

MAH, S. M., BUSKE, C., HUMPHRIES, R. K. & KUCHENBAUER, F. 2010. miRNA*: a passenger stranded in RNA-induced silencing complex? *Crit Rev Eukaryot Gene Expr,* 20**,** 141-8.

MAIR, B., KUBICEK, S. & NIJMAN, S. M. 2014. Exploiting epigenetic vulnerabilities for cancer therapeutics. *Trends Pharmacol Sci,* 35**,** 136-45.

MARCUS, P. M., VINEIS, P. & ROTHMAN, N. 2000. NAT2 slow acetylation and bladder cancer risk: a meta-analysis of 22 case-control studies conducted in the general population. *Pharmacogenetics,* 10**,** 115-22.

MARSH, H. P., HALDAR, N. A., BUNCE, M., MARSHALL, S. E., LE MONIER, K., WINSEY, S. L., CHRISTODOULOS, K., CRANSTON, D., WELSH, K. I. & HARRIS, A. L. 2003. Polymorphisms in tumour necrosis factor (TNF) are associated with risk of bladder cancer and grade of tumour at presentation. *Br J Cancer,* 89**,** 1096-101.

MARTUZA, R. L. 2000. Conditionally replicating herpes vectors for cancer therapy. *J Clin Invest,* 105**,** 841-6.

MASTERS, J. R., BEDFORD, P., KEARNEY, A., POVEY, S. & FRANKS, L. M. 1988. Bladder cancer cell line cross-contamination: identification using a locus-specific minisatellite probe. *Br J Cancer,* 57**,** 284-6.

MATIC, M., PEKMEZOVIC, T., DJUKIC, T., MIMIC-OKA, J., DRAGICEVIC, D., KRIVIC, B., SUVAKOV, S., SAVIC-RADOJEVIC, A., PLJESA-ERCEGOVAC, M., TULIC, C., CORIC, V. & SIMIC, T. 2013. GSTA1, GSTM1, GSTP1, and GSTT1 polymorphisms and

susceptibility to smoking-related bladder cancer: a case-control study. *Urol Oncol,* 31**,** 1184-92.

MCCONKEY, D. J., CHOI, W. & DINNEY, C. P. 2015. Genetic subtypes of invasive bladder cancer. *Curr Opin Urol,* 25**,** 449-58.

MEDRANO, M., COMMUNAL, L., BROWN, K. R., IWANICKI, M., NORMAND, J., PATERSON, J., SIRCOULOMB, F., KRZYZANOWSKI, P., NOVAK, M., DOODNAUTH, S. A., SAIZ, F. S., CULLIS, J., AL-AWAR, R., NEEL, B. G., MCPHERSON, J., DRAPKIN, R., AILLES, L., MES-MASSONS, A. M. & ROTTAPEL, R. 2017. Interrogation of Functional Cell-Surface Markers Identifies CD151 Dependency in High-Grade Serous Ovarian Cancer. *Cell Rep,* 18**,** 2343-2358.

MELAMED, M. R. 1992. Flow cytometry for detection and evaluation of urinary bladder carcinoma. *Semin Surg Oncol,* 8**,** 300-7.

MELIKER, J. R. & NRIAGU, J. O. 2007. Arsenic in drinking water and bladder cancer: review of epidemiological evidence. *Trace Metals and other Contaminants in the Environment.* Elsevier.

MESSING, E. M., FAHEY, J. L., DEKERNION, J. B., BHUTA, S. M. & BUBBERS, J. E. 1982. Serum-free medium for the in vitro growth of normal and malignant urinary bladder epithelial cells. *Cancer Res,* 42**,** 2392-7.

MIRSAIDI, N., BURNS, M. P., MCCLAIN, S. A., FORSYTH, E., LI, J., DUKES, B., LIN, D., NAHVI, R., GIRALDO, J., PATTON, M., WANG, P., LIN, K., MILLER, E., RATLIFF, T., HAMIDI, S., CRIST, S., TAKEMARU, K. I. & SZEMA, A. 2017. Enhanced Mortality to Metastatic Bladder Cancer Cell Line MB49 in Vasoactive Intestinal Peptide Gene Knockout Mice. *Front Endocrinol (Lausanne),* 8**,** 162.

MITRA, A. P., DATAR, R. H. & COTE, R. J. 2006. Molecular pathways in invasive bladder cancer: new insights into mechanisms, progression, and target identification. *J Clin Oncol,* 24**,** 5552-64.

MITRE, M., MARIGA, A. & CHAO, M. V. 2017. Neurotrophin signalling: novel insights into mechanisms and pathophysiology. *Clin Sci (Lond),* 131**,** 13-23.

MONDUL, A. M., WEINSTEIN, S. J., MANNISTO, S., SNYDER, K., HORST, R. L., VIRTAMO, J. & ALBANES, D. 2010. Serum vitamin D and risk of bladder cancer. *Cancer Res,* 70**,** 9218-23.

MOODY, T. W., NUCHE-BERENGUER, B. & JENSEN, R. T. 2016a. Vasoactive intestinal peptide/pituitary adenylate cyclase activating polypeptide, and their receptors and cancer. *Curr Opin Endocrinol Diabetes Obes,* 23**,** 38-47.

MOODY, T. W., NUCHE-BERENGUER, B., NAKAMURA, T. & JENSEN, R. T. 2016b. EGFR Transactivation by Peptide G Protein-Coupled Receptors in Cancer. *Curr Drug Targets,* 17**,** 520-8.

MOORE, L. E., PFEIFFER, R. M., POSCABLO, C., REAL, F. X., KOGEVINAS, M., SILVERMAN, D., GARCIA-CLOSAS, R., CHANOCK, S., TARDON, A., SERRA, C., CARRATO, A., DOSEMECI, M., GARCIA-CLOSAS, M., ESTELLER, M., FRAGA, M., ROTHMAN, N. & MALATS, N. 2008. Genomic DNA hypomethylation as a biomarker for bladder cancer susceptibility in the Spanish Bladder Cancer Study: a case-control study. *Lancet Oncol,* 9**,** 359-66.

MOSTAFA, M. H., SHEWEITA, S. A. & O'CONNOR, P. J. 1999. Relationship between schistosomiasis and bladder cancer. *Clin Microbiol Rev,* 12**,** 97-111.

MOUSAVI ARDEHAIE, R., HASHEMZADEH, S., BEHROUZ SHARIF, S., GHOJAZADEH, M., TEIMOORI-TOOLABI, L. & SAKHINIA, E. 2017. Aberrant methylated EDNRB can act as a potential diagnostic biomarker in sporadic colorectal cancer while KISS1 is controversial. *Bioengineered,* 8**,** 555-564.

MULLER, A. J., DUHADAWAY, J. B., JALLER, D., CURTIS, P., METZ, R. & PRENDERGAST, G. C. 2010. Immunotherapeutic suppression of indoleamine 2,3-dioxygenase and tumor growth with ethyl pyruvate. *Cancer Res,* 70**,** 1845-53.

MUNARI, E., CHAUX, A., VAGHASIA, A. M., TAHERI, D., KARRAM, S., BEZERRA, S. M., GONZALEZ ROIBON, N., NELSON, W. G., YEGNASUBRAMANIAN, S., NETTO, G. J. & HAFFNER, M. C. 2016. Global 5-Hydroxymethylcytosine Levels Are Profoundly Reduced in Multiple Genitourinary Malignancies. *PLoS One,* 11**,** e0146302.

NAIK, D. S., SHARMA, S., RAY, A. & HEDAU, S. 2011. Epidermal growth factor receptor expression in urinary bladder cancer. *Indian J Urol,* 27**,** 208-14.

NG, K. W., ABRAHAM, M. C., LEONG, D. T. W., MORRIS, C. & SCHANTZ, J. T. 2011. Primary culture of specific cell types and the establishment of cell lines. *Animal cell culture: essential methods***,** 205-230.

NICKERSON, M. L., DANCIK, G. M., IM, K. M., EDWARDS, M. G., TURAN, S., BROWN, J., RUIZ-RODRIGUEZ, C., OWENS, C., COSTELLO, J. C., GUO, G., TSANG, S. X., LI, Y., ZHOU, Q., CAI, Z., MOORE, L. E., LUCIA, M. S., DEAN, M. & THEODORESCU, D. 2014. Concurrent alterations in TERT, KDM6A, and the BRCA pathway in bladder cancer. *Clin Cancer Res,* 20**,** 4935-48.

NICKERSON, M. L., WITTE, N., IM, K. M., TURAN, S., OWENS, C., MISNER, K., TSANG, S. X., CAI, Z., WU, S., DEAN, M., COSTELLO, J. C. & THEODORESCU, D. 2017. Molecular analysis of urothelial cancer cell lines for modeling tumor biology and drug response. *Oncogene,* 36**,** 35-46.

NIELSEN, M. E., SHARIAT, S. F., KARAKIEWICZ, P. I., LOTAN, Y., ROGERS, C. G., AMIEL, G. E., BASTIAN, P. J., VAZINA, A., GUPTA, A., LERNER, S. P., SAGALOWSKY, A. I., SCHOENBERG, M. P. & PALAPATTU, G. S. 2007. Advanced age is associated with poorer bladder cancer-specific survival in patients treated with radical cystectomy. *Eur Urol,* 51**,** 699-706; discussion 706-8.

OBIER, N. & MULLER, A. M. 2010. Chromatin flow cytometry identifies changes in epigenetic cell states. *Cells Tissues Organs,* 191**,** 167-74.

OCHS, R. L., FENSTERER, J., OHORI, N. P., WELLS, A., GABRIN, M., GEORGE, L. D. & KORNBLITH, P. 2003. Evidence for the isolation, growth, and characterization of malignant cells in primary cultures of human tumors. *In Vitro Cell Dev Biol Anim,* 39**,** 63-70.

OWAKI, H., SADAHIRO, S. & TAKAKI, M. 2015. Characterizations of the alpha1-adrenoceptor subtypes mediating contractions of the human internal anal sphincter. *J Pharmacol Sci,* 127**,** 424-9.

OXFORD, G. & THEODORESCU, D. 2003. The role of Ras superfamily proteins in bladder cancer progression. *J Urol,* 170**,** 1987-93.

PAN, H., XU, X., WU, D., QIU, Q., ZHOU, S., HE, X., ZHOU, Y., QU, P., HOU, J., HE, J. & ZHOU, J. 2016. Novel somatic mutations identified by whole-exome sequencing in muscle-invasive transitional cell carcinoma of the bladder. *Oncol Lett,* 11**,** 1486-1492.

PANTELIDES, N. M., IVAZ, S. L., FALCONER, A., HAZELL, S., WINKLER, M., HROUDA, D. & MAYER, E. K. 2012. Lymphoepithelioma-like carcinoma of the urinary bladder: A case report and review of systemic treatment options. *Urol Ann,* 4**,** 45-7.

PAPAFOTIOU, G., PARASKEVOPOULOU, V., VASILAKI, E., KANAKI, Z., PASCHALIDIS, N. & KLINAKIS, A. 2016. KRT14 marks a subpopulation of bladder basal cells with pivotal role in regeneration and tumorigenesis. *Nat Commun,* 7**,** 11914.

PAPAVRAMIDOU, N., PAPAVRAMIDIS, T. & DEMETRIOU, T. 2010. Ancient Greek and Greco-Roman methods in modern surgical treatment of cancer. *Ann Surg Oncol,* 17**,** 665-7.

PARADA, L. F., TABIN, C. J., SHIH, C. & WEINBERG, R. A. 1982. Human EJ bladder carcinoma oncogene is homologue of Harvey sarcoma virus ras gene. *Nature,* 297**,** 474-8.

PARKIN, D. M. 2006. The global health burden of infection-associated cancers in the year 2002. *Int J Cancer,* 118**,** 3030-44.

PARSONS, C. L. 1993. The role of the glycosaminoglycan layer in bladder defense mechanisms and interstitial cystitis. *International Urogynecology Journal,* 4**,** 373-379.

PASIN, E., JOSEPHSON, D. Y., MITRA, A. P., COTE, R. J. & STEIN, J. P. 2008. Superficial bladder cancer: an update on etiology, molecular development, classification, and natural history. *Rev Urol,* 10**,** 31-43.

PEI, N., MAO, Y., WAN, P., CHEN, X., LI, A., CHEN, H., LI, J., WAN, R., ZHANG, Y., DU, H., CHEN, B., JIANG, G., XIA, M., SUMNERS, C., HU, G., GU, D. & LI, H. 2017. Angiotensin II type 2 receptor promotes apoptosis and inhibits angiogenesis in bladder cancer. *J Exp Clin Cancer Res,* 36**,** 77.

PELUCCHI, C., BOSETTI, C., NEGRI, E., MALVEZZI, M. & LA VECCHIA, C. 2006. Mechanisms of disease: The epidemiology of bladder cancer. *Nat Clin Pract Urol,* 3**,** 327-40.

PERROTTA, C., CERVIA, D., DI RENZO, I., MOSCHENI, C., BASSI, M. T., CAMPANA, L., MARTELLI, C., CATALANI, E., GIOVARELLI, M., ZECCHINI, S., COAZZOLI, M., CAPOBIANCO, A., OTTOBRINI, L., LUCIGNANI, G., ROSA, P., ROVERE-QUERINI, P., DE PALMA, C. & CLEMENTI, E. 2018. Nitric Oxide Generated by Tumor-Associated Macrophages Is Responsible for Cancer Resistance to Cisplatin and Correlated With Syntaxin 4 and Acid Sphingomyelinase Inhibition. *Front Immunol,* 9**,** 1186.

PETERS, T. J., BUCKLEY, M. J., STATHAM, A. L., PIDSLEY, R., SAMARAS, K., V LORD, R., CLARK, S. J. & MOLLOY, P. L. 2015. De novo identification of differentially methylated regions in the human genome. *Epigenetics & Chromatin,* 8**,** 6.

PFEIFER, G. P., KADAM, S. & JIN, S. G. 2013. 5-hydroxymethylcytosine and its potential roles in development and cancer. *Epigenetics Chromatin,* 6**,** 10.

PFEIFER, G. P., XIONG, W., HAHN, M. A. & JIN, S. G. 2014. The role of 5-hydroxymethylcytosine in human cancer. *Cell Tissue Res,* 356**,** 631-41.

PHILIPPEOS, C., HUGHES, R. D., DHAWAN, A. & MITRY, R. R. 2012. Introduction to cell culture. *Methods Mol Biol,* 806**,** 1-13.

PIPER, J. M., TONASCIA, J. & MATANOSKI, G. M. 1985. Heavy phenacetin use and bladder cancer in women aged 20 to 49 years. *N Engl J Med,* 313**,** 292-5.

PIPERI, C. & PAPAVASSILIOU, A. G. 2011. Strategies for DNA methylation analysis in developmental studies. *Dev Growth Differ,* 53**,** 287-99.

POLLACK, A., CZERNIAK, B., ZAGARS, G. K., HU, S. X., WU, C. S., DINNEY, C. P., CHYLE, V. & BENEDICT, W. F. 1997. Retinoblastoma protein expression and radiation response in muscle-invasive bladder cancer. *Int J Radiat Oncol Biol Phys,* 39**,** 687-95.

PONTI, D., COSTA, A., ZAFFARONI, N., PRATESI, G., PETRANGOLINI, G., CORADINI, D., PILOTTI, S., PIEROTTI, M. A. & DAIDONE, M. G. 2005. Isolation and in vitro propagation of tumorigenic breast cancer cells with stem/progenitor cell properties. *Cancer Res,* 65**,** 5506-11.

POUESSEL, D., NEUZILLET, Y., MERTENS, L. S., VAN DER HEIJDEN, M. S., DE JONG, J., SANDERS, J., PETERS, D., LEROY, K., MANCEAU, A., MAILLE, P., SOYEUX, P., MOKTEFI, A., SEMPREZ, F., VORDOS, D., DE LA TAILLE, A., HURST, C. D., TOMLINSON, D. C., HARNDEN, P., BOSTROM, P. J., MIRTTI, T., HORENBLAS, S., LORIOT, Y., HOUEDE, N., CHEVREAU, C., BEUZEBOC, P., SHARIAT, S. F., SAGALOWSKY, A. I., ASHFAQ, R., BURGER, M., JEWETT, M. A., ZLOTTA, A. R., BROEKS, A., BAPAT, B., KNOWLES, M. A., LOTAN, Y., VAN DER KWAST, T. H., CULINE, S., ALLORY, Y. & VAN RHIJN, B. W. 2016. Tumor heterogeneity of fibroblast growth factor receptor 3 (FGFR3) mutations in invasive bladder cancer: implications for perioperative anti-FGFR3 treatment. *Ann Oncol,* 27**,** 1311-6.

POYET, C., HERMANNS, T., ZHONG, Q., DRESCHER, E., EBERLI, D., BURGER, M., HOFSTAEDTER, F., HARTMANN, A., STOHR, R., ZWARTHOFF, E. C., SULSER, T. & WILD, P. J. 2015. Positive fibroblast growth factor receptor 3 immunoreactivity is associated with low-grade non-invasive urothelial bladder cancer. *Oncol Lett,* 10**,** 2753-2760.

POZAROWSKI, P. & DARZYNKIEWICZ, Z. 2004. Analysis of cell cycle by flow cytometry. *Methods Mol Biol,* 281**,** 301-11.

PUNTONI, M., ZANARDI, S., BRANCHI, D., BRUNO, S., CUROTTO, A., VARALDO, M., BRUZZI, P. & DECENSI, A. 2007. Prognostic effect of DNA aneuploidy from bladder washings in superficial bladder cancer. *Cancer Epidemiol Biomarkers Prev,* 16**,** 979-83.

QIANG, M., DENNY, A., LIEU, M., CARREON, S. & LI, J. 2011. Histone H3K9 modifications are a local chromatin event involved in ethanol-induced neuroadaptation of the NR2B gene. *Epigenetics,* 6**,** 1095-104.

QIU, W., LIN, J., ZHU, Y., ZHANG, J., ZENG, L., SU, M. & TIAN, Y. 2017. Kaempferol Modulates DNA Methylation and Downregulates DNMT3B in Bladder Cancer. *Cell Physiol Biochem,* 41**,** 1325-1335.

RAHMAN, Z., REEDY, E. A. & HEATFIELD, B. M. 1987. Isolation and primary culture of urothelial cells from normal human bladder. *Urol Res,* 15**,** 315-20.

RAIBER, E. A., MURAT, P., CHIRGADZE, D. Y., BERALDI, D., LUISI, B. F. & BALASUBRAMANIAN, S. 2015. 5-Formylcytosine alters the structure of the DNA double helix. *Nat Struct Mol Biol,* 22**,** 44-49.

REAL, F. X., SANTOS, C. P., LAPI, E., ALVARO-ESPINOSA, L., FERNANDEZ-BARRAL, A., BARBACHANO, A., MEGIAS, D. & MUNOZ, A. 2018. Urothelial organoids originate from Cd49f-High stem cells and display Notch-dependent differentiation capacity. *bioRxiv*.

RIGBY, C. C. & FRANKS, L. M. 1970. A human tissue culture cell line from a transitional cell tumour of the urinary bladder: growth, chromosone pattern and ultrastructure. *Br J Cancer,* 24**,** 746-54.

ROBERTSON, A. G., KIM, J., AL-AHMADIE, H., BELLMUNT, J., GUO, G., CHERNIACK, A. D., HINOUE, T., LAIRD, P. W., HOADLEY, K. A., AKBANI, R., CASTRO, M. A. A., GIBB, E. A., KANCHI, R. S., GORDENIN, D. A., SHUKLA, S. A., SANCHEZ-VEGA, F., HANSEL,

D. E., CZERNIAK, B. A., REUTER, V. E., SU, X., DE SA CARVALHO, B., CHAGAS, V. S., MUNGALL, K. L., SADEGHI, S., PEDAMALLU, C. S., LU, Y., KLIMCZAK, L. J., ZHANG, J., CHOO, C., OJESINA, A. I., BULLMAN, S., LERAAS, K. M., LICHTENBERG, T. M., WU, C. J., SCHULTZ, N., GETZ, G., MEYERSON, M., MILLS, G. B., MCCONKEY, D. J., WEINSTEIN, J. N., KWIATKOWSKI, D. J. & LERNER, S. P. 2017. Comprehensive Molecular Characterization of Muscle-Invasive Bladder Cancer. *Cell,* 171**,** 540-556.e25.

ROMANENKO, A., KAKEHASHI, A., MORIMURA, K., WANIBUCHI, H., WEI, M., VOZIANOV, A. & FUKUSHIMA, S. 2009. Urinary bladder carcinogenesis induced by chronic exposure to persistent low-dose ionizing radiation after Chernobyl accident. *Carcinogenesis,* 30**,** 1821-1831.

ROSENBERG, J. E., HOFFMAN-CENSITS, J., POWLES, T., VAN DER HEIJDEN, M. S., BALAR, A. V., NECCHI, A., DAWSON, N., O'DONNELL, P. H., BALMANOUKIAN, A., LORIOT, Y., SRINIVAS, S., RETZ, M. M., GRIVAS, P., JOSEPH, R. W., GALSKY, M. D., FLEMING, M. T., PETRYLAK, D. P., PEREZ-GRACIA, J. L., BURRIS, H. A., CASTELLANO, D., CANIL, C., BELLMUNT, J., BAJORIN, D., NICKLES, D., BOURGON, R., FRAMPTON, G. M., CUI, N., MARIATHASAN, S., ABIDOYE, O., FINE, G. D. & DREICER, R. 2016. Atezolizumab in patients with locally advanced and metastatic urothelial carcinoma who have progressed following treatment with platinum-based chemotherapy: a single-arm, multicentre, phase 2 trial. *Lancet,* 387**,** 1909-20.

ROTTERUD, R., FOSSA, S. D. & NESLAND, J. M. 2007. Protein networking in bladder cancer: immunoreactivity for FGFR3, EGFR, ERBB2, KAI1, PTEN, and RAS in normal and malignant urothelium. *Histol Histopathol,* 22**,** 349-63.

ROY, S. & PARWANI, A. V. 2011. Adenocarcinoma of the urinary bladder. *Arch Pathol Lab Med,* 135**,** 1601-5.

RUDEN, D. M., GARFINKEL, M. D., SOLLARS, V. E. & LU, X. 2003. Waddington's widget: Hsp90 and the inheritance of acquired characters. *Semin Cell Dev Biol,* 14**,** 301-10.

RUSHTON, L., HUTCHINGS, S. J., FORTUNATO, L., YOUNG, C., EVANS, G. S., BROWN, T., BEVAN, R., SLACK, R., HOLMES, P., BAGGA, S., CHERRIE, J. W. & VAN TONGEREN, M. 2012. Occupational cancer burden in Great Britain. *Br J Cancer,* 107 Suppl 1**,** S3-7.

SADIKOVIC, B., AL-ROMAIH, K., SQUIRE, J. A. & ZIELENSKA, M. 2008. Cause and consequences of genetic and epigenetic alterations in human cancer. *Curr Genomics,* 9**,** 394-408.

SALA, A., PENCHARZ, P. & BARR, R. D. 2004. Children, cancer, and nutrition--A dynamic triangle in review. *Cancer,* 100**,** 677-87.

SAM, P. & LAGRANGE, C. A. 2018. Anatomy, Pelvis, Bladder, Muscles, Detrusor. *StatPearls.* Treasure Island (FL): StatPearls Publishing

StatPearls Publishing LLC.

SANCHEZ-CARBAYO, M. & CORDON-CARDO, C. 2003. Applications of array technology: identification of molecular targets in bladder cancer. *Br J Cancer,* 89**,** 2172-7.

SANGAR, V. K., RAGAVAN, N., MATANHELIA, S. S., WATSON, M. W. & BLADES, R. A. 2005. The economic consequences of prostate and bladder cancer in the UK. *BJU Int,* 95**,** 59-63.

SANNU, A., RADHA, R., MATHEWS, A., PADMAKUMARI MONY, R., PRAHLADAN, A. & JAMES, F. V. 2017. Ifosfamide-Induced Malignancy of Ureter and Bladder. *Cureus,* 9**,** e1594.

SANTARPIA, L., LIPPMAN, S. M. & EL-NAGGAR, A. K. 2012. Targeting the MAPK-RAS-RAF signaling pathway in cancer therapy. *Expert Opin Ther Targets,* 16**,** 103-19.

SANTOS, C. P., LAPI, E., ÁLVARO, L., BARBÁCHANO, A., BARRAL, A., MUÑOZ, A. & REAL, F. X. 2017. CD49f labels an organoid-forming mouse urothelial cell population with stem cell features. *Urologic Oncology: Seminars and Original Investigations,* 35**,** 617.

SANTOS, L., PEREIRA, S., LEITE, R. P., SOUTO, M., AMARO, T. & CRIADO, B. 2003. Chromosome instability and progression in urothelial cell carcinoma of the bladder. *Acta Oncol,* 42**,** 169-73.

SAWICKA, A. & SEISER, C. 2012. Histone H3 phosphorylation - a versatile chromatin modification for different occasions. *Biochimie,* 94**,** 2193-201.

SCHMITZ-DRAGER, B. J., SCHULZ, W. A., JURGENS, B., GERHARZ, C. D., VAN ROEYEN, C. R., BULTEL, H., EBERT, T. & ACKERMANN, R. 1997. c-myc in bladder cancer. Clinical findings and analysis of mechanism. *Urol Res,* 25 Suppl 1**,** S45-9.

SCHNEIDER, A. C., HEUKAMP, L. C., ROGENHOFER, S., FECHNER, G., BASTIAN, P. J., VON RUECKER, A., MULLER, S. C. & ELLINGER, J. 2011. Global histone H4K20 trimethylation predicts cancer-specific survival in patients with muscle-invasive bladder cancer. *BJU Int,* 108**,** E290-6.

SCHUBELER, D., MACALPINE, D. M., SCALZO, D., WIRBELAUER, C., KOOPERBERG, C., VAN LEEUWEN, F., GOTTSCHLING, D. E., O'NEILL, L. P., TURNER, B. M., DELROW, J., BELL, S. P. & GROUDINE, M. 2004. The histone modification pattern of active genes revealed through genome-wide chromatin analysis of a higher eukaryote. *Genes Dev,* 18**,** 1263-71.

SCHULZ, W. A. 2006. Understanding urothelial carcinoma through cancer pathways. *Int J Cancer,* 119**,** 1513-8.

SCOSYREV, E., GOLIJANIN, D., WU, G. & MESSING, E. 2012. The burden of bladder cancer in men and women: analysis of the years of life lost. *BJU Int,* 109**,** 57-62.

SCOTT, S. N., OSTROVNAYA, I., LIN, C. M., BOUVIER, N., BOCHNER, B. H., IYER, G., SOLIT, D., BERGER, M. F. & LIN, O. 2017. Next-generation sequencing of urine specimens: A novel platform for genomic analysis in patients with non-muscle-invasive urothelial carcinoma treated with bacille Calmette-Guerin. *Cancer Cytopathol,* 125**,** 416-426.

SEARS, R. C. & NEVINS, J. R. 2002. Signaling networks that link cell proliferation and cell fate. *J Biol Chem,* 277**,** 11617-20.

SEDAGHAT, S., GHEYTANCHI, E., ASGARI, M., ROUDI, R., KEYMOOSI, H. & MADJD, Z. 2017. Expression of Cancer Stem Cell Markers OCT4 and CD133 in Transitional Cell Carcinomas. *Appl Immunohistochem Mol Morphol,* 25**,** 196-202.

SEHGAL, S. S., WEIN, A. J., BING, Z., MALKOWICZ, S. B. & GUZZO, T. J. 2010. Neuroendocrine tumor of the bladder. *Rev Urol,* 12**,** e197-201.

SEIFERT, H. H., MEYER, A., CRONAUER, M. V., HATINA, J., MULLER, M., RIEDER, H., HOFFMANN, M. J., ACKERMANN, R. & SCHULZ, W. A. 2007. A new and reliable culture system for superficial low-grade urothelial carcinoma of the bladder. *World J Urol,* 25**,** 297-302.

SEILER, R., ASHAB, H. A. D., ERHO, N., VAN RHIJN, B. W. G., WINTERS, B., DOUGLAS, J., VAN KESSEL, K. E., FRANSEN VAN DE PUTTE, E. E., SOMMERLAD, M., WANG, N. Q., CHOEURNG, V., GIBB, E. A., PALMER-ARONSTEN, B., LAM, L. L., BUERKI, C., DAVICIONI, E., SJODAHL, G., KARDOS, J., HOADLEY, K. A., LERNER, S. P., MCCONKEY, D. J., CHOI, W., KIM, W. Y., KISS, B., THALMANN, G. N., TODENHOFER, T., CRABB, S. J., NORTH, S., ZWARTHOFF, E. C., BOORMANS, J. L., WRIGHT, J., DALL'ERA, M., VAN DER HEIJDEN, M. S. & BLACK, P. C. 2017. Impact of Molecular Subtypes in Muscle-invasive Bladder Cancer on Predicting Response and Survival after Neoadjuvant Chemotherapy. *Eur Urol,* 72**,** 544-554.

SEOK JU, Y. 2017. The mutational signatures and molecular alterations of bladder cancer. *Translational Cancer Research***,** S689-S701.

SHACKNEY, S. E., BERG, G., SIMON, S. R., COHEN, J., AMINA, S., POMMERSHEIM, W., YAKULIS, R., WANG, S., UHL, M., SMITH, C. A. & ET AL. 1995. Origins and clinical implications of aneuploidy in early bladder cancer. *Cytometry,* 22**,** 307-16.

SHAMIR, E. R. & EWALD, A. J. 2014. Three-dimensional organotypic culture: experimental models of mammalian biology and disease. *Nat Rev Mol Cell Biol,* 15**,** 647-64.

SHARMA, S., KELLY, T. K. & JONES, P. A. 2010. Epigenetics in cancer. *Carcinogenesis,* 31**,** 27-36.

SHEN, Z., SHEN, T., WIENTJES, M. G., O'DONNELL, M. A. & AU, J. L. 2008. Intravesical treatments of bladder cancer: review. *Pharm Res,* 25**,** 1500-10.

SHIIO, Y. & EISENMAN, R. N. 2003. Histone sumoylation is associated with transcriptional repression. *Proc Natl Acad Sci U S A,* 100**,** 13225-30.

SHOKEIR, A. A. 2004. Squamous cell carcinoma of the bladder: pathology, diagnosis and treatment. *BJU Int,* 93**,** 216-20.

SIEGEL, R. L., MILLER, K. D. & JEMAL, A. 2016. Cancer statistics, 2016. *CA Cancer J Clin,* 66**,** 7-30.

SIEVERT, K. D., AMEND, B., NAGELE, U., SCHILLING, D., BEDKE, J., HORSTMANN, M., HENNENLOTTER, J., KRUCK, S. & STENZL, A. 2009. Economic aspects of bladder cancer: what are the benefits and costs? *World J Urol,* 27**,** 295-300.

SINCLAIR, W. K. 2012. Cyclic X-ray responses in mammalian cells in vitro. 1968. *Radiat Res,* 178**,** AV112-24.

SINGAL, R. & GINDER, G. D. 1999. DNA methylation. *Blood,* 93**,** 4059-70.

SJODAHL, G., LAUSS, M., LOVGREN, K., CHEBIL, G., GUDJONSSON, S., VEERLA, S., PATSCHAN, O., AINE, M., FERNO, M., RINGNER, M., MANSSON, W., LIEDBERG, F., LINDGREN, D. & HOGLUND, M. 2012. A molecular taxonomy for urothelial carcinoma. *Clin Cancer Res,* 18**,** 3377-86.

SKOWRON, M. A., NIEGISCH, G., FRITZ, G., ARENT, T., VAN ROERMUND, J. G., ROMANO, A., ALBERS, P., SCHULZ, W. A. & HOFFMANN, M. J. 2015. Phenotype plasticity rather

than repopulation from CD90/CK14+ cancer stem cells leads to cisplatin resistance of urothelial carcinoma cell lines. *J Exp Clin Cancer Res,* 34**,** 144.

SLOAN, F. A. & GELBAND, H. 2007. Cancer Control Opportunities in Low- and Middle-Income Countries. *The National Academies Collection: Reports funded by National Institutes of Health.* Washington (DC): National Academies Press (US).

SMITH, A. K., HANSEL, D. E. & JONES, J. S. 2008. Role of Cystitis Cystica et Glandularis and Intestinal Metaplasia in Development of Bladder Carcinoma. *Urology,* 71**,** 915-918.

SMOLENSKY, D., RATHORE, K. & CEKANOVA, M. 2016. Molecular targets in urothelial cancer: detection, treatment, and animal models of bladder cancer. *Drug Des Devel Ther,* 10**,** 3305-3322.

SONG, C. X., YIN, S., MA, L., WHEELER, A., CHEN, Y., ZHANG, Y., LIU, B., XIONG, J., ZHANG, W., HU, J., ZHOU, Z., DONG, B., TIAN, Z., JEFFREY, S. S., CHUA, M. S., SO, S., LI, W., WEI, Y., DIAO, J., XIE, D. & QUAKE, S. R. 2017. 5-Hydroxymethylcytosine signatures in cell-free DNA provide information about tumor types and stages. *Cell Res,* 27**,** 1231-1242.

SOUTHGATE, J., HUTTON, K. A., THOMAS, D. F. & TREJDOSIEWICZ, L. K. 1994. Normal human urothelial cells in vitro: proliferation and induction of stratification. *Lab Invest,* 71**,** 583-94.

SPADA, F., HAEMMER, A., KUCH, D., ROTHBAUER, U., SCHERMELLEH, L., KREMMER, E., CARELL, T., LANGST, G. & LEONHARDT, H. 2007. DNMT1 but not its interaction with the replication machinery is required for maintenance of DNA methylation in human cells. *J Cell Biol,* 176**,** 565-71.

STEIN, J. P., LIESKOVSKY, G., COTE, R., GROSHEN, S., FENG, A. C., BOYD, S., SKINNER, E., BOCHNER, B., THANGATHURAI, D., MIKHAIL, M., RAGHAVAN, D. & SKINNER, D.

G. 2001. Radical cystectomy in the treatment of invasive bladder cancer: long-term results in 1,054 patients. *J Clin Oncol,* 19**,** 666-75.

STEINER, H., BERGMEISTER, M., VERDORFER, I., GRANIG, T., MIKUZ, G., BARTSCH, G., STOEHR, B. & BRUNNER, A. 2008. Early results of bladder-cancer screening in a high-risk population of heavy smokers. *BJU Int,* 102**,** 291-6.

STERNE-WEILER, T. & SANFORD, J. R. 2014. Exon identity crisis: disease-causing mutations that disrupt the splicing code. *Genome Biol,* 15**,** 201.

STEWART, S. K., MORRIS, T. J., GUILHAMON, P., BULSTRODE, H., BACHMAN, M., BALASUBRAMANIAN, S. & BECK, S. 2015. oxBS-450K: a method for analysing hydroxymethylation using 450K BeadChips. *Methods,* 72**,** 9-15.

STRAND, S. H., ORNTOFT, T. F. & SORENSEN, K. D. 2014. Prognostic DNA methylation markers for prostate cancer. *Int J Mol Sci,* 15**,** 16544-76.

SUDHAKAR, A. 2009. History of Cancer, Ancient and Modern Treatment Methods. *J Cancer Sci Ther,* 1**,** 1-4.

SUGIBAYASHI, K., HAYASHI, T., MATSUMOTO, K. & HASEGAWA, T. 2004. Utility of a three-dimensional cultured human skin model as a tool to evaluate the simultaneous diffusion and metabolism of ethyl nicotinate in skin. *Drug Metab Pharmacokinet,* 19**,** 352-62.

SUN, L., ZHAO, H., XU, Z., LIU, Q., LIANG, Y., WANG, L., CAI, X., ZHANG, L., HU, L., WANG, G. & ZHA, X. 2007. Phosphatidylinositol 3-kinase/protein kinase B pathway stabilizes DNA methyltransferase I protein and maintains DNA methylation. *Cell Signal,* 19**,** 2255-63.

SVATEK, R. S., HOLLENBECK, B. K., HOLMANG, S., LEE, R., KIM, S. P., STENZL, A. & LOTAN, Y. 2014. The economics of bladder cancer: costs and considerations of caring for this disease. *Eur Urol,* 66**,** 253-62.

SWEIS, R. F., SPRANGER, S., BAO, R., PANER, G. P., STADLER, W. M., STEINBERG, G. & GAJEWSKI, T. F. 2016. Molecular Drivers of the Non-T-cell-Inflamed Tumor Microenvironment in Urothelial Bladder Cancer. *Cancer Immunol Res,* 4**,** 563-8.

TAHILIANI, M., KOH, K. P., SHEN, Y., PASTOR, W. A., BANDUKWALA, H., BRUDNO, Y., AGARWAL, S., IYER, L. M., LIU, D. R., ARAVIND, L. & RAO, A. 2009. Conversion of 5-methylcytosine to 5-hydroxymethylcytosine in mammalian DNA by MLL partner TET1. *Science,* 324**,** 930-5.

TAKAI, D. & JONES, P. A. 2002. Comprehensive analysis of CpG islands in human chromosomes 21 and 22. *Proc Natl Acad Sci U S A,* 99**,** 3740-5.

TAKEUCHI, T., TONOOKA, A., OKUNO, Y., HATTORI-KATO, M. & MIKAMI, K. 2016. Oct4B, CD90, and CD73 are upregulated in bladder tissue following electro-resection of the bladder. *J Stem Cells Regen Med,* 12**,** 10-5.

TALAR-WILLIAMS, C., HIJAZI, Y. M., WALTHER, M. M., LINEHAN, W. M., HALLAHAN, C. W., LUBENSKY, I., KERR, G. S., HOFFMAN, G. S., FAUCI, A. S. & SNELLER, M. C. 1996. Cyclophosphamide-induced cystitis and bladder cancer in patients with Wegener granulomatosis. *Ann Intern Med,* 124**,** 477-84.

TARAYRAH, L. & CHEN, X. 2013. Epigenetic regulation in adult stem cells and cancers. *Cell Biosci,* 3**,** 41.

TARNOK, A., ULRICH, H. & BOCSI, J. 2010. Phenotypes of stem cells from diverse origin. *Cytometry A,* 77**,** 6-10.

THIEDE, T. & CHR. CHRISTENSEN, B. 2009. *Bladder tumors induced by chlornaphazine*.

THOMSEN, M. B. H., NORDENTOFT, I., LAMY, P., VANG, S., REINERT, L., MAPENDANO, C. K., HOYER, S., ORNTOFT, T. F., JENSEN, J. B. & DYRSKJOT, L. 2017. Comprehensive multiregional analysis of molecular heterogeneity in bladder cancer. *Sci Rep,* 7**,** 11702.

TIAN, W., GUNER, G., MIYAMOTO, H., CIMINO-MATHEWS, A., GONZALEZ-ROIBON, N., ARGANI, P., LI, X., SHARMA, R., SUBHAWONG, A. P., REZAEI, K., BIVALACQUA, T. J., EPSTEIN, J. I., BISHOP, J. A. & NETTO, G. J. 2015. Utility of uroplakin II expression as a marker of urothelial carcinoma. *Hum Pathol,* 46**,** 58-64.

TILLEY, S. K., KIM, W. Y. & FRY, R. C. 2017. Analysis of bladder cancer tumor CpG methylation and gene expression within The Cancer Genome Atlas identifies GRIA1 as a prognostic biomarker for basal-like bladder cancer. *Am J Cancer Res,* 7**,** 1850-1862.

TOH, T. B., LIM, J. J. & CHOW, E. K. 2017. Epigenetics in cancer stem cells. *Mol Cancer,* 16**,** 29.

TUNCER, M., FAYDACI, G., ALTIN, G., ERDOGAN, B. A., KIBAR, S., SANLI, A. & BILGICI, D. 2014. Metastasis of non-muscle-invasive bladder cancer into the thyroid gland: a literature review accompanied by a rare case. *Korean J Urol,* 55**,** 222-5.

VALE, C. 2005. Neoadjuvant chemotherapy in invasive bladder cancer: update of a systematic review and meta-analysis of individual patient data: advanced bladder cancer (ABC) meta-analysis collaboration. *European urology,* 48**,** 202-206.

VAN BATAVIA, J., YAMANY, T., MOLOTKOV, A., DAN, H., MANSUKHANI, M., BATOURINA, E., SCHNEIDER, K., OYON, D., DUNLOP, M., WU, X. R., CORDON-CARDO, C. & MENDELSOHN, C. 2014. Bladder cancers arise from distinct urothelial sub-populations. *Nat Cell Biol,* 16**,** 982-91, 1-5.

VAN DER WEYDEN, L. & ADAMS, D. J. 2007. The Ras-association domain family (RASSF) members and their role in human tumourigenesis. *Biochim Biophys Acta,* 1776**,** 58-85.

VAN RHIJN, B. W., VAN TILBORG, A. A., LURKIN, I., BONAVENTURE, J., DE VRIES, A., THIERY, J. P., VAN DER KWAST, T. H., ZWARTHOFF, E. C. & RADVANYI, F. 2002. Novel fibroblast growth factor receptor 3 (FGFR3) mutations in bladder cancer previously identified in non-lethal skeletal disorders. *Eur J Hum Genet,* 10**,** 819-24.

VAZ-DRAGO, R., CUSTODIO, N. & CARMO-FONSECA, M. 2017. Deep intronic mutations and human disease. *Hum Genet,* 136**,** 1093-1111.

VEILLETTE, A. & CHEN, J. 2018. SIRPalpha-CD47 Immune Checkpoint Blockade in Anticancer Therapy. *Trends Immunol,* 39**,** 173-184.

VETTER, I. R. & WITTINGHOFER, A. 2001. The guanine nucleotide-binding switch in three dimensions. *Science,* 294**,** 1299-304.

VINEIS, P., ALAVANJA, M., BUFFLER, P., FONTHAM, E., FRANCESCHI, S., GAO, Y. T., GUPTA, P. C., HACKSHAW, A., MATOS, E., SAMET, J., SITAS, F., SMITH, J., STAYNER, L., STRAIF, K., THUN, M. J., WICHMANN, H. E., WU, A. H., ZARIDZE, D., PETO, R. & DOLL, R. 2004. Tobacco and cancer: recent epidemiological evidence. *J Natl Cancer Inst,* 96**,** 99-106.

VOLKMER, J. P., SAHOO, D., CHIN, R. K., HO, P. L., TANG, C., KURTOVA, A. V., WILLINGHAM, S. B., PAZHANISAMY, S. K., CONTRERAS-TRUJILLO, H., STORM, T. A., LOTAN, Y., BECK, A. H., CHUNG, B. I., ALIZADEH, A. A., GODOY, G., LERNER, S. P., VAN DE RIJN, M., SHORTLIFFE, L. D., WEISSMAN, I. L. & CHAN, K. S. 2012. Three differentiation states risk-stratify bladder cancer into distinct subtypes. *Proc Natl Acad Sci U S A,* 109**,** 2078-83.

WANG, L., LIU, R., RIBICK, M., ZHENG, P. & LIU, Y. 2010. FOXP3 as an X-linked tumor suppressor. *Discov Med,* 10**,** 322-8.

WANG, Y., YU, Y., YE, R., ZHANG, D., LI, Q., AN, D., FANG, L., LIN, Y., HOU, Y., XU, A., FU, Y., LU, W., CHEN, X., CHEN, M., ZHANG, M., JIANG, H., ZHANG, C., DONG, P., LI, C., CHEN, J., YANG, G., LIU, C., CAI, Z., ZHOU, F. & WU, S. 2016. An epigenetic biomarker combination of PCDH17 and POU4F2 detects bladder cancer accurately by methylation analyses of urine sediment DNA in Han Chinese. *Oncotarget,* 7**,** 2754-64.

WASCO, M. J., DAIGNAULT, S., ZHANG, Y., KUNJU, L. P., KINNAMAN, M., BRAUN, T., LEE, C. T. & SHAH, R. B. 2007. Urothelial carcinoma with divergent histologic differentiation (mixed histologic features) predicts the presence of locally advanced bladder cancer when detected at transurethral resection. *Urology,* 70**,** 69-74.

WASFY, R. E. & EL-GUINDY, D. M. 2017. CD133 and CD44 as cancer stem cell markers in bladder carcinoma: an immunohistochemical study. *Egyptian Journal of Pathology,* 37**,** 204-208.

WEI, X., WALIA, V., LIN, J. C., TEER, J. K., PRICKETT, T. D., GARTNER, J., DAVIS, S., STEMKE-HALE, K., DAVIES, M. A., GERSHENWALD, J. E., ROBINSON, W., ROBINSON, S., ROSENBERG, S. A. & SAMUELS, Y. 2011. Exome sequencing identifies GRIN2A as frequently mutated in melanoma. *Nat Genet,* 43**,** 442-6.

WEISSBACH, A. 1993. A chronicle of DNA methylation (1948-1975). *EXS,* 64**,** 1-10.

WELBY, E., LAKOWSKI, J., DI FOGGIA, V., BUDINGER, D., GONZALEZ-CORDERO, A., LUN, A. T. L., EPSTEIN, M., PATEL, A., CUEVAS, E., KRUCZEK, K., NAEEM, A., MINNECI, F., HUBANK, M., JONES, D. T., MARIONI, J. C., ALI, R. R. & SOWDEN, J. C. 2017. Isolation and Comparative Transcriptome Analysis of Human Fetal and iPSC-Derived Cone Photoreceptor Cells. *Stem Cell Reports,* 9**,** 1898-1915.

WEST, D. A., CUMMINGS, J. M., LONGO, W. E., VIRGO, K. S., JOHNSON, F. E. & PARRA, R. O. 1999. Role of chronic catheterization in the development of bladder cancer in patients with spinal cord injury. *Urology,* 53**,** 292-7.

WOLFF, E. M., LIANG, G., CORTEZ, C. C., TSAI, Y. C., CASTELAO, J. E., CORTESSIS, V. K., TSAO-WEI, D. D., GROSHEN, S. & JONES, P. A. 2008. RUNX3 methylation reveals that bladder tumors are older in patients with a history of smoking. *Cancer Res,* 68**,** 6208-14.

WOLFF, E. M., LIANG, G. & JONES, P. A. 2005. Mechanisms of Disease: genetic and epigenetic alterations that drive bladder cancer. *Nature Clinical Practice Urology,* 2**,** 502.

WOODMAN, J. R., MANSFIELD, K. J., LAZZARO, V. A., LYNCH, W., BURCHER, E. & MOORE, K. H. 2011. Immunocytochemical characterisation of cultures of human bladder mucosal cells. *BMC Urol,* 11**,** 5.

WU, C. S., POLLACK, A., CZERNIAK, B., CHYLE, V., ZAGARS, G. K., DINNEY, C. P., HU, S. X. & BENEDICT, W. F. 1996. Prognostic value of p53 in muscle-invasive bladder cancer treated with preoperative radiotherapy. *Urology,* 47**,** 305-10.

WU, C. T., LIN, W. Y., CHANG, Y. H., CHEN, W. C. & CHEN, M. F. 2017. Impact of CD44 expression on radiation response for bladder cancer. *J Cancer,* 8**,** 1137-1144.

WU, C. T., WU, C. F., LU, C. H., LIN, C. C., CHEN, W. C., LIN, P. Y. & CHEN, M. F. 2011. Expression and function role of DNA methyltransferase 1 in human bladder cancer. *Cancer,* 117**,** 5221-33.

WU, H., WU, X. & ZHANG, Y. 2016. Base-resolution profiling of active DNA demethylation using MAB-seq and caMAB-seq. *Nat Protoc,* 11**,** 1081-100.

XING, J., GINTY, D. D. & GREENBERG, M. E. 1996. Coupling of the RAS-MAPK pathway to gene activation by RSK2, a growth factor-regulated CREB kinase. *Science,* 273**,** 959-63.

XING, X. W., LIU, Y. L., VARGAS, M., WANG, Y., FENG, Y. Q., ZHOU, X. & YUAN, B. F. 2013. Mutagenic and cytotoxic properties of oxidation products of 5-methylcytosine revealed by next-generation sequencing. *PLoS One,* 8**,** e72993.

YANG, W. H., CHANG, A. C., WANG, S. W., WANG, S. J., CHANG, Y. S., CHANG, T. M., HSU, S. K., FONG, Y. C. & TANG, C. H. 2016. Leptin promotes VEGF-C production and induces lymphangiogenesis by suppressing miR-27b in human chondrosarcoma cells. *Sci Rep,* 6**,** 28647.

YANG, X., HAN, H., DE CARVALHO, D. D., LAY, F. D., JONES, P. A. & LIANG, G. 2014. Gene body methylation can alter gene expression and is a therapeutic target in cancer. *Cancer Cell,* 26**,** 577-90.

YANG, Y. M. & CHANG, J. W. 2008. Bladder cancer initiating cells (BCICs) are among EMA-CD44v6+ subset: novel methods for isolating undetermined cancer stem (initiating) cells. *Cancer Invest,* 26**,** 725-33.

YAP, K. L., KIYOTANI, K., TAMURA, K., ANTIC, T., JANG, M., MONTOYA, M., CAMPANILE, A., YEW, P. Y., GANSHERT, C., FUJIOKA, T., STEINBERG, G. D., O'DONNELL, P. H. & NAKAMURA, Y. 2014. Whole-exome sequencing of muscle-invasive bladder cancer identifies recurrent mutations of UNC5C and prognostic importance of DNA repair gene mutations on survival. *Clin Cancer Res,* 20**,** 6605-17.

YE, F., WANG, L., CASTILLO-MARTIN, M., MCBRIDE, R., GALSKY, M. D., ZHU, J., BOFFETTA, P., ZHANG, D. Y. & CORDON-CARDO, C. 2014. Biomarkers for bladder cancer management: present and future. *Am J Clin Exp Urol,* 2**,** 1-14.

YOU, J. S. & JONES, P. A. 2012. Cancer genetics and epigenetics: two sides of the same coin? *Cancer Cell,* 22**,** 9-20.

YOUSSEF, R. F. & LOTAN, Y. 2011. Predictors of outcome of non-muscle-invasive and muscle-invasive bladder cancer. *ScientificWorldJournal,* 11**,** 369-81.

YU, C., HEQUN, C., LONGFEI, L., LONG, W., ZHI, C., FENG, Z., JINBO, C., CHAO, L. & XIONGBING, Z. 2017. GSTM1 and GSTT1 polymorphisms are associated with increased bladder cancer risk: Evidence from updated meta-analysis. *Oncotarget,* 8**,** 3246-3258.

YUAN, S. S., CHUNG, Y. F., CHEN, H. W., TSAI, K. B., CHANG, H. L., HUANG, C. H. & SU, J. H. 2004. Aberrant expression and possible involvement of the leptin receptor in bladder cancer. *Urology,* 63**,** 408-13.

ZAGHLOUL, M. S. 2012. Bladder cancer and schistosomiasis. *J Egypt Natl Canc Inst,* 24**,** 151-9.

ZARAVINOS, A., LAMBROU, G. I., BOULALAS, I., DELAKAS, D. & SPANDIDOS, D. A. 2011. Identification of common differentially expressed genes in urinary bladder cancer. *PLoS One,* 6**,** e18135.

ZHANG, H., PRADO, K., ZHANG, K. X., PEEK, E. M., LEE, J., WANG, X., HUANG, J., LI, G., PELLEGRINI, M. & CHIN, A. I. 2016. Biased Expression of the FOXP3Delta3 Isoform in Aggressive Bladder Cancer Mediates Differentiation and Cisplatin Chemotherapy Resistance. *Clin Cancer Res,* 22**,** 5349-5361.

ZHANG, W. & LIU, H. T. 2002. MAPK signal pathways in the regulation of cell proliferation in mammalian cells. *Cell Res,* 12**,** 9-18.

ZHAO, J. 2016. Cancer stem cells and chemoresistance: The smartest survives the raid. *Pharmacol Ther,* 160**,** 145-58.

ZHU, F., QIAN, W., ZHANG, H., LIANG, Y., WU, M., ZHANG, Y., ZHANG, X., GAO, Q. & LI, Y. 2017. SOX2 Is a Marker for Stem-like Tumor Cells in Bladder Cancer. *Stem Cell Reports,* 9**,** 429-437.

ZIEGER, K., MARCUSSEN, N., BORRE, M., ORNTOFT, T. F. & DYRSKJOT, L. 2009. Consistent genomic alterations in carcinoma in situ of the urinary bladder confirm the presence of two major pathways in bladder cancer development. *Int J Cancer,* 125**,** 2095-103.

ZUIVERLOON, T. C., BEUKERS, W., VAN DER KEUR, K. A., MUNOZ, J. R., BANGMA, C. H., LINGSMA, H. F., EIJKEMANS, M. J., SCHOUTEN, J. P. & ZWARTHOFF, E. C. 2012. A methylation assay for the detection of non-muscle-invasive bladder cancer (NMIBC) recurrences in voided urine. *BJU Int,* 109**,** 941-8.

APPENDIX 1

Table 1: Details of all tissue samples used in primary culture

Patient	Gender	Age	Stage	Grade	Cis	Type	Treatment	Appearance	Medium used	Method used
Pt 44	F	75	pT2	G3	No	UCC	Radiotherapy	2 large pieces	DMEM full (20% FCS)	Explant method
Pt 45	F	92	pT1	G3	No	UCC	None	brown fragment	N/A	N/A
Pt 46	M	83	pT3b	G3	No	UCC	None	2 medium pieces	1- DMEM Full. 2- KSFMc. 3- Epilife.	Explant method + Stripping method
Pt 47	M	85	pT2	G3	No	UCC	None	2 large pieces	1- DMEM Full. 2- Epilife.	Explant method
Pt 48	M	49	pT4	n/a	N/a	ADC	None	very small piece	1- DMEM Full. 2- Epilife.	Explant method
Pt 51	M	77	pT2b	G3	No	UCC	None	2 medium pieces	1- DMEM Full. 2- Epilife. 3- Stem pro.	Explant method
Pt 54	M	81	pT3a	G3	No	TCC	None	2 large pieces	1- DMEM Full.	Explant method
Pt 55	M	71	pT3a	G3	No	TCC	None	2 pieces	1-DMEM Full.	Explant method
Pt 56	M	81	pT1	G3	No	TCC	None	3 small pieces	1- KSFMc. 2- Epilife. 3 -Stem pro medium.	Explant method
Pt 59	M	74	pT2	G3	Cis	TCC	None	Many small pieces	1-DMEM Full	Stripping method
Pt 61	F	74	pT3	G3	Cis	TCC	None	1 small piece	1-DMEM Full. 2- KSFMc. 3- Stem pro.	Stripping method

Pt 62	M	83	pT3b	G3	No	Tcc	None	2 pieces: small and medium	1-DMEM Full. 2- Stem pro +10%FCS.	CTOS isolation methods
Pt 63	M	79	pT2	G3	No	TCC	None	2 small pieces	1-Stem pro + 10%FCS	Explant method
Pt 65	M	90	pT1	G3	No	TCC	None	1 small piece	1-Stem pro + 10%FCS	Explant method
Pt 66	M	74	pT3b	G3	No	SCC	None	1 large piece	1-Stem pro + 10%FCS	Explant method
Pt 70	M	78	pTa	G3	Cis	TCC	None	1 small piece	1-Stem pro medium + 10%FCS	Explant method
Pt 72	F	78	pTa	G2	No	TCC	None	3 medium pieces	1-Stem pro medium + 10%FCS	Explant method
Pt 73	M	75	pT1	G3	No	TCC	None	4 large pieces	1-Stem pro medium.	Explant method
Pt 75	F	73	pT1	G3	No	ADC	None	1 small piece	1-Stem pro medium.	Explant method
Pt 76	M	72	pT2a	G3	No	TCC	None	1 small piece	1-Stem pro medium.	Explant method
Pt 78	M	73	pTa	G2	No	TCC	Yes	3 small pieces	1-Stem pro medium.	Explant method
Pt 79	M	74	pT4a	G3	No	TCC	None	1 large piece	1-Stem pro medium.	Explant method
Pt 81	M	71	n/a	n/a	Cis	TCC	None	1 small piece	1-Stem pro + 1%FCS	Explant method
Pt 84	M	98	pTx	G2	No	UCC	None	Many pieces	1-Stem pro + patient serum	Explant method
Pt 85	M	77	pT1	G3	Cis	UCC	None	Many small pieces	1-Stem pro + patient serum	Explant method
Pt 87	M	87	pT3a	G3	No	UCC	None	2 small pieces	1-Stem pro.	Explant method
Pt 90	M	75	pT1a	G3	No	UCC	None	Many small pieces	1-Stem pro.	Explant method
Pt 97	F	90	pT2	G3	Cis	UCC	None	2 pieces	1-Stem pro.	Explant method
Pt 100	M	87	pTa	G2	No	UCC	None	Many small pieces	1-Stem pro.	Explant method
Pt 103	F	63	pT2	G3	Yes	UCC	None	1 small piece	1-Stem pro.	Explant method

Table 2: Details of all tissue (normal and tumour) samples used in fluorescence-activated cell sorting (FACS)

Patient	Gender	Age	Tissue	Operation	Pre-op treatment	Sample appearance
Pt 113	M	71	Bladder normal	Radical prostatectomy	N/A	One large piece
Pt 123	M	68	Bladder normal	Radical prostatectomy	N/A	One medium piece
Pt 127	M	64	Bladder normal	Radical prostatectomy	N/A	One medium piece
Pt 128	M	71	Bladder normal	Radical prostatectomy	N/A	One medium piece

Patient	Gender	Age	Tissue	Stage	Grade	Cis	Type	Pre-op treatment	Sample appearance
Pt 112	M	49	Bladder tumour	pT3	G3	Yes	TCC	None	1 medium piece
Pt 114	M	90	Bladder tumour	pT1	G3	No	SCC	None	Many pieces (necrotic)
Pt 115	M	77	Bladder tumour	pT1	G3	Cis	TCC	None	Many small pieces
Pt 116	F	59	Bladder tumour	pTa	G2	No	TCC	None	One small piece (necrotic)
Pt 117	F	87	Bladder tumour	pT1	G2	No	TCC	None	Two large pieces
Pt 118	F	71	Bladder tumour	pTa	G2	No	UCC	None	Many pieces (necrotic)
Pt 119	M	72	Bladder tumour	pT2	G3	No	TCC	None	Medium piece
Pt 120	M	72	Bladder tumour	pT2a	G3	No	TCC	None	Two small pieces (necrotic)
Pt 121	M	76	Bladder tumour	pT2	G3	No	TCC	None	Small piece (necrotic)
Pt 122	F	83	Bladder tumour	pTa	G2	No	TCC	Yes	One medium piece
Pt 124	M	71	Bladder tumour	pTa	G3	No	UCC	None	Two pieces and one small
Pt 125	F	80	Bladder tumour	pT2b	G3	No	UCC	None	One medium piece
Pt 126	M	87	Bladder tumour	pTa	G2	No	UCC	Yes	One medium piece

Pt 129	M	54	Bladder tumour	pT1	G3	Cis	UCC	None	Very thin piece
Pt 130	M	89	Bladder tumour	pT1+	G3	No	UCC	None	Many pieces
Pt 131	M	63	Bladder tumour	N/A	benign	N/A	UCC	None	Many clean pieces
Pt 133	M	66	Bladder tumour	pT1	G3	Cis	TCC	None	One medium piece
Pt 134	M	75	Bladder tumour	pT1	G3	Cis	TCC	None	One medium piece
Pt 136	M	67	Bladder tumour	pT2	G3	No	TCC	None	One medium piece
Pt 137	F	90	Bladder tumour	pT1+	G2	No	SCC	None	One medium piece
Pt 138	M	77	Bladder tumour	pTa	G1	No	TCC	None	One small piece
Pt 139	F	81	Bladder tumour	pTa	G3	Cis	TCC	None	One medium piece
Pt 140	M	51	Bladder tumour	pTa	G2	No	TCC	None	Many large pieces
Pt 141	M	82	Bladder tumour	pTa	G3	No	Adc	None	One medium piece
Pt 142	M	74	Bladder tumour	pT2b	G3	No	TCC	None	Two small pieces
Pt 143	M	75	Bladder tumour	pTa	G2	No	TCC	None	Two small pieces
Pt 145	F	86	Bladder tumour	pT1+	G3	No	TCC	None	Three small pieces
Pt 146	F	68	Bladder tumour	pT3	G3	No	TCC	None	Three medium pieces
Pt 147	M	77	Bladder tumour	pTa	G2	No	UCC	None	One medium piece
Pt 148	M	71	Bladder tumour	pT1	G3	No	UCC	None	Medium piece
Pt 149	M	67	Bladder tumour	pT3b	G3	No	UCC	None	One medium piece
Pt 150	F	70	Bladder tumour	pT3b	G3	Cis	UCC	None	Two small pieces
Pt 151	M	67	Bladder tumour	pT2	G3	No	UCC	None	Two medium pieces
Pt 152	M	80	Bladder tumour	pTa	G2	No	UCC	None	One medium piece

Table 3: Details of all tissue (normal and tumour) samples used in Infinium HumanMethylation450 BeadChip array

Patient	Study number	Gender	Age	Grade	Tissue	Treatment
NT1	4480	male	67	N/A	normal	None
NT2	4305	male	70	N/A	normal	None
NT3	4341	male	70	N/A	normal	None
BC1	3191	male	64	G3	Tumour	None
BC2	4237	male	85	G3	Tumour	None
BC3	4038	female	81	G3	Tumour	None
BC4	4229	male	78	G3	Tumour	None
BC5	4166	male	87	G3	Tumour	None
BC6	3129	female	79	G3	Tumour	None
BC9	4028	male	78	G3	Tumour	None

APPENDIX 2

Details of primers used for 5hmC qPCR detection kit

Probe ID	Oligo name	Oligo sequence (5' to 3")	Chromosome	Position	Amplicon position
cg12068908	Forward 01	AGGGTGCAGGTAGAGACAGG	chr11	14270521	Start: 14270457
cg12068908	Reverse 01	TTGTAGGAAATCTGGGCATTTTC			End: 14270556
cg20340596	Forward 02	TCCTCAGCTGATCCCTTCT	chr10	100206925	Start: 100206891
cg20340596	Reverse 02	CAGGGAGAGCAGTCACAAA			End: 100206996
cg10967023	Forward 03	GTGATCGAATAAGAGGCAGTGG	chr12	115134886	Start: 115134821
cg10967023	Reverse 03	GCAAAGCTGGTGGGAAGTAA			End: 115134944
cg09307193	Forward 04	GCCAGTTATCCAGAGCAGTTAG	chr14	69430369	Start: 69430336
cg09307193	Reverse 04	GAAAGGACAAGCGGAGAAGAA			End: 69430461
cg24092939	Forward 05	CTTCAGCCTCCTCCATTCAC	chr12	49181056	Start: 49180980
cg24092939	Reverse 05	TTGGAACATGGCCAGAAACTA			End: 49181096
cg06044662	Forward 06	CGCAGGGCTAAGGTTACC	chr16	30386144	Start: 30386044
cg06044662	Reverse 06	GCAGGGGTTGGAGGATTCT			End: 30386207
cg24327132	Forward 07	CATTAATCAAGTCCCAGGAGAGG	chr15	72520632	Start: 72520548
cg24327132	Reverse 07	GCTTAAGTGTAGACTGGCAGAG			End: 72520657